

DYNAMIC RESPONSE OF STRUCTURES
IN LAYERED SOILS

by

VICTOR CHANG LIANG

Ing. Civil, Univ. de San Carlos de Guatemala
(1969)

Submitted in partial fulfillment
of the requirements for the degree of
Doctor of Science

at the
Massachusetts Institute of Technology
(February 1974)

Signature redacted

Signature of Author
Department of Civil Engineering, February 1974

Signature redacted

Certified by
Thesis Supervisor

Signature redacted

Accepted by
Chairman, Departmental Committee on Graduate Students
of the Department of Civil Engineering



ABSTRACT

DYNAMIC RESPONSE OF STRUCTURES
IN LAYERED SOILS

by

VICTOR CHANG LIANG

Submitted to the Department of Civil Engineering on January 16, 1974, in partial fulfillment of the requirements for the degree of Doctor of Science.

The dynamic response of a strip footing resting on or embedded in a soil stratum is studied. The cases investigated cover the excitation of the footing by horizontal forces and rocking moments, and the motion due to a specified displacement at bedrock.

The study is based on an extension of a method originally developed by G. Waas. It is a finite element formulation, with appropriate energy absorbing boundaries, which consist of semi-infinite layered regions extending to the left and right of the finite element region.

The effect of layer thickness and the convergence towards the half-space solution are investigated first. The effect of embedment is then considered, comparing the response of an embedded footing to that of the same footing at the surface. The interaction between adjacent footings is finally studied.

The results obtained suggest that some of the effects studied might be reasonably well reproduced by applying simple correction factors to the half-space solutions.

Thesis Supervisor:

José Manuel Roësset

Title:

Associate Professor of Civil Engineering

ACKNOWLEDGEMENTS

In the first place, I would like to express my gratitude to Exploraciones y Explotaciones Mineras de Izabal (EXMIBAL) for supporting most of my studies at MIT. Thanks are also extended to the National Science Foundation, who made this research possible through Grant No. GI-35139.

My sincere appreciation is given to Professor José M. Roësset, who supervised my research with patience and encouragement, and offered continuous advice and help throughout my studies at MIT. Special recognition is given to Dr. Günter Waas, whose valuable comments and ideas made this work possible. Finally, I want to thank Mrs. Jessica Malinofsky for her patience in typing the manuscript; and my wife, France-Anne, for her help in the final drafting of the figures.

TABLE OF CONTENTS

	Page
Title Page	1
Abstract	2
Acknowledgements	3
Table of Contents	4
List of Figures	6
List of Symbols	10
Chapter 1. INTRODUCTION	13
1.1 General Considerations	13
1.2 Review of Past Work	14
1.3 Scope of this Work	20
Chapter 2. THEORETICAL CONSIDERATIONS	22
2.1 Introduction	22
2.2 Soil Properties	24
2.3 Basic Equations	27
2.4 Mathematical Model	29
2.5 Rock Motion	39
2.6 Compliance Functions	53
2.7 Response of Structures with Mass	59
2.8 Structure - Soil - Structure Interaction	65
2.8.1 Generalities	65
2.8.2 Stiffness Functions	66
2.8.3 Effect of Mass	72
2.8.4 Rock Motion	73
Chapter 3. EFFECT OF LAYER THICKNESS	75
3.1 Introduction	75
3.2 Amplification Functions	75

3.3	Compliance and Stiffness Functions	80
	3.3.1 General Characteristics	80
	3.3.2 Effect of Damping. Approximation.	88
	3.3.3 Effect of Layer Thickness	91
3.4	Effect of Mass	103
Chapter 4.	EFFECT OF EMBEDMENT	118
	4.1 Introduction	118
	4.2 Amplification Functions	118
	4.3 Compliance Functions	129
	4.4 Effect of Mass	136
Chapter 5.	STRUCTURE - SOIL - STRUCTURE INTERACTION	149
	5.1 Introduction	149
	5.2 Method of Solution	149
	5.3 Response to Exciting Forces	151
	5.4 Response to a Prescribed Motion of the Soil	165
Chapter 6.	CONCLUSIONS AND RECOMMENDATIONS	178
	6.1 Summary	178
	6.2 Conclusions	179
	6.3 Recommendations for Further Work	183
References		185
Biography		191
Appendix -	User's Manual for PLAXLY2	192

LIST OF FIGURES

<u>Figure</u>	<u>Description</u>	<u>Page</u>
2-1a	Typical plane strain system	23
2-1b	Typical axisymmetric system	23
2-2a	Hysteretic stress-strain relationship at different strains	25
2-2b	Representation of stress and strain in the complex plane	25
2-3	Typical modelling of plane strain system	31
2-4	Form of matrices in eq. (2.20)	33
2-5	Discretization for 1-D amplification	40
2-6	Forces acting at boundaries of layered regions for motion at bedrock	47
2-7	System including rigid structure with mass	61
2-8	Geometry for two adjacent structures	65
2-9	Discretization for mathematical solutions	67
3-1	Geometry for footing on soil surface	76
3-2	1-D amplification for different amounts of damping	78
3-3	Effect of damping on maximum 1-D amplification	79
3-4	Effect of damping on compliance function F_{xx}	83
3-5	Effect of damping on compliance function $F_{\phi\phi}$	84
3-6	Effect of damping on stiffness function K_{xx}	86
3-7	Effect of damping on stiffness function $K_{\phi\phi}$	87
3-8a	Comparison of "exact" K_{xx} vs. same by correspondence principle for $\beta = 10\%$	89
3-8b	Comparison of "exact" $K_{\phi\phi}$ vs. same by correspondence principle for $\beta = 10\%$	90
3-9a	Effect of layer thickness on static compliances	92
3-9b	Effect of layer thickness on static stiffnesses	93
3-10a	Effect of layer thickness on $\text{Re} (F_{xx})$	96
3-10b	Effect of layer thickness on $\text{Im} (F_{xx})$	97
3-11a	Effect of layer thickness on $\text{Re} (F_{\phi\phi})$	98
3-11b	Effect of layer thickness on $\text{Im} (F_{\phi\phi})$	99

3-12a	Half-space solutions for F_{xx}	101
3-12b	Half-space solutions for $F_{\phi\phi}$	102
3-13	Rigid structure with mass on soil surface	104
3-14	Effect of mass on horizontal amplification, $H/B = 1$	105
3-15	Effect of mass on horizontal amplification, $H/B = 2$	106
3-16	Effect of high mass ratios on horizontal amplification	108
3-17	Effect of height of homogeneous structure on horizontal amplification, $H/B = 2$	109
3-18	Geometry used in approximations to explain phenomena of two peaks in amplification curves	112
3-19	Effect of layer thickness on interaction, $B_x = 2$	113
3-20	Effect of mass on interaction, $H/B = 2$	114
3-21	Effect of height of center of gravity and radius of gyration on horizontal amplification	116
4-1	Geometry for embedded footing	119
4-2	Horizontal amplification of massless embedded footings, $H/B = 2$	121
4-3	1-D amplification at level of embedment in Fig. 4-2	122
4-4	Rotation amplification of massless embedded footings, $H/B = 2$	123
4-5	Phase angles for horizontal displacements and rotations of massless embedded footings	125
4-6	Effect of layer thickness on horizontal amplification	126
4-7	Effect of embedment for several layer thicknesses, $D/B = 2/3$	127
4-8	Effect of embedment for several layer thicknesses, $D/H = 1/3$	128
4-9a	Normalized compliance function F_{xx} for different embedment ratios	130
4-9b	Normalized compliance function $F_{\phi\phi}$ for different embedment ratios	131
4-9c	Normalized compliance function $F_{x\phi}$ for different embedment ratios	132
4-10	Effect of layer thickness on static compliances for different embedment ratios	134

4-11	Effect of embedment on static compliances for different layer thicknesses	135
4-12	Effect of mass on horizontal amplification, $H/B=1$, $D/H = 1/3$	137
4-13	Effect of mass on horizontal amplification, $H/B=2$, $D/H = 1/3$	138
4-14	Effect of embedment on horizontal amplification, $H/B=2$, $B_x = 2$	140
4-15	Effect of embedment on rotation amplification, $H/B=2$, $B_x = 2$	141
4-16	Horizontal amplification of embedded footing with respect to same for footing on surface of soil	143
4-17	Effect of mass on maximum horizontal and rotation amplification and frequency at peaks, $H/B=1$	145
4-18	Effect of mass on maximum horizontal and rotation amplification and frequency at peak, $H/B=2$	146
4-19	Effect of mass on maximum horizontal and rotation amplification and frequency at peak, $H/B=4$	147
4-20	Effect of mass on maximum horizontal amplification at center of gravity and at bottom of structure, $H/B=2$	148
5-1	Geometry for two adjacent structures	150
5-2	Horizontal displacement in excited footing due to a horizontal force on same, $H/B=4$, $L/B=5$	152
5-3	Horizontal displacement in unexcited footing due to a horizontal force on the other, $H/B=4$, $L/B=5$	153
5-4	Rotations in the two footings due to a horizontal force in one of them, $H/B=4$, $L/B=5$	154
5-5	Rotations in the two footings due to a rocking moment in one of them, $H/B=4$, $L/B=5$	155
5-6	Horizontal displacement in excited footing due to a horizontal force on same, $H/B=1$, $L/B=5$	158
5-7	Rotation in excited footing due to a rocking moment on same, $H/B=1$, $L/B=5$	159
5-8	Rotation in excited footing due to a horizontal force on same, $H/B=1$, $L/B=5$	160
5-9	Horizontal displacement in unexcited footing due to horizontal force on the other, $H/B=1$, $L/B=5$	161
5-10	Effect of distance between footings on horizontal displacement of excited footing due to horizontal force on same	163

5-11	Effect of distance between footings on horizontal displacement of unexcited footing due to a horizontal force on the other	164
5-12a	Effect of mass of second footing on amplification of soil motion in first, $B_{x_1} = 1$	166
5-12b	Effect of mass of second footing on amplification of soil motion in same, $B_{x_1} = 1$	167
5-13	Effect of mass of second footing on amplification of soil motion in first, $B_{x_1} = 4$	168
5-14	Effect of adjacent mass on amplification of soil motion	170
5-15	Effect of adjacent footing on amplification of soil motion	171
5-16	Effect of mass of second footing on amplification of soil motion in first, $B_2 = 4B_1$, $B_{x_1} = 1$	173
5-17	Effect of mass of second footing on amplification of soil motion in first, $B_2 = 4B_1$, $B_{x_1} = 4$	174
5-18	Effect of small footing on a larger footing for amplification of soil motion	175
5-19	Effect of adjacent larger footing on amplification of soil motion	176

NOTATION

Note: Only the symbols often used are shown in this list.

- $a = \frac{\Omega H}{C_s}$ = frequency ratio (with respect to layer thickness)
- $a_0 = \frac{\Omega B}{C_s}$ = frequency ratio (with respect to footing half-width)
- $A(\Omega)$ = amplification function
- B = half-width of strip footing
- $B_x = \frac{M}{\rho B^2}$ = mass ratio for horizontal translation
- $B_\phi = \frac{I_c}{\rho B^4}$ = $B_x^2 s^2$ = inertia ratio for rocking
- c = phase velocity
- C_p = dilatational (P) wave velocity
- C_s = shear (S) wave velocity
- $d = D/H$ = embedment ratio (with respect to layer thickness)
- D = embedment of footing
- $e = E/B$ = height, center of gravity ratio; or base of natural logarithms = 2.718.....
- E = height of center of gravity of rigid structure
- f = frequency in cycles per second
- $f_{xx}, f_{\phi\phi}, f_{x\phi}$ = normalized $F_{xx}, F_{\phi\phi}, F_{x\phi}$ with respect to their static values, respectively
- F_{xx} = horizontal (sliding,swaying) compliance function
- $F_{\phi\phi}$ = rocking compliance function
- $F_{x\phi}$ = cross-compliance function
- $[F]$ = compliance matrix

G	=	shear modulus
h_j	=	thickness of j^{th} layer in a layered soil stratum
H	=	height of soil stratum
[J]	=	inertia matrix
K	=	wave number
K_{xx}	=	horizontal (sliding, swaying) stiffness function
$K_{\phi\phi}$	=	rocking stiffness function
$K_{x\phi}$	=	cross-stiffness function
[K]	=	stiffness matrix
[K*]	=	reduced stiffness matrix for structure - soil - structure interaction
L	=	distance between center-lines of two footings
M	=	mass of rigid structure
P_x	=	horizontal force
P_z	=	vertical force
P_ϕ	=	rocking moment
r, θ, z	=	cylindrical coordinates for axisymmetric systems
s	=	radius of gyration ratio
S	=	radius of gyration of rigid structure
t	=	time
u	=	horizontal displacement
w	=	vertical displacement
x, y, z	=	rectangular (Cartesian) coordinates for plane strain systems
α_s	=	participation factor for s^{th} mode in layered system
β	=	percentage of hysteretic damping

ϵ	=	strain
η	=	viscosity coefficient
λ	=	Lamé constant
ν	=	Poisson's ratio
π	=	3.14159.....
ρ	=	density of soil
ρ_{st}	=	density of homogeneous structure
σ	=	normal stress
τ	=	shear stress
ϕ	=	rotation (rocking)
ω_n	=	n^{th} natural frequency
Ω	=	frequency of excitation

CHAPTER 1 - INTRODUCTION

1.1 General Considerations

The design of foundations to resist dynamic loadings, either from supported machinery or from external sources, e.g. earthquakes, must meet certain performance criteria. These usually relate to the dynamic response of the foundation, as expressed in terms of a limiting amplitude of vibration at a particular frequency or a limiting value of peak velocity or peak acceleration. It must also be ensured that the vibrations transmitted through the ground will not affect other structures or humans in the neighborhood.

Since a foundation is resting on, or embedded in, the ground, the characteristics of the soil will affect its behavior. If the soil foundation system vibrates with small amplitudes, it can be considered to behave linearly; and then the response to periodic loads can be obtained by superposition of the harmonic response at different frequencies. Transient loads can also be dealt with, by using the Fourier transformation techniques.

The evaluation of the structure's response considering soil-structure interaction is a complicated problem. Even if the structure is considered rigid (e.g. a rigid footing for machinery, a nuclear reactor containment vessel), the problem is quite involved from a mathematical point of view. It is a wave propagation problem with boundary conditions of the mixed type, i.e., both displacement and force boundary conditions arise. Displacements must be compatible in the area of contact of the structure with the soil, and

the free surface of the ground is stress-free. There may be rock underlying the soil stratum, which may itself consist of different layers with different properties.

For these reasons, the mathematical model must be a very idealized one. Most of the research done on this subject assumes a perfectly elastic half-space, where the only existing boundary for the soil is the free surface. Besides, the footing is usually considered axisymmetric, thus reducing the number of spatial dimensions to two, instead of three.

In this work, a rigid strip footing is considered as the model of the structure. Therefore, this is also a two-dimensional problem of plane strain. This model is adequate if the actual footing is comparatively long with respect to its width. Instead of assuming a half-space, a soil stratum of limited depth overlying a rigid rock from which waves are totally reflected is considered here.

To obtain numerical solutions to this problem, finite elements were used, using as a starting point the model developed by Waas [56], as summarized in Chapter 2.

1.2 Review of Past Work

There are numerous studies on the vibrations of a rigid circular footing supported by a homogeneous, isotropic and perfectly elastic half-space. The excitation by a harmonic vertical force was studied first by Reissner [43] in 1936. He assumed a uniform stress distribution under the footing. Bycroft [9] assumed the

static stress distribution as valid for the dynamic case in the low frequency range. Lysmer and Richart [35], and Awojobi and Grootenhuis [5] derived solutions for this problem taking into consideration the frequency dependence of the stress distribution under the footing. Robertson [46] used a series solution valid in the low frequency range. Lysmer and Kuhlemeyer [34] used a finite element method with an energy absorbing boundary (consisting of lumped dashpots) to analyze this problem, with capabilities to study the effect of embedment.

When rock or hard layers are encountered at relatively shallow depths, the half-space theory does not provide a good solution to the "real" situation. Warburton [57] studied the vertical vibration of a rigid circular footing supported by a homogeneous elastic layer that extends to infinity in the horizontal direction, and rests on a rigid base. He assumed a stress distribution and considered a frictionless contact between the soil and the rigid base. Kuhlemeyer [29] used the energy absorbing boundary mentioned above to study the vertical motion of a footing supported by a stratified half-space, but found that the results were inconclusive when the deeper layers were stiffer than the surface layer, which is a usual case in foundation vibration problems. Waas [56] studied this problem using also finite elements, and developed dynamic stiffness matrices for the layered regions of infinite horizontal extent, adjoining the finite element irregular region, thereby accounting for dissipation of waves through the layered media.

The study of the horizontal and rocking vibrations of circular footings has received considerable attention recently. Arnold, Bycroft and Warburton [3], Bycroft [9], and Warburton [57] considered all four modes of vibration. They assumed a uniform shear stress distribution for horizontal vibration and a linear variation of stress for rocking vibration. Gladwell [16] considered the actual mixed boundary-value problem, but introduced simplifying assumptions with regard to the conditions of contact at the footing-soil interface. Luco and Westmann [30] used a similar method, and covered a wider range of frequencies. These solutions neglected the coupling between sliding and rocking. Wei [60] found an "exact" solution, without making an a priori assumption concerning the distribution of contact pressure, covering a wide range of frequencies.

By a reorganization of Reissner's equations, Hsieh [19] developed expressions for frequency-dependent stiffness and damping functions. Utilizing Bycroft's solutions and the force-displacement relationships given by Hsieh, Hall [18] determined a solution for the rocking and sliding oscillations of a circular plate on the surface of an elastic half-space. Ratay [42] used a similar approach to obtain the simultaneous rocking and sliding motion of a rigid mass with a circular base. Whitman and Richart [61] presented useful expressions for the determination of the spring and dashpot constants and the equivalent mass of soil to represent the dynamic properties of the soil. Veletsos and Wei [55] presented results for an equivalent spring-dashpot representation of the disk-foundation system. Meek

and Veletsos [37] considered a semi-infinite truncated cone of circular cross section as effective in transmitting the energy from a dynamically loaded circular footing, and developed expressions for frequency-independent spring and dashpot constants for the horizontal motion, whereas the rocking expressions are frequency-dependent. Veletsos and Verbic [54] found simple approximate solutions for the steady-state response of a massless circular rigid disk supported on the surface of a linear viscoelastic half-space, idealized as either a standard Voigt solid or as a constant hysteretic solid.

Less research has been done on the vibrations of strip footings. Karasudhi, Keer and Lee [22] presented an approximate analytical solution for the vertical and coupled horizontal and rocking vibration of an infinitely long rigid footing resting on the surface of an elastic half-space; and showed that the coupling effects are quite significant. Luco and Westmann [31] also studied this problem and found an exact analytical solution when the Poisson's ratio of the soil is $1/2$, and a first approximation for other values of this ratio, valid in the range of low frequencies. Awojobi [4] considered the high frequency range, but did not cover the case of horizontal motion. Ang and Harper [2] developed a lumped-parameter consisting of mass-points and stress-points to simulate the semi-infinite, linearly elastic, homogeneous, isotropic medium for plane strain problems. This model was modified by Agabain, Parmelee and Lee [1] to include finite boundaries, and developed a fairly general two-dimensional scheme for the study of seismic soil-structure inter-

action problems. Gupta, Parmelee, and Krizek [17] used this extended model to examine the coupled sliding and rocking of a strip footing resting on the surface of an elastic half-space.

Rectangular foundations have been studied by Elorduy, Nieto and Szekely [13] for vertical loading. Kobori, Minai, Suzuki and Kusakabe [25] have obtained numerical solutions for the four modes of vibration of rectangular bases on an elastic half-space. In another paper [26] they considered the same problem, but including material damping in the soil. Later on, Kobori and Suzuki [27] considered a viscoelastic multi-layered medium, while Kobori, Minai and Suzuki [24] determined the solutions for a viscoelastic stratum of soil overlying a rigid base.

The effect of embedment of footings has been recently considered. No rigorous analytical solution of embedded footings is available because of the obvious mathematical difficulties.

An approximate analytical approach was formulated by Baranov [6], who assumed an elastic half-space under the footing base and a series of thin independent elastic layers between the force-surface of the ground and this half-space. Novak and Beredugo [40] have used this model to compute series solutions for stiffness and damping functions for vertical vibrations of a circular footing in either a half-space or a stratum. Also, in another paper, Beredugo and Novak [7] considered the case of coupled horizontal and rocking vibrations of the same system studied above. Krizek, Gupta and Parmelee [28] used the extended model of Ang and Harper to study the coupled

sliding and rocking vibrations of a rigid strip footing embedded in an elastic half-space, and made a parametric study of the effect of embedment. Lysmer and Kuhlemeyer [34] used the energy absorbing boundary mentioned before to study this effect; and Waas [56] also used the finite element method with appropriate boundaries to simulate the layered systems. Both studied in detail the case of vertical vibrations for axisymmetric systems. Recently, Urlich and Kuhlemeyer [53] studied the effect of embedment for coupled rocking and lateral vibrations of circular footings in a half-space, using a viscous boundary. Novak [39] suggested an approximate method to get corrections to the solutions of circular footings on the surface of a soil stratum, for any vibration mode.

There has been evidence that soil-structure interaction affects the response of structures subjected to seismic loadings. Several approximate models have been used to take care of the foundation flexibility [10, 14, 32, 38, 50, 52, 61]. The common method of separating this dynamic problem into two parts, with a one-dimensional soil amplification of the input motion considered first and the resulting motion at the soil surface applied next as input to the structure, will not be exact if there is embedment.

It has also been recognized that the structures in a neighborhood affect each other through the soil. If they are close enough, it may not be appropriate to study each one separately. When one structure is excited by forces like those produced by machinery, waves are generated, and these disturb other structures in the vicinity [20].

The response to seismic motions is also modified by the presence of neighboring bodies. Several authors [41, 45, 51] have considered the motion of a rigid footing due to waves travelling along the ground surface. Richardson [50] and Warburton, Richardson and Webster [58] considered two circular cylinders on the surface of a half-space and used an averaging procedure for the free surface motion to find the effect of the mutual interaction of the two structures. Other approaches to this problem have been suggested by Kobori and Minai [23], who studied the statistical properties of a random flow of energy between structures on a viscoelastic soil; Sakurai and Minami [49], who used a truss as a model of the buildings and the soil, and determined the response to earthquake motions and pulse waves by modal superposition; and MacCalden and Matthiesen [36], who used Bycroft's compliances for the half-space to study the transmission of surface vibrations from one circular footing to another in an analytical form.

1.3 Scope of this Work

The problems considered here are the steady-state harmonic vibrations of one or two strip footings due to exciting forces applied to them, or to motions of the soil stratum due to a specified displacement at the soil-rock interface. The soil is considered homogeneous, isotropic and linearly elastic with hysteretic damping. Poisson's ratio has been kept as $\nu = 0.30$ throughout the whole study. The rock is considered as a rigid half-space. The structure is

idealized as a rigid strip footing.

The theory pertaining to these problems is presented in Chapter 2. The starting point to this work was given by Waas [56].

In Chapter 3, a strip footing on the surface of the soil stratum is considered. Compliance and stiffness functions are determined for a range of layer thickness to footing width ratio, from relatively shallow to relatively deep strata. Comparison is made with some available solutions for the half-space. The amplification of the motion of the soil is then studied, for footings with different masses. The effect of the soil-structure interaction is then isolated.

Embedded strip footings are considered in Chapter 4. Studies similar to those of Chapter 3 are conducted. The variation of static compliances for different embedment ratios gives an insight into the effect of embedment. Summary curves giving the maximum amplification of the soil motion for different mass and embedment ratios are given.

Chapter 5 considers the interaction of two parallel strip footings through the soil. Both the cases of excitation of one of the footings by external forces and of soil motion are considered. The number of parameters involved in this problem is very large; but the cases presented give a picture of the phenomenon of structure - soil - structure interaction.

Conclusions and recommendations are finally given in Chapter 6.

CHAPTER 2 - THEORETICAL CONSIDERATIONS

2.1 Introduction

The majority of studies on foundation vibrations have dealt with the case of a circular footing on a homogeneous, isotropic and perfectly elastic half-space. This has often been adopted as a typical foundation-ground model.

Karasudhi, Keer and Lee [22] have studied the vibratory motion of a rigid strip-footing on an elastic half-plane. The present work also deals with an infinitely long strip footing, but under more realistic conditions, by including material dissipation properties (internal damping) and limiting the thickness of the soil to a finite stratum with one or more layers of different properties. These studies have concentrated on a homogeneous soil, while the computer program used has the capabilities to deal with a horizontally layered system, consisting of a series of homogeneous, isotropic and viscoelastic layers, perfectly connected at the interfaces. The region in the neighborhood of the footing can be irregular. The whole system is limited at the bottom boundary by a rigid half-space, which will be referred to as "rock." Fig. 2-1 depicts the coordinate system and significant dimensions.

This work presents the response of the foundation to harmonic exciting forces on the rigid footing, and also the response of a structure represented by the footing, to a harmonically varying prescribed displacement in the rock. Finally, it presents the dynamic interaction of two structures through the soil.

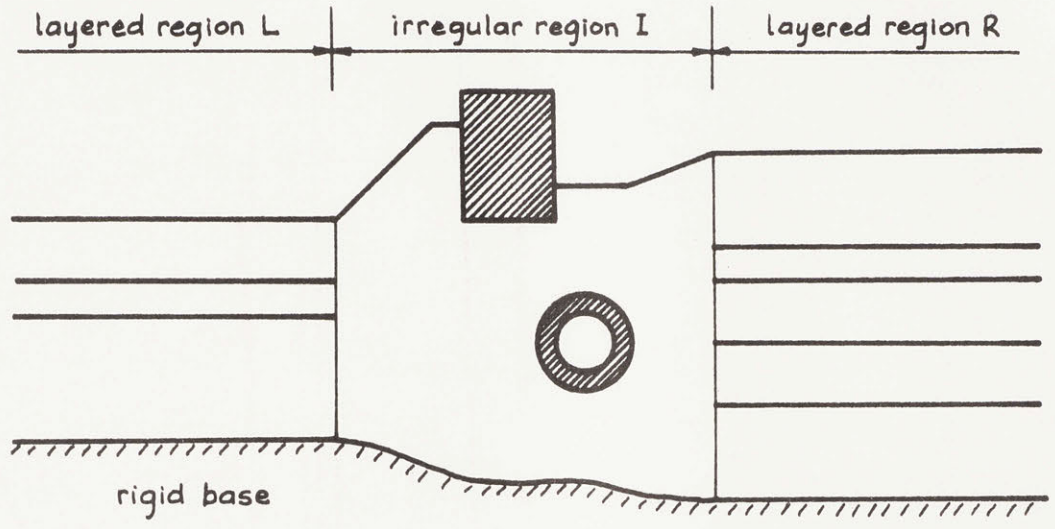
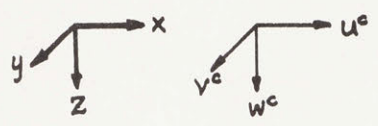


Figure 2-1a Typical Plane Stress System

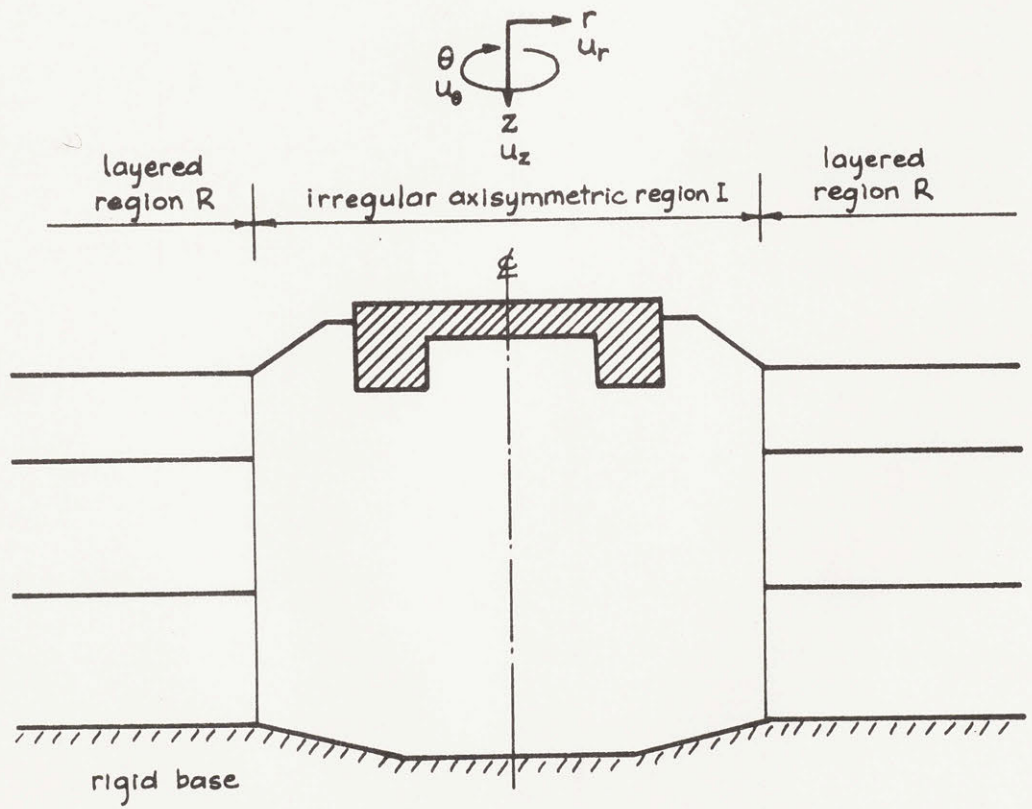


Figure 2-1b Typical Axisymmetric System

2.2 Soil Properties

The soil is represented by a homogeneous, isotropic and visco-elastic material. The stress-strain relationship of most soils subjected to symmetric cyclic loading conditions is of the form shown in Fig. 2-2. The hysteretic stress-strain behavior can be represented by the secant modulus, which is determined by the extreme points of the hysteresis loop, and by the damping capacity, which is proportional to the area inside the loop. These parameters depend on the magnitude of the strain except for very small strains, where the soil response is approximately linear. The modulus and damping factor used in analyses of foundation vibration problems are assumed, however, to be independent of the strain amplitude, leading to what is called a linear hysteretic model.

For loads varying harmonically in time, the stress-strain behavior of a linear hysteretic material can be represented by complex moduli. Then, if

$$\sigma^c = \sigma_1 + i\sigma_2 \quad (2.1)$$

$$\epsilon^c = \epsilon_1 + i\epsilon_2 \quad (2.2)$$

are, respectively, the complex stress and strain, and $i = \sqrt{-1}$ (the superscript c denotes a complex quantity, and will be dropped when no confusion might arise), the complex modulus relating stress and strain is generally frequency dependent. The moduli that characterize the soil are the complex Lamé's constants,

$$G^c = G_1(\omega) + i G_2(\omega) \quad (2.3)$$

$$\lambda^c = \lambda_1(\omega) + i \lambda_2(\omega) \quad (2.4)$$

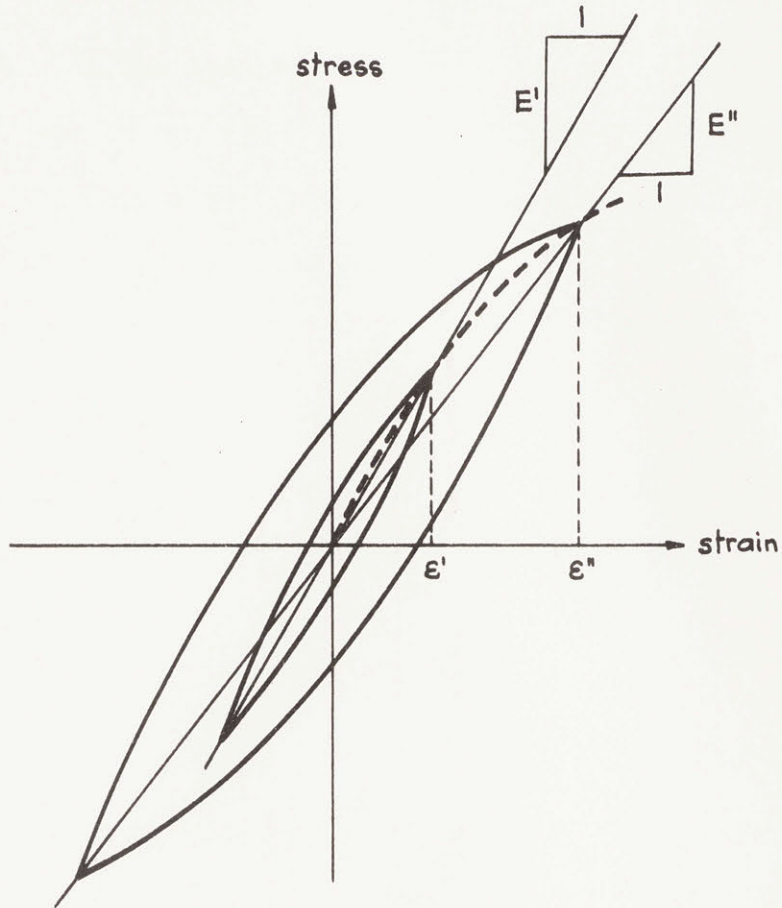


Figure 2-2a Hysteretic Stress-Strain Relationship at Different Strains

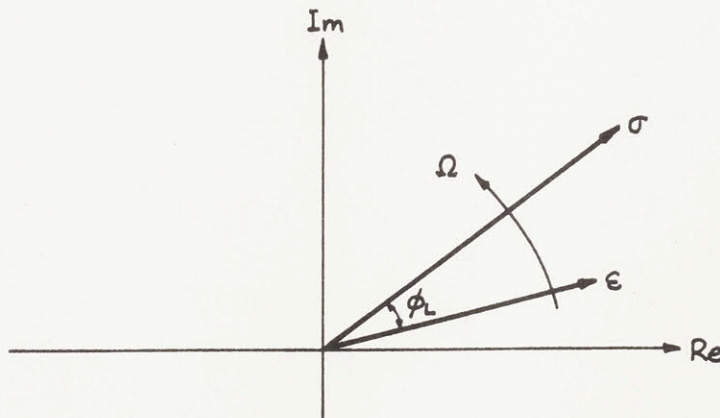


Figure 2-2b Representation of Stress and Strain in the Complex Plane

where ω is the circular frequency.

It is clearer to use the shear modulus G^C and the Poisson's ratio ν (taken as a real quantity) to represent the stress-strain behavior. The parameter λ^C is related to G^C and ν by

$$\lambda^C = \frac{2\nu G^C}{1-2\nu} \quad (2.5)$$

The imaginary part of the shear modulus is associated with an energy loss due to hysteretic damping. The ratio

$$\tan \phi_L = \frac{G_2}{G_1} \quad (2.6)$$

is called the "loss tangent." The loss angle, ϕ_L , is the angle (in terms of ωt , where t denotes time) by which the strain response lags behind the corresponding stress at any given time. The loss tangent is related to the fraction of critical damping, β , and to the logarithmic decrement, D , by

$$\tan \phi_L \approx 2\beta \approx \frac{D}{\pi} \quad (2.7)$$

for small damping, which is the usual case in foundation vibration problems. Thus, the complex shear modulus can be written as

$$G^C = G(1 + i2\beta) \quad (2.8)$$

The symbol G will be referred to simply as "shear modulus."

In wave propagation problems, the velocity of shear waves (S-waves, distortional or equivoluminal waves) and the velocity of dilatational waves (P-waves, compression or irrotational waves) are of great importance. They are:

$$C_s = \left[\operatorname{Re} \sqrt{\frac{\rho}{G^C}} \right]^{-1} \quad (2.9)$$

$$C_p = \left[\operatorname{Re} \sqrt{\frac{\rho}{\lambda^C + 2G^C}} \right]^{-1} \quad (2.10)$$

where ρ is the mass density of the soil. For small damping,

$$C_s \approx \operatorname{Re} \sqrt{\frac{G^C}{\rho}} = \sqrt{\frac{G}{\rho}} \quad (2.11)$$

$$C_p \approx \operatorname{Re} \sqrt{\frac{\lambda^C + 2G^C}{\rho}} \approx \sqrt{\frac{\lambda + 2G}{\rho}} \quad (2.12)$$

where $G = \operatorname{Re}(G^C)$ and $\lambda = \operatorname{Re}(\lambda^C)$. Both C_s and C_p vary with frequency, but are nearly constant for small damping.

2.3 Basic Equations.

As shown in Fig. 2.1, the displacements in the x , y , z directions are respectively u^C , v^C , w^C . For plane strain problems, all derivatives with respect to y vanish. When there are no external forces, the differential equations of motion are:

$$G^C \left(\frac{\partial^2 u^C}{\partial x^2} + \frac{\partial^2 u^C}{\partial z^2} \right) + (\lambda^C + G^C) \left(\frac{\partial^2 u^C}{\partial x^2} + \frac{\partial^2 w^C}{\partial x \partial z} \right) = \rho \frac{\partial^2 u^C}{\partial t^2} \quad (2.13a)$$

$$G^C \left(\frac{\partial^2 w^C}{\partial x^2} + \frac{\partial^2 w^C}{\partial z^2} \right) + (\lambda^C + G^C) \left(\frac{\partial^2 u^C}{\partial x \partial z} + \frac{\partial^2 w^C}{\partial z^2} \right) = \rho \frac{\partial^2 w^C}{\partial t^2} \quad (2.13b)$$

which are coupled equations governing motion in the x-z plane, and

$$G^C \left(\frac{\partial^2 v^C}{\partial x^2} + \frac{\partial^2 v^C}{\partial z^2} \right) = \rho \frac{\partial^2 v^C}{\partial t^2} \quad (2.13c)$$

governing motion in the y-direction.

For axisymmetric conditions, when all derivatives with respect to the angular direction θ vanish, the motion can be described by displacements u_r^C , u_z^C , u_θ^C corresponding to the coordinate directions r (radial), z (vertical), θ (angular) respectively. The equations of motion are:

$$\begin{aligned} (\lambda^C + 2G^C) \left(\frac{\partial^2 u_r^C}{\partial r^2} + \frac{1}{r} \frac{\partial u_r^C}{\partial r} - \frac{u_r^C}{r^2} + \frac{\partial^2 u_z^C}{\partial r \partial z} \right) + G^C \left(\frac{\partial^2 u_r^C}{\partial z^2} - \frac{\partial^2 u_z^C}{\partial r \partial z} \right) \\ = \rho \frac{\partial^2 u_r^C}{\partial t^2} \end{aligned} \quad (2.14a)$$

$$\begin{aligned} (\lambda^C + 2G^C) \left(\frac{\partial^2 u_r^C}{\partial r \partial z} + \frac{1}{r} \frac{\partial u_r^C}{\partial z} + \frac{\partial^2 u_r^C}{\partial z^2} \right) + G^C \left(\frac{\partial^2 u_z^C}{\partial r^2} + \frac{1}{r} \frac{\partial u_z^C}{\partial r} \right. \\ \left. - \frac{\partial^2 u_r^C}{\partial r \partial z} - \frac{1}{r} \frac{\partial u_r^C}{\partial r} \right) = \rho \frac{\partial^2 u_z^C}{\partial t^2} \end{aligned} \quad (2.14b)$$

which are coupled equations governing motion in the r-z plane, and

$$G \left(\frac{\partial^2 u_\theta^C}{\partial r^2} + \frac{1}{r} \frac{\partial u_\theta^C}{\partial r} - \frac{u_\theta^C}{r^2} + \frac{\partial^2 u_\theta^C}{\partial z^2} \right) = \rho \frac{\partial^2 u_\theta^C}{\partial t^2} \quad (2.14c)$$

The plane strain case is of main interest here. For harmonic excitation varying as $e^{i\Omega t}$, the steady state displacement response will also vary as $e^{i\Omega t}$. That is,

$$u^C = \hat{u}(x, z) e^{i\Omega t} \quad (2.15a)$$

$$w^C = \hat{w}(x, z) e^{i\Omega t} \quad (2.15b)$$

Assuming that

$$\hat{u}(x,z) = u(z) g(x) \quad (2.16a)$$

and

$$\hat{w}(x,z) = w(z) g(x) \quad (2.16b)$$

the displacements in the soil can be expressed as

$$u^c = u(z) \exp(i\Omega t - ikx) \quad (2.17a)$$

$$w^c = w(z) \exp(i\Omega t - ikx) \quad (2.17b)$$

since $g(x) = \exp(-ikx)$ is found after introducing eqs. (2.16a) and (2.16b) into eqs. (2.14a) and (2.14b). The parameter k is called the wave number, and is related to the circular frequency and the phase velocity, c , by

$$k^2 c^2 = \Omega^2 \quad (2.18)$$

This assumption considers then a plane wave travelling in the x -direction. Eqs. (2.17a) and (2.17b) define a plane generalized Rayleigh wave motion, since Rayleigh waves in layered media are described mathematically in the same way, but usually with real wave numbers. Here, k can be either real, imaginary or complex, and depends on the frequency of the wave; so, the medium is dispersive.

The mode shapes $u(z)$ and $w(z)$ are, in general, complex.

2.4 Mathematical Model

The mathematical model used in this study was developed by G. Waas [56]. Following is a summary of the basic features of this model, and then, an extension of it is presented.

Waas used the well-known finite element method to analyze plane

strain and axisymmetric vibration problems for footings resting on the surface of or embedded in a layered stratum of soil. Fig. 2-3 shows this model. It consists of an irregular region I subdivided into subregions which form the finite elements of arbitrary quadrilateral cross-sections. The displacements are assumed to vary linearly along the boundaries of the elements, which are themselves connected at the nodal joints. Each joint j has two degrees of freedom, u_j and w_j .

By using the principle of virtual work applied to viscoelastic media and specialized for harmonic motion, stiffness and mass matrices for the elements can be computed, and then assembled by the direct stiffness method [62] to get a complex stiffness matrix $[K]$ and a real mass matrix $[M]$.

Since loads vary harmonically with time at a circular frequency Ω , the equations of motion are:

$$([K] - \Omega^2 [M])\{u\} = \{b\} \quad (2.19)$$

where $\{u\}$ is the vector containing the nodal displacements, and $\{b\}$ is the vector of nodal forces.

Attached to the irregular region I, there are two layered regions R and L, to the right and left, respectively. They must be considered in the stiffness and mass matrices of eq. (2.19). The displacements in the layered region are considered to vary linearly within each layer along the z -direction, and exponentially in the x -direction, according to eqs. (2.17a) and (2.17b). The details of the derivation of the corresponding matrices are shown in Waas' thesis.

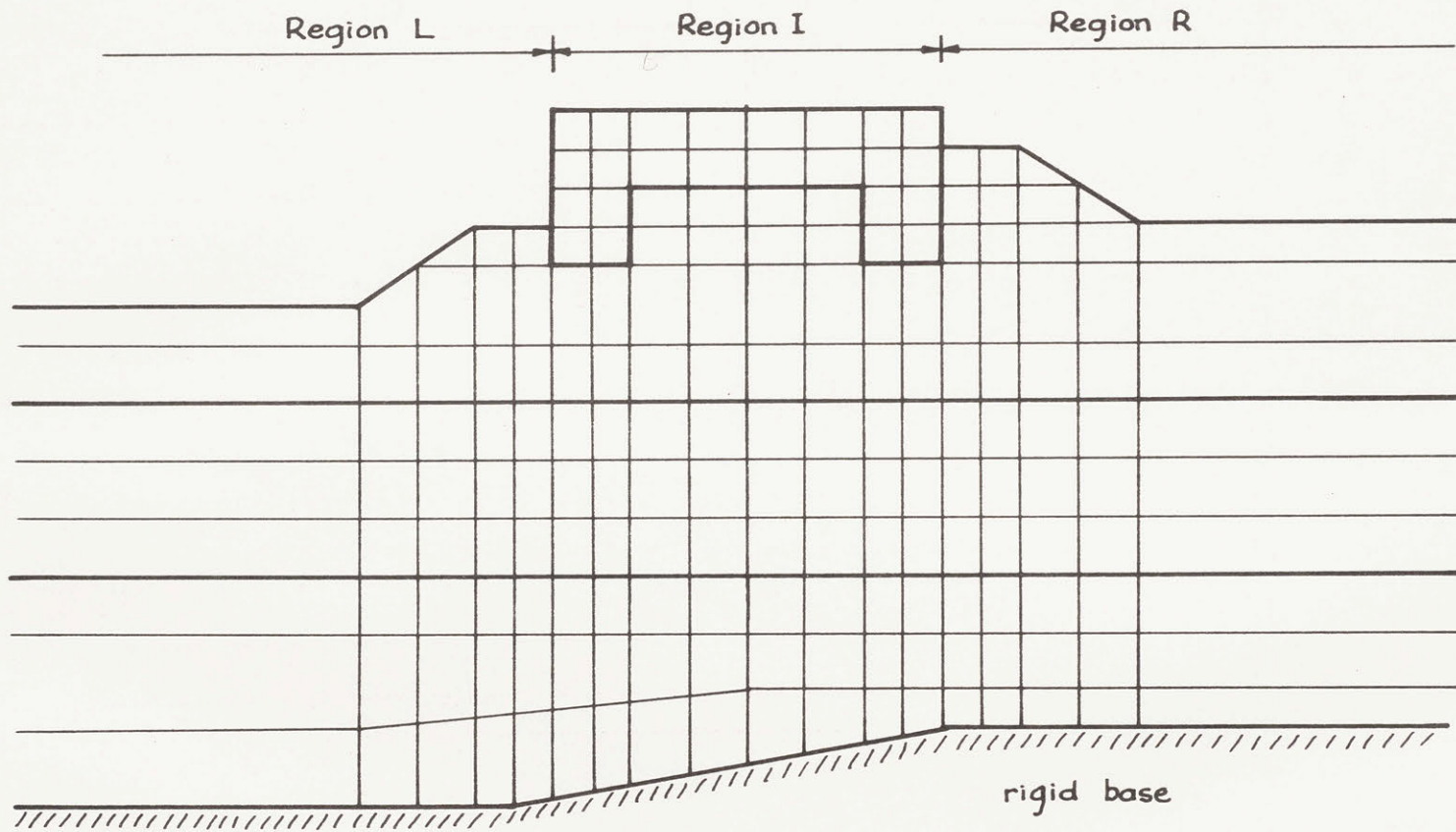


Figure 2-3 Typical Modelling of Plane Strain System

For free harmonic Rayleigh wave motion under plane strain conditions, the result is a set of equations of the form

$$(k^2[A] - ik[D] + ik[D]^T + [G] - \Omega^2 [M]) \{v\} = \{0\} \quad (2.20)$$

where the vector $\{v\}$ contains $2n$ complex displacements v_j , $j=1, \dots, 2n$ for the n layers, each having two degrees of freedom u_j and w_j . The $2n \times 2n$ matrices $[A]$, $[D]$, $[G]$ and $[M]$ consist of the contributions from the individual layers, and can therefore be assembled by addition of layer submatrices as indicated in Fig. 2-4. The submatrices to be substituted for $[x_j]$ in that figure are:

$$[A]_j = \frac{1}{6} h_j \begin{bmatrix} 2(2G_j + \lambda_j) & 0 & (2G_j + \lambda_j) & 0 \\ 0 & 2G_j & 0 & G_j \\ (2G_j + \lambda_j) & 0 & 2(2G_j + \lambda_j) & 0 \\ 0 & G_j & 0 & 2G_j \end{bmatrix} \quad (2.21a)$$

$$[D]_j = \frac{1}{2} \begin{bmatrix} 0 & \lambda_j & 0 & -\lambda_j \\ G_j & 0 & -G_j & 0 \\ 0 & \lambda_j & 0 & -\lambda_j \\ G_j & 0 & -G_j & 0 \end{bmatrix} \quad (2.21b)$$

$$[G]_j = \frac{1}{h_j} \begin{bmatrix} G_j & 0 & -G_j & 0 \\ 0 & (2G_j + \lambda_j) & 0 & -(2G_j + \lambda_j) \\ -G_j & 0 & G_j & 0 \\ 0 & -(2G_j + \lambda_j) & 0 & (2G_j + \lambda_j) \end{bmatrix} \quad (2.21c)$$

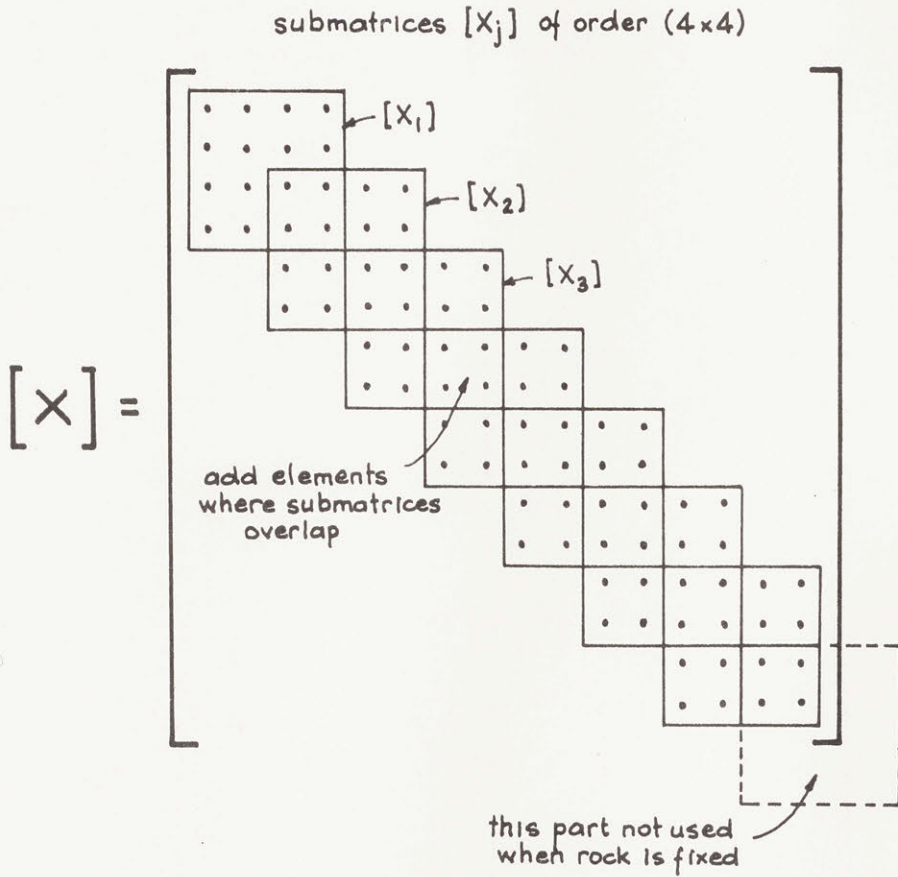


Figure 2-4 Form of Matrices in Eq. (2.20)

$$[M]_j = \rho_j h_j \begin{bmatrix} 1/3 & 0 & 1/6 & 0 \\ 0 & 1/3 & 0 & 1/6 \\ 1/6 & 0 & 1/3 & 0 \\ 0 & 1/6 & 0 & 1/3 \end{bmatrix} \quad (2.21d)$$

where $j = 1, \dots, n$; and h_j is the thickness of the j^{th} layer, ρ_j its mass density, and G_j and λ_j its complex Lamé's constants, which reduce to real values in the undamped case.

The matrices $[A]$, $[D]$ and $[G]$ are related to the stiffness of the layers, and the matrix $[M]$ is a consistent mass matrix.

The solutions to eq. (2.20) satisfy equilibrium in the layered region between the vertical planes $\hat{x} = 0$ at the right (or left) boundary of the finite element region, and $\hat{x} = \xi$, where ξ is arbitrary, and can then be taken as infinitely large.

For any given circular frequency Ω , let

$$[C] = [G] - \Omega^2 [M] \quad (2.22a)$$

and

$$[B] = [D]^T - [D] \quad (2.22b)$$

Introducing these into eq. (2.20),

$$([A]k^2 + i[B]k + [C]) \{v\} = \{0\} \quad (2.23)$$

is obtained. The matrices $[A]$ and $[C]$ are symmetric and the matrix $[B]$ is skew symmetric. Eq. (2.23) constitutes a set of $2n$ linear homogeneous equations which have non-trivial solutions only if the determinant of the coefficient matrix vanishes. Hence, for any given frequency Ω , the secular equation

$$|[A] k^2 + i[B] k + [C]| = 0 \quad (2.24)$$

defines the possible wave members for generalized Rayleigh waves in the layered region. Eq. (2.23) is thus an eigenvalue problem which has $4n$ generally complex roots k_s , $s = 1, \dots, 4n$. The corresponding eigenvectors $\{v\}_s$ are the mode shapes.

Each eigenvalue k_s and its corresponding eigenvector $\{v\}_s$ define a Rayleigh wave mode which can exist in the layered region and has the displacements $\{\delta\}_s$ given by

$$\{\delta\}_s = \alpha_s \{v\}_s \cdot \exp(i\omega t - ik_s x) \quad (2.25)$$

where α_s is the participation factor for the s^{th} mode. If

$$\{\tilde{v}\}^T = \langle -v_1 \ v_2 \ -v_3 \ v_4 \ \dots \ -v_{2n-1} \ v_{2n} \rangle \quad (2.26)$$

is the "adjoined" of $\{v\}$, obtained by changing the sign on all horizontal displacements (odd elements) in $\{v\}$, and \bar{k} , $\{\bar{v}\}$ and $\{\bar{\tilde{v}}\}$ are the complex conjugates of k , $\{v\}$ and $\{\tilde{v}\}$, respectively; then the eigenvalue problem, eq. (2.23) has the property that if

(a) k with $\{v\}$

is a solution, then

(b) $-k$ with $\{\tilde{v}\}$

is another solution, and, in the undamped case,

(c) \bar{k} with $\{\bar{\tilde{v}}\}$ and

(d) $-\bar{k}$ with $\{\bar{v}\}$

are also solutions.

These solutions are linearly independent with the exception that the solutions (c) and (d) depend on (a) and (b) if k is purely real or purely imaginary. The eigenvectors are orthonormal in the sense that they satisfy the matrix equation

$$[K][\tilde{V}]^T[A][V][K] - [\tilde{V}]^T[C][V] = 2 [K]^2 \quad (2.27)$$

in which $[K]$ is a $2n \times 2n$ diagonal matrix containing one of each of the eigenvalues $\pm k_s$, $s=1, \dots, 2n$, and $[V]$ and $[\tilde{V}]$ are $2n \times 2n$ modal matrices containing the corresponding mode shapes $\{v_s\}$ and $\{\tilde{v}_s\}$, $s=1, \dots, 2n$, columnwise. So, the eigenvectors are orthogonal for $k_r \neq k_s$; and the case of $k_r = k_s$ is used to normalize them.

However, since the motion is generated by external forces acting in the irregular region, and the layered regions R and L are open in the positive x -direction and negative x -direction, respectively (see Fig. 2-1), energy considerations dictate that the transmission of energy must be positive—that is, away from the source—so that energy density does not increase with distance. Then, from the $4n$ solutions, only $2n$ wave numbers k_s must be selected, which are those which decay or propagate energy away.

Then, a dynamic stiffness matrix for the infinite layered region R can be found, given by

$$[R] = i[A][V][K][V]^{-1} + [D] \quad (2.28)$$

where $[A]$ and $[D]$ are determined from eqs. (2.21a) and [2.21b]. Matrix $[R]$ relates the modal forces at the boundary of the finite element region with the layered region R, with the corresponding nodal displace-

ments. This matrix is symmetric, according to the dynamic reciprocal theorem [12].

The dynamic stiffness matrix $[L]$ for the left layered region L may be computed as in eq. (2.28) just by changing the sign of all coefficients that relate horizontal forces to vertical displacements or vertical forces to horizontal displacements.

These matrices $[R]$ and $[L]$ are added to the matrices in eq. (2.19) and the system of equations is solved, giving as solution the displacements $\{u\}$. Representing by $\{u\}^R$ the displacements in the boundary nodes, the mode participation factors $\{\alpha\}$ to be used in eq. (2.25) are given by

$$\{\alpha\} = [V]^{-1} \{u\}^R \quad (2.29)$$

The analysis of axisymmetric Rayleigh wave motion in a layered system is similar to that for plane Rayleigh wave motion described above. This analysis leads to the determination of the pertinent dynamic stiffness matrix $[R]$ for the layered region R around the finite element region I , as

$$[R] = r_0 (i[A][\psi][K][\phi]^{-1} + [D] + [E]) \quad (2.30)$$

where r_0 is the radius of the region I . Matrices $[A]$ and $[D]$ have already been defined. The matrix $[\phi]$ contains the vectors $\{\phi\}_s$, $s=1, \dots, 2n$ columnwise, which in turn are found from the eigenvalues k_s and eigenvectors $\{v\}_s$ as in eq. (2.23). The elements of $\{\phi\}_s$ are

$$\phi_j^s = v_j^s a_s \quad j = 1, 3, \dots, 2n-1 \quad (2.31a)$$

$$\text{and } \phi_j^S = v_j^S b_S \quad j = 2, 4, \dots, 2n \quad (2.31b)$$

$$\text{with } a_S = H_1^{(2)}(k_S r_0) \quad \text{and} \quad b_S = i H_0^{(2)}(k_S r_0) \quad (2.31c)$$

where odd values of j refer to radial displacements and even values to vertical displacements. The matrix $[\psi]$ consists of the column vectors $\{\psi\}_S$, $s = 1, \dots, 2n$, which have the elements

$$\psi_S = v_j^S a_S \quad j = 2, 4, \dots, 2n \quad (2.32a)$$

$$\text{and } \psi_S = v_j^S a_S \quad j = 2, 4, \dots, 2n \quad (2.32b)$$

The functions $H_0^{(2)}$ and $H_1^{(2)}$ are the Hankel functions of order zero and one of the second kind, respectively.

The matrix $[E]$ is assembled from matrices $[E]_j$, $j = 1, \dots, n$ given by

$$[E]_j = \frac{1}{3} \frac{G_j}{r_0} \begin{bmatrix} 2 & 0 & 1 & 0 \\ 0 & 0 & 0 & 0 \\ 1 & 0 & 2 & 0 \\ 0 & 0 & 0 & 0 \end{bmatrix} \quad (2.33)$$

as shown on Fig. 2-4, by substituting $[X]_j$ by $[E]_j$.

Matrix $[R]$ is symmetric, and relates the nodal forces per radian to the simultaneous nodal displacements at the boundary $r = r_0$.

The equations and the procedure described above for both plane and axisymmetric Rayleigh wave motion were developed and programmed by G. Wass [56]. The result is a program called PLAXLY (University of California at Berkeley, June 1972) written originally for a CDC 6400

computer. Since then, PLAXLY was revised to run in an IBM 370 and extended to include rock motion, either horizontal or vertical for the plane strain case, and only vertical for the axisymmetric case. This originated the PLAXLY2. A Users' Manual is provided in the Appendix.

2.5 Rock Motion

The determination of the transfer functions of the soil due to harmonic base motion (at the rock level) is of importance for earthquake studies. These functions can be found by prescribing either a horizontal or vertical displacement, harmonically varying with time, at the bottom boundary of the soil stratum. Then, the resulting motion at a point of the structure resting on the soil, or the displacements at any point of it can be determined. Of particular interest are the free-field displacements at the surface of the stratum and the motion of the base of the structure, the latter defined by the horizontal and vertical displacements at its bottom and the rocking about an axis perpendicular to the x-z plane.

The inclusion of rock motion is described below, first for the plane strain case, and then for the axisymmetric case, which has as limitation the analysis of vertical motion only.

(i) One-dimensional amplification.

This will be referred to as 1-D amplification. This simple theory considers a horizontally layered soil, extending to infinity at both left and right. Its motion can then be analyzed from a vertical slice of the stratum. This method is well understood [48] and will be de-

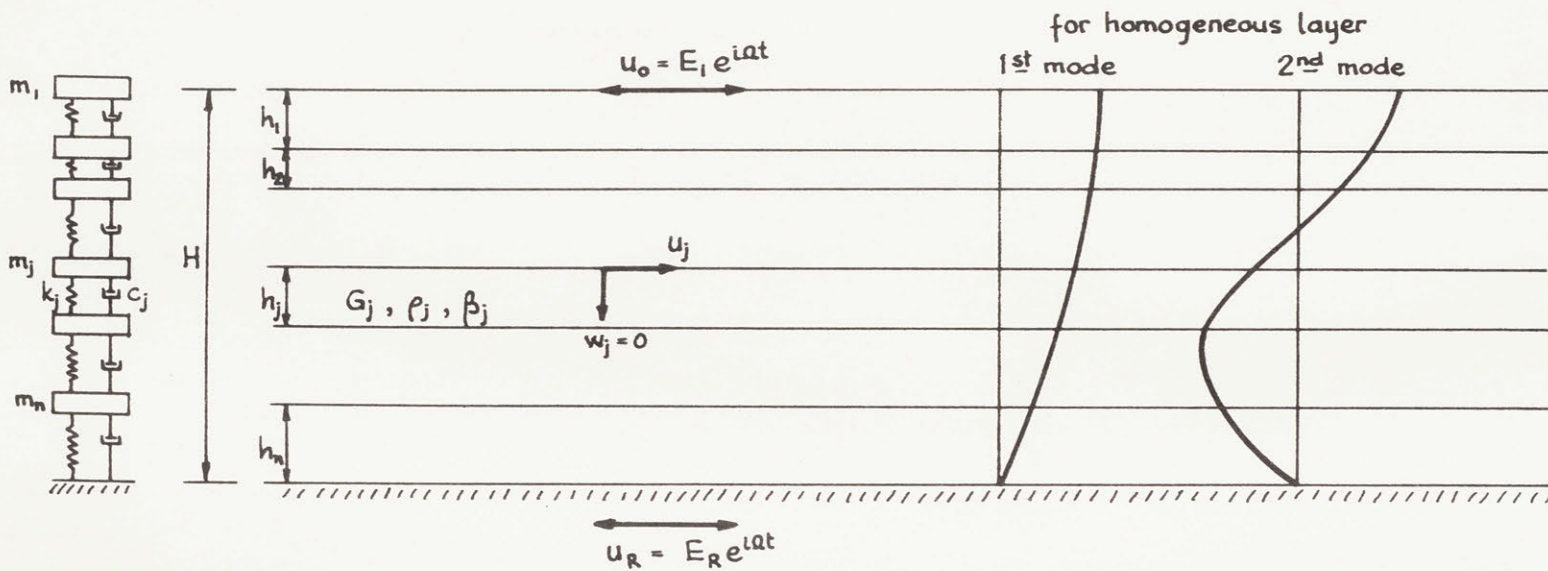


Figure 2-5 Discretization for 1-D Amplification

scribed only briefly. Refer to Fig. 2-5.

Let u_R be the motion at the rock, $z = H$; and

$\bar{u} = u(0) - u_R$ be the relative displacement of the soil.

The differential equation of motion for a one-layered system is

$$\rho \frac{\partial^2 \bar{u}}{\partial t^2} = G \frac{\partial^2 \bar{u}}{\partial z^2} + \eta \frac{\partial^3 \bar{u}}{\partial x^2 \partial t} - \rho \frac{\partial^2 u_R}{\partial t^2} \quad (2.34)$$

where

ρ = mass density

G = shear modulus

η = coefficient of viscosity

If the base motion is harmonic,

$$\ddot{u}_R = C e^{i\Omega t} \quad (2.35)$$

the steady state solution is of the form

$$\bar{u} = U(z) e^{i\Omega t} \quad (2.36)$$

Now, letting

$$p^2 = \frac{\rho \Omega^2}{G + i\eta \Omega} \quad (2.37)$$

and applying the boundary conditions

$$U(H) = 0, \quad U'(0) = 0 \quad (2.38)$$

where H is the thickness of the layer, the amplification function

$A(\Omega)$ is obtained as

$$A(\Omega) = \frac{\ddot{u}(0)}{\ddot{u}_R} = \frac{u(0)}{u_R} = \frac{1}{\cos pH} \quad (2.39)$$

Calling

$$\bar{c}_1 = \frac{1}{\sqrt{2}} H\Omega \sqrt{\frac{\rho}{G}} \sqrt{\frac{\sqrt{1 + (\eta\Omega/G)^2} + 1}{1 + (\eta\Omega/G)^2}} \quad (2.40a)$$

$$\bar{c}_2 = \frac{1}{\sqrt{2}} H\Omega \sqrt{\frac{\rho}{G}} \sqrt{\frac{\sqrt{1 + (\eta\Omega/G)^2} - 1}{1 + (\eta\Omega/G)^2}} \quad (2.40b)$$

the amplification function can be written as

$$|A(\Omega)| = \frac{1}{\sqrt{\cos^2 \bar{c}_1 \cosh^2 \bar{c}_2 + \sin^2 \bar{c}_1 \sinh^2 \bar{c}_2}} \quad (2.41)$$

If there is no viscosity, i.e., $\eta = 0$,

$$A(\Omega) = \frac{1}{\cos \bar{c}_2} \quad (2.42)$$

and $A(\Omega) = \infty$ if $\cos \bar{c}_2 = 0$, which implies

$$\Omega = \frac{(2n-1)\pi}{2H} \sqrt{\frac{G}{\rho}} = \omega_n \quad (2.43)$$

the n^{th} natural frequency of the layer.

The critical value of the viscosity, above which no harmonic motion can occur, is given by

$$\eta_{\text{crit}} = \frac{4H}{\pi} \sqrt{G\rho} \quad (2.44)$$

Consider the case when the viscosity is inversely proportional to the frequency (hysteretic damping), that is

$$\tan \delta = \frac{\eta\Omega}{G} = \text{constant} \quad (2.45)$$

and small. Then, the amplification at $\Omega = \omega_n$ will be

$$|A(\omega_n)| = \frac{4}{(2n-1)\pi \tan \delta} \quad (2.46)$$

In this case,

$$\tan \delta = 2 \frac{\eta \Omega}{(\eta \omega)_{\text{crit}}} = 2\beta \quad (2.47)$$

giving

$$|A(\omega_n)| = \frac{4}{(2n-1)\pi \cdot 2\beta} \quad (2.48)$$

which implies that the successive peaks are in the relation 1, 1/3, 1/5

For this case of considering a constant percentage of (hysteretic) damping β at all frequencies, the maximum amplification occurs when

$$c_1 \sin 2 c_1 a = c_2 \sinh 2 c_2 a \quad (2.49)$$

where

$$c_1 = \frac{1}{\sqrt{2}} \sqrt{\frac{\sqrt{1 + 4\beta^2} + 1}{1 + 4\beta^2}} \quad (2.50a)$$

$$c_2 = \frac{1}{\sqrt{2}} \sqrt{\frac{\sqrt{1 + 4\beta^2} - 1}{1 + 4\beta^2}} \quad (2.50b)$$

$$a = \Omega H \sqrt{\frac{\rho}{G}} = \frac{\Omega H}{C_s} \quad (2.51)$$

giving, for the value of a which satisfies eq. (2.49),

$$A_{\text{max}} = \frac{1}{\sqrt{\cos^2 c_1 a \cdot \cosh^2 c_2 a + \sin^2 c_1 a \cdot \sinh^2 c_2 a}} \quad (2.52)$$

It is worthwhile to note that, when $\beta > 0$, the maximum amplification A_{\max} is finite, and occurs at a value $a > \pi/2$. The value $a = \pi/2$ corresponds to infinite amplification in the undamped case, for the first natural frequency.

A multi-layered medium can be considered as a discrete closed-coupled model of masses, springs and dashpots, as shown in Fig. 2-6, where

$$M_1 = \frac{1}{2} \rho_1 h_1 \quad (2.53a)$$

$$M_j = \frac{1}{2} (\rho_{j-1} h_{j-1} + \rho_j h_j), \quad j = 2, \dots, n \quad (2.53b)$$

$$K_j = \frac{G_j}{h_j} \quad (2.53c)$$

$$C_j = \frac{\eta_j}{h_j} \quad (2.53d)$$

Considering a harmonic base motion,

$$u_R = E_R e^{i\Omega t}, \quad \dot{u}_R = i\Omega E_R e^{i\Omega t}, \quad \ddot{u}_R = -\Omega^2 E_R e^{i\Omega t} \quad (2.54)$$

the steady state solution, assuming that all the masses are vibrating with the same frequency Ω is, for the j^{th} layer,

$$u_j = E_j e^{i\Omega t}, \quad \dot{u}_j = i\Omega E_j e^{i\Omega t}, \quad \ddot{u}_j = -\Omega^2 E_j e^{i\Omega t} \quad (2.55)$$

and noting that

$$\begin{aligned} K_j + i\Omega C_j &= \frac{1}{h_j} (G_j + i\Omega\eta) \\ &= \frac{1}{h_j} (1 + i2\beta_j) \\ &= \frac{1}{h_j} G_j^C \end{aligned} \quad (2.56)$$

where G_j^C is the complex shear modulus of layer j , $j = 1, \dots, n$, the dynamic equations of motion can be written as

with

$$[G]_j = \frac{1}{h_j} \begin{bmatrix} G_j^C & -G_j^C \\ -G_j^C & G_j^C \end{bmatrix} \quad (2.61a)$$

$$[M]_j = \rho_j h_j \begin{bmatrix} 1/3 & 1/6 \\ 1/6 & 1/3 \end{bmatrix} \quad (2.61b)$$

$j = 1, \dots, n$, where n is the number of layers, and

$$p_n = \left(\frac{G_n^C}{h_n} + \frac{1}{6} \Omega^2 h_n \rho_n \right) u_R \quad (2.62)$$

is known.

For vertical motion caused by a harmonic vertical prescribed displacement w_R at the rock, the analysis is essentially the same as above, the only difference being the use of $(2G_j^C + \lambda_j^C)$ instead of G_j^C in the preceding equations, and that

$$p_n = \left(\frac{2G_n^C + \lambda_n^C}{h_n} + \frac{1}{6} \Omega^2 h_n \rho_n \right) w_R \quad (2.63)$$

is used in eq. (2.59)

(ii) The problem of including base motion in the system shown in Fig. 2-6 can be formulated as follows:

— differential equations:

$$L_x(u,w) = 0 \quad , \quad L_z(u,w) = 0 \quad (2.64)$$

— boundary conditions:

$$u(x,H) = u_R \quad , \quad w(x,H) = w_R \quad (2.65a)$$

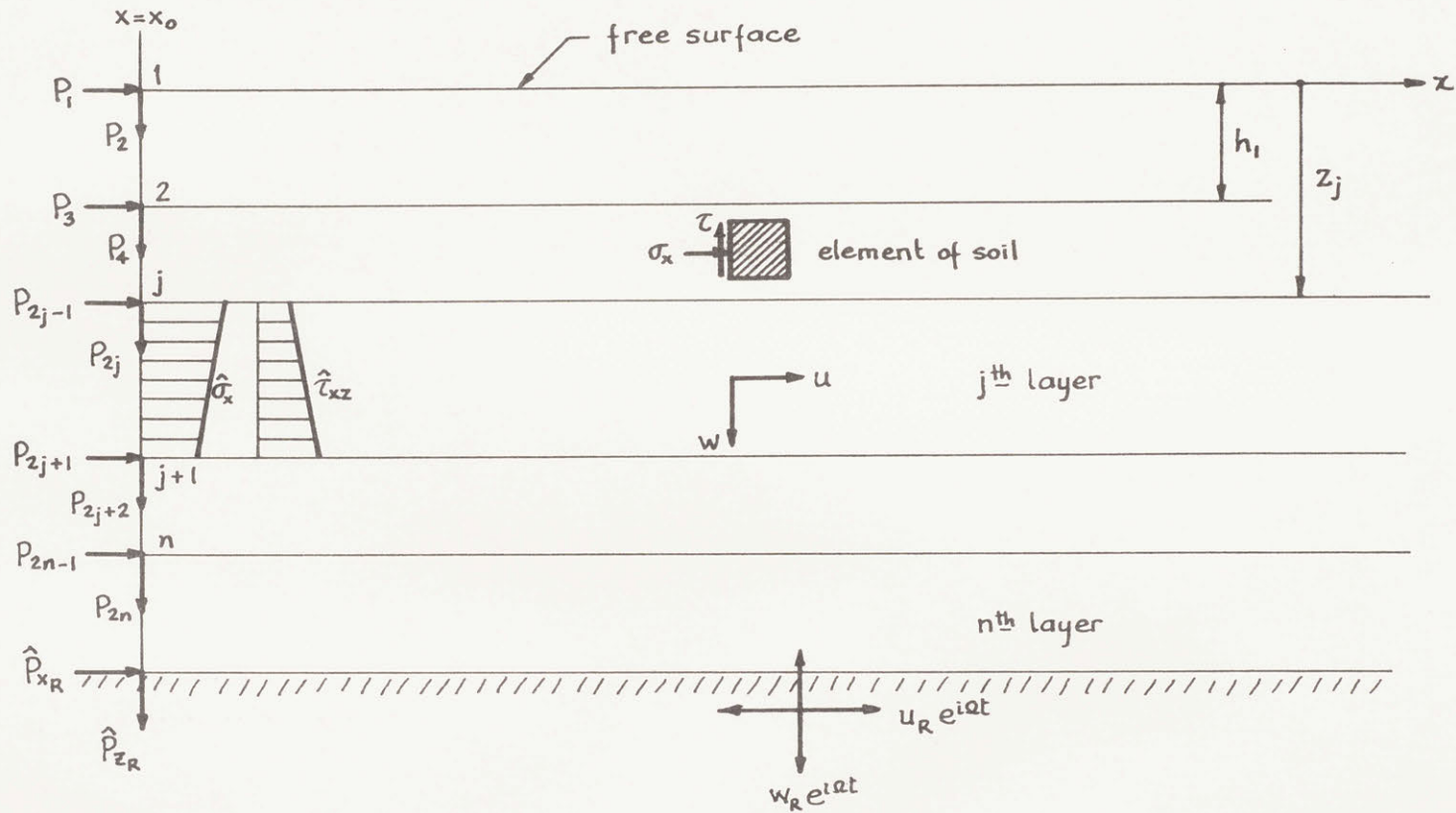


Figure 2-6 Forces Acting at Boundaries for Motion at Bedrock

$$\sigma_z(x,0) = 0 \quad , \quad \tau_{xz}(x,0) = 0 \quad , \quad x > x_0 \quad (2.65b)$$

$$u(x_0,z) = f(z) \quad , \quad w(x_0,z) = g(z) \quad (2.65c)$$

where $x = x_0$ corresponds to the boundary between the finite element region and the layered system; and σ_z and τ_{xz} are the vertical normal stress and shear stress, respectively. The derivations will be made for the right layers.

This problem can be split in two parts, as follows:

A. Consider the homogeneous boundary conditions, with solution $(u,w) = (\tilde{u}, \tilde{w})$. Then

$$L_x(\tilde{u}, \tilde{w}) = 0 \quad , \quad L_z(\tilde{u}, \tilde{w}) = 0 \quad (2.66)$$

$$\tilde{u}(x,H) = 0 \quad , \quad \tilde{w}(x,H) = 0 \quad (2.67a)$$

$$\tilde{\sigma}_z(x,0) = 0 \quad , \quad \tilde{\tau}_{xz}(x,0) = 0 \quad , \quad x > x_0 \quad (2.67b)$$

$$\tilde{u}(x_0,z) = \tilde{f}(z) \quad , \quad \tilde{w}(x_0,z) = \tilde{g}(z) \quad (2.67c)$$

These partial displacements \tilde{u} and \tilde{w} can be written as linear combinations of modal shapes \tilde{u}_j and \tilde{w}_j , $j = 1, \dots, n$, respectively,

$$\tilde{u}(x,z) = \sum \alpha_j \tilde{u}_j(x,z) \quad (2.68a)$$

$$\tilde{w}(x,z) = \sum \alpha_j \tilde{w}_j(x,z) \quad (2.68b)$$

where

$$\tilde{u}(x_0,z) = \sum \alpha_j \tilde{u}_j(x_0,z) = \tilde{f}(z) \quad (2.69a)$$

$$\tilde{w}(x_0,z) = \sum \alpha_j \tilde{w}_j(x_0,z) = \tilde{g}(z) \quad (2.69b)$$

B. Now, take the actual boundary conditions, and obtain a particular solution $(u,w) = (\hat{u}, \hat{w})$,

$$L_x(\hat{u}, \hat{w}) = 0 \quad , \quad L_z(\hat{u}, \hat{w}) = 0 \quad (2.70)$$

$$\hat{u}(x, H) = u_R \quad , \quad \hat{w}(x, H) = w_R \quad (2.71a)$$

$$\hat{\sigma}_z(x, 0) = 0 \quad , \quad \hat{\tau}_{xz}(x, 0) = 0 \quad , \quad x > x_0 \quad (2.71b)$$

$$\hat{u}(x_0, z) = \hat{f}(z) \quad , \quad \hat{w}(x_0, z) = \hat{g}(z) \quad (2.71c)$$

and then

$$\hat{u}(x, z) = \hat{u}(z) = \hat{f}(z) \quad (2.72a)$$

$$\hat{w}(x, z) = \hat{w}(z) = \hat{g}(z) \quad (2.72b)$$

satisfy eqs. (2.70) and (2.71a) through (2.71c), where $\hat{f}(z)$ and $\hat{g}(z)$ are the displacements caused at $x \geq x_0$ due to the base motion as in the 1-D theory.

Superimposing solutions (A) and (B),

$$u = \tilde{u} + \hat{u} \quad , \quad w = \tilde{w} + \hat{w} \quad (2.73)$$

$$f = \tilde{f} + \hat{f} \quad , \quad g = \tilde{g} + \hat{g} \quad (2.74)$$

eqs. (2.64) and (2.65a) through (2.65c) are satisfied.

Therefore, for $x \geq x_0$,

$$u = u(x, z) = \sum \alpha_j \tilde{u}(x, z) + \hat{u}(z) \quad (2.75a)$$

$$w = w(x, z) = \sum \alpha_j \tilde{w}(x, z) + \hat{w}(z) \quad (2.75b)$$

The participation factors α_j , $j = 1, \dots, 2n$ are found from eq. (2.29), where $\{u\}^R$ is the vector representing $\tilde{u}(x_0, z)$ and $\tilde{w}(x_0, z)$.

The boundary nodal forces at $x = x_0$ acting on the right layered system are given by

$$\{\tilde{P}\} = [R] \{\tilde{\delta}\} \quad (2.76)$$

for displacements \tilde{u} and \tilde{w} , where the matrix $[R]$ is found from eq. (2.28), and

$$\{\tilde{\delta}\}^T = \langle \tilde{u}_1 \tilde{w}_1 \tilde{u}_2 \tilde{w}_2 \dots \tilde{u}_n \tilde{w}_n \rangle \quad (2.77)$$

where n is the number of right layers. And for the displacements \hat{u} and \hat{w} , these forces are

$$\{\hat{P}\} = [T]\{\hat{\delta}\} \quad (2.78)$$

where the matrix $[T]$ is of order $2n \times (2n + 2)$, which will be determined by eq. (2.83), and the vector $\{\hat{\delta}\}$ is

$$\{\hat{\delta}\}^T = \langle \hat{u}_1 \hat{w}_1 \hat{u}_2 \hat{w}_2 \dots \hat{u}_{n+1} \hat{w}_{n+1} \rangle \quad (2.79)$$

has $(2n + 2)$ displacement components. The vector $\{\hat{P}\}$ is the force vector which has to be applied on the layered region at $x = x_0$ to preserve the one-dimensional motion. The elements \hat{u}_{n+1} and \hat{w}_{n+1} are clearly the prescribed horizontal and vertical displacements at the rock level, respectively.

The forces $\{\hat{P}\}$ must be statically equivalent to the stresses at $x = x_0$; the stresses are obtained from the strains at that boundary, which in turn are obtained from the displacements,

$$\hat{\epsilon}_x = \frac{\partial \hat{u}}{\partial x} = 0 \quad (2.80a)$$

$$\hat{\epsilon}_z = \frac{1}{h_j} (\hat{w}_{j+1} - \hat{w}_j) \quad (2.80b)$$

$$\hat{\gamma}_{xz} = \frac{1}{h_j} (\hat{u}_{j+1} - \hat{u}_j) \quad (2.80c)$$

$$\hat{\sigma}_x = \lambda_j \hat{\epsilon}_z = \frac{\lambda_j}{h_j} (\hat{w}_{j+1} - \hat{w}_j) \quad (2.81a)$$

$$\hat{\tau}_{xz} = G_j \hat{\gamma}_{xz} = \frac{G_j}{h_j} (\hat{u}_{j+1} - \hat{u}_j) \quad (2.81b)$$

for the j^{th} layer. Therefore

$$\begin{Bmatrix} \hat{p}_{2j-1} \\ \hat{p}_{2j} \\ \hat{p}_{2j+1} \\ \hat{p}_{2j+2} \end{Bmatrix} = \frac{1}{2} \begin{bmatrix} 0 & -\lambda_j & 0 & \lambda_j \\ -G_j & 0 & G_j & 0 \\ 0 & -\lambda_j & 0 & \lambda_j \\ -G_j & 0 & G_j & 0 \end{bmatrix} \begin{Bmatrix} \hat{v}_{2j-1} \\ \hat{v}_{2j} \\ \hat{v}_{2j+1} \\ \hat{v}_{2j+2} \end{Bmatrix} \quad (2.82)$$

and, after assembling the n submatrices, it is found that

$$\{\hat{p}\} = [D; D_R] \{\hat{\delta}\} = [T] \{\hat{\delta}\} \quad (2.83)$$

where the submatrix $[D]$ is determined from eq. (2.21b), and the submatrix $[D_R]$ relates the displacements and forces at the rock level.

Considering now the finite element region I, where external forces $\{P\}_I$ may be acting, the equations of equilibrium are

$$([K] - \Omega^2 [M])\{\delta\} = \{P\}_I - \{P\}_R \quad (2.84)$$

where

$$\begin{aligned} \{P\}_R &= \{\tilde{p}\} + \{\hat{p}\} \\ &= [R]\{\tilde{\delta}\} + [T]\{\hat{\delta}\} \end{aligned} \quad (2.85)$$

with the convention that the forces $\{P\}_R$ are put in the proper position according to the $2m$ -element vector $\{\delta\}$, where n is the number of nodes in the finite element region, and that the matrix $[R]$ and the displacement vectors $\{\tilde{\delta}\}$ and $\{\hat{\delta}\}$ are extended to order $2m$ by filling with zero elements the positions not corresponding to the boundary. So,

$$\{P\}_R = [R] \{\delta\} - [R] \{\hat{\delta}\} + [T] \{\hat{\delta}\} \quad (2.86)$$

$$([K] - \Omega^2 [M] + [R]) \{\delta\} = \{P\}_I + [R] \{\hat{\delta}\} - [T] \{\hat{\delta}\} \quad (2.87)$$

Eq. (2.87) then gives the desired equations of equilibrium if only the right layer system exists, with equivalent forces given by

$$\begin{aligned} \{P\} &= \{P\}_I + ([R] - [T]) \{\hat{\delta}\} \\ &= \{P\}_I + ([R] - [D \mid D_R]) \{\hat{\delta}\} \end{aligned} \quad (2.88)$$

where it must be remembered that the elements of the matrices and vectors have to be positioned properly. The vector $\{\hat{\delta}\}$ is clearly the solution of eq. (2.59) of the 1-D theory.

For the left layered system, due to the antisymmetry of signs, the boundary forces are

$$\{P\}_L = [L] \{\delta\} - ([L] + [D \mid D_L]) \{\hat{\delta}\} \quad (2.89)$$

where matrices $[L]$, $[D]$ and $[D_L]$ have a similar meaning as above.

Adding the two layered systems, a complete set of equations of equilibrium is obtained as

$$\begin{aligned} &([K] - \Omega^2 [M] + [R] + [L]) \{\delta\} \\ &= \{P\}_I + ([L] + [D \mid D_L]) \{\hat{\delta}\}_L + ([R] - [D \mid D_R]) \{\hat{\delta}\}_R \end{aligned} \quad (2.90)$$

where $\{\hat{\delta}\}_L$ and $\{\hat{\delta}\}_R$ are the 1-D solutions for left and right layered regions, respectively.

(iii) For the axisymmetric case, with boundary of the layered system at $r = r_0$, an analysis parallel to the one described in section (ii) gives the equivalent forces

$$\{P\} = \{P\}_I + ([R] - r_0 [D \mid D_R])\{\delta\} \quad (2.91)$$

with $[R]$ given now by eq. (2.30), and where only vertical forces exist due to the one-dimensional motion, since only vertical prescribed displacements at the rock are considered in this case. Then, the equilibrium equations are

$$([K] - \Omega^2 [M] + [R])\{\delta\} = \{P\}_I + ([R] - r_0 [D \mid D_R])\{\hat{\delta}\} \quad (2.92)$$

Eqs. (2.90) and (2.92) must be modified to account for the prescribed displacements in the bottom of the finite element element region. To avoid obvious complications, all the interface of the soil with the rock is assumed to vibrate with the same amplitude and phase.

2.6 Compliance Functions

By dynamic ground compliance is understood the ratio between the response of the (rigid) footing, in the sense of displacements or rotations produced, and the exciting force. If there is a harmonic force P_j applied on the footing in Fig. 2-1, there will be displacements $u_k(j, k = x, z, \phi)$ at a given reference point on the footing, such that if

$$P_j = |P_j| e^{i\Omega t} \quad (2.93)$$

then

$$u_k = |u_k| e^{i(\Omega t - \theta_{kj})} \quad (2.94)$$

where θ_{kj} is the "phase angle" by which the response u_k lags the excitation P_j .

Therefore, for a given frequency Ω , the dynamic ground compliance relating u_k and P_j is

$$F_{kj} = \frac{u_k}{P_j} = \left| \frac{u_k}{P_j} \right| e^{-i\theta_{kj}} = |F_{ij}| e^{-i\theta_{kj}} \quad (2.95)$$

which can be expressed as

$$F_{kj} = F'_{kj} + i F''_{kj} \quad (2.96)$$

where

$$F'_{kj} = \text{Re} (F_{kj}) = |F_{kj}| \cos \theta_{kj} \quad (2.97a)$$

$$F''_{kj} = \text{Im} (F_{kj}) = - |F_{kj}| \sin \theta_{kj} \quad (2.97b)$$

If $k = j$, the dynamic ground compliance will be referred to simply as "compliance." Otherwise, it will be called "cross-compliance."

The functional relation between the compliance (or cross-compliance) and the frequency is called the "compliance function." It depends on Poisson's ratio ν of the soil. Then

$$F_{kj} = F_{kj} (\nu, \Omega) \quad (2.98)$$

It will be useful to introduce dimensionless parameters

$$a = \frac{\Omega H}{C_s} \quad (2.99)$$

$$a_0 = \frac{\Omega B}{C_s} \quad (2.100)$$

$$f_{kj} = \frac{F_{kj}}{F_{kj}(0)} \quad (2.101)$$

where

$$C_s = \sqrt{\frac{G}{\rho}} = \text{velocity of S-waves in the medium}$$

H = stratum thickness

B = half-width of (rigid) footing

$$F_{kj}(0) = \text{Re}(F_{kj}) \text{ for } \Omega = 0, \text{ i.e. static}$$

These parameters are adequate for a uniform stratum. Otherwise, reference variables have to be chosen.

Three kinds of exciting forces are considered:

- (1) A vertical force P_z
- (2) A horizontal force P_x
- (3) A rotational moment P_ϕ about the y-axis.

The system used has a vertical axis of symmetry. Therefore, the vertical motion w is an independent and uncoupled motion. However, the horizontal translation u (swaying), and the rotational motion ϕ (rocking) are coupled motions.

The relationships between forces and displacements (in the generalized sense) can then be written

$$F_z P_z = w \quad (2.102)$$

for the vertical motion, and

$$\begin{bmatrix} F_{xx} & F_{x\phi} \\ F_{\phi x} & F_{\phi\phi} \end{bmatrix} \begin{Bmatrix} P_x \\ P_\phi \end{Bmatrix} = \begin{Bmatrix} u \\ \phi \end{Bmatrix} \quad (2.103)$$

for the coupled swaying and rocking, where $F_{x\phi} = F_{\phi x}$

Energy considerations dictate that the imaginary part of the compliance functions has to be always negative. The external energy (work rate) for harmonic motion is

$$E = \frac{\Omega}{2} \text{Im} (\{\delta\}^* \{P\}) \quad (2.104)$$

where $\{\delta\}$ designates either w or $\{u, \phi\}^T$ and $\{P\}$ designates either P_z or $\{P_x, P_\phi\}^T$. The vector $\{\delta\}^*$ is the conjugate transpose of $\{\delta\}$. To have $E > 0$, it is necessary to have

$$\text{Im} (\{\delta\}^* \{P\}) > 0 \quad (2.105)$$

giving the conditions

$$F_z'' P_z^2 < 0 \quad (2.106a)$$

and

$$F_{xx}'' P_x^2 + 2 F_{x\phi}'' P_x P_\phi + F_{\phi\phi}'' P_\phi^2 < 0 \quad (2.106b)$$

by virtue of eqs. (2.102) and (2.103), respectively.

This implies then, that

$$F_z'' < 0 \quad (2.107a)$$

$$F_{xx}'' < 0 \quad (2.107b)$$

$$F_{\phi\phi}'' < 0 \quad (2.107c)$$

$$F_{x\phi}''^2 < F_{xx}'' F_{\phi\phi}'' \quad (2.107d)$$

since eqs. (2.106a) and (2.106b) have to hold true for arbitrary values of P_z , P_x and P_ϕ independently. Note that, however, the imaginary part

of the cross-compliance function $F_{x\phi}$ can be either positive or negative, but with the restriction given by the inequality (2.107d).

The compliance functions can also be thought as the Fourier transform with respect to time t , i.e., a complex transfer function, of displacement components to an exciting force associated with the dynamic problem of a massless foundation-ground system considered here. That is, if

$$\bar{u}(\Omega) = F[\{w, u, \phi\}] = F[u(t)] \quad (2.108a)$$

and

$$\bar{P}(\Omega) = F[\{P_z, P_x, P_\phi\}] = F[P(t)] \quad (2.108b)$$

where F is the operator indicating the Fourier transform with respect to time t , the compliance functions $F(\Omega)$ are the output-input ratio

$$F(\Omega) = \frac{\bar{u}(\Omega)}{\bar{P}(\Omega)} \quad (2.109)$$

in the frequency domain.

The dynamic ground compliance converges to a finite value as the stratum thickness H increases, and for any frequency Ω , except that in the case of the half-space (or more properly, half-plane), the static solution, $\Omega = 0$, is undefined within an arbitrary constant [].

The compliance functions are affected by the percentage of critical damping, β . If these functions are known for the purely elastic case, $F_{kj,E}$, the solutions for a given $\beta > 0$ can be found [8] approximately by setting

$$\begin{aligned}
 F'_{kj} + i F''_{kj} &= \frac{F'_{kj,E} + i F''_{kj,E}}{1 + i2\beta} \\
 &= \frac{(F'_{kj,E} + 2\beta F''_{kj,E}) + i(F''_{kj,E} - 2\beta F'_{kj,E})}{1 + 4\beta^2}
 \end{aligned}
 \tag{2.110a}$$

Therefore, the relation between elastic and viscoelastic compliances are

$$F'_{kj} = \frac{F'_{kj,E} + 2\beta F''_{kj,E}}{1 + 4\beta^2}
 \tag{2.110b}$$

$$F''_{kj} = \frac{F''_{kj,E} - 2\beta F'_{kj,E}}{1 + 4\beta^2}
 \tag{2.110c}$$

This approximation neglects the coupling between sliding and rocking, and is undefined when either $F'_{kj,E}$ or $F''_{kj,E}$ tends to $\pm \infty$ at resonance frequencies, since the presence of damping limits the compliance functions to finite values. In the elastic case, there is no radiation damping until the first resonant frequency of the layer is reached.

The inverse of the dynamic ground compliance gives the displacement-force transfer function of a massless foundation-ground system, which means the complex stiffness of the system. Then, denoting by K_{kj} the stiffness relating a displacement u_k to a force P_j ,

$$K_z = \frac{1}{F_z}
 \tag{2.111}$$

for the vertical motion, and

$$\begin{bmatrix} K_{xx} & K_{x\phi} \\ K_{\phi x} & K_{\phi\phi} \end{bmatrix} = \begin{bmatrix} F_{xx} & F_{x\phi} \\ F_{\phi x} & F_{\phi\phi} \end{bmatrix}^{-1}
 \tag{2.112}$$

for the coupled sliding and rocking, where $K_{x\phi} = K_{\phi x}$.

The knowledge of the compliance functions offers the basic data for estimating the effects of soil-structure interaction. These functions have applicability to various dynamic problems of structures founded on or embedded in soils; for example, in foundations for machinery or in seismic response.

2.7 Response of Structures with Mass

The present study assumes a rigid structure represented by a rigid strip footing resting on or embedded in a soil stratum for either horizontal or vertical excitation; and the possibility of having a circular rigid footing is provided also for vertical excitation. It is of interest to know the response of a structure with mass due to a prescribed harmonic motion of the rock underlying the soil stratum, as well as to compare this response with the free-field motion induced at the ground surface.

(i) Vertical Motion

Let M be the mass of the structure, w_A its vertical displacement, and w_{A0} the response of the structure without mass. These responses are related to the stiffness function K_z given by eq. (2.111) as

$$K_z(w_A - w_{A0}) = \Omega^2 M w_A \quad (2.113a)$$

Then,

$$w_A = \frac{K_z}{K_z - \Omega^2 M} w_{A0} \quad (2.113b)$$

which can be expressed in terms of the compliance function F_z as

$$w_A = \frac{1}{1 - \Omega^2 M F_z} w_{A0} \quad (2.114)$$

ii) Coupled swaying and rocking

The equations of equilibrium for the structure shown in Fig. 2-7 can be written as

$$[K_A]({\delta}_A - {\delta}_{A0}) = [J_A]{\delta}_A \quad (2.115)$$

where

$[K_A]$ = stiffness matrix at point A

$[J_A]$ = inertia matrix at point A

${\delta}_A$ = displacement vector at point A, for structure with mass

${\delta}_{A0}$ = displacement vector at point A, for massless structure

The stiffness matrix $[K_A]$ is the same stiffness matrix $[K]$ given by eq. (2.112), since the stiffness (and compliance) functions are referred to point A. The inertia matrix for point A can be found from that at the center of gravity C, $[J_C]$, by the following transformation:

$$[J_C] = M \begin{bmatrix} 1 & 0 \\ 0 & S^2 \end{bmatrix} \quad (2.116)$$

where M is the mass of the structure, and S is its radius of gyration about the center of gravity. From Fig. 2-7, it is seen that

$$\begin{Bmatrix} P_x \\ P_\phi \end{Bmatrix}_A = \begin{bmatrix} 1 & 0 \\ -E & 1 \end{bmatrix} \begin{Bmatrix} P_x \\ P_\phi \end{Bmatrix}_C \quad (2.117a)$$

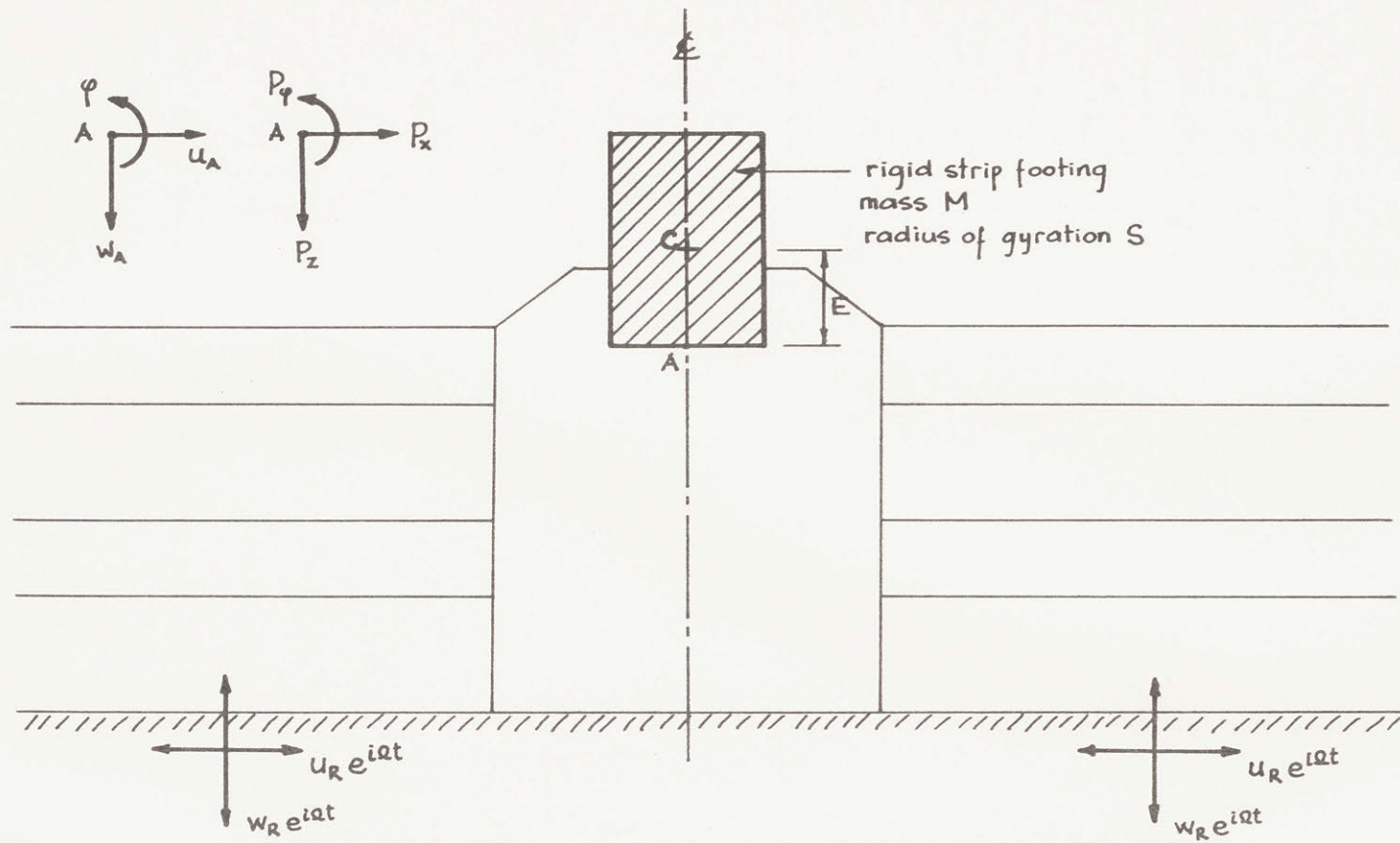


Figure 2-7 System with Rigid Mass

$$\begin{Bmatrix} u \\ \phi \end{Bmatrix}_C = \begin{bmatrix} 1 & -E \\ 0 & 1 \end{bmatrix} \begin{Bmatrix} u \\ \phi \end{Bmatrix}_A \quad (2.117b)$$

But

$$\begin{Bmatrix} P_x \\ P_\phi \end{Bmatrix}_C = \Omega^2 M \begin{bmatrix} 1 & 0 \\ 0 & S^2 \end{bmatrix} \begin{Bmatrix} u \\ \phi \end{Bmatrix}_C = \Omega^2 [J_C] \{\delta\}_C \quad (2.117c)$$

Then,

$$\begin{Bmatrix} P_x \\ P_\phi \end{Bmatrix}_A = \Omega^2 M \begin{bmatrix} 1 & 0 \\ -E & 1 \end{bmatrix} \begin{bmatrix} 1 & 0 \\ 0 & S^2 \end{bmatrix} \begin{bmatrix} 1 & -E \\ 0 & 1 \end{bmatrix} \begin{Bmatrix} u \\ \phi \end{Bmatrix}_A = \Omega^2 [J_A] \{\delta\}_A \quad (2.117d)$$

and calling

$$[A] = \begin{bmatrix} 1 & 0 \\ -E & 1 \end{bmatrix} \quad (2.118)$$

the result is

$$[J_A] = [A] [J_C] [A]^T = M \begin{bmatrix} 1 & -E \\ -E & E^2 + S^2 \end{bmatrix} \quad (2.119)$$

To simplify notation, the subscript A will be dropped, which will be understood, unless explicitly noted. The equations of equilibrium for a structure with mass can be put in a dimensionless form by setting

$$[f] = \begin{bmatrix} f_{xx} & f_{x\phi} \\ f_{\phi x} & f_{\phi\phi} \end{bmatrix} \quad (2.120a)$$

as the normalized compliance matrix, where any element f_{ij} is

$$f_{ij}(\Omega) = \frac{F_{ij}(\Omega)}{\text{Re}[F_{ij}(0)]} = F_{ij}(\Omega) \cdot \bar{k}_{ij0} \quad (2.120b)$$

where \bar{k}_{ij0} is a pseudo-static stiffness, equal to the reciprocal of the real part of the static compliance function, which in turn can be written as

$$\bar{k}_{xx0} = \kappa_{xx} G \quad (2.121a)$$

$$\bar{k}_{x\phi0} = \bar{k}_{\phi x0} = \kappa_{x\phi} GB \quad (2.121b)$$

$$\bar{k}_{\phi\phi0} = \kappa_{\phi\phi} GB^2 \quad (2.121c)$$

with B being the half-width of the strip footing, and G the shear modulus of the soil. The compliance matrix [F] can then be written as

$$\begin{aligned} [F] &= \begin{bmatrix} F_{xx} & F_{x\phi} \\ F_{\phi x} & F_{\phi\phi} \end{bmatrix} \\ &= \frac{1}{G} \begin{bmatrix} 1 & 0 \\ 0 & 1/B \end{bmatrix} \begin{bmatrix} f_{xx}/\kappa_{xx} & f_{x\phi}/\kappa_{x\phi} \\ f_{x\phi}/\kappa_{x\phi} & f_{\phi\phi}/\kappa_{\phi\phi} \end{bmatrix} \begin{bmatrix} 1 & 0 \\ 0 & 1/B \end{bmatrix} \\ &= \frac{1}{G} [B]^{-T} [\bar{F}] [B]^{-1} \quad (2.122) \end{aligned}$$

where

$$[B] = \begin{bmatrix} 1 & 0 \\ 0 & B \end{bmatrix} \quad (2.123)$$

and

$$[\overline{F}] = \begin{bmatrix} f_{xx}/\kappa_{xx} & f_{x\phi}/\kappa_{x\phi} \\ f_{x\phi}/\kappa_{x\phi} & f_{\phi\phi}/\kappa_{\phi\phi} \end{bmatrix} \quad (2.124)$$

is dimensionless; and $[B]^{-T}$ denotes $([B]^{-1})^T = ([B]^T)^{-1}$

Since $[K] = [F]^{-1}$,

$$[K] = G [B] [\overline{F}]^{-1} [B]^T \quad (2.125)$$

Letting

$$b = \frac{B}{H} \quad (2.126a)$$

$$e = \frac{E}{B} \quad (2.126b)$$

$$s = \frac{S}{B} \quad (2.126c)$$

$$B_x = \frac{M}{\rho B^2} \quad (2.126d)$$

$$B_\phi = \frac{I_c}{\rho B^4} = \frac{MS^2}{\rho B^4} = B_x^2 s^2 \quad (2.126e)$$

$$a = \frac{\Omega H}{C_s} \quad (1.127a)$$

$$a_o = \frac{\Omega B}{C_s} \quad (1.127b)$$

$$[J] = \begin{bmatrix} 1 & -e \\ -e & e^2 + s^2 \end{bmatrix} \quad (2.128)$$

eq. (2.115) can be written as

$$\{\delta_A\} = ([\overline{F}]^{-1} - B_x a_o^2 [J])^{-1} [\overline{F}]^{-1} \{\delta_{A0}\} \quad (2.129)$$

where the coefficient matrix of $\{\delta_{A_0}\}$ is dimensionless. Therefore, once the compliance function and the response $\{\delta_{A_0}\}$ due to a certain excitation are known for a structure without mass, the response for a given combination of mass M and mass-moment of inertia I_C can be determined using eq. (2.129).

2.8 Structure - Soil - Structure Interaction

2.8.1 Generalities

The problem of structure - soil - structure interaction is concerned with the influence of an adjacent body on the response of a given structure. This mutual influence takes place because both bodies are connected through the foundation soil, as shown in Fig. 2-8.

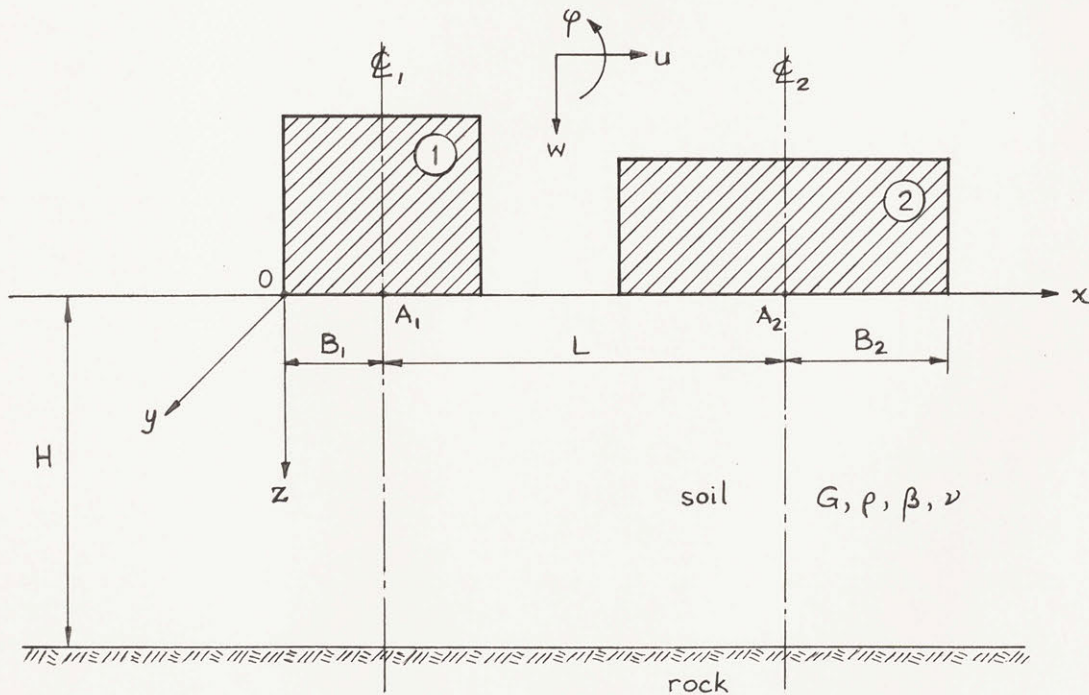


Figure 2-8

If one of the structures is excited, both of them will experience displacements u_i , ϕ_i and w_i , $i = 1, 2$. Also, if the soil is set in motion, the response of the two structures will be different than if only one of them existed. As before, only harmonic motion will be considered in this work; and the soil is homogeneous, isotropic and linearly elastic with hysteretic damping. The two structures are represented by parallel rigid strip footings in the y -direction. The global system of coordinates and the basic variables are shown in Fig. 2-8.

In principle, this problem can be solved by using the program PLAXLY2 described before; but the large number of finite elements that would be needed to cover the area between the two footings makes its use uneconomical. Furthermore, symmetry cannot be used in the general case. The approach that is explained in the next subsection is an indirect one, but it is more expedient and general.

Only structures founded on the surface of the soil will be studied here.

2.8.2 Stiffness Functions

Consider a set of equally spaced points on the surface of a soil stratum of unit depth, as shown in Fig. 2-9. Either a horizontal or a vertical line load (in the y -direction) will produce both horizontal and vertical displacements throughout the soil surface. Since the points under consideration are equally spaced, it suffices to determine the displacement patterns for the loads applied at the origin of

global coordinates; and for a load at any other point a distance x away, this pattern just shifts the same distance x .

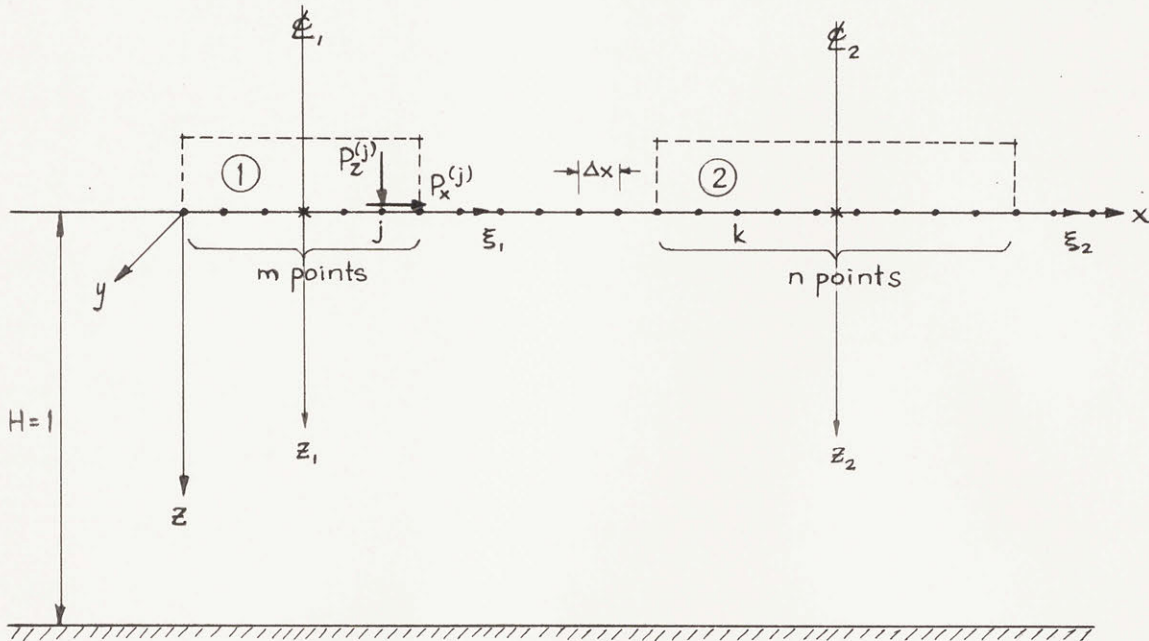


Figure 2-9

The first footing (Fig. 1) covers m points, and has a total width $2B_1 = (m-1) \cdot \Delta x$, and the second footing (Fig. 2) covers n points, with a total width $2B_2 = (n-1) \cdot \Delta x$.

Now, an influence matrix $[F]$ can be written, with elements f_{kj} , relating forces at j and displacements at k . This matrix is frequency-dependent, that is, $[F] = [F(\omega)]$. Order the forces and displacements so that odd position-numbers correspond to the horizontal direction, i.e., P_x and u ; and even to the vertical direction, i.e., P_z and w . Then, the following relation holds,

$$\begin{bmatrix} [F_{11}] & [F_{12}] \\ (2m \times 2m) & (2m \times 2n) \\ \hline [F_{21}] & [F_{22}] \\ (2n \times 2m) & (2n \times 2n) \end{bmatrix} \begin{Bmatrix} \{P_1\} \\ (2m \times 1) \\ \hline \{P_2\} \\ (2n \times 1) \end{Bmatrix} = \begin{Bmatrix} \{V_1\} \\ (2m \times 1) \\ \hline \{V_2\} \\ (2n \times 1) \end{Bmatrix} \quad (2.130)$$

where the order of the submatrices or subvectors are shown in parentheses. The vectors $\{P_i\}$ are the forces applied at the points in the location of footing i , $i = 1, 2$; and $\{V_i\}$ are the corresponding displacements.

A vertical line load produces symmetric vertical and antisymmetric horizontal displacements, and a horizontal load produces symmetric horizontal and antisymmetric vertical displacements. Also, u at point k due to a unit force $P_z^{(j)}$ applied at point j is equal but opposite in sign to w at point k due to a unit force $P_x^{(j)}$ applied at point j . Therefore, the influence matrix $[F]$ is symmetrical, satisfying the law of reciprocity [15]. This matrix can be thought of as a (frequency-dependent) flexibility matrix for the soil surface.

The matrix $[F]$ is of order $(2m \times 2n)$. Considering that the two footings are rigid bodies, there are only three independent degrees of freedom for each of them, namely, a horizontal displacement u_i , a rotation about the center-line ϕ_i , and a vertical displacement w_i .

Denoting by superscripts the number of the points under either footing, the conditions of rigid body motion are

$$u_i^{(1)} = u_i^{(2)} = \dots = u_i^{(r)} = u_i \quad (2.131a)$$

$$w_i^{(\ell)} = w_i - \xi_i^{(\ell)} \phi_i \quad (2.131b)$$

where $r = m$ or n , $i = 1$ or 2 , and $1 \leq \ell \leq r$. The local coordinate $\xi_i^{(\ell)}$ of point ℓ under footing i is just the distance between that point and the center-line of the footing.

Calling

$$\{V^*\} = \{u_1 \ \phi_1 \ w_1 \ \vdots \ u_2 \ \phi_2 \ w_2\}^T \quad (2.132a)$$

and

$$\{P^*\} = \{P_{x1} \ P_{\phi1} \ P_{z1} \ \vdots \ P_{x2} \ P_{\phi2} \ P_{z2}\}^T \quad (2.132b)$$

the condensed displacement and force vectors, respectively, a condensed stiffness matrix can be found by imposing conditions (2.131). They are equivalent to writing

$$\{V\} = [T] \{V^*\} \quad (2.133)$$

where $[T]$ is a transformation matrix of order $(2m + 2n) \times 6$, given by

Therefore

$$[F]\{P\} = \{V\} = [T] \{V^*\}$$

$$\therefore P = [F]^{-1} [T] \{V^*\} \quad (2.135)$$

Now, the total forces acting on the footings are just the resultants of the reaction forces at the r , $r = m$ or n , points under each footing, i.e.,

$$\left. \begin{aligned} P_{x_i} &= \sum_{\ell=1}^r p_{x_i}^{(\ell)} \\ P_{z_i} &= \sum_{\ell=1}^r p_{z_i}^{(\ell)} \\ P_{\phi_i} &= - \sum_{\ell=1}^r \xi_i^{(\ell)} p_{z_i}^{(\ell)} \end{aligned} \right\} \begin{array}{l} i = 1 \text{ or } 2 \\ \ell = m \text{ or } n \end{array} \quad (2.136a)$$

It can be easily observed that this statement is equivalent to premultiplying the vector $\{P\}$ by $[T]^T$; so,

$$\{P^*\} = [T]^T \{P\} \quad (2.136b)$$

which, after introducing into eq. (2.135) gives

$$\begin{aligned} \{P^*\} &= ([T]^T [F]^{-1} [T]) \{V^*\} \\ &= [K^*] \{V^*\} \end{aligned} \quad (2.137)$$

where

$$[K^*] = [T]^T [F]^{-1} [T] \quad (2.138)$$

is the desired condensed stiffness matrix, of order (6×6) .

2.8.3 Effect of Mass

The effect of including mass in the footings is just to add an inertia term to the stiffness matrix $[K^*]$. The inertia matrix is given by

$$[J] = \left[\begin{array}{c|c} [J_1] & [0] \\ \hline [0] & [J_2] \end{array} \right] \quad (2.139)$$

where

$$[J_i] = M_i \begin{bmatrix} 1 & -E_i & 0 \\ -E_i & E_i^2 + S_i^2 & 0 \\ 0 & 0 & 1 \end{bmatrix}, \quad i = 1, 2 \quad (2.140)$$

The meaning of E and S is the same as in Section 2.7. Since the inertia term is

$$[J] \{\ddot{V}^*\} = -\Omega^2 [J] \{V^*\} \quad (2.141)$$

the relation between forces and displacements in the two footings is

$$([K^*] - \Omega^2 [J]) \{V^*\} = \{P^*\} \quad (2.142)$$

Note that the stiffness matrix $[K^*]$ already includes the effect of the mass of the soil.

The displacements for a given pair of masses can be expressed in dimensionless form. For a set of loads $P_{x_1}, P_{\phi_1}, P_{z_1}, P_{x_2}, P_{\phi_2}$ and P_{z_2} acting independently, the load vector $\{P^*\}$ is now a diagonal matrix,

$$[P^*] = \text{diag} (P_{x_1} \quad P_{\phi_1} \quad P_{z_1} \quad | \quad P_{x_2} \quad P_{\phi_2} \quad P_{z_2}) \quad (2.143)$$

and the resulting displacements form a (6 x 6) matrix $[V^*]$, where each column is the vector of displacements for one of the applied individual loads. Calling

$$[B] = \text{diag} (0 \quad B_1 \quad 0 \quad \Big| \quad 0 \quad B_2 \quad 0) \quad (2.144)$$

the dimensionless displacements $[\bar{V}^*]$ are expressed by

$$[\bar{V}^*] = G[B]^T [V^*] [B] [P^*]^{-1} \quad (2.145)$$

2.8.4 Rock Motion

If a horizontal motion $u_R e^{i\Omega t}$ is prescribed at the rock level, the displacements at the free surface of the soil are $u_0 e^{i\Omega t}$, with only horizontal components, as predicted by the 1-D theory.

The displacements on the footings are given by

$$[K^*] (\{V^*\} - \{V_0\}) = \Omega^2 [J] \{V^*\} = \{0\} \quad (2.146)$$

where

$$\begin{aligned} \{V_0\} &= \{u_0 \quad 0 \quad 0 \quad \Big| \quad u_0 \quad 0 \quad 0\}^T \\ &= u_0 \{1 \quad 0 \quad 0 \quad \Big| \quad 1 \quad 0 \quad 0\}^T \end{aligned} \quad (2.147)$$

and $(\{V^*\} - \{V_0\})$ is then the relative motion of the footings with respect to the free-field motion. Then,

$$([K^*] - \Omega^2 [J]) \{V^*\} = [K^*] \{V_0\} \quad (2.148)$$

The right-hand member is equivalent to $u_0 \{R\}$, where $\{R\}$ is the vector formed by adding the first and fourth columns of $[K^*]$. The

amplification of the motion u_0 is then given by

$$([\mathbf{K}^*] - \Omega^2 [\mathbf{J}]) \left(\frac{1}{u_0} \{V^*\} \right) = \{R\} \quad (2.149)$$

In terms of dimensionless displacements, the amplification is

$$\{u_1/u_0 \quad \phi_1 B_1/u_0 \quad w_1/u_0 \quad | \quad u_2/u_0 \quad \phi_2 B_2/u_0 \quad w_2/u_0\}^T \quad (2.150)$$

CHAPTER 3 - EFFECT OF LAYER THICKNESS

3.1 Introduction

The majority of studies on the dynamics of ground-foundation systems have dealt with the case of a footing resting on an elastic half-space. In actual situations, the soil (as distinguished from rock) has a limited depth, and the foundation may be partially embedded. In this work, the soil is represented by a homogeneous, isotropic and viscoelastic material resting on a rigid half-space (rigid rock). For simplicity, the layer has been assumed homogeneous throughout the whole domain, and of uniform thickness. The foundation is represented by a rigid strip of infinite length.

This chapter explores the nature of the amplification, compliance and stiffness functions, for a strip footing resting on the surface of the soil as a function of the layer thickness. The effect of embedment is then studied in Chapter 4.

3.2 Amplification Functions

The amplification function, as used here, is the transfer function for the motion from the rock level to the surface of the soil or to the bottom of the footing (point A in Fig. 3-1). Therefore, this function is given by u_A/u_R , where u_A is the magnitude of the horizontal displacement at point A, and u_R is the magnitude of the horizontal displacement at the soil-rock interface.

Resonance phenomena do not appear in the case of a half-space. On the other hand, in the case of a stratum over a rigid medium, waves

are reflected at both boundary surfaces of the soil layer. There will be as a result a set of frequencies, function of the layer thickness and the elastic properties of the soil, at which resonance occurs for harmonic motion. If the medium is perfectly elastic, the amplitude of the resulting displacements becomes infinity at these frequencies; but if some amount of material damping exists, the displacements are limited in magnitude, due to the energy loss in the viscoelastic medium.

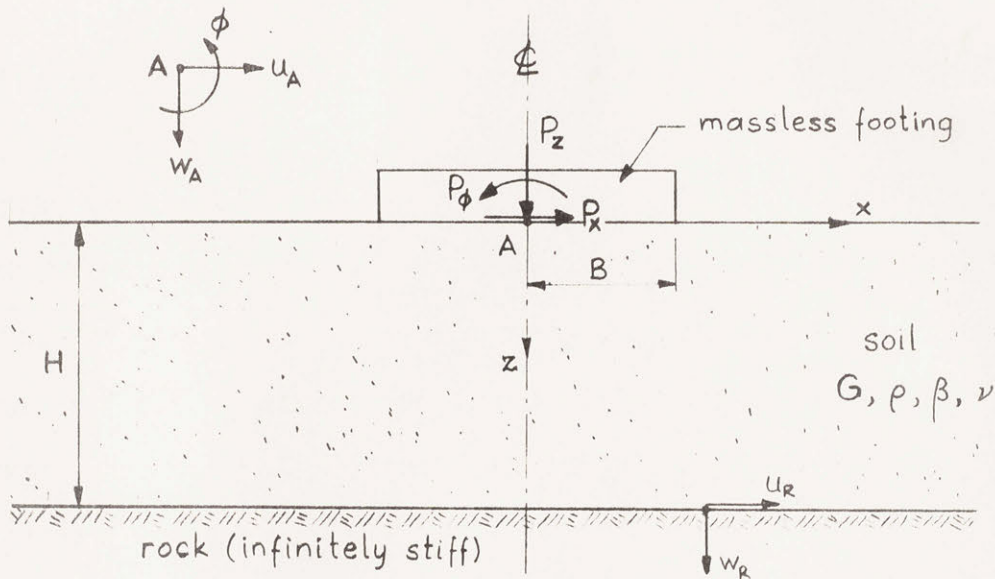


Figure 3-1

According to the theory of one-dimensional amplification [], the resonant frequencies of the stratum considered in this study coincide with the natural frequencies of vibration of a prismatic beam having the same mass density ρ as the soil, and with a length equal to the layer thickness. For horizontal vibrations, this equivalent beam has the same shear modulus G as the soil, but an infinite bending stiffness, i.e., it is a pure shear beam. For vertical vibrations,

the equivalent beam has a modulus $(\lambda + 2G)$, where λ and G are the Lamé's constants of the soil, and deforms only axially. The boundary conditions are in both cases the same as for the actual soil stratum, one end fixed and the other free.

For transverse (horizontal) vibrations, the resonant frequencies ω_n are

$$\omega_n = \frac{2n-1}{2H} \pi \sqrt{\frac{G}{\rho}}, \quad n = 1, 2, \dots \quad (3.1)$$

and with

$$c_s = \sqrt{\frac{G}{\rho}} = \text{shear-wave velocity} \quad (3.2)$$

$$a = \frac{\Omega H}{c_s} = \text{frequency ratio} \quad (3.3)$$

these resonant frequencies can be expressed as resonant frequency ratios.

$$a_n = \frac{2n-1}{2} \pi \quad (3.4)$$

For longitudinal (vertical) vibrations, the resonant frequencies are

$$\omega_n = \frac{2n-1}{2H} \pi \sqrt{\frac{\lambda+2G}{\rho}}, \quad n = 1, 2, \dots \quad (3.5)$$

The amplification function for horizontal vibrations is shown in Fig. 3-2, where u_o/u_R is the 1-D amplification, u_o being the amplitude of motion at the free surface. This function is shown for four different percentages of hysteretic damping β . The amplitudes of successive peaks go in the ratio of 1, 1/3, 1/5, Fig. 3-3 shows the maximum amplification, corresponding to the first resonant frequency,

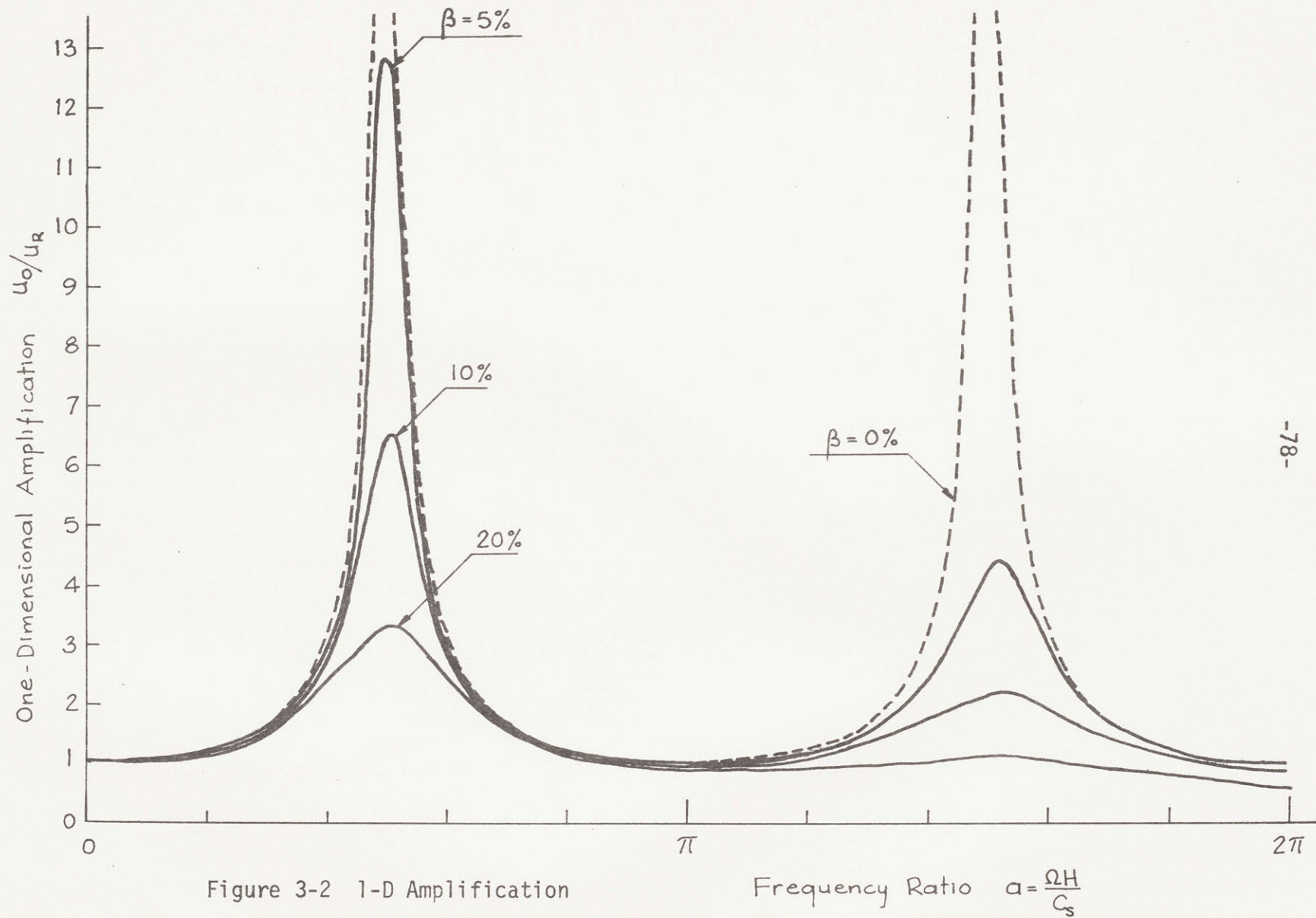


Figure 3-2 1-D Amplification

Frequency Ratio $a = \frac{\Omega H}{C_s}$

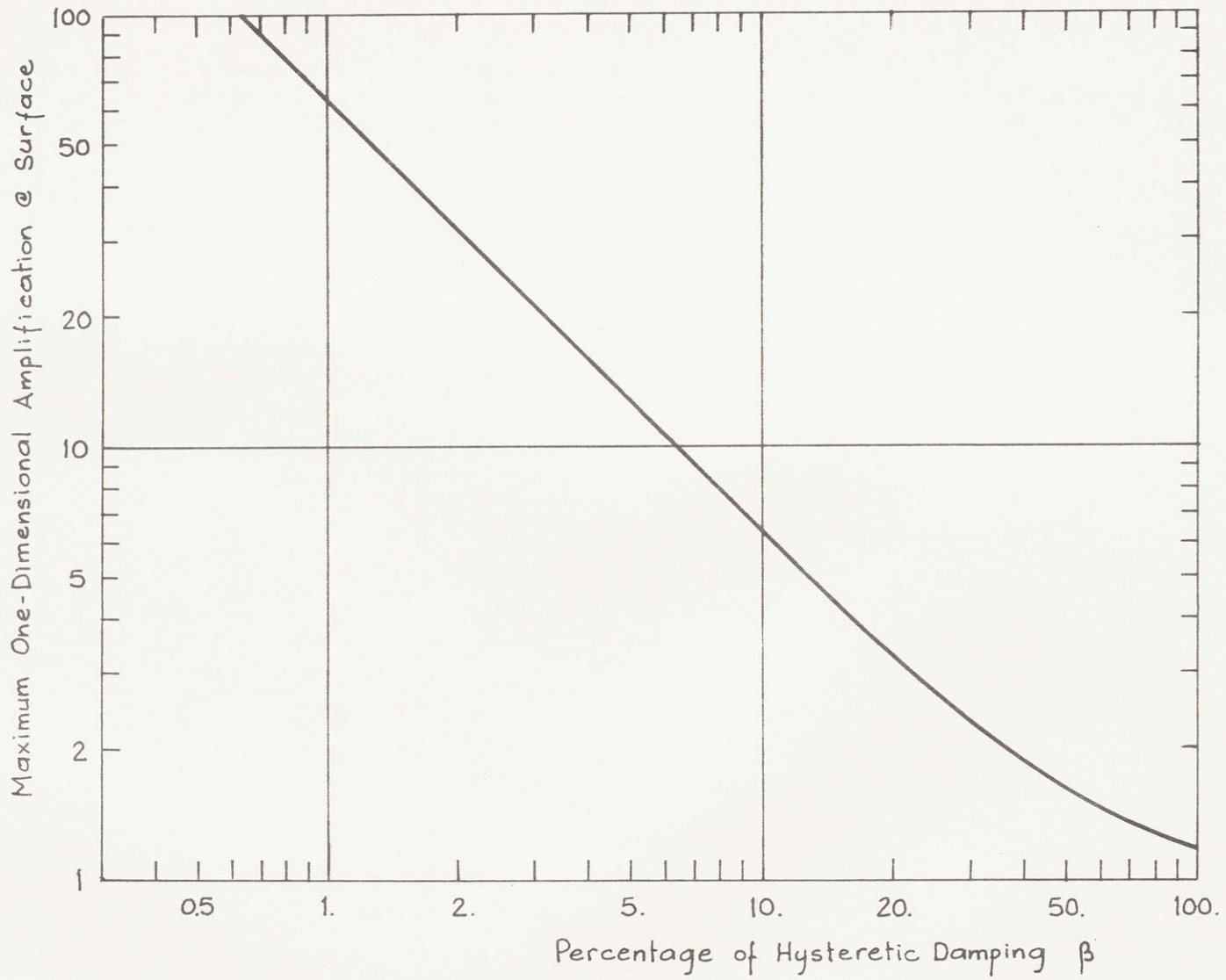


Figure 3-3 Effect of Damping on Maximum 1-D Amplification

vs. the percentage of hysteretic damping. In the range of small β , say less than 20%, the maximum amplification is inversely proportional to the amount of damping. It is clearly seen that an error in the prediction of damping can lead to significant under- or over-estimations of the surface motion in the neighborhood of the resonant frequencies.

For the case of a massless strip footing resting on the surface of the soil stratum, this 1-D amplification is the same as the transfer function given by u_A/u_R , that is $u_A = u_0$.

3.3 Compliance and Stiffness Functions

3.3.1 General Characteristics

Consider a rigid massless footing welded to the soil, and a harmonic force or moment applied at its base. The resulting displacement and rotation provide the frequency dependent flexibility coefficients:

F_{xx} = horizontal displacement due to unit horizontal force;

$F_{\phi\phi}$ = rotation due to unit moment;

$F_{x\phi}$ = horizontal displacement due to unit moment; and,

$F_{\phi x}$ = rotation due to unit horizontal force;

where $F_{x\phi} = F_{\phi x}$ according to the law of reciprocity [15]. The compliance, or flexibility, matrix $[F]$ is then defined as

$$[F] = \begin{bmatrix} F_{xx} & F_{x\phi} \\ F_{\phi x} & F_{\phi\phi} \end{bmatrix} \quad (3.6)$$

The inverse of this matrix is the stiffness matrix $[K]$, given by

$$[K] = [F]^{-1} = \begin{bmatrix} K_{xx} & K_{x\phi} \\ K_{\phi x} & K_{\phi\phi} \end{bmatrix} \quad (3.7)$$

which relates resulting forces to prescribed displacements.

Then, the following relations can be written:

$$[F] \{P\} = \{U\} \quad (3.8)$$

or

$$[K] \{U\} = \{P\} \quad (3.9)$$

where

$$\{U\} = \begin{Bmatrix} u \\ \phi \end{Bmatrix} = \text{displacement vector} \quad (3.10)$$

$$\{P\} = \begin{Bmatrix} P_x \\ P_\phi \end{Bmatrix} = \text{force vector} \quad (3.11)$$

with the displacement and force components as shown in Fig. 3-1.

The compliance functions were computed in the frequency ratio range $0 \leq a \leq 2\pi$ for ratios of layer thickness to half-width of footing, H/B , of 1, 2, 4, 8 and 16, by means of the computer program PLAXLY2 described in Chapter 2. The finite elements used had a maximum dimension of 1/12 of the minimum wavelength, except that for the cases of high H/B ratio, the lower half of the soil stratum was modeled with elements 1/6 of the minimum wavelength in depth, but 1/12 in width. The error introduced by using such an apparently coarse mesh was sufficiently small, since the largest part of energy transmission occurs in the upper part of the layer in the form of Rayleigh

waves, especially at high frequencies (small wavelengths). A Poisson's ratio $\nu = 0.30$ was used throughout, and the percentage of hysteretic damping was taken as 10%, except for the case of $H/B = 2$, where other values of β were considered as well.

Figs. 3-4 and 3-5 show the compliance functions F_{xx} and $F_{\phi\phi}$ for the case of $H/B = 2$ and different percentages of damping. For the case of no material damping, $\beta = 0\%$, F_{xx} shows singularities at frequencies ω_n' slightly higher than those corresponding to the resonant frequencies ω_n of the stratum, since only a small part of the stratum surface is excited by external forces. The first resonant frequency ratio is $a_{1H} = \pi/2$, and the second is $a_{2H} = 3\pi/2$, as shown in these figures by (1_H) and (2_H) . The real part of F_{xx} tends to infinity as the excitation frequency approaches ω_n' , and starts again from zero just above it; the imaginary part is zero throughout all frequencies smaller than ω_1' , indicating that no radiation of energy takes place in this range, and goes from $-\infty$ to 0 between successive resonant frequencies, showing a finite peak at a frequency just above that corresponding to resonance for vertical vibrations, ($a_{1V} = (C_p/C_s)(\pi/2)$), as indicated in the figures by (1_V) . Similarly, $F_{\phi\phi}$ has a singularity at a frequency close to a_{1V} , but the imaginary part has a non-zero value below this frequency, since rocking is also influenced by shear waves, which have a resonant frequency lower than that of compressional waves. For finite amounts of damping, the compliance functions follow the general trend of the undamped case, but both the real and imaginary parts are finite throughout the whole frequency range.

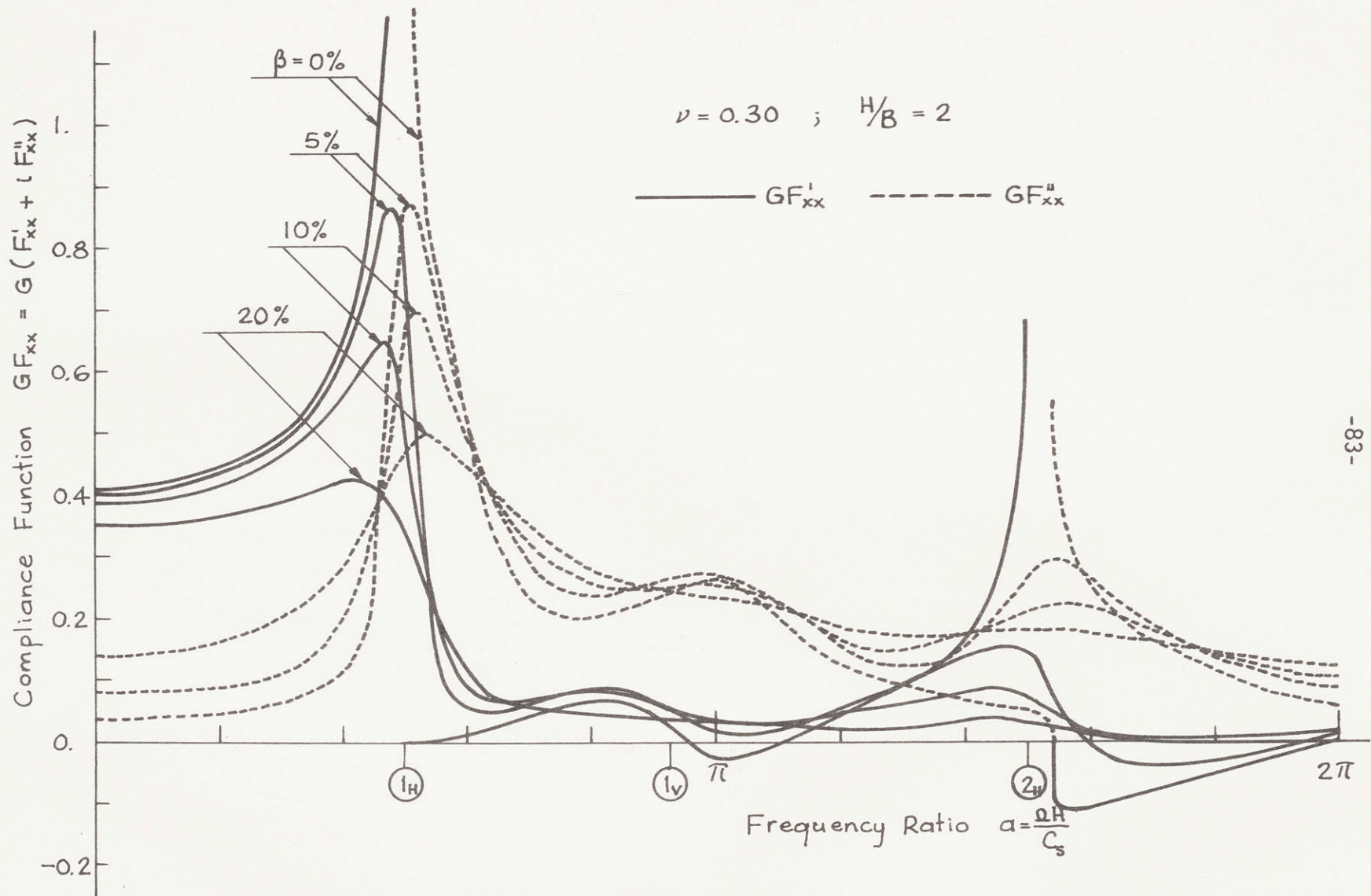


Figure 3-4 Effect of Damping on F_{xx}

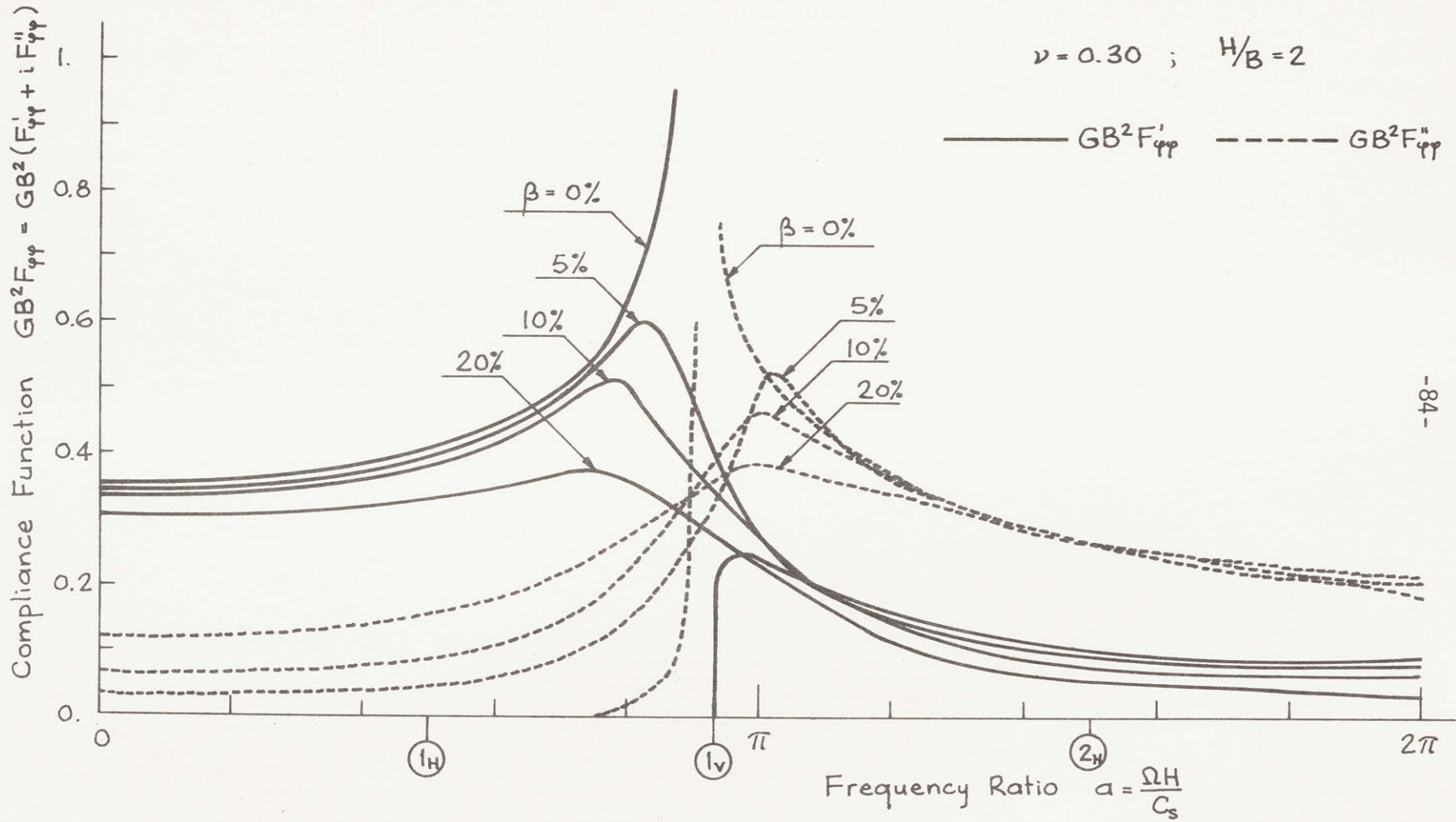


Figure 3-5 Effect of Damping on $F_{\phi\phi}$

The stiffness functions K_{xx} and $K_{\phi\phi}$ for the same system are shown in Figs. 3-6 and 3-7. The horizontal stiffness for zero damping becomes zero at $a \approx a_{1H}$ and shows a singularity at a frequency ratio close to a_{1V} , as seen from the change in $\text{Re}(K_{xx})$ from $-\infty$ to $+\infty$ across this frequency. The rocking stiffness also shows a disturbance around this peak. Both functions are very wavy for low values of damping, but smooth out as damping increases. In contrast to the compliance functions, the stiffness functions have less identifiable features with respect to location of peaks, but they show clearly that radiation damping occurs only for frequencies larger than that of the first shear mode.

While simple consideration of the one-dimensional resonant frequencies of the stratum explains some of the basic features of these curves, it can only afford a partial explanation for their complete shape. It must be realized that at any frequency the motion is the result of a complex combination of waves. As discussed in ref. [56] the solution can be expressed in terms of generalized Rayleigh wave modes. These modes are dispersive; that is, their phase velocity (velocity of propagation along the surface) depends on the wave number (and therefore on the frequency). These modes may not propagate below critical values of the frequency and their wave numbers may change abruptly from complex to real or pure imaginary with a corresponding change in the modal shape. The result of these variations is the waviness of the functions which depends on the relative importance or participation of each mode.

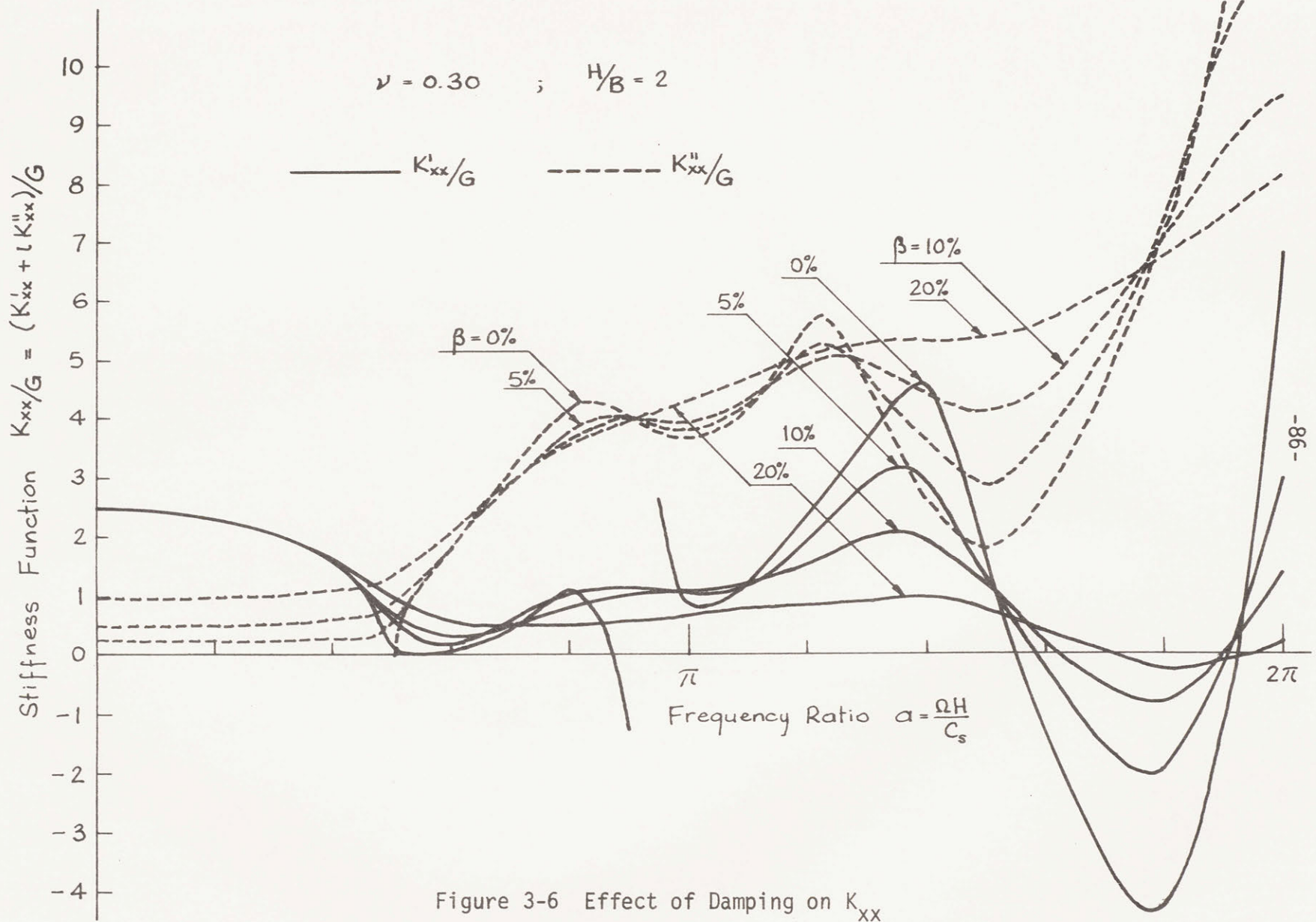


Figure 3-6 Effect of Damping on K_{xx}

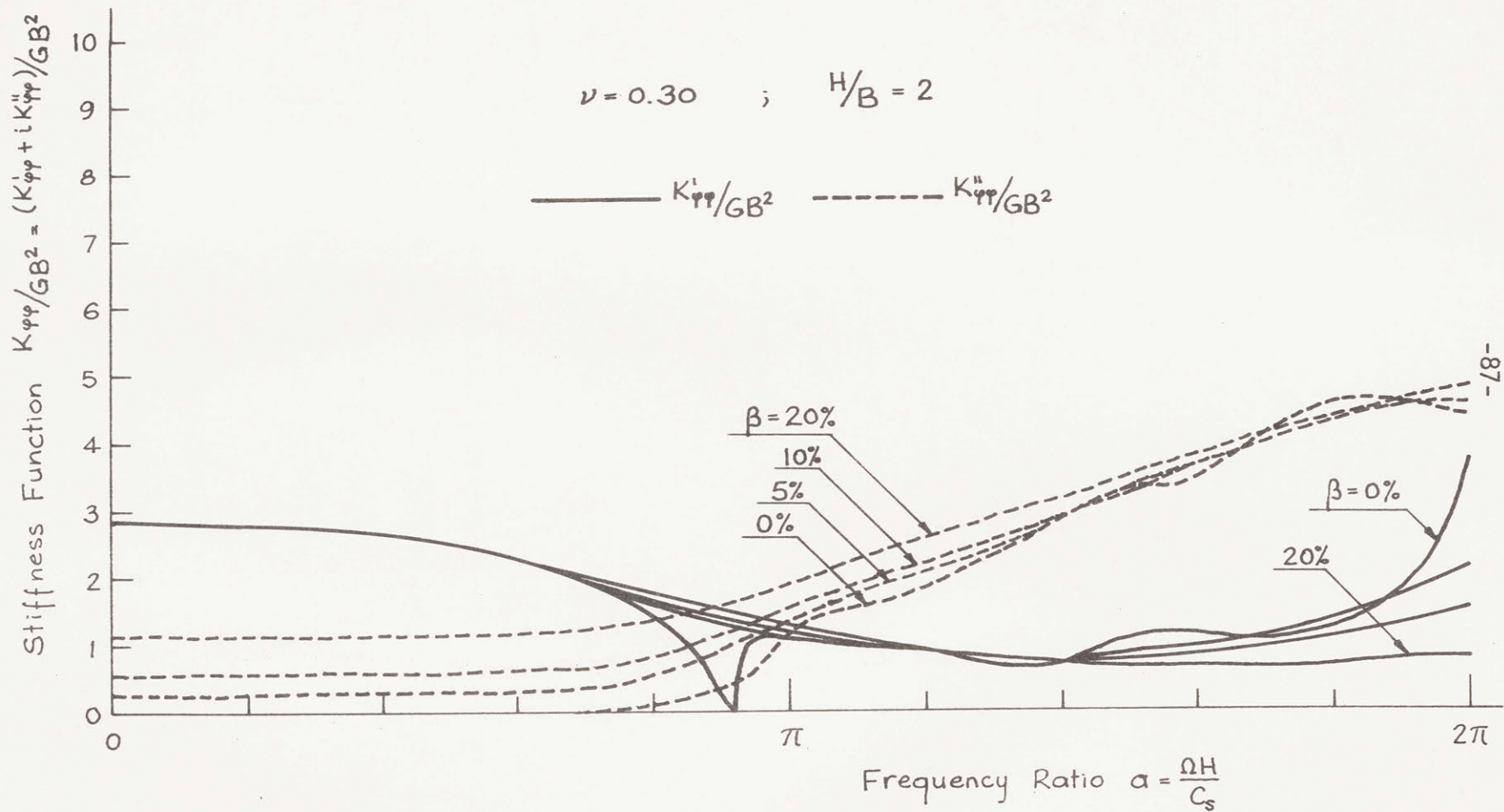


Figure 3-7 Effect of Damping on $K_{\phi\phi}$

Consideration of the group velocity

$$C_g = \frac{d\Omega}{dk} \quad (3.12)$$

shows that both C_g and k become zero at the one-dimensional resonant frequencies. ($C_g = 0$ implies that there is no transmission of energy [], thus a resonance condition). But there are additional frequencies (roots of a transcendental equation) [26, 29] at which C_g may become zero for a mode with $k \neq 0$, or at which two modes have the same phase velocity but opposite directions of propagation, resulting in a net zero group velocity. If there is no damping in the system, very large and narrow peaks will appear in the compliance functions at these frequencies.

Because these effects are essentially due to singularities at resonant frequencies, they are considerably decreased if the system has some internal damping; and as the damping increases, the curves become much smoother.

In general, these resonant frequencies are functions of only the properties of the soil stratum, such as the thickness H , the shear modulus G , and the Poisson's ratio ν . They are independent of the shape and dimensions of the footing.

3.3.2 Effect of Damping. Approximation.

It has often been suggested that the stiffness functions for an elastic stratum or half space can be used for a hysteretic medium just by replacing the static stiffness by a value $k(1+2i\beta)$. The

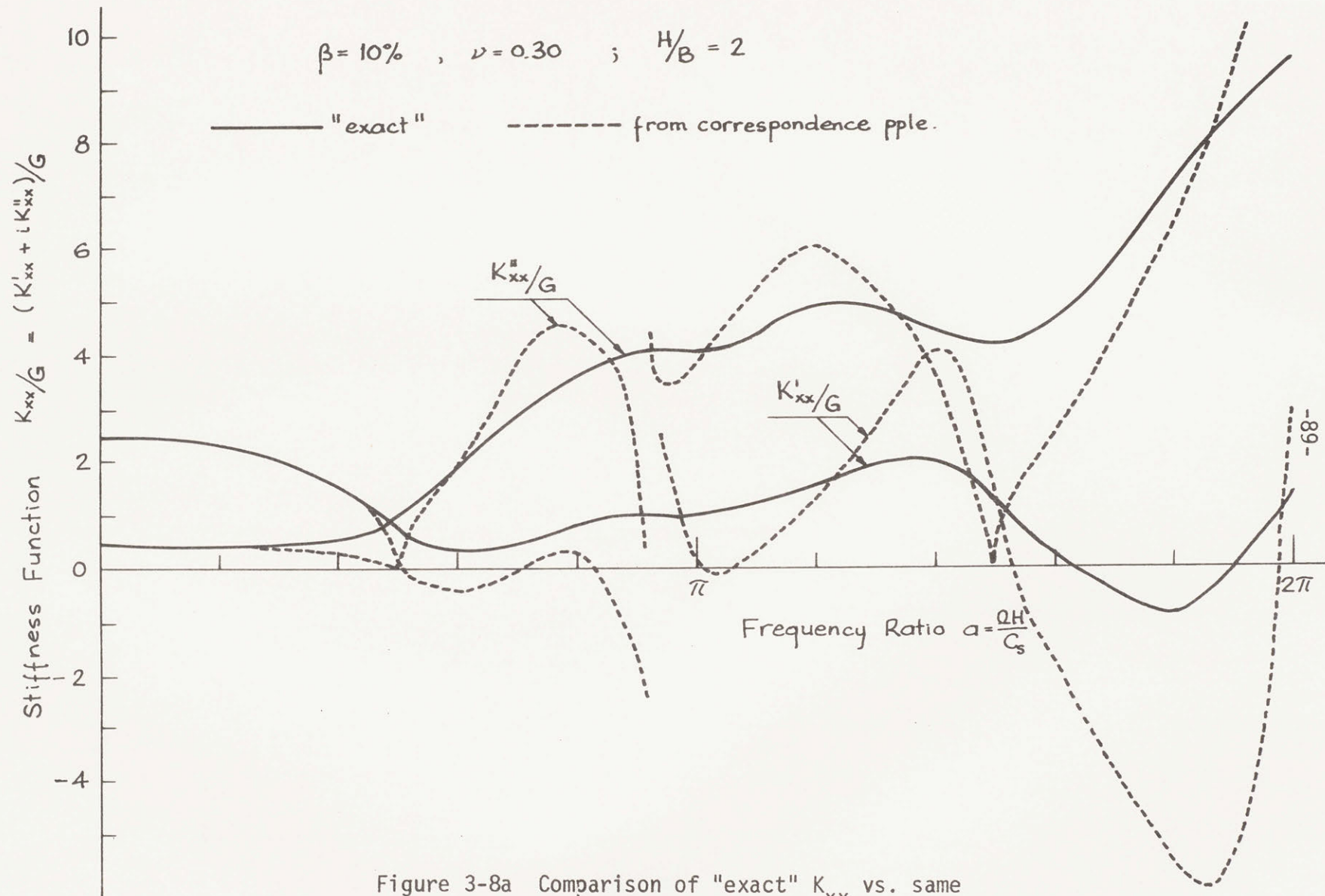


Figure 3-8a Comparison of "exact" K_{xx} vs. same by Correspondence Principle

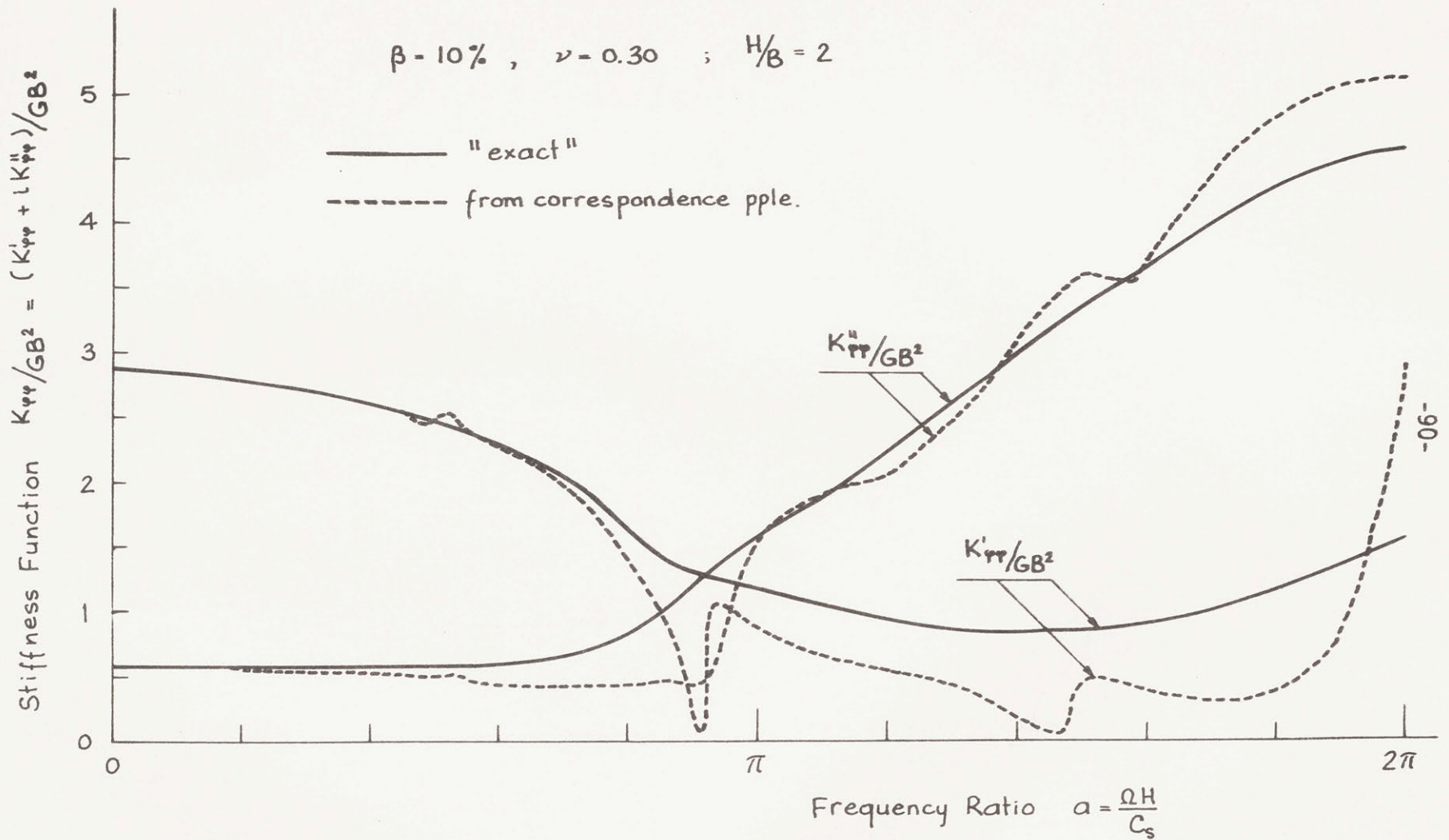


Figure 3-8b Comparison of "exact" $K_{\phi\phi}$ vs. same by Correspondence Principle

real part of the static stiffness is indeed independent of β , although this is not true for the static compliance since

$$F'_{xx} = \frac{K'_{\phi\phi}}{(1 + 4\beta^2)(K'_{xx} K'_{\phi\phi} - K'^2_{x\phi})} \quad (3.13a)$$

and

$$F'_{\phi\phi} = \frac{K'_{xx}}{(1 + 4\beta^2)(K'_{xx} K'_{\phi\phi} - K'^2_{x\phi})} \quad (3.13b)$$

If this approximation were to hold over the complete range of frequencies, one should have

$$K(\beta) = K'(\beta) + iK''(\beta) = (K'(0) + iK''(0))(1 + 2i\beta) \quad (3.14a)$$

or

$$K'(\beta) = K'(0) - 2\beta K''(0) \quad (3.14b)$$

$$K''(\beta) = K''(0) + 2\beta K'(0) \quad (3.14c)$$

Fig. 3-8 shows that these relationships do not hold true and that therefore the application of the correspondence principle in this case, as often used, is only approximate.

3.3.3 Effect of Layer Thickness

It is interesting to look first at the variation of the static compliances and stiffnesses as a function of the thickness of the stratum. The variation of static compliances against the thickness to width ratio is shown in Fig. 3-9a for rigid footings resting on the surface of the soil stratum. These curves apply to the case of $\nu = 0.30$ and $\beta = 10\%$. For other values of damping β , the correspond-

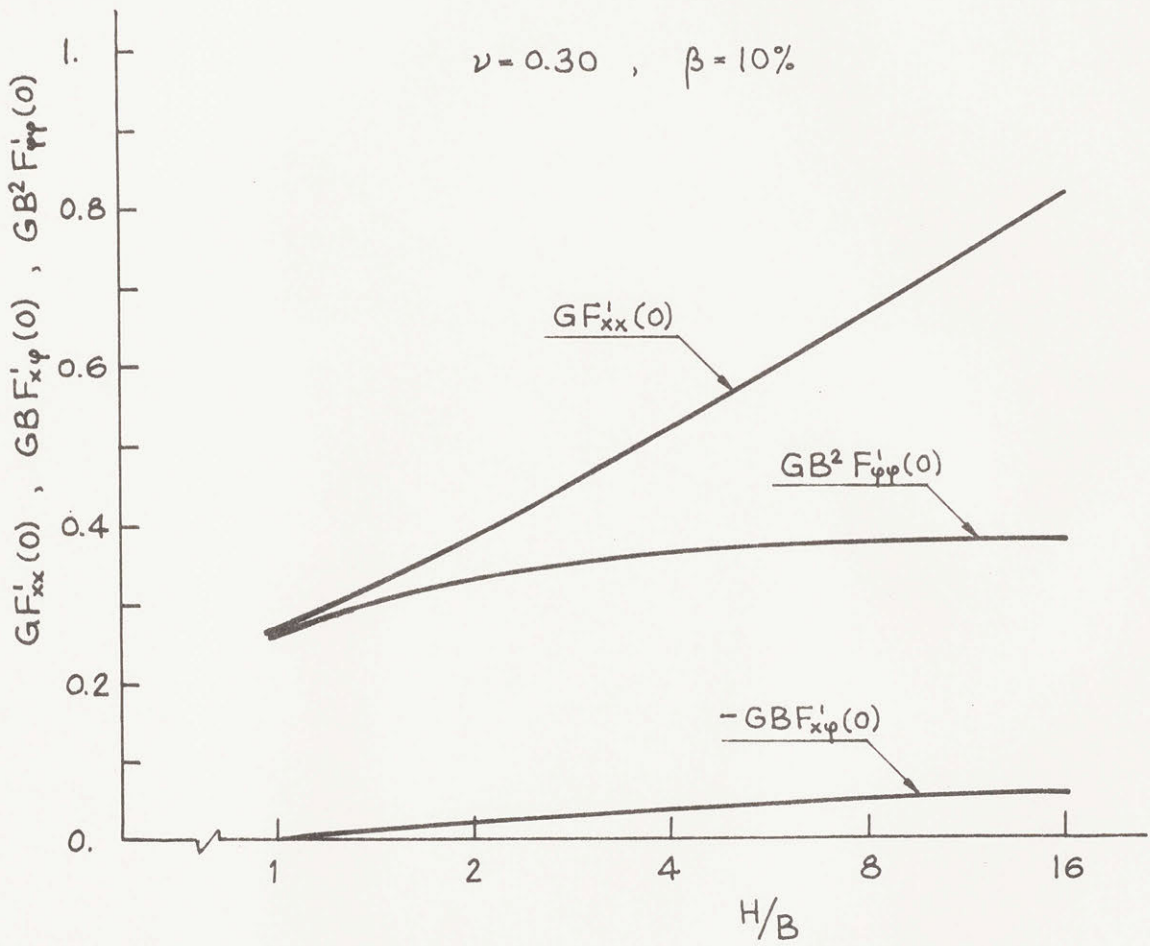


Figure 3-9a Effect of Layer Thickness on Static Compliances

all β , $\nu = 0.30$

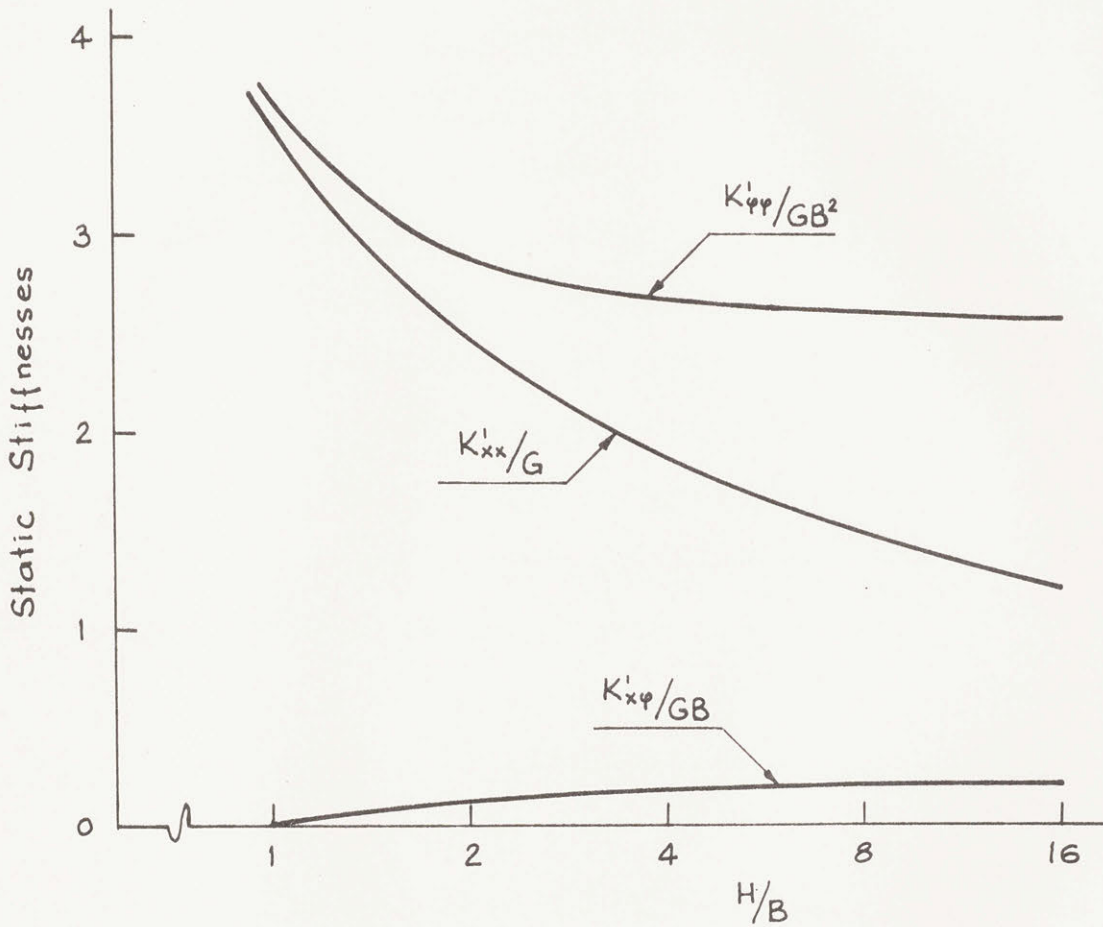


Figure 3-9b Effect of Layer Thickness on Static Stiffnesses

ing curves can be found by multiplying the respective ordinates by $1.04/(1+4\beta^2)$. The swaying compliance keeps increasing as the layer thickness increases; but the variation is slow, less than linear. In the limit, when $H/B \rightarrow \infty$, which is the case of the half-space, $F'_{xx}(0)$ tends to infinity. Therefore, even with very deep strata, the effect of the rigid rock is felt. On the contrary, the rocking compliance converges very rapidly to a finite value, as seen from the small difference between $GB^2F'_{\phi\phi}(0)$ at $H/B = 8$ and 16 . This suggests that an effective "bulb of pressure" exists for rocking excitation. The fast convergence of $F'_{\phi\phi}$ to the half-space solution in the dynamic case also occurs, as will be shown later.

Fig. 3-9b shows the variation of the static stiffness against the H/B ratio, for the case of $\nu = 0.30$ and any value of damping. The stiffness variation gives a better insight to the problem of static deflections and can be thought of as a coefficient of subgrade reaction. The static deflections would be given by

$$u = \frac{P_x}{K_x} \quad \text{for a horizontal load } P_x \quad (3.15)$$

and

$$\phi = \frac{P_\phi}{K_\phi} \quad \text{for a rocking moment } P_\phi \quad (3.16)$$

where

$$K_x = K'_{xx} - \frac{K'^2_{x\phi}}{K'_\phi\phi} \quad (3.17)$$

$$K_\phi = K'_{\phi\phi} - \frac{K'^2_{x\phi}}{K'_{xx}} \quad (3.18)$$

evaluated at $\Omega = 0$. Of course, $K_x = 1/F_{xx}'$ and $K_\phi = 1/F_{\phi\phi}'$.

For the dynamic case, compliance functions for several H/B ratios are plotted in Figs. 3-10 and 3-11. They apply only for a damping of 10% and Poisson's ratio of 0.30. As the stratum thickness increases, convergence to the half-space solution should be expected. Only F_{xx} and $F_{\phi\phi}$ are shown, because the coupling function $F_{x\phi} = F_{\phi x}$ is small and erratic.

For the horizontal compliance F_{xx} , it is seen that after the first high peak, the functions for different H/B ratios follow a definite trend, similar to that of the half-space solutions shown in Fig. 3-12, as obtained by different authors [22, 31, 47].

The rapid convergence in the case of rotational excitation, namely $F_{\phi\phi}$, is particularly conspicuous. In this case, there are tensile stresses on one-half of the footing and compressive stresses on the other half at the same instant of time, thereby producing some cancelling effect on the dynamic response of the soil. As a consequence, the depth of the supporting rigid rock has less importance than in the case of translational excitation, where the stresses under the footing are most likely of the same sign at any instant of time, increasing the depth of the effective "bulb of pressure."

Except at the first resonance, the compliance functions follow quite well the trend of the half-space solutions of Fig. 3-12. The difference is more marked when the stratum is shallow, since wave reflections at the rock and free surface are then more impor-

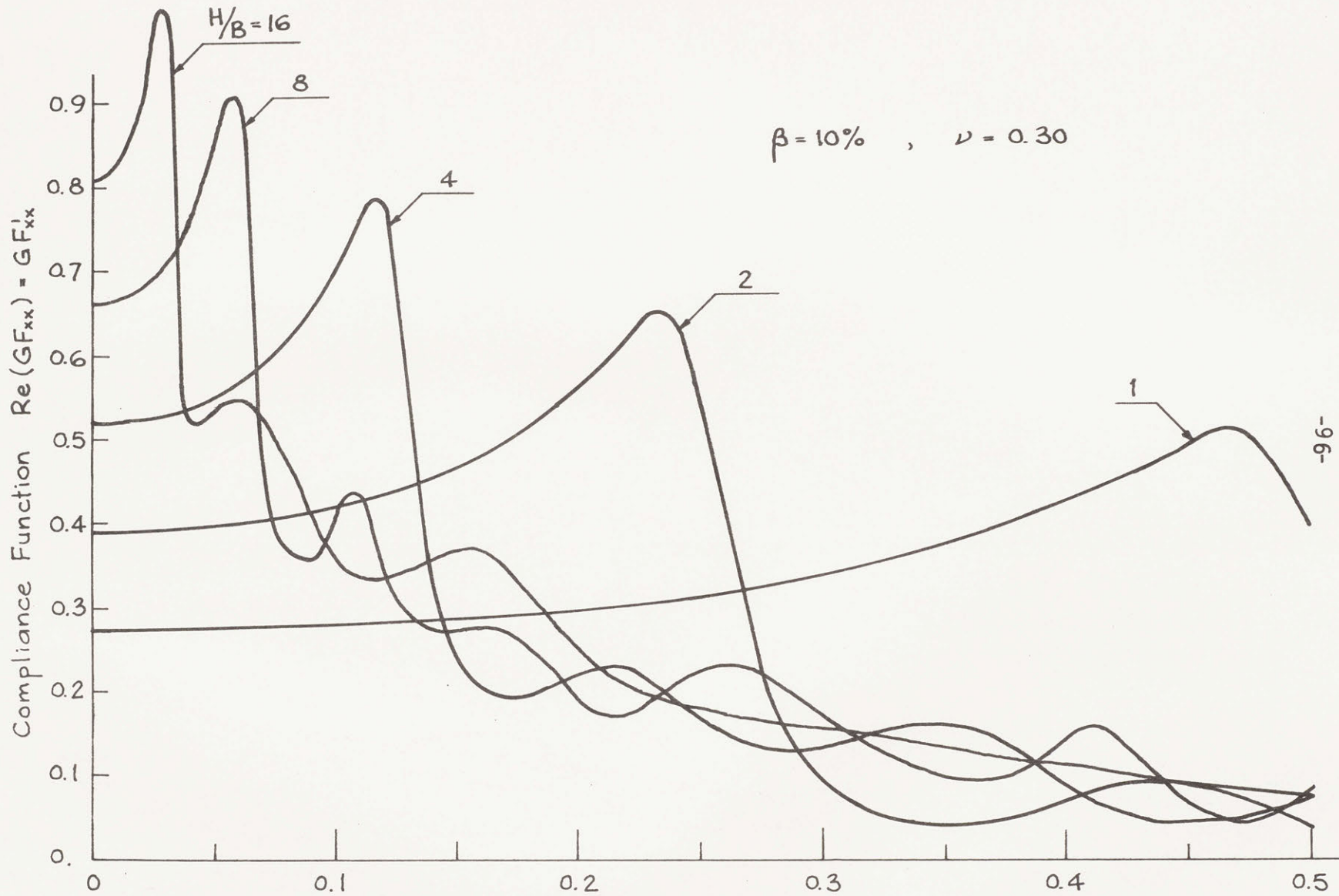
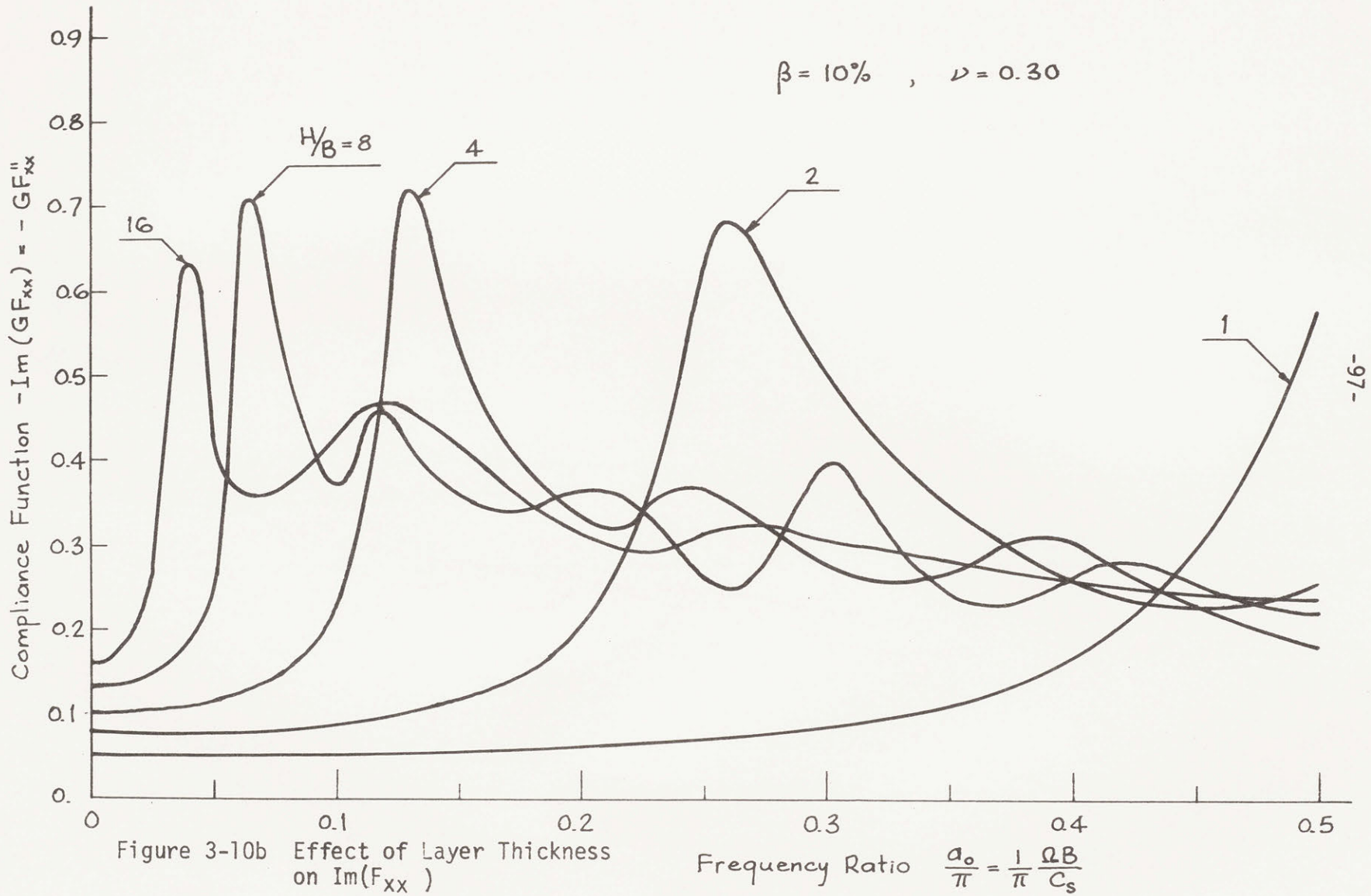
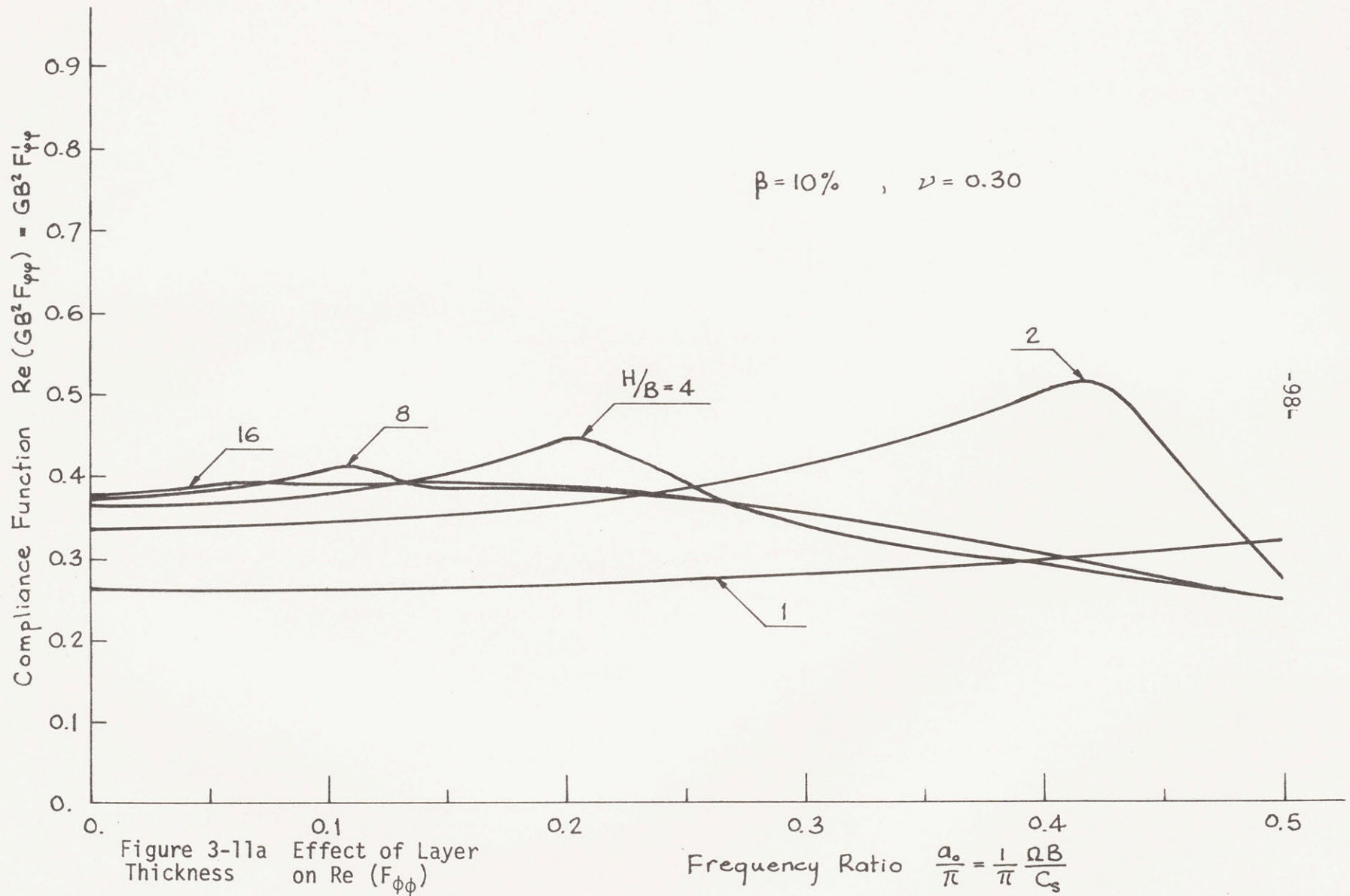
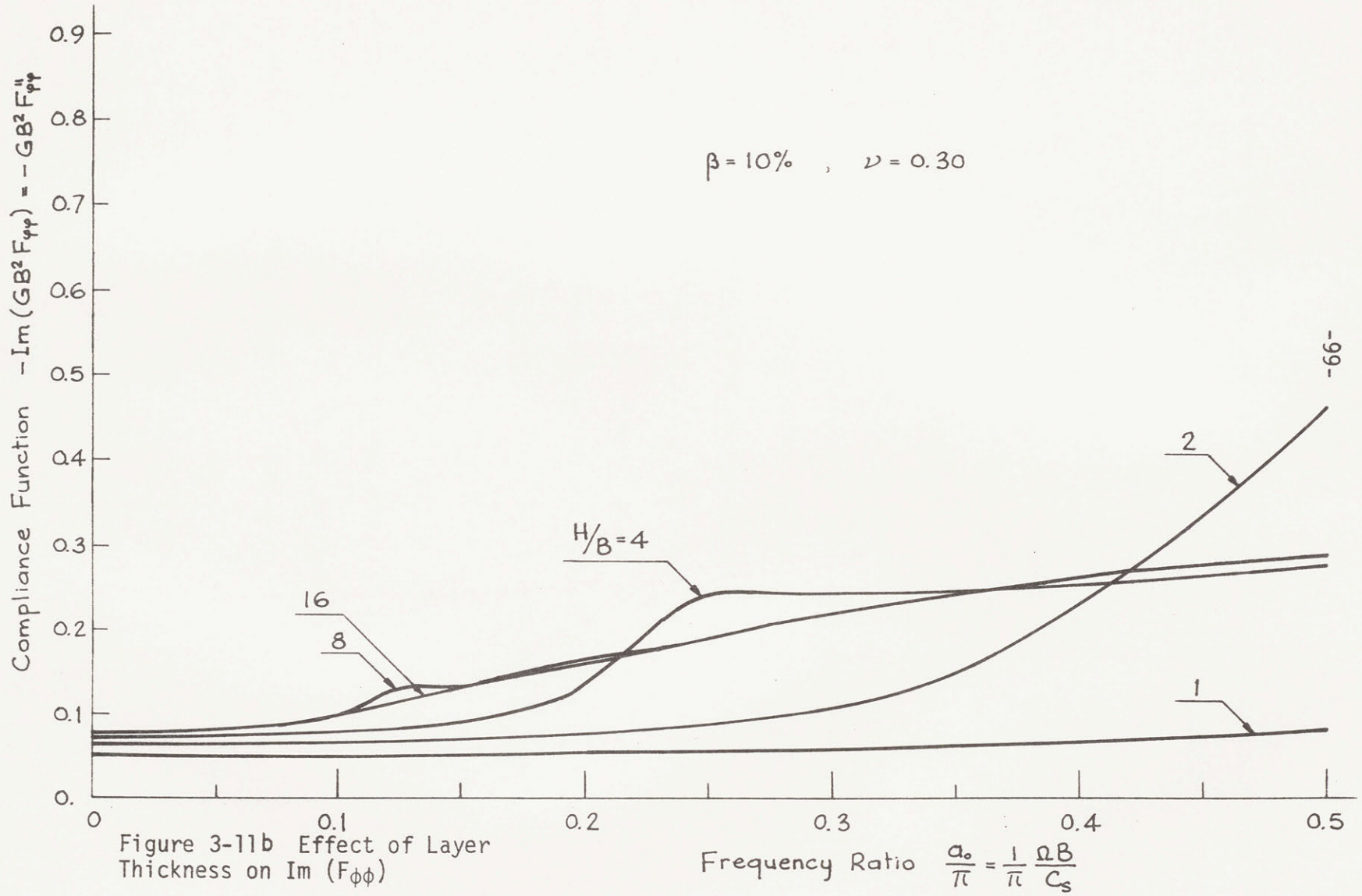


Figure 3-10a Effect of Layer Thickness on $Re(F_{xx})$

Frequency Ratio $\frac{\omega_0}{\pi} = \frac{1}{\pi} \frac{\omega B}{C_s}$







tant. In this case, the closeness of the rigid bottom does not allow enough radiation damping, besides producing a stiffening effect and increasing the resonant frequency.

It is noted that, as the H/B ratio increases, the compliance functions are more wavy, but this is due to the larger number of resonance frequencies occurring in the frequency ratio range under consideration, $0 \leq a_0 \leq 0.5\pi$. However, the series of peaks smooth out as H/B increases, and also as a_0 increases.

The compliance, and hence the stiffness, functions vary considerably with frequency, thus making it difficult to represent the system using a one or two degree of freedom model composed of a mass, springs and dashpots; unless a very small range of frequencies is considered.

The stiffness function K'_{xx} may become negative for some range of frequencies, as illustrated in Fig. 3-4 for the case of H/B = 2. This situation happens only in shallow strata. For H/B = 4 and up this phenomenon does not occur. This implies that, at some frequencies, the restraining action of the stiffness is more than offset by the effect of the inertia forces due to the mass of soil.

In the three solutions for the half-space illustrated in Fig. 3-12, the following comments apply. The solutions by Karasudhi et al. [22] and by Luco and Westmann [31] are analytical; but both make some simplifying assumptions with regard to interface conditions between the footing and the soil. These solutions apply to a perfectly elastic half-space, and they cannot therefore be directly

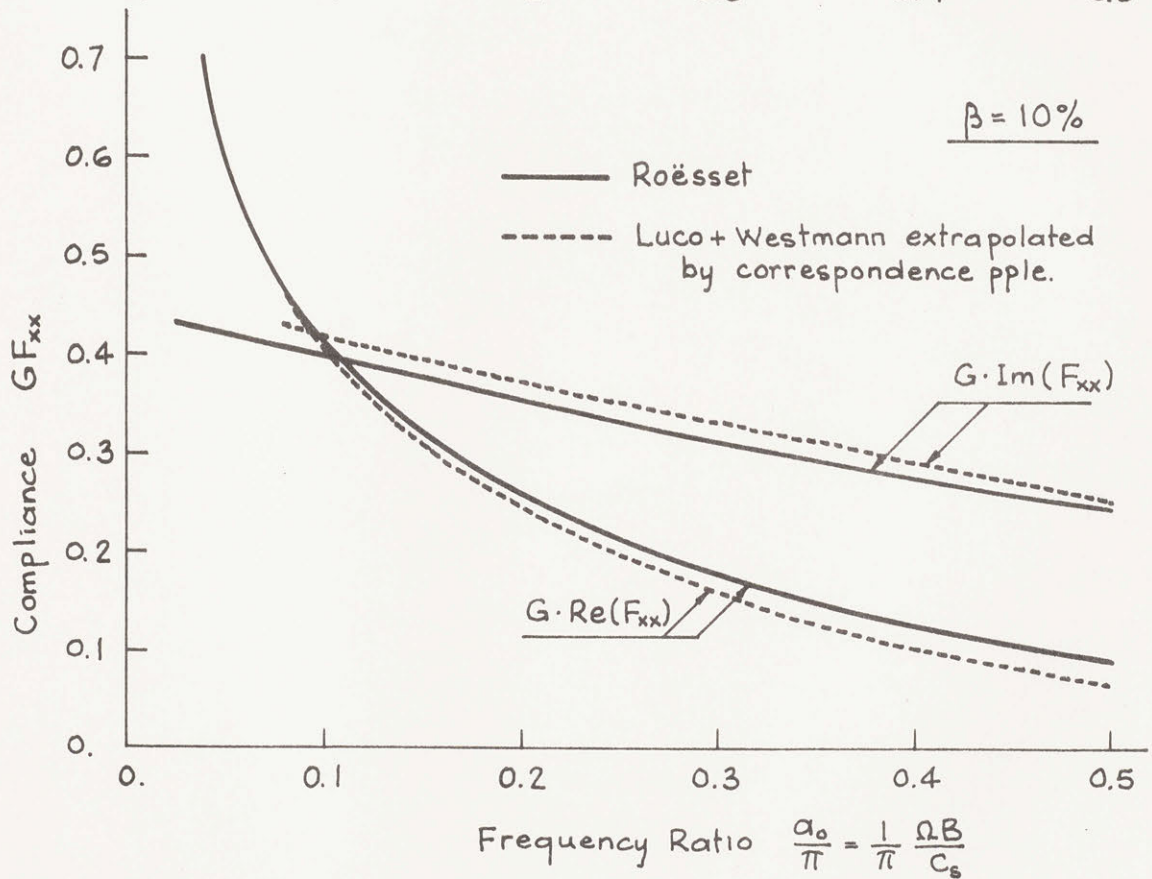
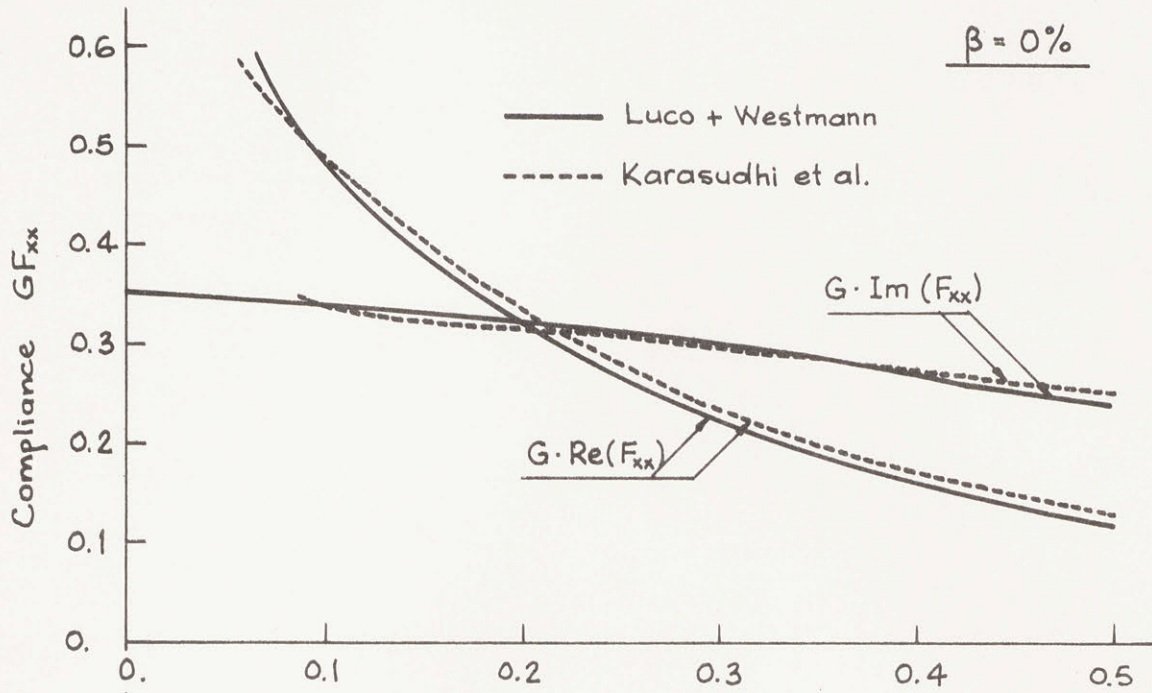


Figure 3-12a Half-Space Solution for F_{xx} , $\nu = 0.30$

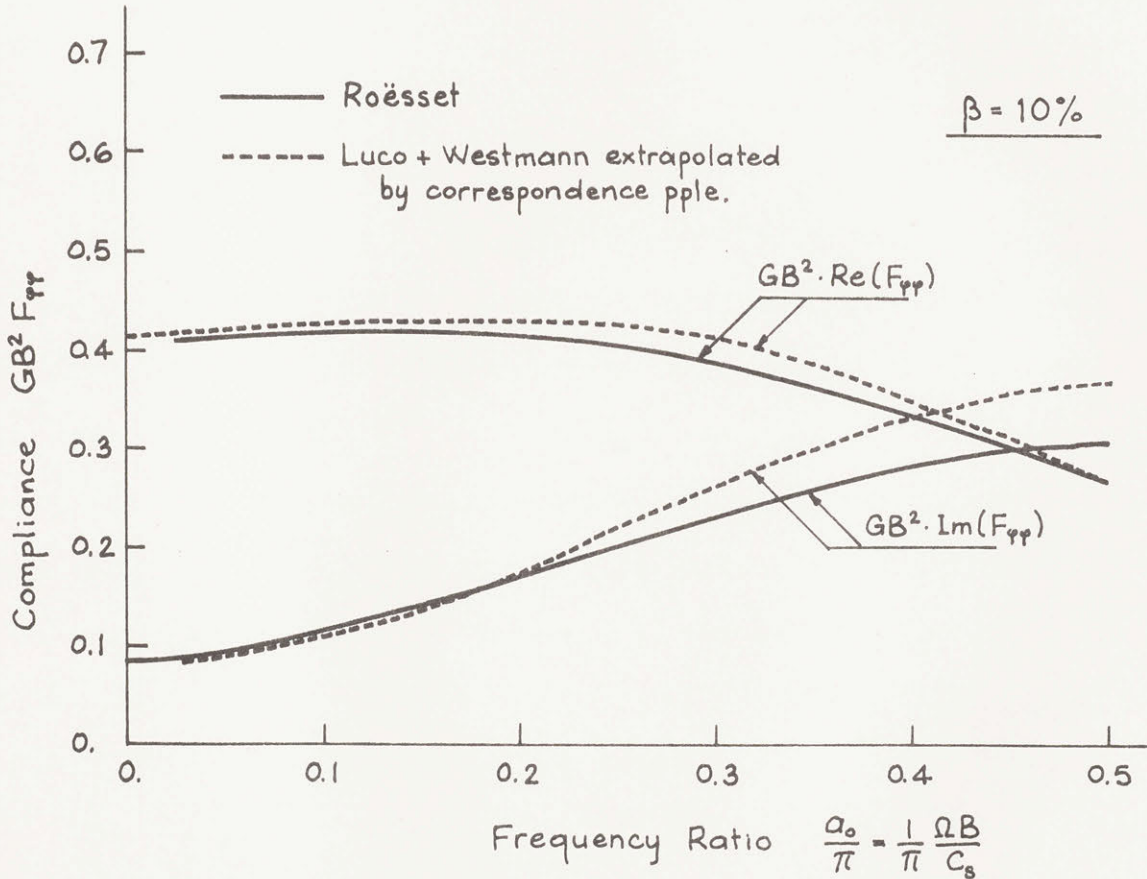
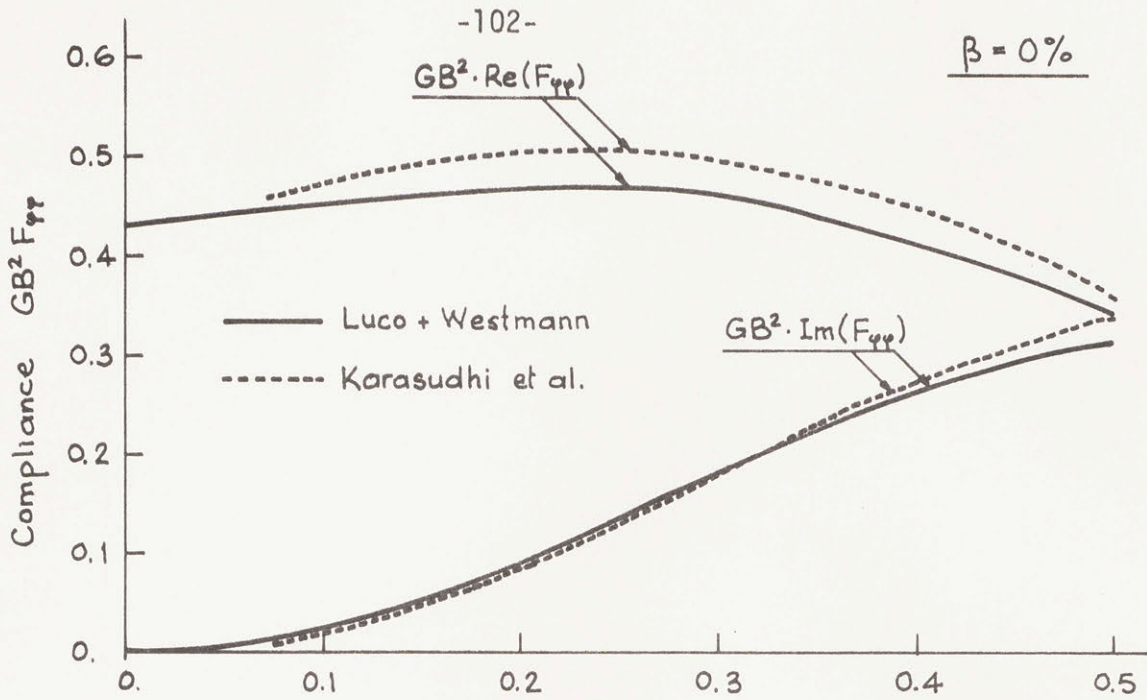


Figure 3-12b Half-Space Solution for $F_{\phi\phi}$, $\nu = 0.30$

compared with the solutions obtained by PLAXLY2, where damping was considered. Application of the corresponding principle [8] to derive a solution for $\beta = 10\%$ is not valid, since inertia terms do not change with hysteretic damping, whereas the elastic moduli do. For low frequencies, the correspondence principle should give fairly good results. The solution by Roësset [47] was derived using a fast Fourier transform [11] for a load under the footing and then integrating across the width and imposing the condition of rigid body motion in this area. This solution can take damping into consideration.

3.4 Effect of Mass

From the knowledge of the compliance and amplification functions, the response of a rigid structure with arbitrary mass distribution (but symmetrical about a vertical axis) can be found, as described in Section 2.4.

Four parameters define the rigid block of infinite length in Fig. 3-13: the width of the base $2B$, the mass M , the height of the center of gravity (C) above the bottom E, and the radius of gyration with respect to the center of gravity S. Three dimensionless parameters can be defined from these four quantities:

$$\text{mass ratio, } B_x = \frac{M}{\rho B^2}$$

$$\text{height of c.g. Ratio, } e = \frac{E}{B}$$

$$\text{radius of gyration ratio, } s = \frac{S}{B}$$

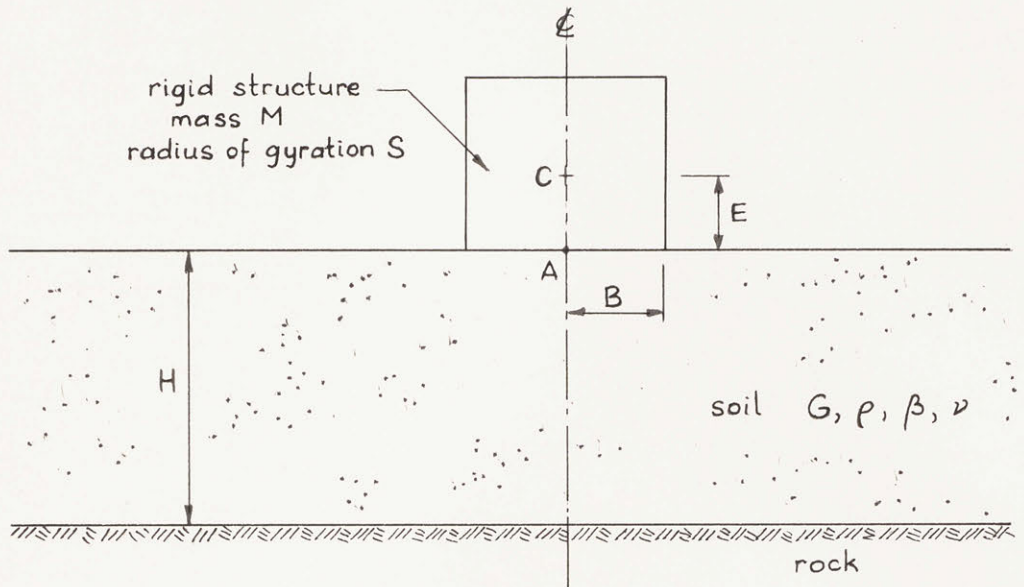


Figure 3-13

Figs. 3-14 and 3-15 show the amplification curves as given by the response of the bottom of the structure u_A/u_R for two different layer depths, $H/B = 1$ and 2 , respectively. They are applicable to the case of $e = 2/3$ and $s = 1$, and with a soil having 10% hysteretic damping and Poisson's ratio of 0.30. The responses for mass ratios $B_x = 0, 1, 2, 4$ are depicted.

Increasing mass ratios shift the resonant frequencies towards lower values, the effect being more pronounced as the stratum gets shallower.

As the mass ratio increases, there is first an increase in the maximum amplification of the first peak, and then it becomes smaller and tends towards a value of 1 at the static frequency. The reason for this behavior is that the "effective" stiffness, $[K] - \Omega^2[J]$, is reduced as the mass of the structure increases, thereby producing

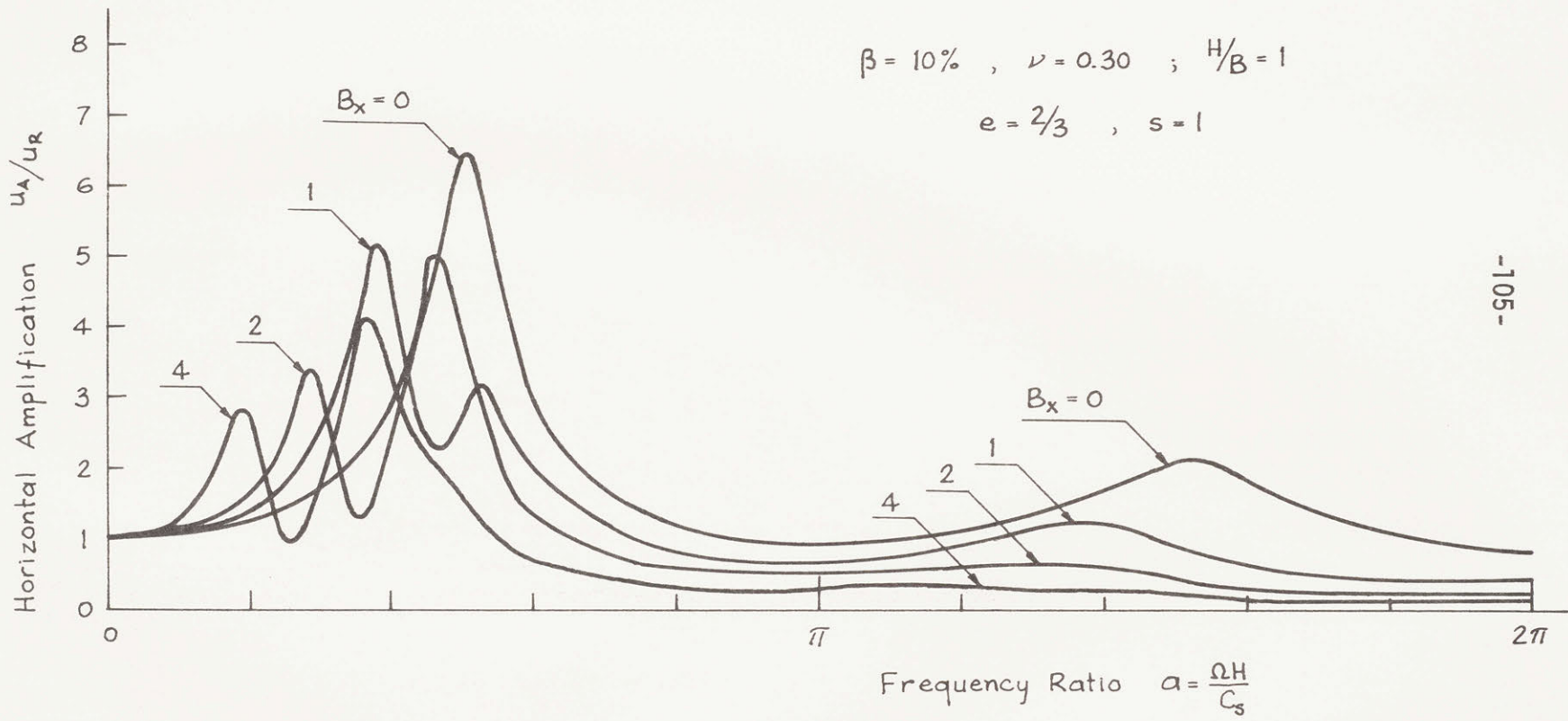


Figure 3-14 Effect of Mass on Horizontal Amplification, $H/B=1$

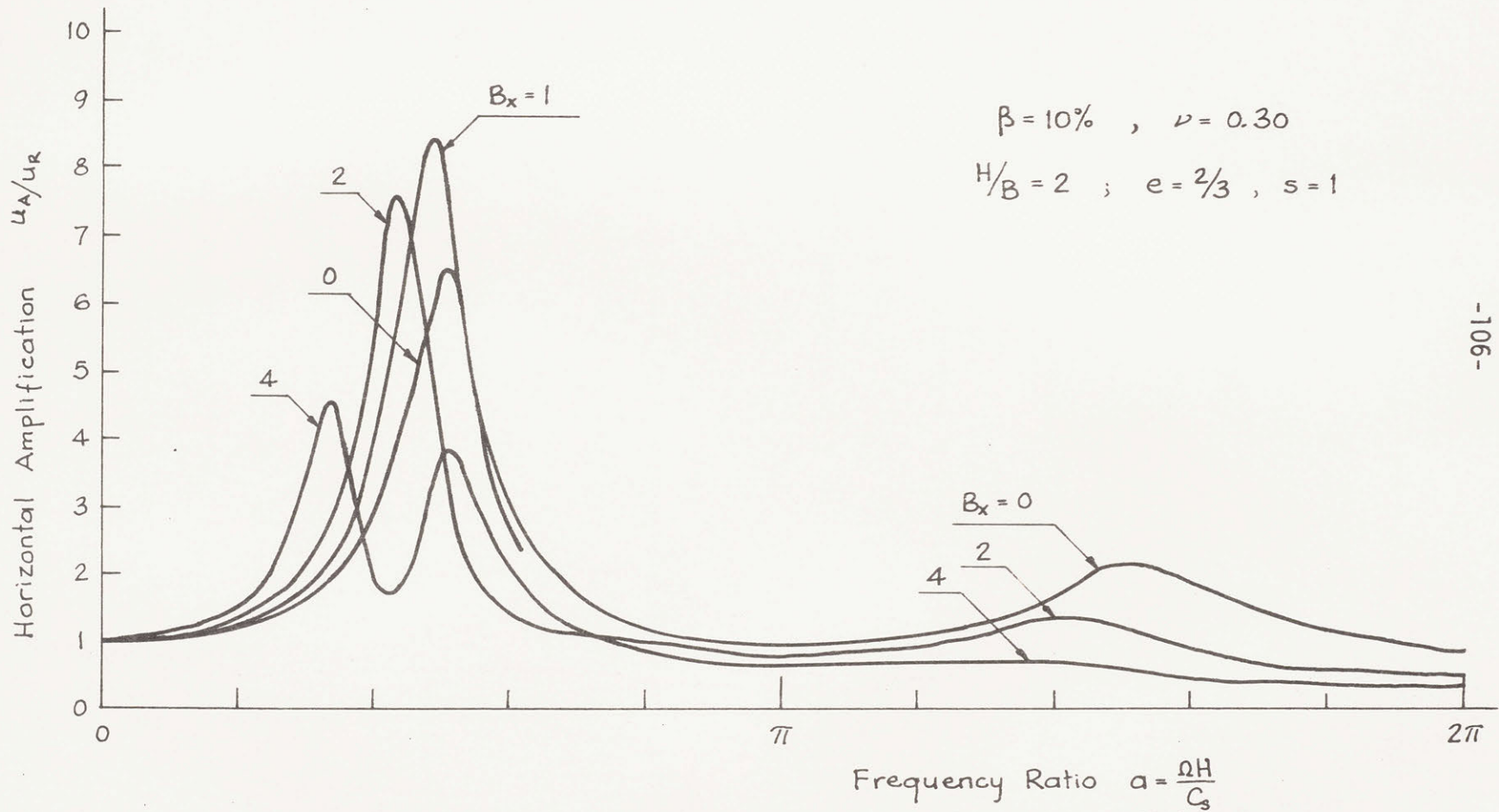


Figure 3-15 Effect of Mass on Horizontal Amplification, $H/B=2$

larger displacements. But for large values of B_x , the inertia term $-\omega^2[J]$ overcomes the stiffness $[K]$; and consequently, the "effective" stiffness increases again, but with the inertia term dominating. This results in smaller displacements. At the same time, the fact that all the soil surface has smaller displacements for low frequencies, adds to the reduction in the height of the peaks for high mass ratios. For deep strata, the range of B_x for which the peaks keep increasing is larger.

Another interesting observation is that as the mass ratio increases, the amplification curve u_A/u_R starts showing two distinctive peaks in the neighborhood of the first resonant frequency. This happens for even low mass ratios when the layer of soil is shallow enough.

The first peak is caused by resonance in swaying. The second peak is due to excitation of the rocking mode, which occurs more easily when the stratum is thin, and/or when the mass moment of inertia is high. This second peak starts forming at the resonant frequency for vertical vibration; and shifts towards the resonant frequency for horizontal excitation (at $a = \pi/2$), as B_x is increased. At the same time, this peak increases in height. After crossing the frequency ratio $a = \pi/2$, it starts becoming smaller again. This is illustrated in the detail of Fig. 3-16. A similar effect occurs when the density ρ_{st} of the structure is kept constant, and its height is varied (with a corresponding change in position of the center of gravity and value of the radius of gyration). This is

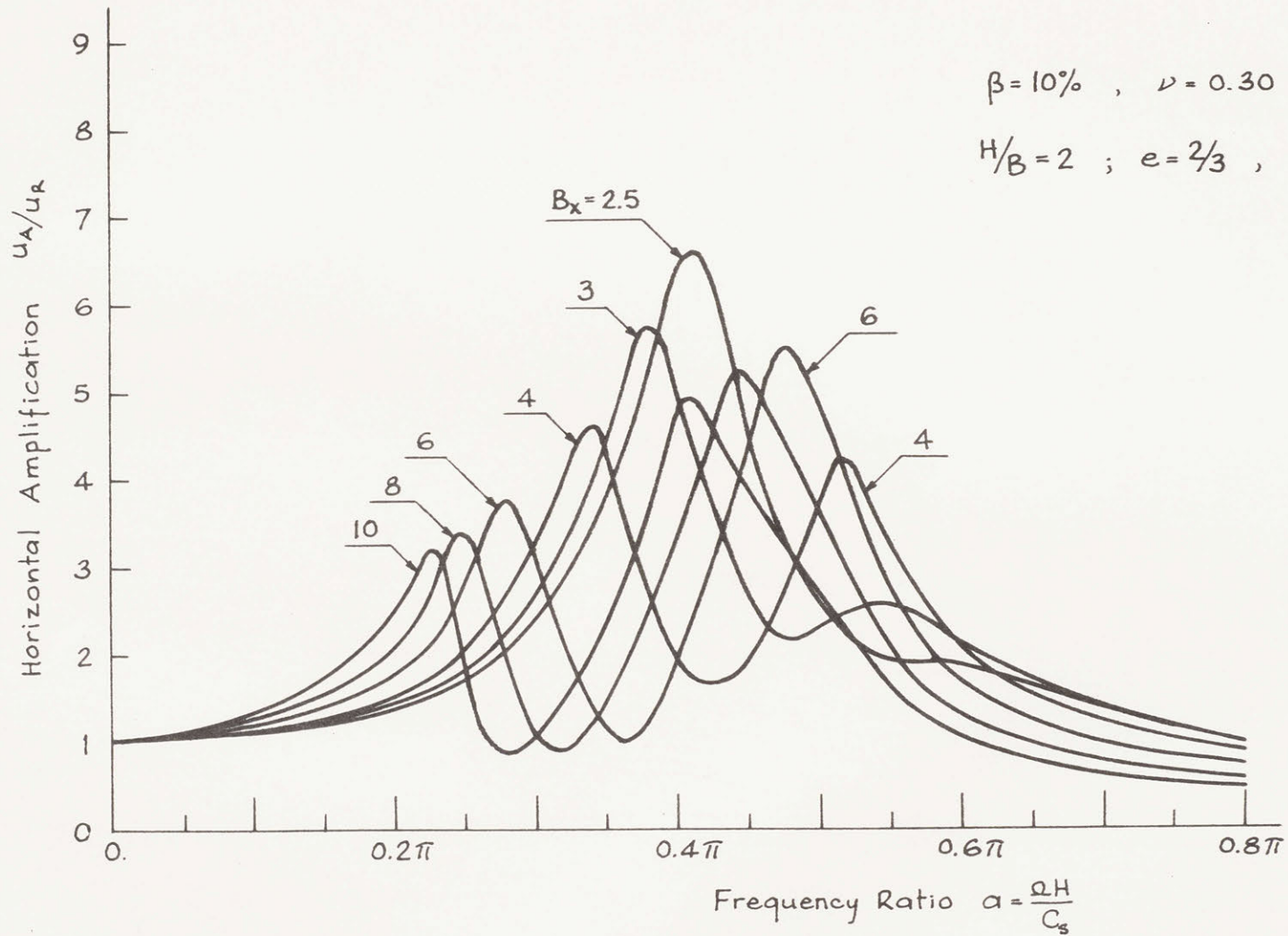


Figure 3-16 Effect of High Mass Ratios on Horizontal Amplification

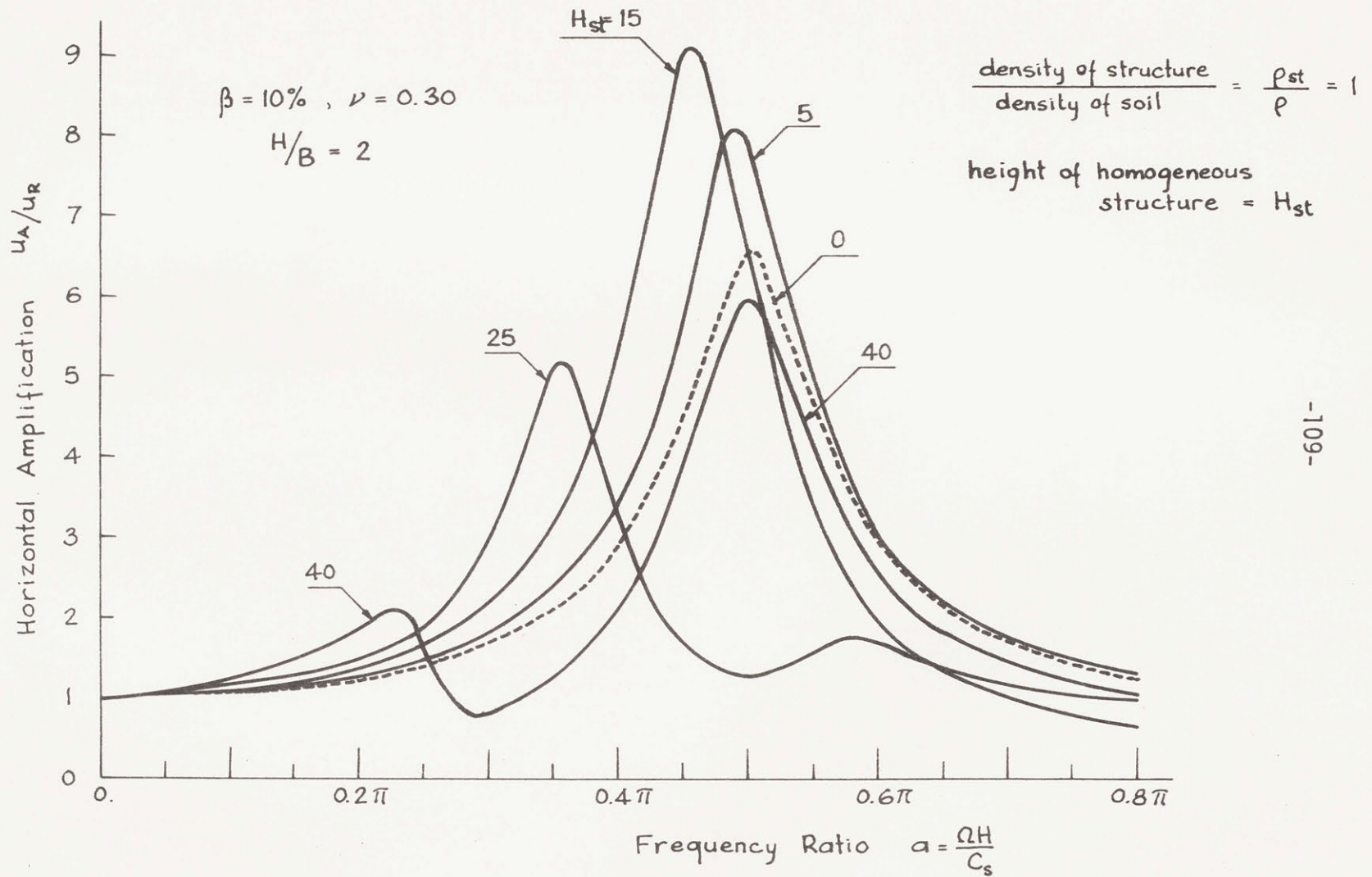


Figure 3-17 Effect of Height of Structure on Horizontal Amplification

shown in Fig. 3-17, where H_{st} is the height of the homogeneous structure of rectangular cross-section, with base-width $2B$.

In order to show that the second peak is due to the excitation of rocking, the following approximate calculations can be done.

Assume that the stiffnesses vary parabolically in the range of frequencies where the two peaks occur. Neglect the cross stiffness $K_{x\phi} = K_{\phi x}$ as well as damping. For the case of $H/B = 2$, Figs. 3-6 and 3-7 show that K'_{xx} and $K'_{\phi\phi}$ can be approximated by

$$K'_{xx} = (2.48 - 0.70 a^2)G$$

$$K'_{\phi\phi} = (2.88 - 0.196 a^2)GB^2$$

Therefore,

$$\begin{aligned} [K] &\cong \begin{bmatrix} K'_{xx} & 0 \\ 0 & K'_{\phi\phi} \end{bmatrix} \\ &\cong G \begin{bmatrix} 1 & 0 \\ 0 & B \end{bmatrix} \begin{bmatrix} (2.48 - 0.70 a^2) & 0 \\ 0 & (2.88 - 0.196 a^2) \end{bmatrix} \begin{bmatrix} 1 & 0 \\ 0 & B \end{bmatrix} \\ &= G[\tilde{B}]^T [\tilde{K}] [\tilde{B}] \end{aligned}$$

where the matrices $[\tilde{B}]$ and $[\tilde{K}]$ are self-explanatory. The inertia term is

$$\Omega^2 [J] = a^2 B_x \left(\frac{B}{H}\right)^2 G[\tilde{B}]^T \begin{bmatrix} 1 & -e \\ -e & e^2 + s^2 \end{bmatrix} [\tilde{B}]$$

where $e = 2/3$ and $s = 1$ for this example. Consider the case of $B_x = 4$, as shown in Fig. 3-18. Then, resonance occurs when

$$([K] - \Omega^2 [J]) \{\delta\} = \{0\} \quad ,$$

and in order to have a non-zero solution,

$$\det ([K] - \Omega^2 [J]) = 0$$

which implies

$$\begin{vmatrix} (2.48 - 0.70 a^2) - a^2 & 0.67 a^2 \\ 0.67 a^2 & (2.88 - 0.196 a^2) - 1.445 a^2 \end{vmatrix} = 0$$

since $B_x \left(\frac{B}{H}\right)^2 = 4 \times \left(\frac{1}{2}\right)^2 = 1$ and $\det [\tilde{B}] \neq 0$

Solving the frequency equation given above, gives two positive real roots, $a = 0.34\pi$ and $a = 0.52\pi$. These frequencies correspond remarkably well to the location of the two peaks. The respective eigenmodes are

$$\begin{Bmatrix} u \\ \phi B \end{Bmatrix} = \begin{Bmatrix} 1 \\ -0.74 \end{Bmatrix} \text{ and } \begin{Bmatrix} 1 \\ 1.17 \end{Bmatrix}$$

which show that for the first peak the swaying predominates, and the structure rotates about a point below the base of the footing (to speak in simple terms); and for the second peak, the rocking predominates, and the rotation occurs about a point higher than the base. The uncoupled resonant frequencies are

$$\omega_x = 1.21 \text{ rad/sec for swaying } (a = 0.385\pi)$$

$$\omega_\phi = 1.33 \text{ rad/sec for rocking } (a = 0.42\pi)$$

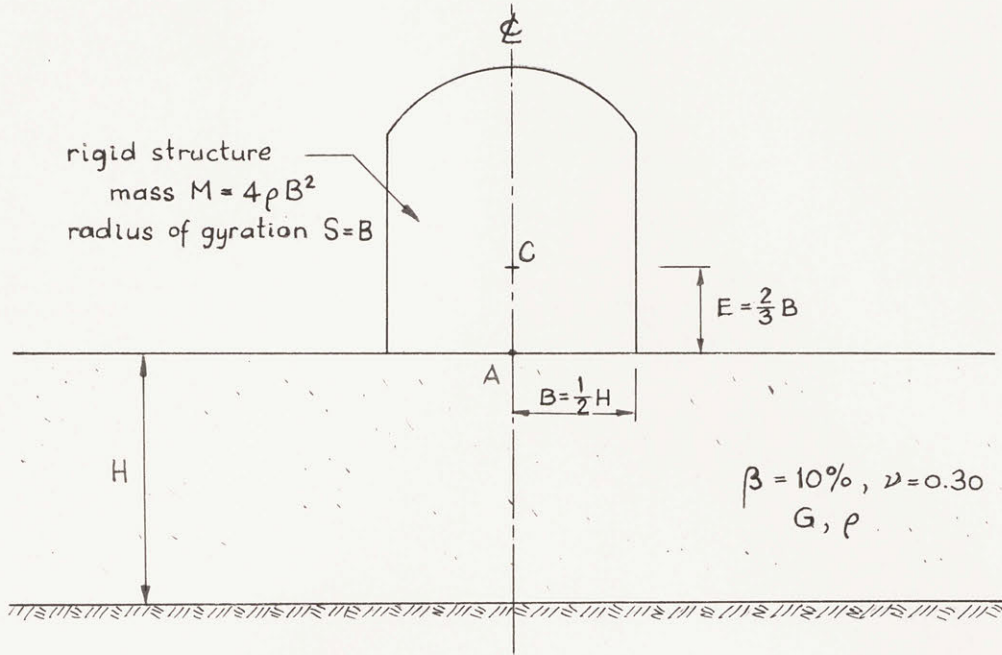


Figure 3-18

The motion of the rigid structure can be decomposed in two parts. The amplification of the soil at the surface, u_0 , and the interaction, given by u_A/u_0 . In this way, the interaction effect can be observed more clearly.

Fig. 3-19 shows the effect of interaction for a mass ratio of 2 and different H/B ratios. It is seen that after the first peak, this effect is basically beneficial; that is, the response under the structure with mass is smaller than the free-field motion (indicated by the line $u_A/u_0 = 1$). For shallow layers, the reduction in amplitude is considerable.

Similarly, Fig. 3-20 shows the interaction for structures of different mass ratios sitting on a layer with a ratio H/B equal to 2. The peaks are higher as B_x increases, but the reduction at higher frequencies is also more pronounced. For deeper strata, the differ-

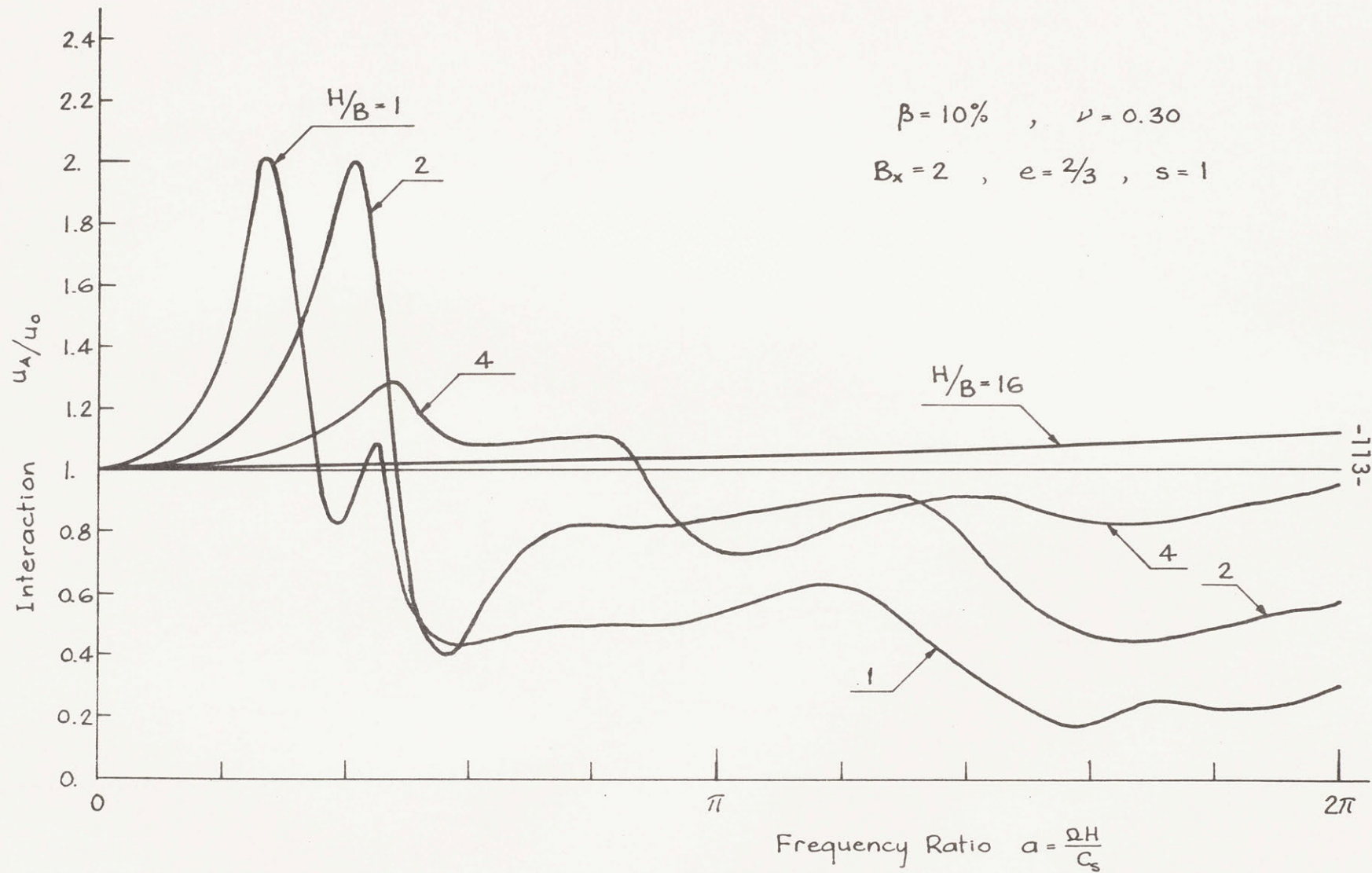


Figure 3-19 Effect of Layer Thickness on Interaction

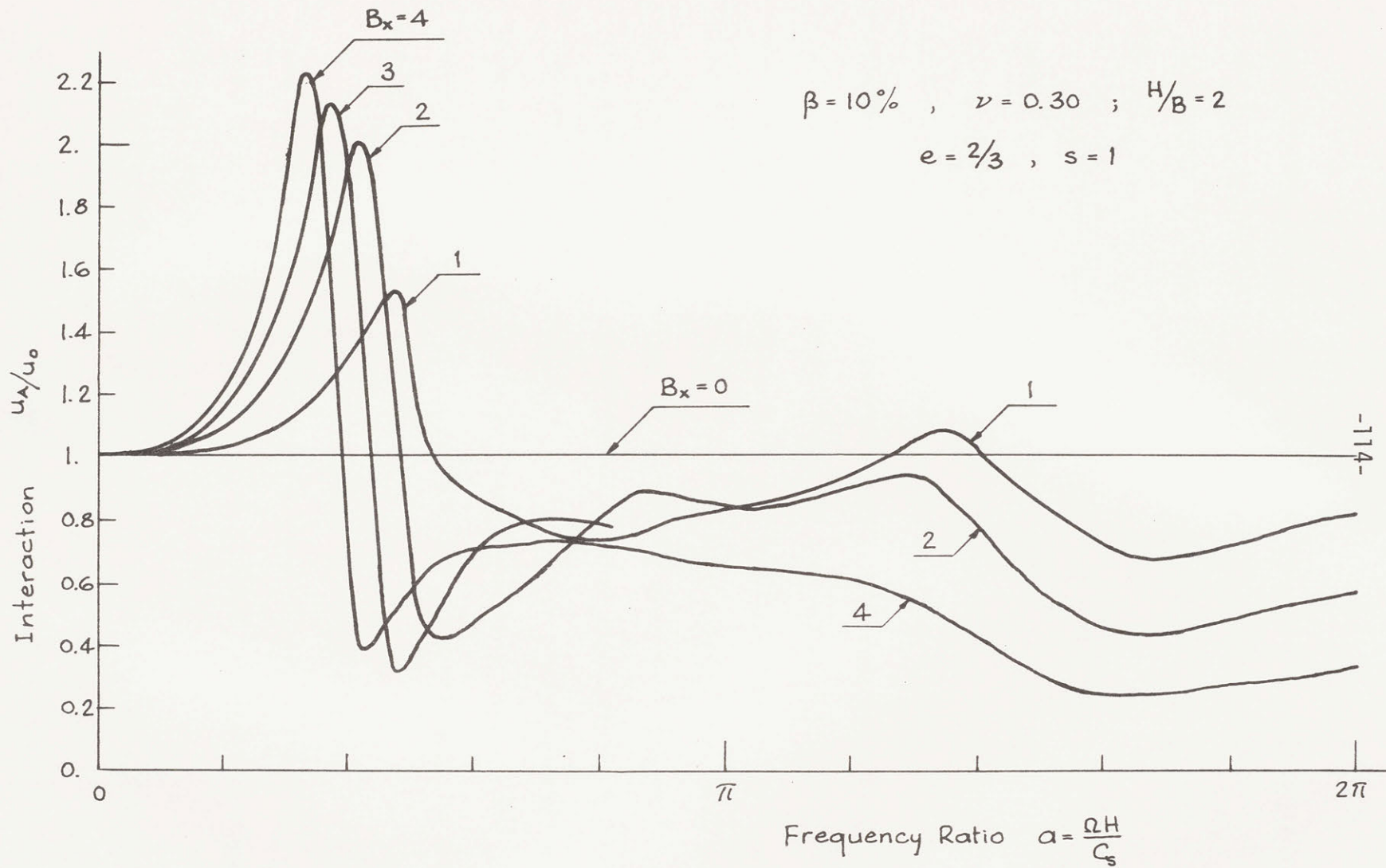


Figure 3-20 Effect of Mass on Interaction

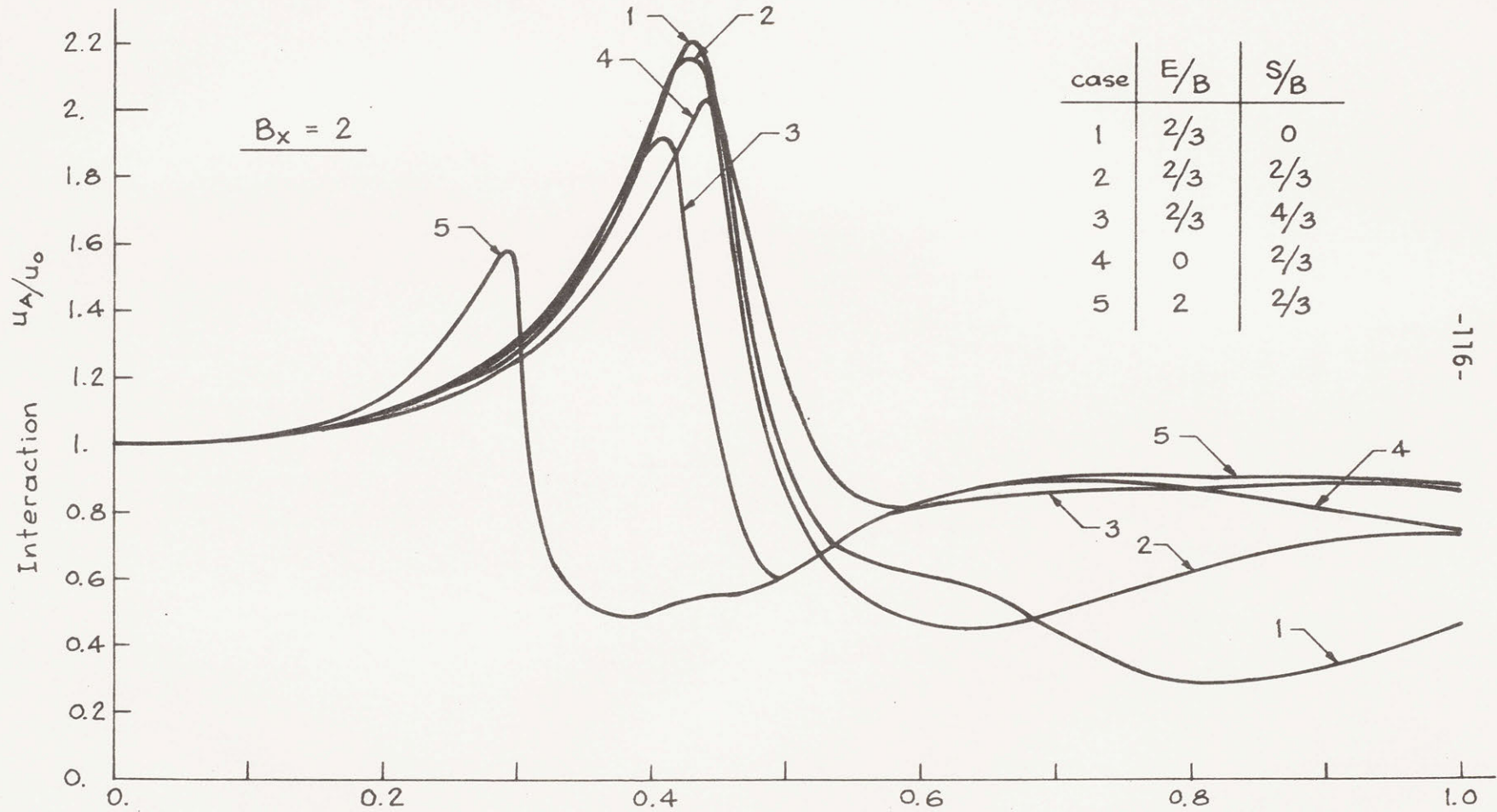
ence between the curves is less perceptible, since then the effect of 1-D amplification is much more important than the effect of interaction; therefore, the interaction curves are closer to a straight line at $u_A/u_0 = 1$.

The effect of changing the location of the center of gravity and/or the radius of gyration while keeping the mass ratio constant is illustrated in Fig. 3-21, for rather extreme values of e and s . Changing the radius of gyration, while keeping B_x and e constant, does not modify the response noticeably for frequencies below resonance; and at higher frequencies, when the interaction effect produces displacements smaller than the free-field motion, it is more beneficial when the mass is concentrated closer to the center of gravity (i.e. small values of s). Changing e while keeping B_x and s constant produces a marked change for low frequencies, as seen from the curves for cases 2, 4 and 5. As the center of gravity moves up, the peak of the interaction curve moves towards the left; whereas increasing the radius of gyration shifts the peak to the right.

For actual structures, the peaks are expected to be flatter than the ones shown in these figures; since there is radiation in three directions, rather than only in a plane, as the cases being studied here consider.

Furthermore, the larger or smaller benefit of the interaction effect depends on the frequency content of the applied earthquake motion. If most of the frequency components of the applied motion

$\beta = 10\%$, $\nu = 0.30$; $H/B = 2$



-116-

Figure 3-21 Effect of Height of Center of Gravity and Radius of Gyration on Interaction Frequency Ratio $\frac{a}{\pi} = \frac{1}{\pi} \frac{\Omega H}{c_s}$

lie in the neighborhood of the peaks of the interaction curves, the resulting motion will be greatly amplified. If the earthquake motion is applied at the rock level, the interaction curves might be misleading, since the total response of the structure depends also on the magnification due to the soil (1-D amplification).

CHAPTER 4 - EFFECT OF EMBEDMENT

4.1 Introduction

The response of a rigid strip footing resting on the surface of a homogeneous layer of soil has been studied in Chapter 3. In many cases, structures are embedded in the soil, and this embedment should affect the response. It is the purpose of this chapter to determine compliance functions for some embedded foundations, and their response to harmonic horizontal motions in the rock underlying the soil stratum. The model used assumes that the soil is capable of resisting tensile stresses, so that, at any moment, the footing remains welded to the soil. Besides, the soil is taken as linearly viscoelastic. Therefore, it is expected that the "actual" footing will experience displacements somewhat larger than predicted in this study.

4.2 Amplification Functions

The one-dimensional amplification theory [21, 48] is no longer strictly applicable for determining the motion at the base of the rigid footing given harmonically varying prescribed displacements in the rock. Fig. 4-1 shows the geometry and parameters involved in this problem. The notation used is basically the same as in Chapter 3. The response of the footing relative to the rock motion, u_A/u_R , is plotted against the frequency factor $a = \Omega H/C_s$ in Fig. 4-2 for different embedment ratios D/H . These curves apply for a layer with $H/B = 2$, $\beta = 10\%$ and $\nu = 0.30$. It can be observed that as

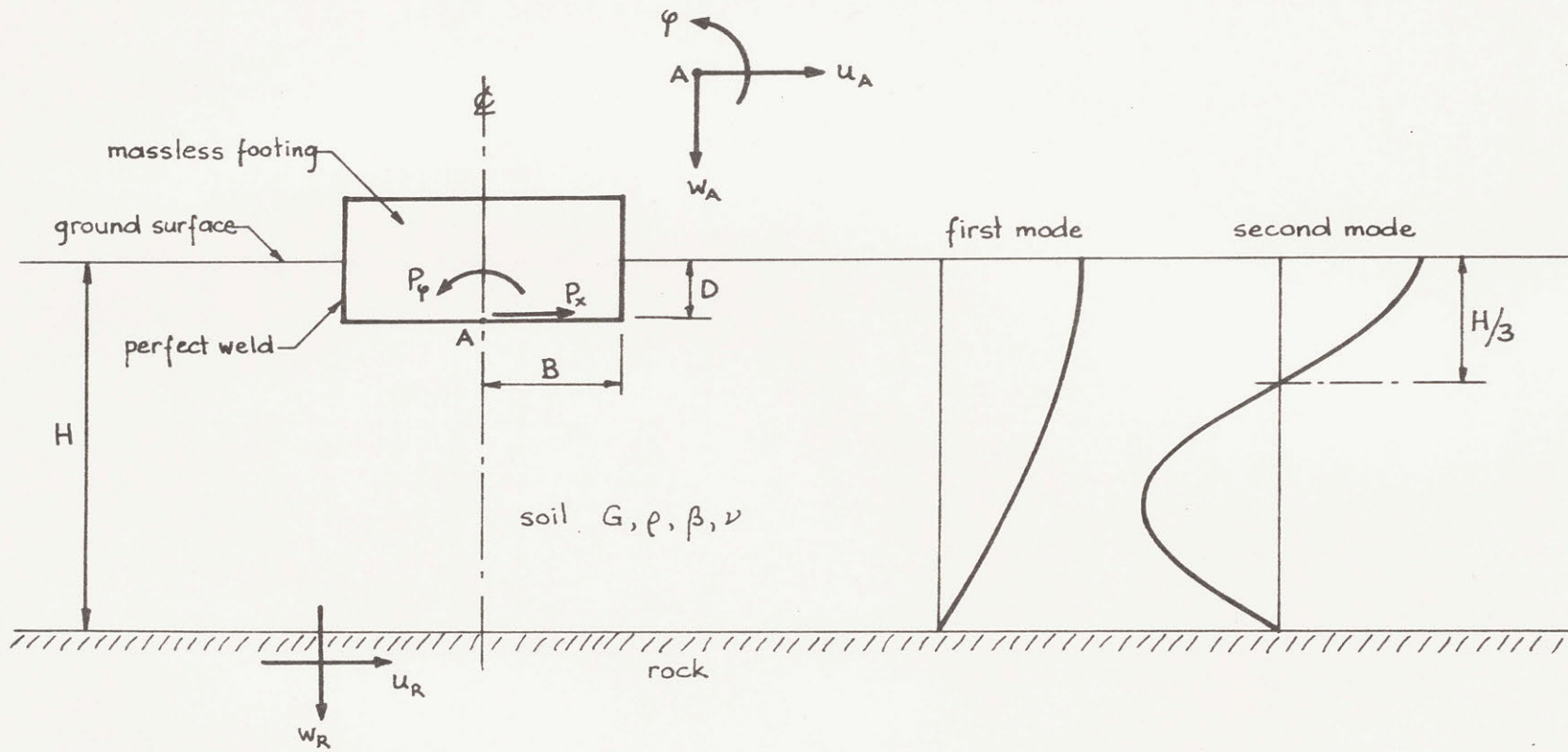


Figure 4-1 Geometry for Embedded Footing

embedment increases, the dynamic response u_A/u_R is reduced for all frequencies. The reduction is particularly strong in the neighborhood of the peaks. The frequency at these peaks is practically unaltered as the massless footing is embedded into the soil, although there is actually a very slight shift towards higher frequencies.

When the footing rests on the ground surface, the response u_A is the same as that given by the 1-D amplification theory. For embedded footings, Fig. 4-3 compares the "actual" response against the motion predicted by the 1-D amplification theory at the level of the base of the footing. It is seen that the latter tends to overestimate the response for low frequencies until past the fundamental resonant frequency; and to underestimate the response thereafter. Notice that the second peak does not develop for the footing embedded one-third of the layer thickness when 1-D theory is used, since at the corresponding frequency ($a = 3\pi/2$) the node of the mode shape is at that level, as shown in Fig. 4-1.

Whereas a massless footing on the surface of the stratum does not exhibit a rocking motion, an embedded footing does, as shown in Fig. 4-4, where the rocking is expressed in terms of the vertical displacement of the footing edge, $\phi B/u_R$. This figure applies for the same stratum of soil used in the preceding figures. In general, as the depth of embedment increases (within the practical range), the rotation becomes larger. While the vertical displacement of the footing edge is only a small percentage of the horizontal motion, it tends to increase as the frequency increases, then making rock-

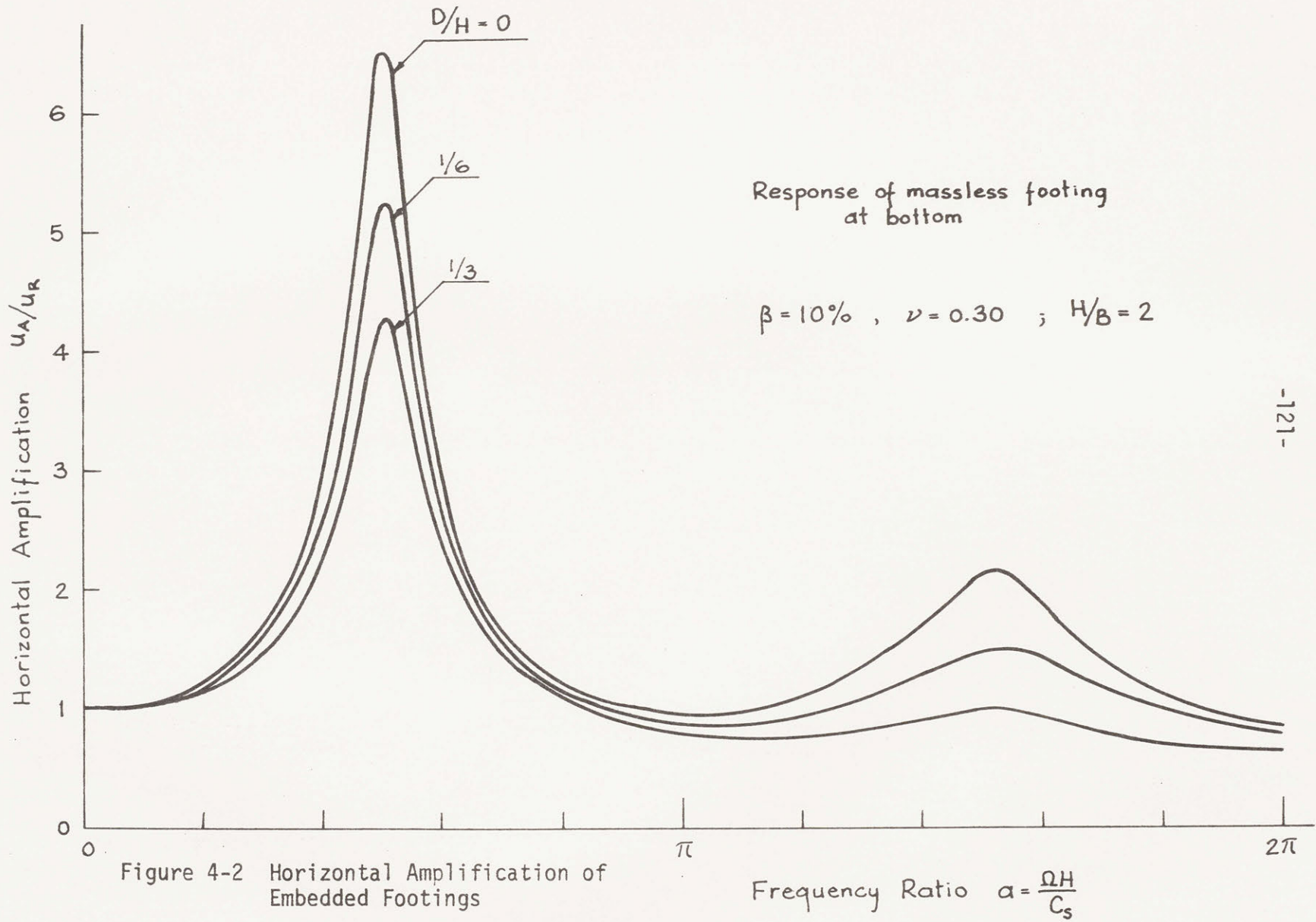


Figure 4-2 Horizontal Amplification of Embedded Footings

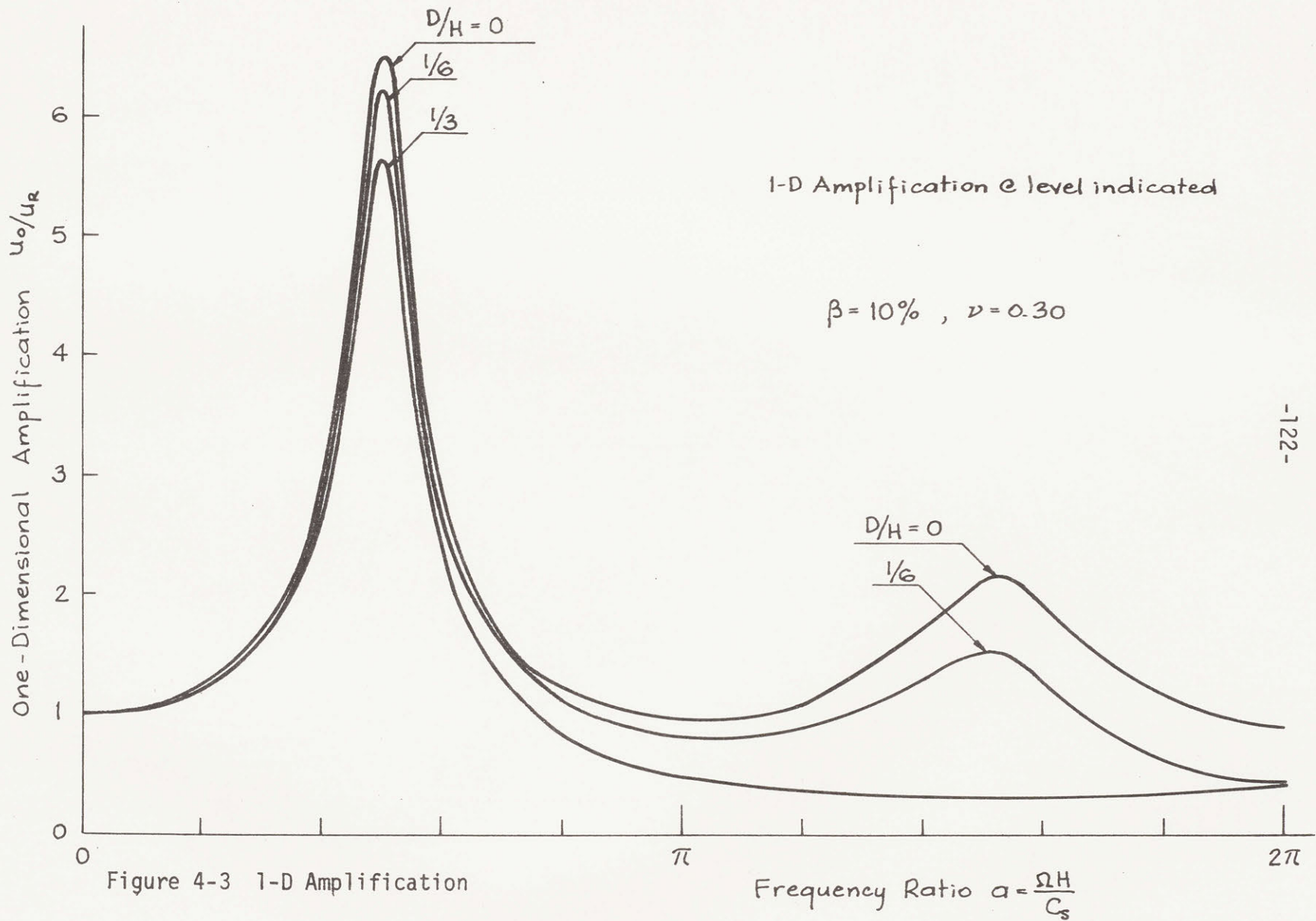


Figure 4-3 1-D Amplification

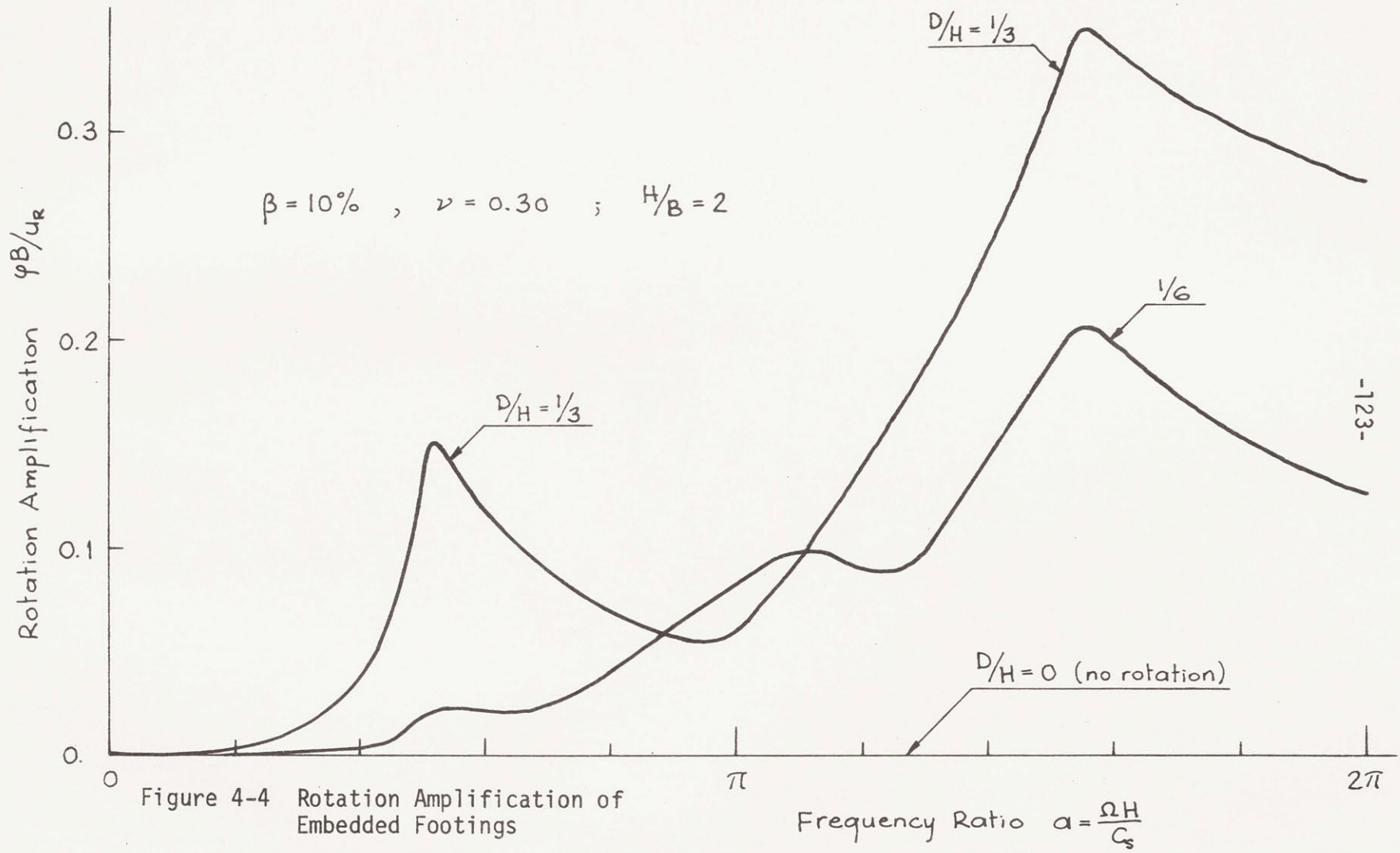


Figure 4-4 Rotation Amplification of Embedded Footings

ing important.

Fig. 4-5 illustrates the phase angles or phase lag of u_A and ϕ with respect to u_R for the same embedment ratios used before. At least for the swaying motion, it can be observed that the response tends to follow more closely the motion of the rock as embedment increases. This is expected, since the base of the footing will be physically closer to the rock.

Fig. 4-6 shows the amplification function for an embedment ratio $D/B = 2/3$, and different layer thicknesses. Logically, for shallow layers, the amplification should be small, tending to 1 as H/B tends to D/B ; and tending to the 1-D amplification at the surface as the layer thickness increases. The reason the amplification for $H/B = 2$ in the neighborhood of the second resonant frequency is smaller than that for $H/B=1$ is that, in the former case, the node of the mode shape of the 1-D amplification is at a depth equal to the level of the footing base (see Fig. 4-3), thereby producing only small displacements at point A.

The effect of embedment is isolated in Fig. 4-7 for the same cases considered in the previous figure. It shows the variation of u_A/u_0 against frequency ratio a , that is, the response of the footing compared to the free-field response at the surface. The embedment produces a beneficial effect, especially around the resonant frequencies, where the reduction is considerable.

The effect of embedment can also be shown in terms of a constant embedment ratio D/H , i.e. depth referred to the layer thickness,

$$\beta = 10\% \quad , \quad \nu = 0.30 \quad ; \quad H/B = 2$$

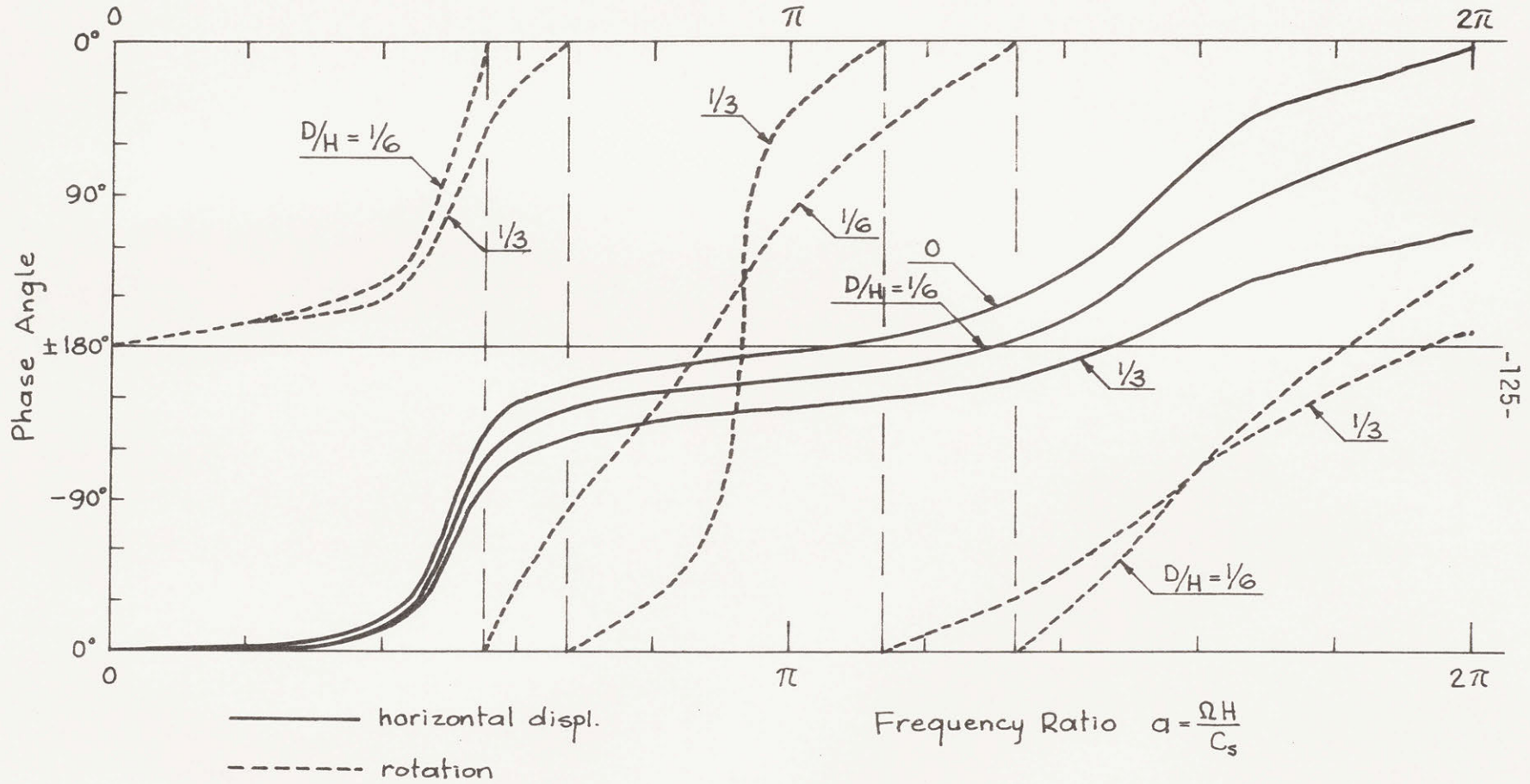
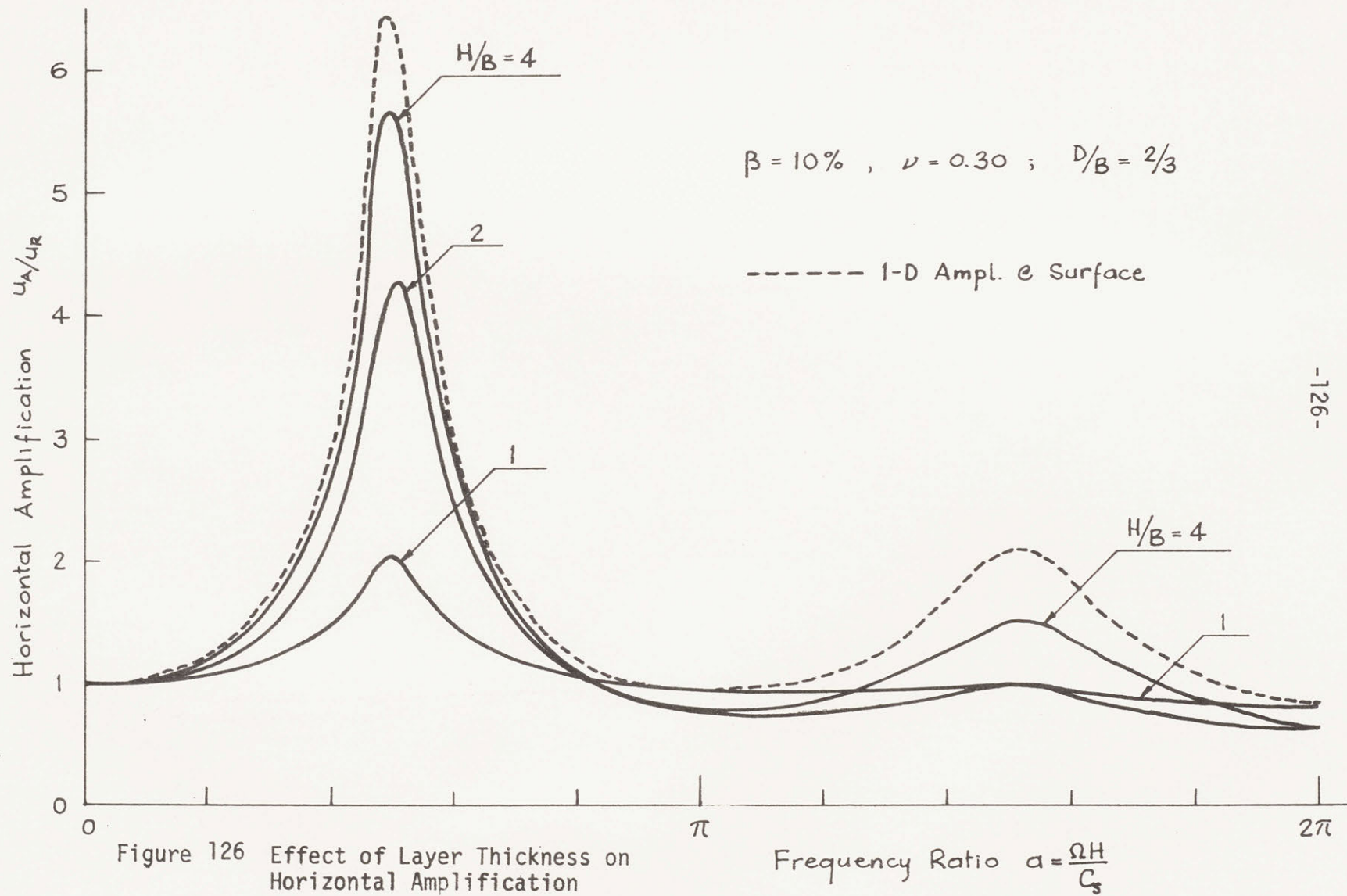


Figure 4-5 Phase Angles for Horizontal Displacements and Rotations of Embedded Footings



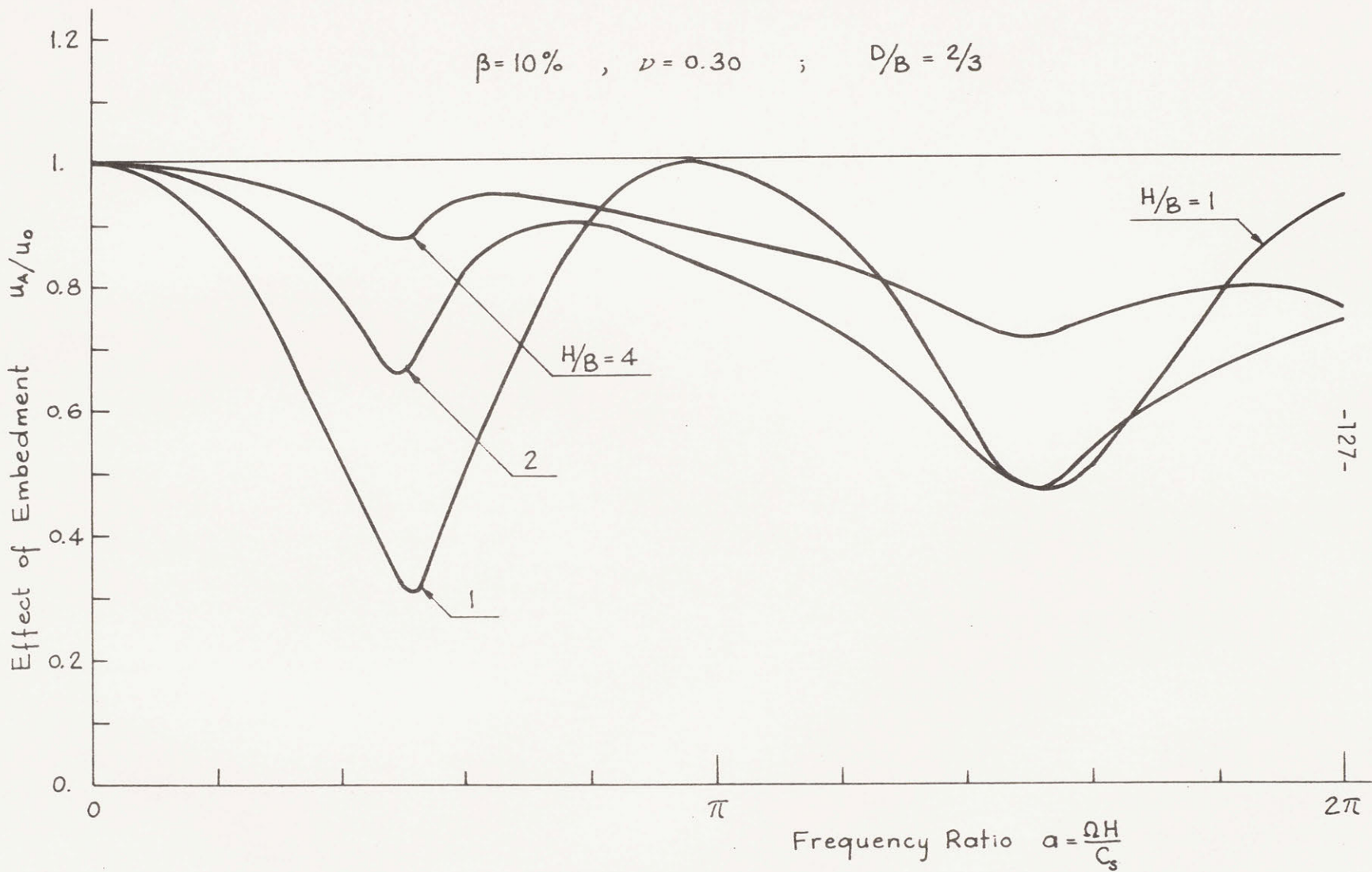


Figure 4-7 Effect of Embedment

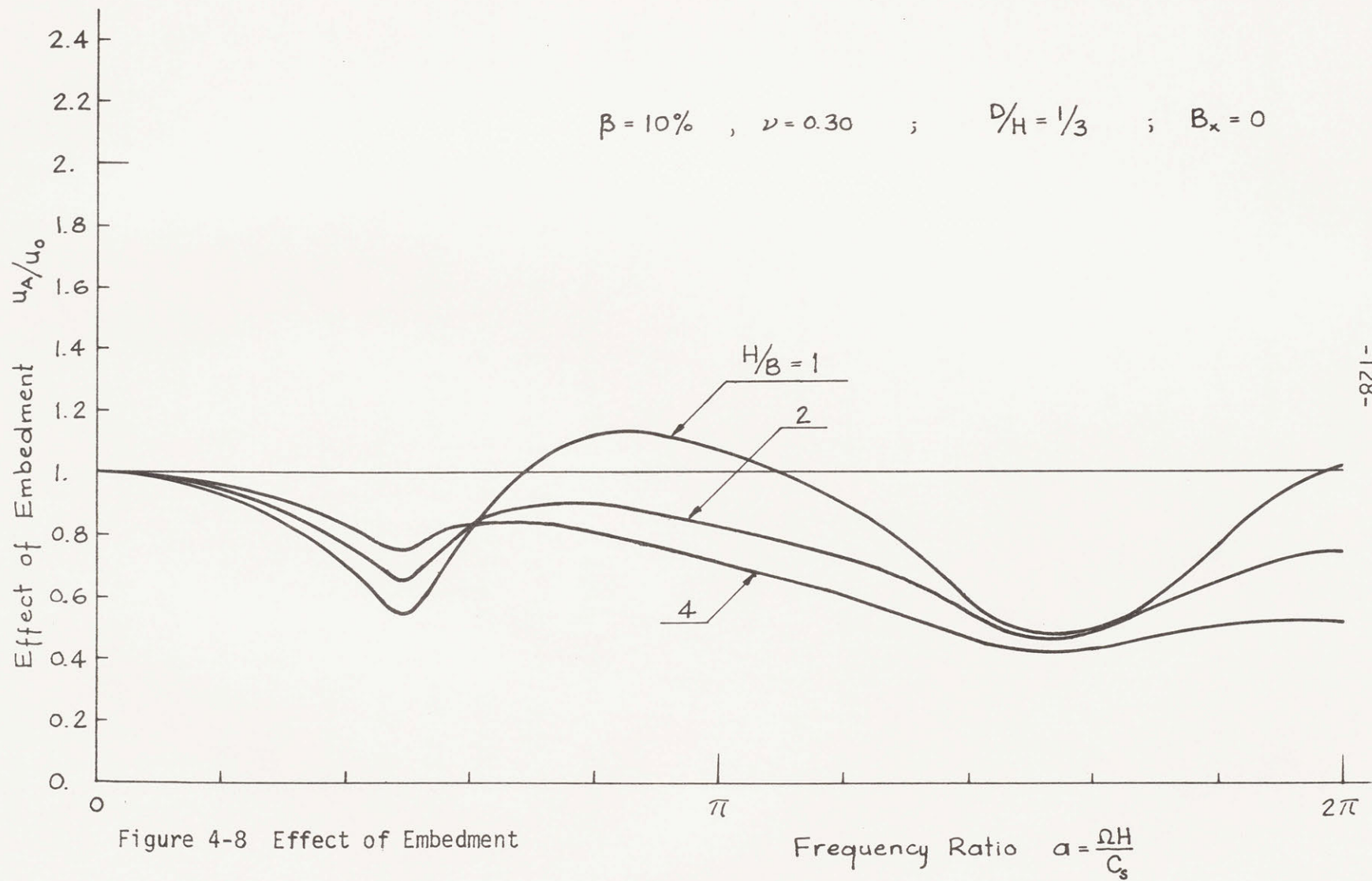


Figure 4-8 Effect of Embedment

rather than to the structure's width. Fig. 4-8 shows the ratio u_A/u_0 for $D/H = 1/3$ and different layer thicknesses. It appears that embedment is, still, beneficial in general; but for shallow strata, the response of the embedded footing can be a little higher than that of the surface footing in some range of frequencies between resonances. However, this increase is in the range where the 1-D amplification is low; so, it is relatively unimportant.

The finite element mesh used to compute u_A/u_R was similar to that used for the footing on the surface. The cases considered for the dynamic response were only $H/B = 1, 2$ and 4 , since deeper layers are less affected by the embedment of the structure.

4.3 Compliance Functions

Compliance functions are determined in a manner similar to the one employed in Chapter 3, by applying a unit horizontal force and a unit rocking moment at the center of the footing base (point A in Fig. 4-1). These functions are shown in Figs. 4-9 for the case of $H/B = 2$, $\beta = 10\%$ and $\nu = 0.30$ for footings embedded $1/6$ and $1/3$ of the layer thickness, and compared to the same functions for a footing resting on the surface. The curves have been normalized, with respect to the real part of the static compliances. It is recalled that these values change with damping. The quantities shown in the tables inserted in the figures represent dimensionless static stiffnesses, approximately.

It can be seen that for this case the main effect of the embed-

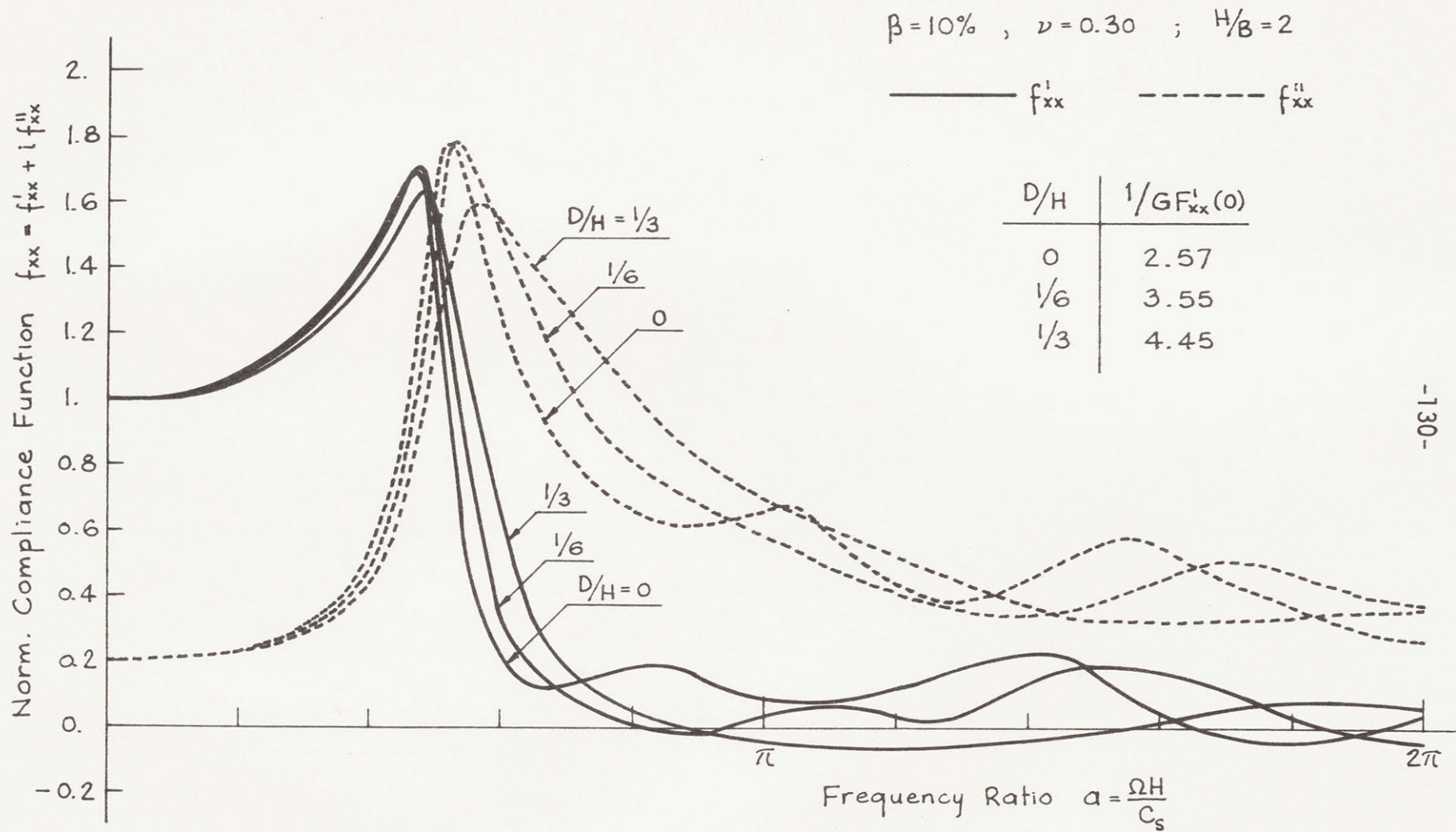


Figure 4-9a Normalized Compliance Function F_{xx}

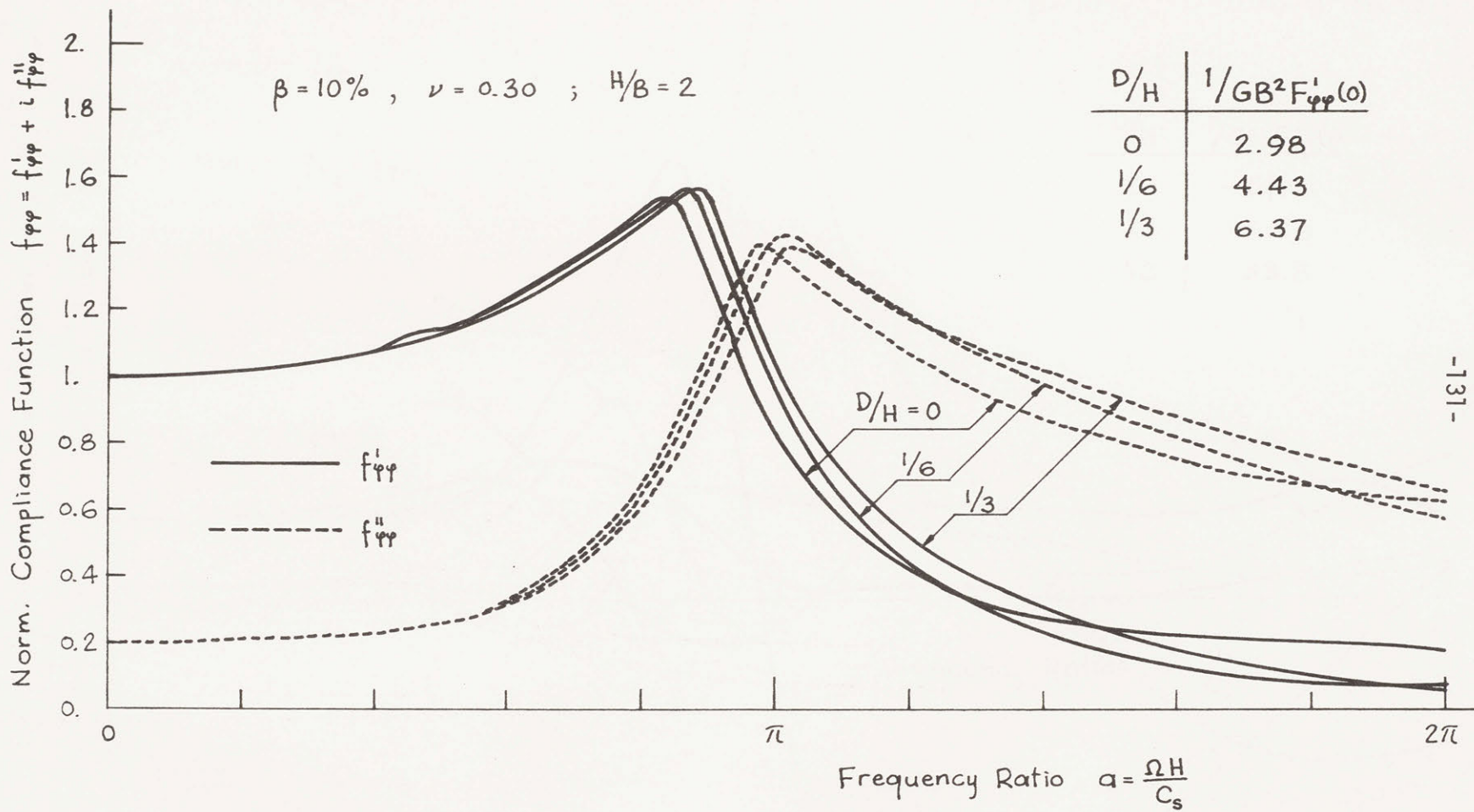


Figure 4-9b Normalized Compliance Function $F_{\phi\phi}$

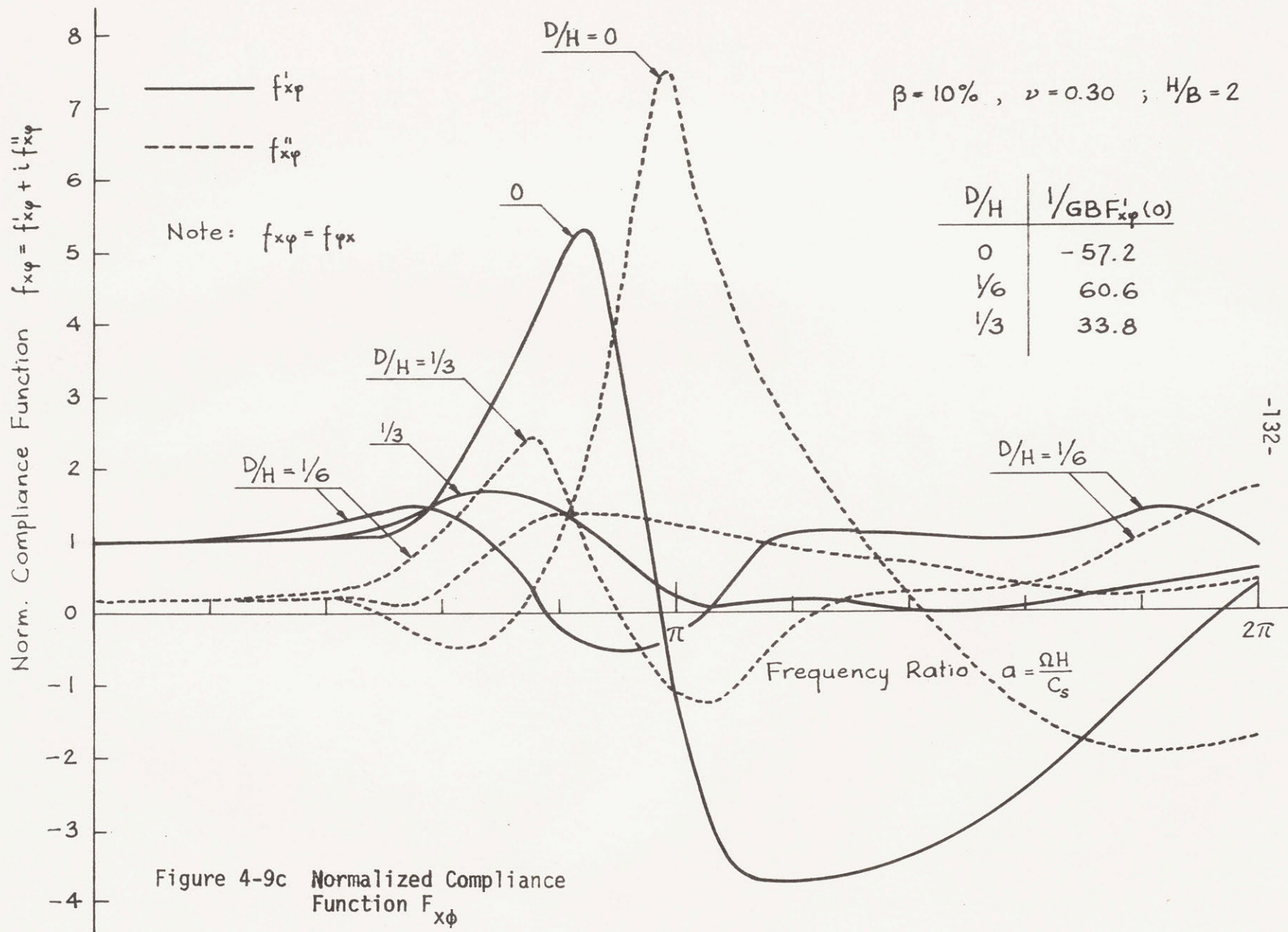


Figure 4-9c Normalized Compliance Function $F_{x\phi}$

ment is the increase in the static stiffnesses. The variation with respect to frequency of the normalized horizontal and rocking compliances is very approximately independent of the embedment. While there is a slight change in the peak frequencies and some variation for higher frequencies, these effects do not seem significant. The cross compliances, on the other hand, show a more significant variation. There is also a more appreciable change for very shallow strata (ratio H/B of the order of unity).

The static compliances are compared in Fig. 4-10 for different embedment to width ratios D/B , and layer thickness to width ratios H/B . The soil is purely elastic and has a Poisson's ratio of 0.30. To consider a percentage of hysteretic damping β , divide the ordinates by $(1 + 4\beta^2)$. Both the swaying and rocking static compliances decrease monotonically with embedment ratio. Whereas the swaying compliance increases with layer thickness for any given D/B ratio, the rocking compliance tends to finite values, corresponding to those of the elastic half-space. For very small embedments and/or deep layers, a horizontal force applied at A (Fig. 4-1) in the positive x -direction (to the right) produces a rotation in the negative ϕ -direction (clockwise), in the static case and at low frequencies. In other cases, the coupling effect is positive.

Fig. 4-11 shows another comparison of the static compliances, but now with respect to the ratio of embedment to layer thickness, D/H . Several curves for different H/B ratios are plotted. These curves seem to show a very fast variation for deep strata as embed-

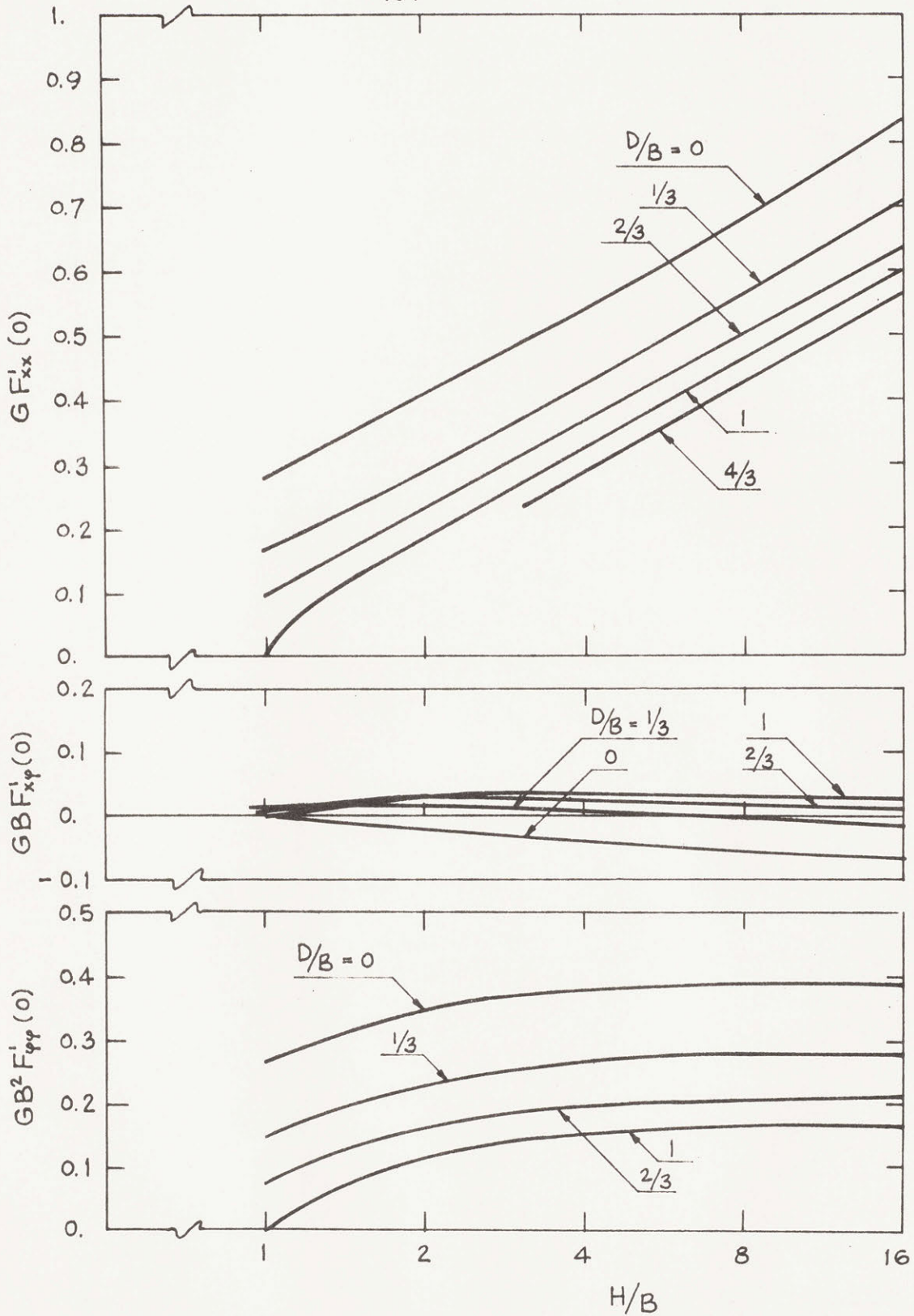


Figure 4-10 Effect of Layer Thickness on Static Compliances

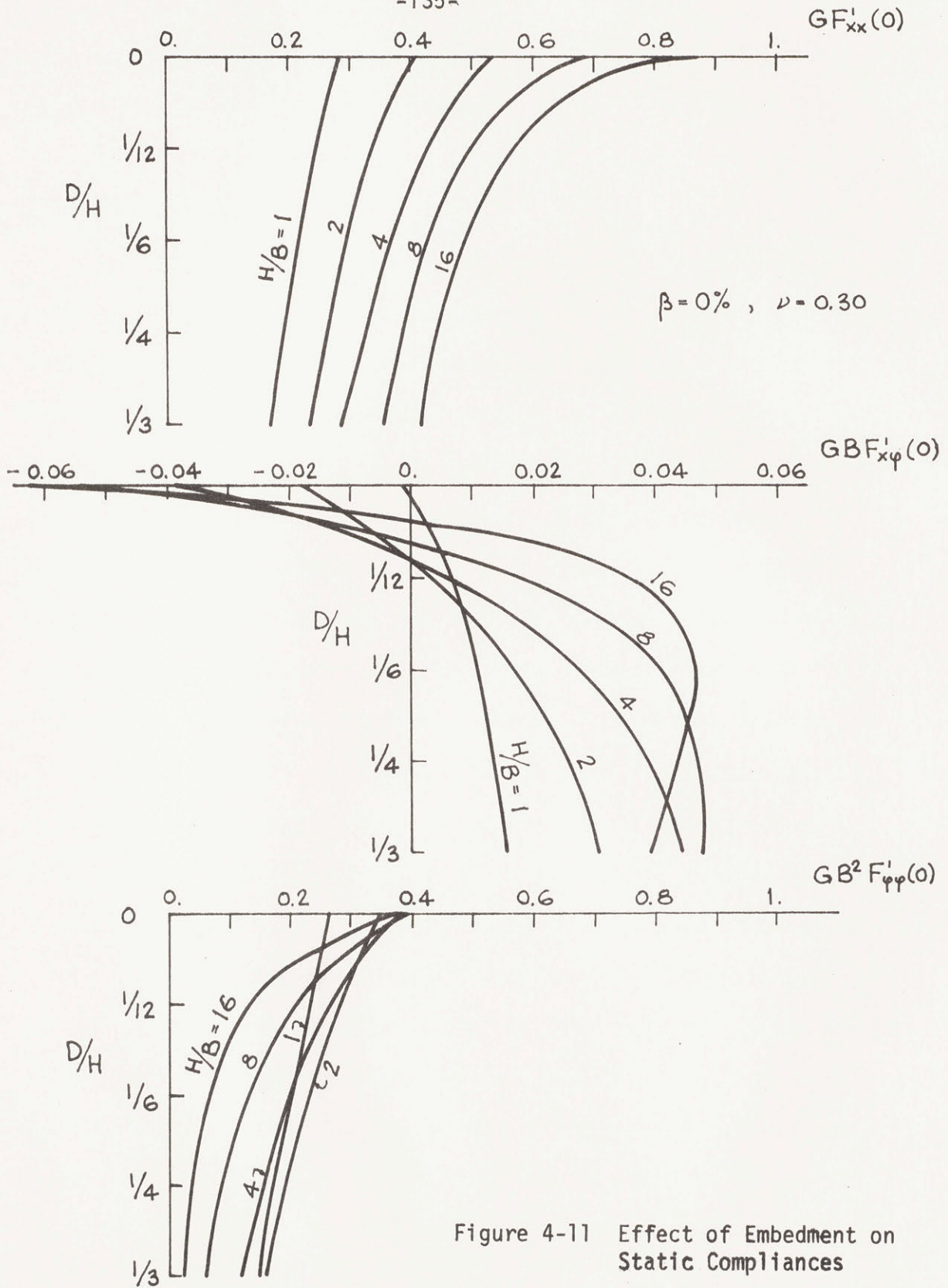


Figure 4-11 Effect of Embedment on Static Compliances

ment increases; but the reason is that for a given D/H ratio, the embedment is larger when H/B is large.

4.4 Effect of Mass

The addition of mass to the rigid strip footing has basically the same effect as for the footing on the surface. For sufficiently high mass ratios and/or for shallow enough strata, the amplification curves u_A/u_R show two peaks. Again, it is seen in Figs. 4-12 and 4-13 that the second peak is produced by the excitation of the rocking mode (compare with discussion in Section 3.4). Fig. 4-12 applies to the case of $H/B = 1$, and Fig. 4-13 to the case $H/B = 2$. Both consider a D/H ratio of 1/3; and the soil has a damping of 10% and a Poisson's ratio of 0.30. The shift in the frequency of the peaks as the mass ratio increases is faster for thinner layers; the maximum amplification is in general lower too. After the first one or two peaks, the amplification drops to a small value; and, actually, for high mass ratios, there is a considerable de-amplification of the rock motion. It must be recalled that although these figures show the general behavior, they are applicable only to a particular set of values of the height of center of gravity ratio E/B and radius of gyration ratio S/B . Notice that the (first) peaks increase in amplitude as the mass ratio increases, and then level off towards $u_A/u_R = 1$. As indicated in Chapter 3, this behavior is due mainly to the effect of the inertia of the structure on the effective stiffness of the system.

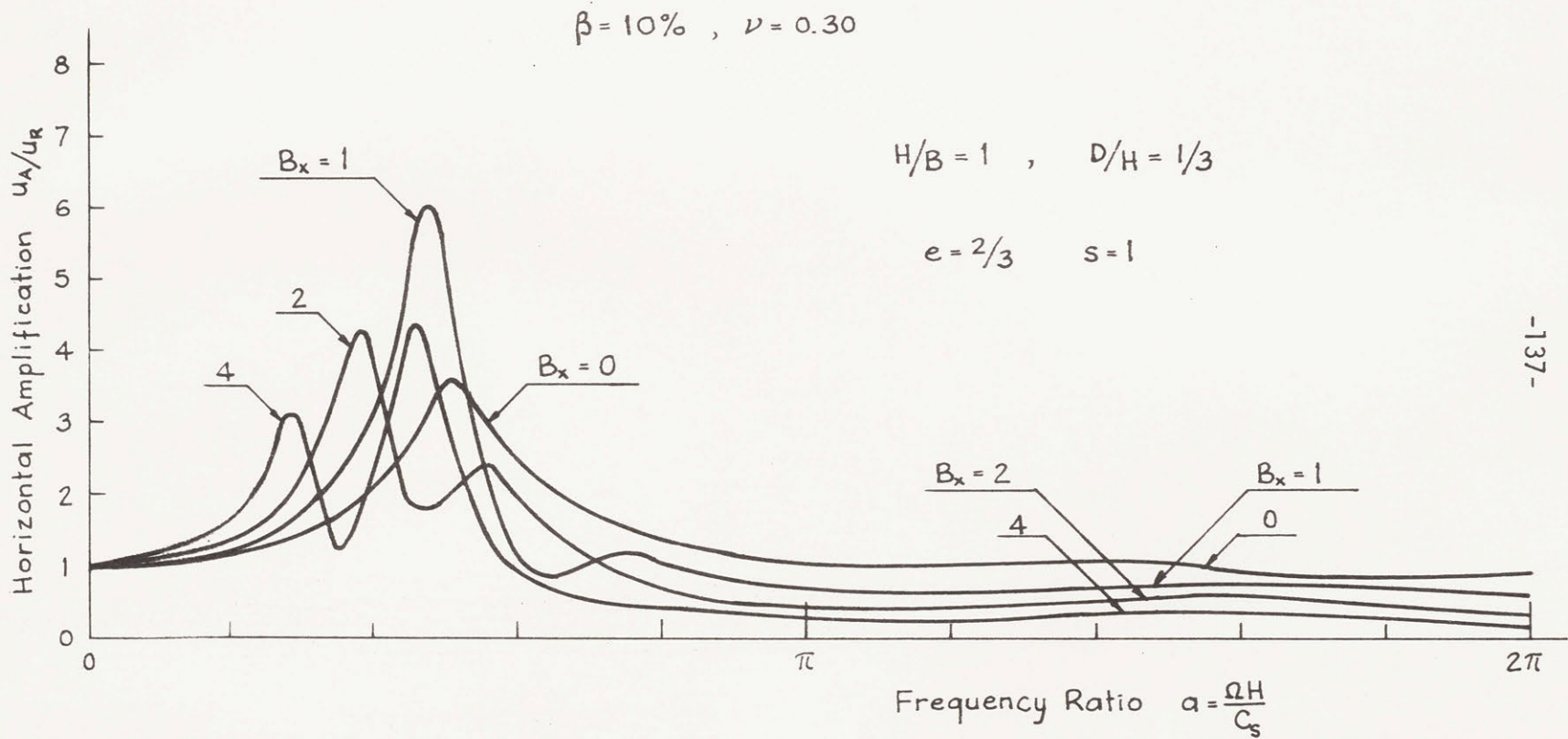


Figure 4-12 Effect of Mass on Horizontal Amplification

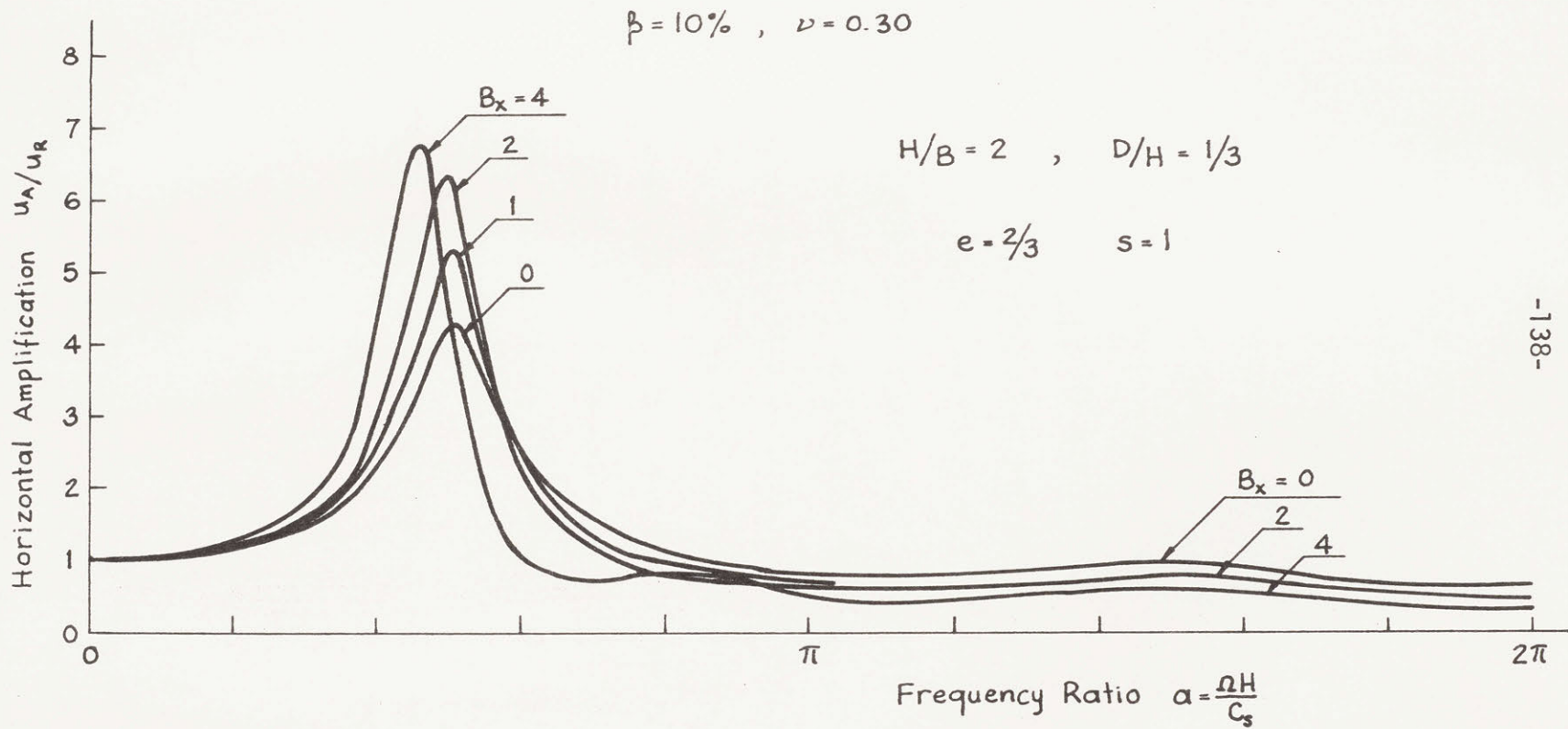


Figure 4-13 Effect of Mass on Horizontal Amplification

To see how embedment affects the horizontal and rocking motion of a rigid structure, a system with the characteristics indicated in Figs. 4-14 and 4-15 was chosen. For the swaying motion, the resonant frequencies increase with embedment, and the peaks tend to be smaller. Whereas for a massless footing, rotation increased with embedment (within the usual embedment ratios), for a footing with the selected mass ratio, the behavior is opposite. There is a remarkable decrease in rocking motion as the footing penetrates into the soil. The reason behind these results is that a massless footing is equivalent to a loss of mass of soil due to the excavation; and then, it is easier for the rest of the soil to move a weightless block as it gets larger because of an increased embedment. But the situation is opposite when the structure weighs more than the volume of soil lost in the excavation. For example, for the case of $D/H = 1/3$, a rectangular block filling the excavation with the given mass ratio of 2 would have a mass density 1.5 times higher than the excavated soil. There is of course the influence of the relative values of B_x , e and s ; and the response is somewhat affected too by a change in the last two parameters (see Fig. 3-21 for a footing on the surface). At high frequencies, the rotatory inertia of the structure prevents it from attaining a large amplification. But for large H/B ratios, the rocking amplification curves follow the behavior of the massless footing; that is, they increase, slowly, with frequency. It has to be noted, however, that for a massless footing the rotation is very small; whereas for structures with considerable mass,

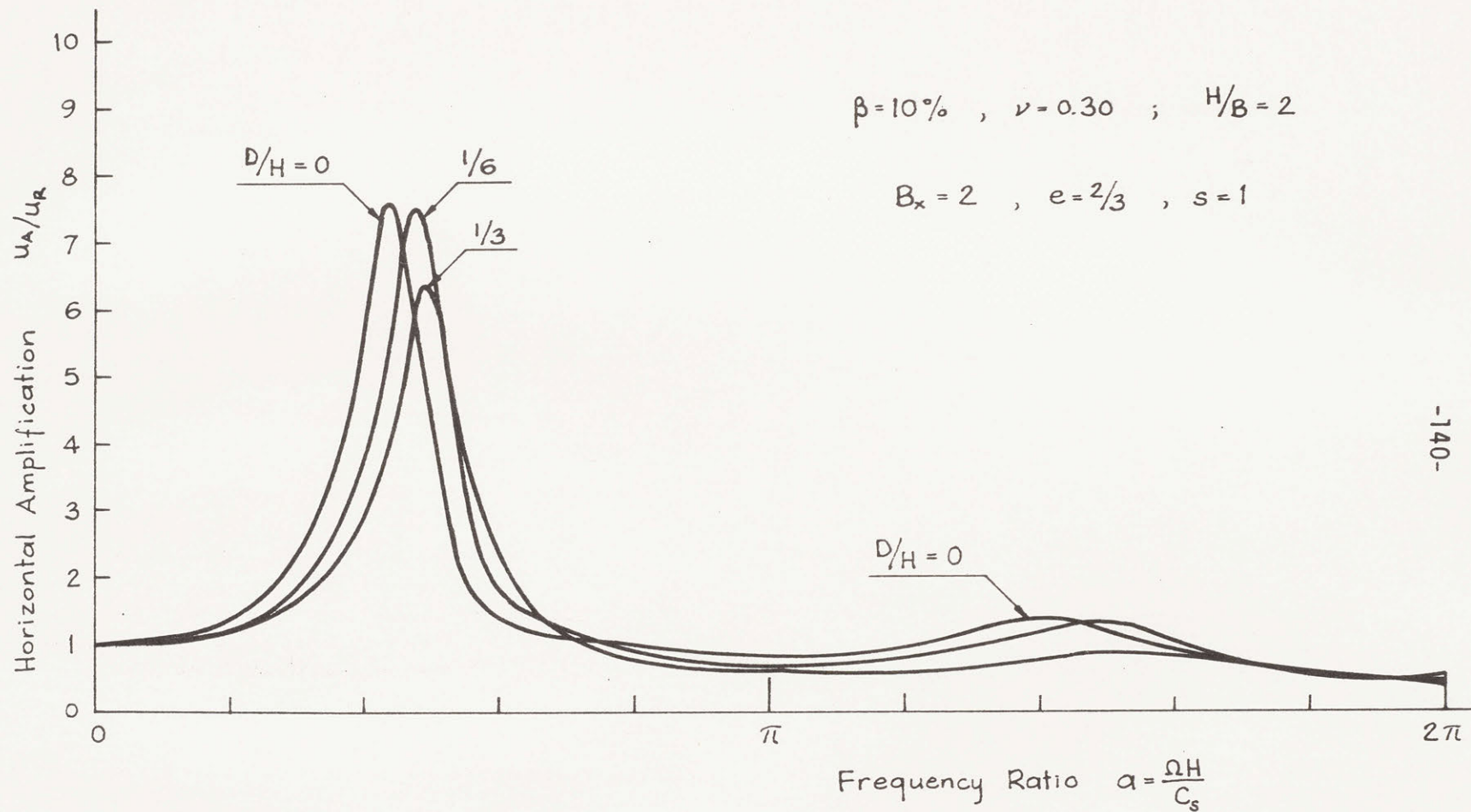


Figure 4-14 Effect of Embedment on Horizontal Amplification

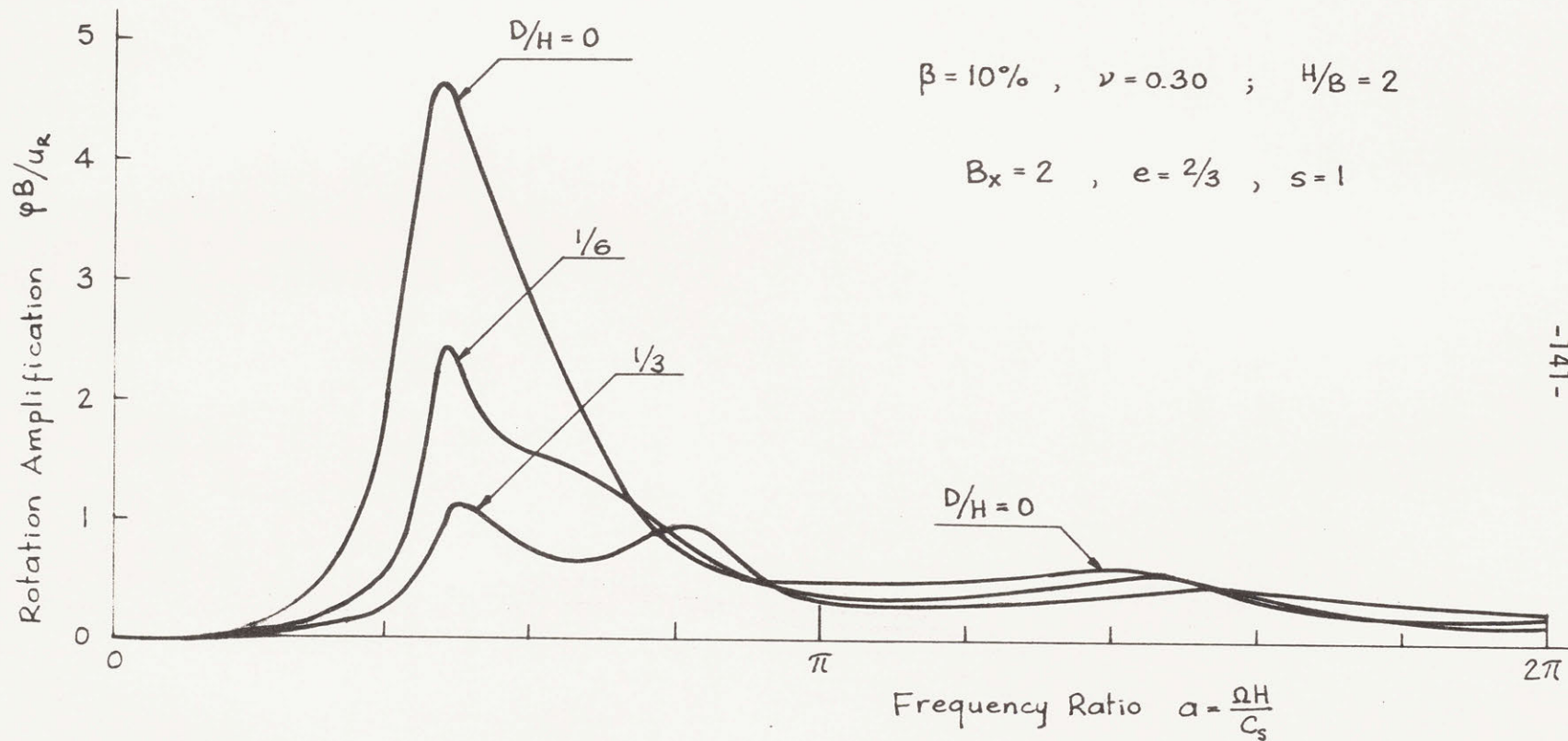


Figure 4-15 Effect of Embedment on Rotation Amplification

the rocking motion, as expressed by the vertical displacements of the edges, is of the same order of magnitude as the swaying motion.

Fig. 4-16 isolates the effect of embedment for the same system considered above. It gives the ratio of the swaying response of an embedded structure against the response of the same structure resting on the ground surface.

The main effect reproduced by these figures is the shift in the fundamental frequency of the mass-soil system due to the increase of stiffness with embedment. The effect of embedment on the motion of the mass under an earthquake-type excitation at the rock would thus depend on the frequency content of the earthquake.

Finally, Figs. 4-17 through 4-19 give a summary of the maximum swaying and rocking response, and position of resonant frequencies, against mass ratio. They consider constant values of height of c.g. ratio, $e = 2/3$, and radius of gyration ratio, $s = 1$; and the soil has the characteristics used throughout this chapter. Fig. 4-17 applies for $H/B = 1$, Fig. 4-18 for $H/B = 2$, and Fig. 4-19 for $H/B = 4$. The embedment ratios are given against the layer thickness; that is, the parameter D/H is used. The second peak is shown in dotted lines when its amplitude is higher than the first. It is seen that the resonant frequency is reduced as the mass ratio increases. Besides, the maximum possible amplification is obtained at lower mass ratios when the layer is thin. As seen from Figs. 4-17 and 4-18, the peak response for embedded footings can be larger than for the same footing on the ground surface, when the mass ratio is high enough. For thin

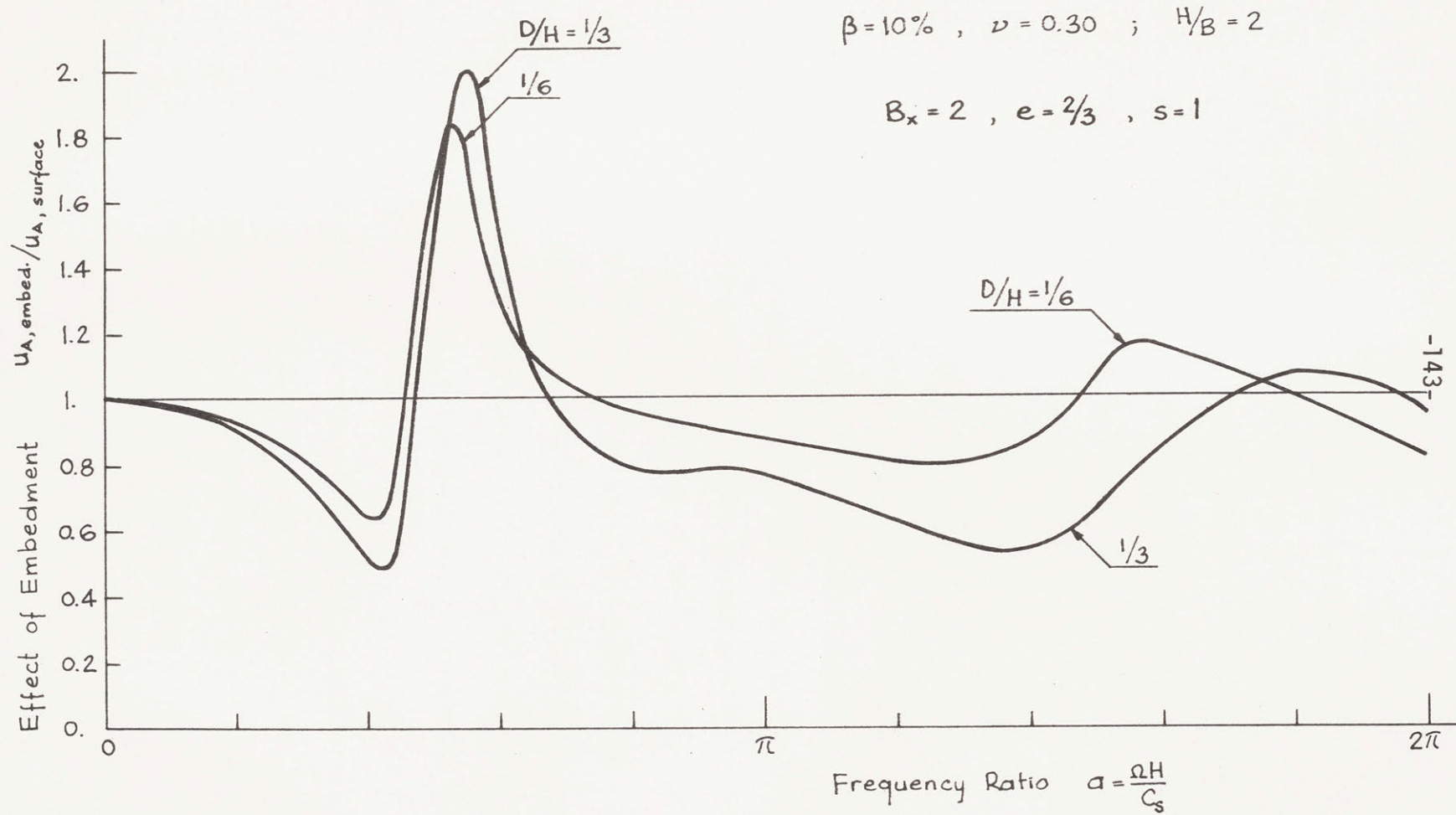


Figure 4-16 Effect of Embedment

layers, that behavior occurs even for small mass ratios. Of course, for massless footings, the maximum swaying amplification is always lower when embedment is deeper. When there is a second peak in the swaying response, its magnitude increases rapidly with increasing mass ratio, but suddenly it levels off. However, this second peak remains higher than the first peak, at least in all cases considered. The fall-off of resonant frequencies is faster for thin layers, and is more pronounced when the embedment ratio is small. With regard to rotation, the increase in rocking peak amplification is faster for thin layers. Embedment reduces the rate of increase.

It is also interesting to compare the horizontal displacements of the center of gravity against those at the bottom of the structure, for different mass ratios, as done in Fig. 4-20, for $H/B = 2$, $e = 2/3$ and $s = 1$. At least for this case, the peak motion of the center of gravity is somewhat higher than that of the bottom; and they are more similar when embedment increases, reflecting the reduction in rocking motion. Fig. 4-18b and 4-20d illustrate this point.

In summary, the general trends with increasing mass are: First, an increase in peak amplification as interaction is added to site effects; then a decrease as the peak frequency shifts off the site effects peak; and, finally, an increase again as the second peak develops.

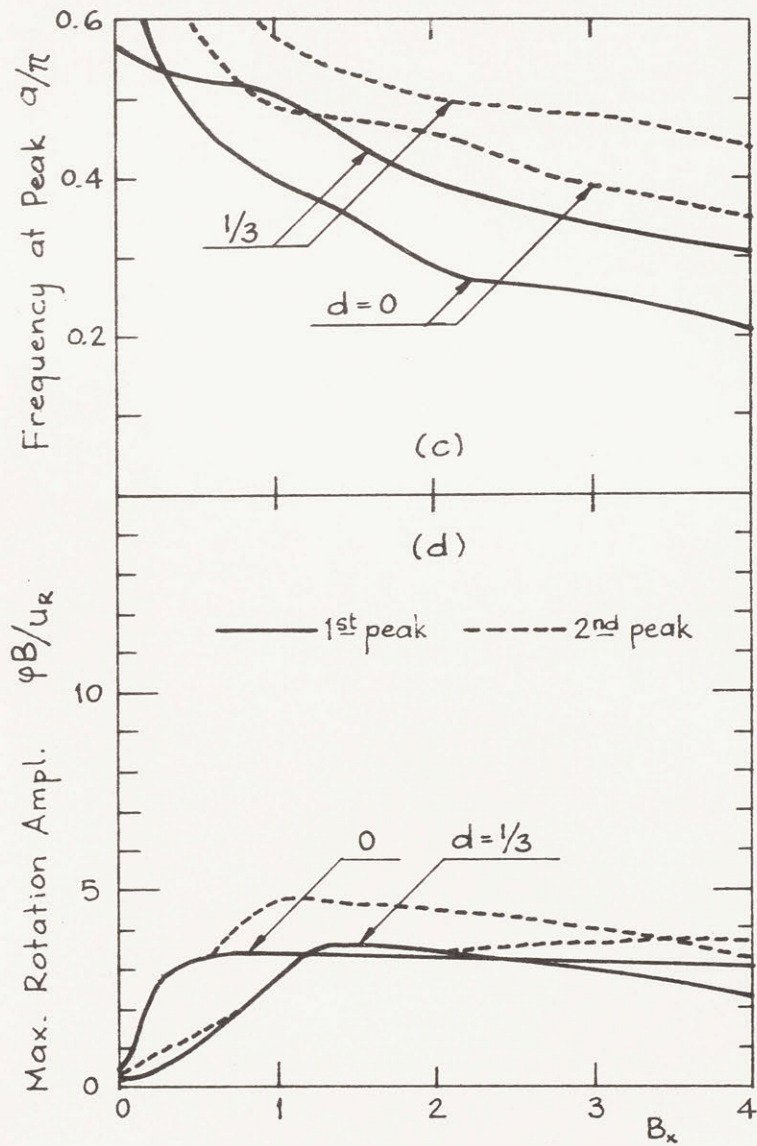
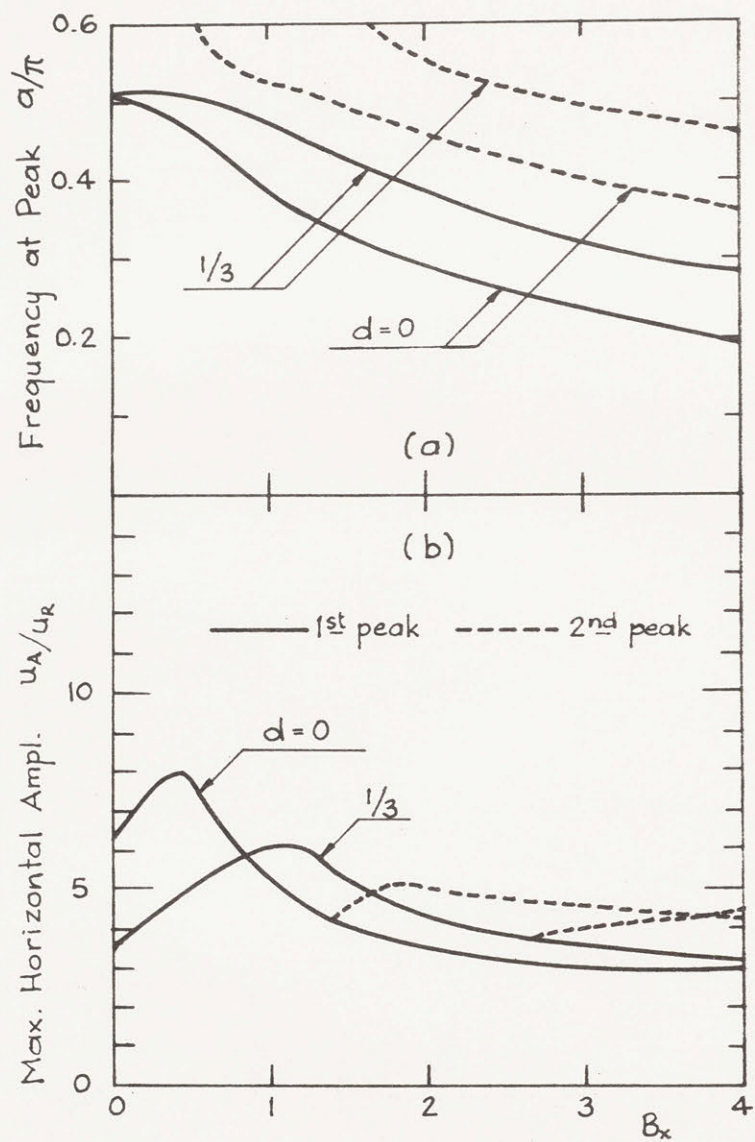


Figure 4-17 Effect of Mass

$\beta=10\%$, $\nu=0.30$; $H/B=1$; $e=2/3$, $s=1$

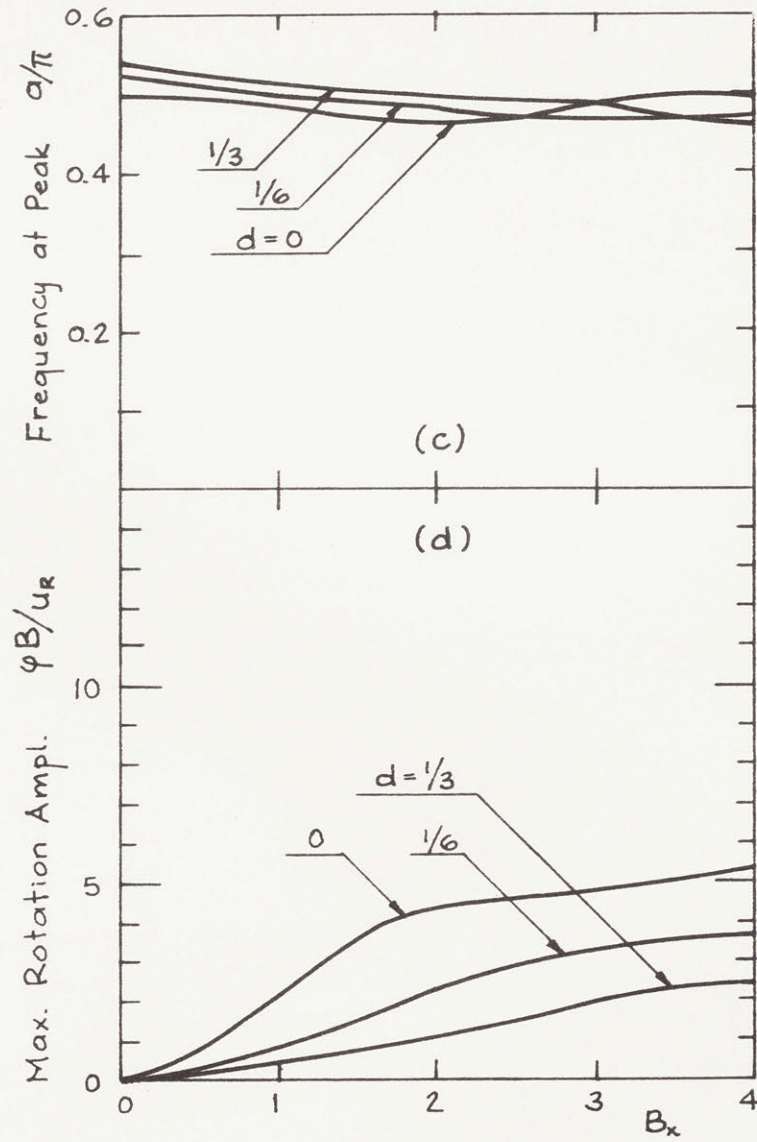
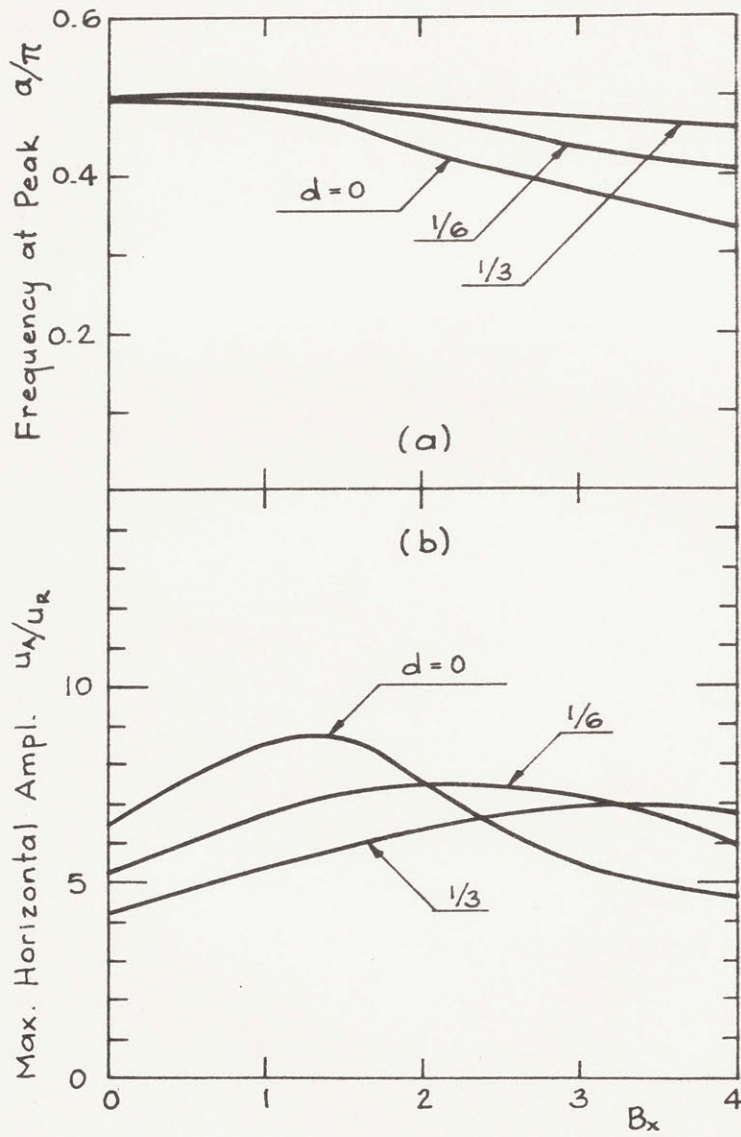


Figure 4-18 Effect of Mass $\beta = 10\%$, $\nu = 0.30$; $H/B = 2$; $e = 2/3$, $s = 1$

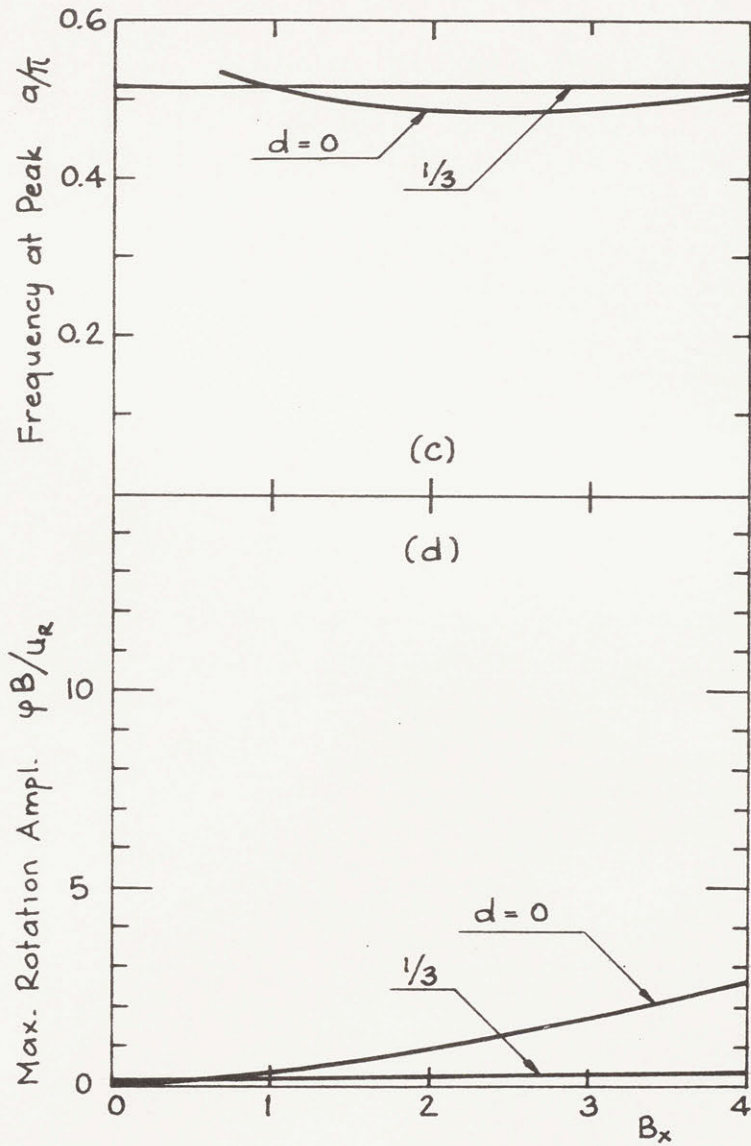
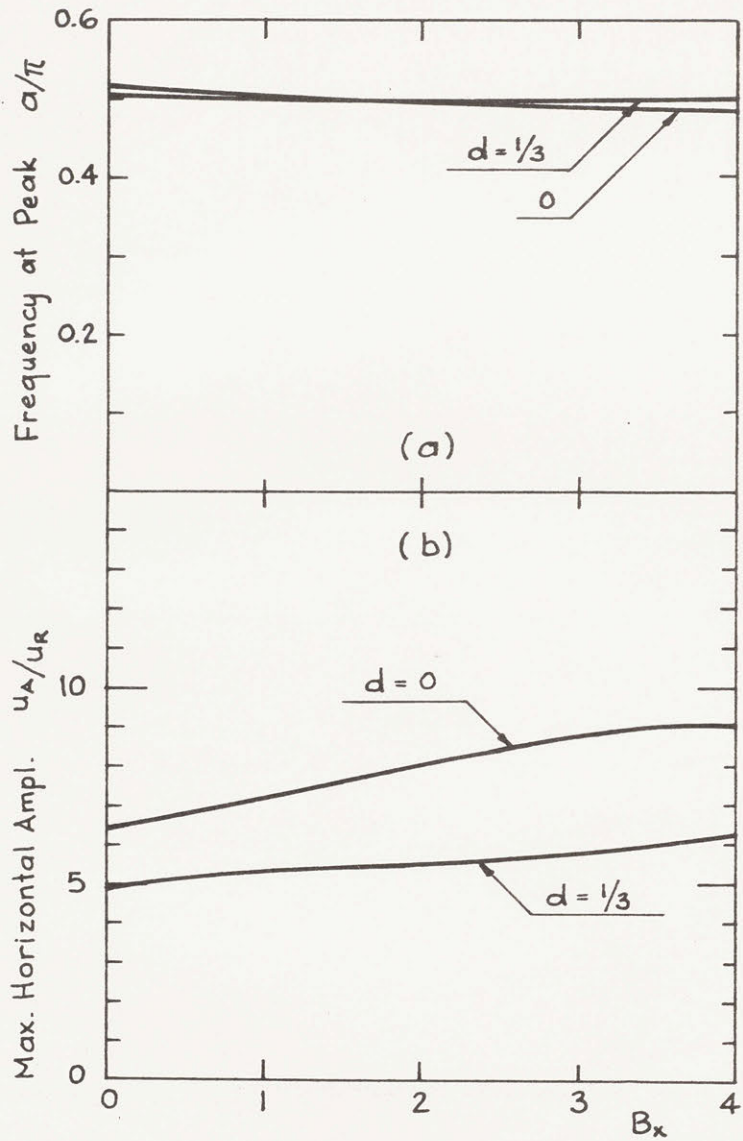


Figure 4-19 Effect of Mass

$\beta=10\%$, $\nu=0.30$, $H/B=4$; $e=2/3$, $s=1$

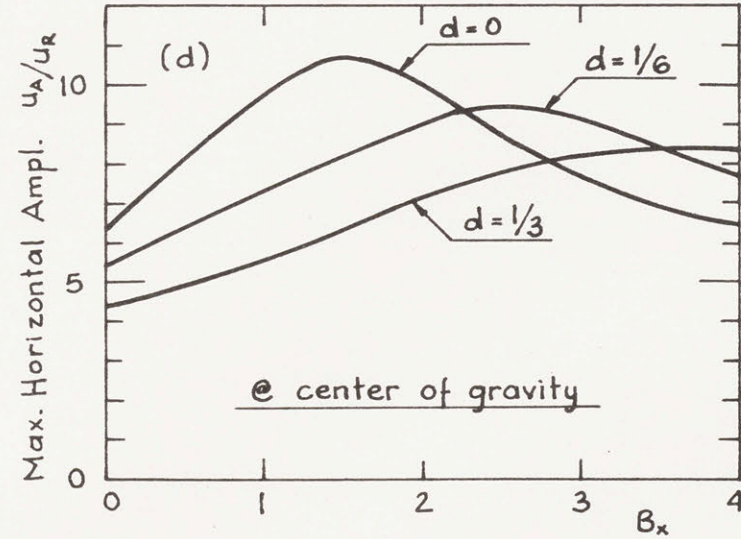
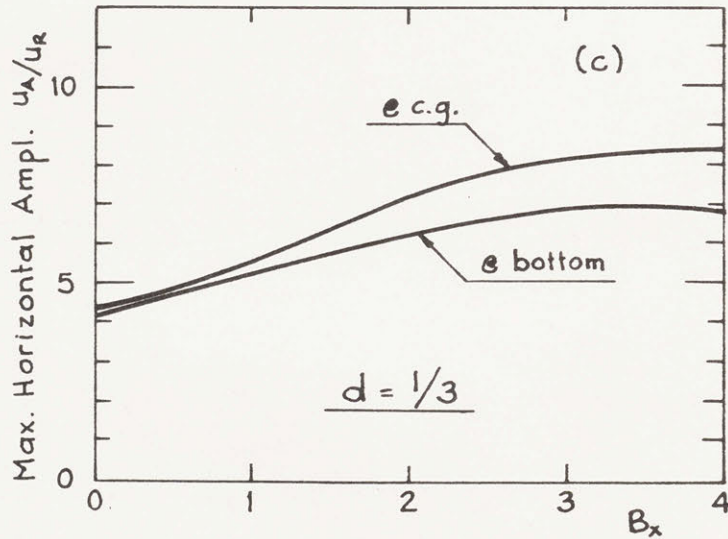
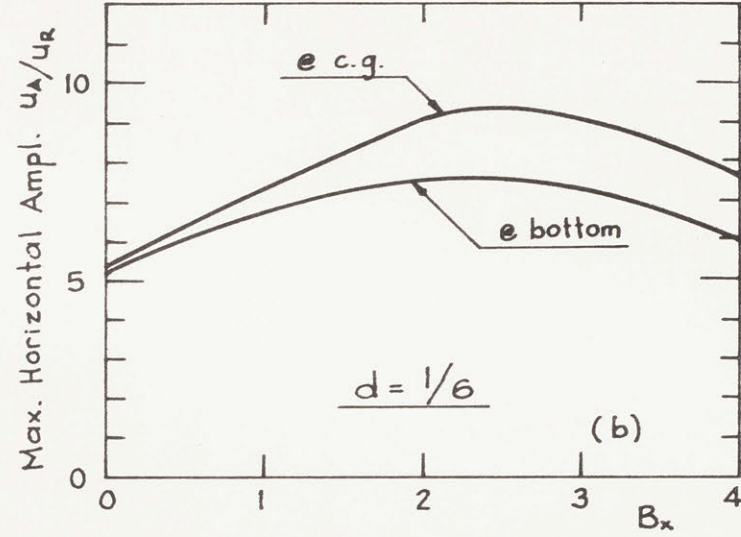
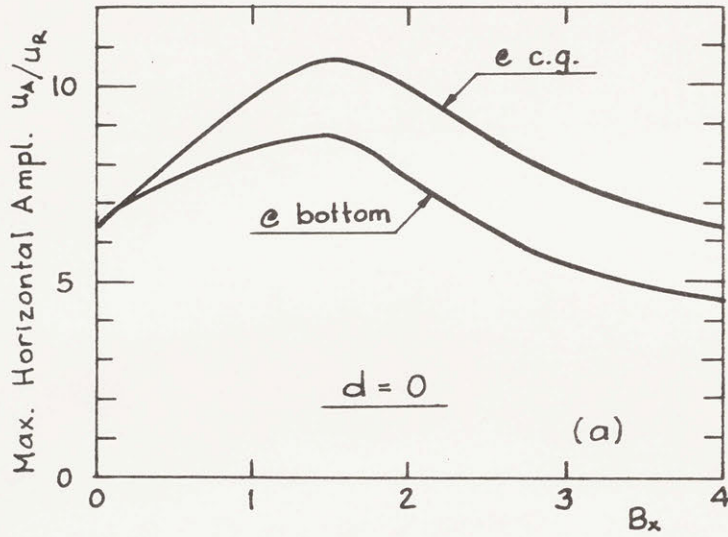


Figure 4-20 Effect of Mass

$\beta = 10\%$, $\nu = 0.30$; $H/B = 2$; $e = 2/3$, $s = 1$

CHAPTER 5 - STRUCTURE - SOIL - STRUCTURE INTERACTION

5.1 Introduction

It is recognized that the response of a structure to exciting forces or to seismic motions is affected by the presence of other bodies in the neighborhood. Also, this structure will be set into motion if an adjacent structure is excited. The coupling between the responses of structures through the foundation soil is called here "structure - soil - structure interaction."

Richardson [44] and Warburton, Richardson and Webster [58,59] have investigated this problem for the case of circular footings resting on the surface of an elastic half-space. In this chapter, two parallel rigid strip footings of arbitrary width and separation are considered. They are welded to the surface of a homogeneous, isotropic and viscoelastic layer. The soil has a Poisson's ratio $\nu = 0.30$ and a percentage of hysteretic damping $\beta = 10\%$. This is a plane-strain problem under harmonic motion.

5.2 Method of Solution

Using the program PLAXLY2 described in Chapter 2, the displacements in the surface of the soil layer were computed for both a unit horizontal and a unit vertical line load and stored in disc. A series of points separated $\Delta x = 0.1H$ were taken, where H is the layer thickness, covering a total distance of $12H$. The structure - soil - interaction is important when the two (or more) structures are close enough. By varying the widths of the footings, different depth-to-half-width

ratios H/B_i , $i = 1, 2$, can be taken. The half-width B_i is an integer multiple of Δx , and the distance between center-lines of the footings L is an integer multiple of $\Delta x/2$.

Only two structures were considered in this study. The mathematical approach was presented in Section 2.8. The (rigid) structures were restricted to have a height of center of gravity of $2/3$ of B_i and a radius of gyration equal to B_i , $i = 1, 2$, to reduce the number of parameters involved in the problem. The mass-ratios $B_{x_i} = M_i / \rho B_i^2$, where M_i is the total mass of the i^{th} footing, were taken as 0, 1, 2 and 4. These conditions can be thought of as taking two geometrically similar structures (just scaled up or down), and varying their densities.

The geometry of this problem is shown in Fig. 5-1. The notation follows closely the one used in the preceding chapters. A subscript 1 or 2 has been added where necessary to identify the two footings.

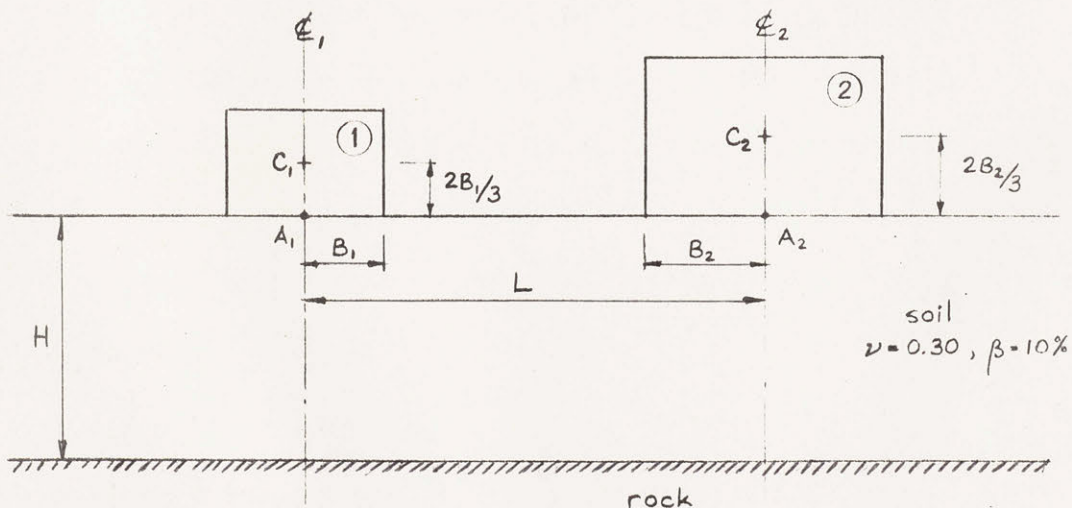


Figure 5-1

The exciting forces P_{x_i} , P_{ϕ_i} , P_{z_i} $i = 1, 2$ were applied at points A_1 or A_2 .

5.3 Response to Exciting Forces

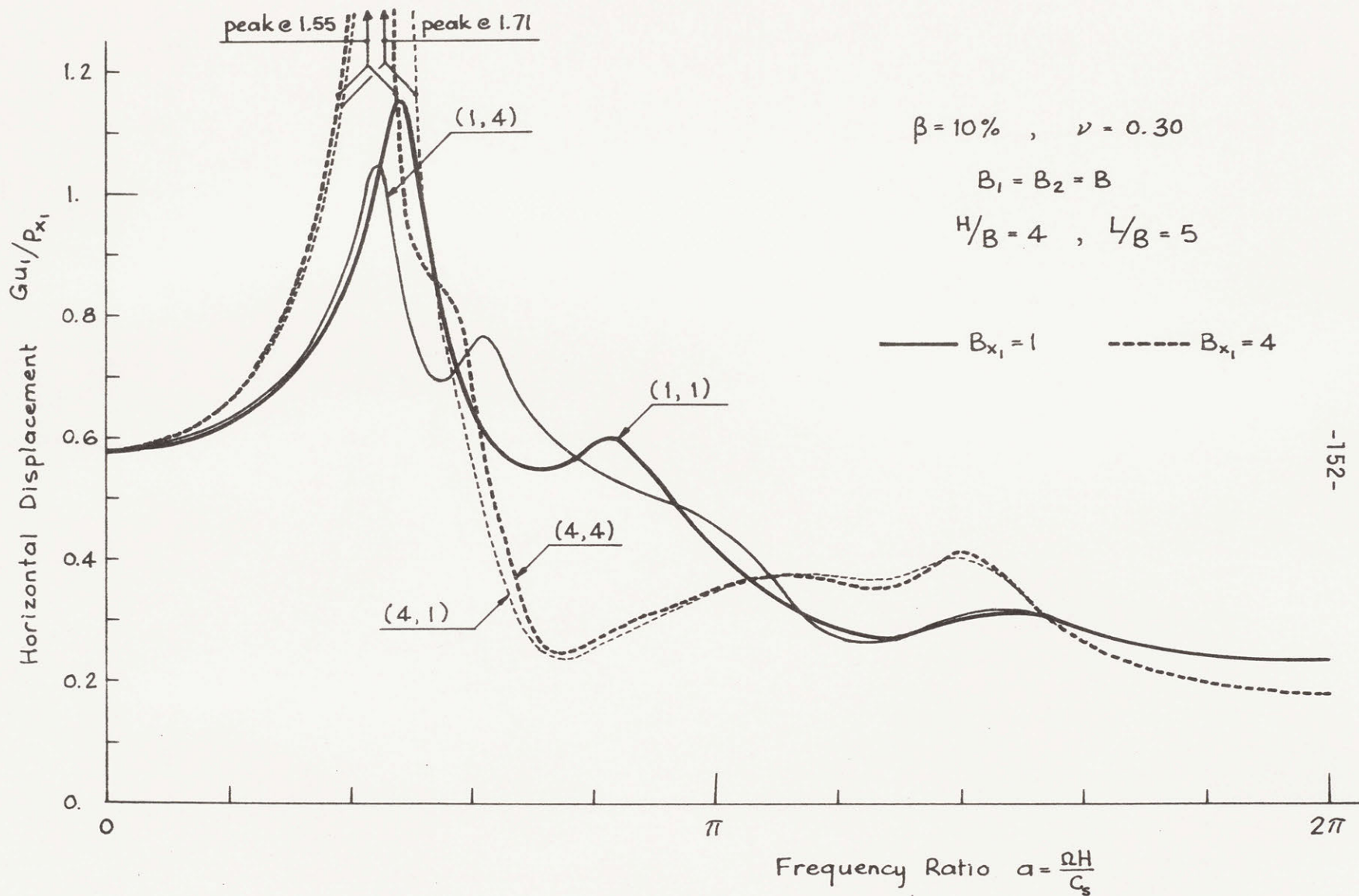
Two geometrically similar structures were considered, i.e.

$$B_1 = B_2 = B.$$

The case of a relatively deep layer, $H/B = 4$ was first considered, with a separation between the centers of the footings $L/B = 5$ ($L/H = 1.25$). Figs. 5-2 through 5-5 show the selected responses to different exciting forces, in terms of dimensionless displacements. Only those responses which are significant are illustrated. The case of vertical excitation has been omitted; but it is emphasized that all three degrees of freedom of each structure are coupled in this problem, as opposed to the one-structure situation treated in Chapters 3 and 4.

The different figures are identified with an ordered pair of numbers (B_{x_1}, B_{x_2}) , e.g. (1,4) means $B_{x_1} = 1, B_{x_2} = 4$.

Fig. 5-2 shows the horizontal displacement in one of the footings when it is excited by a horizontal force. When the mass-ratio of the footing is small, varying the mass-ratio of the adjacent (unexcited) footing so that $B_{x_2} \geq B_{x_1}$ changes the response slightly, especially in the location of the peaks. At high frequencies, the influence of the foreign mass practically disappears. When the excited footing is heavy ($B_x = 4$) the influence of a second smaller mass ($B_{x_2} \leq B_{x_1}$) is even less perceptible. In all these cases, the difference is mostly marked around the first peak, corresponding to the fundamental frequency of the system for horizontal motion.



-152-

Figure 5-2 Horizontal Displacement in Excited Footing Due to Horizontal Force

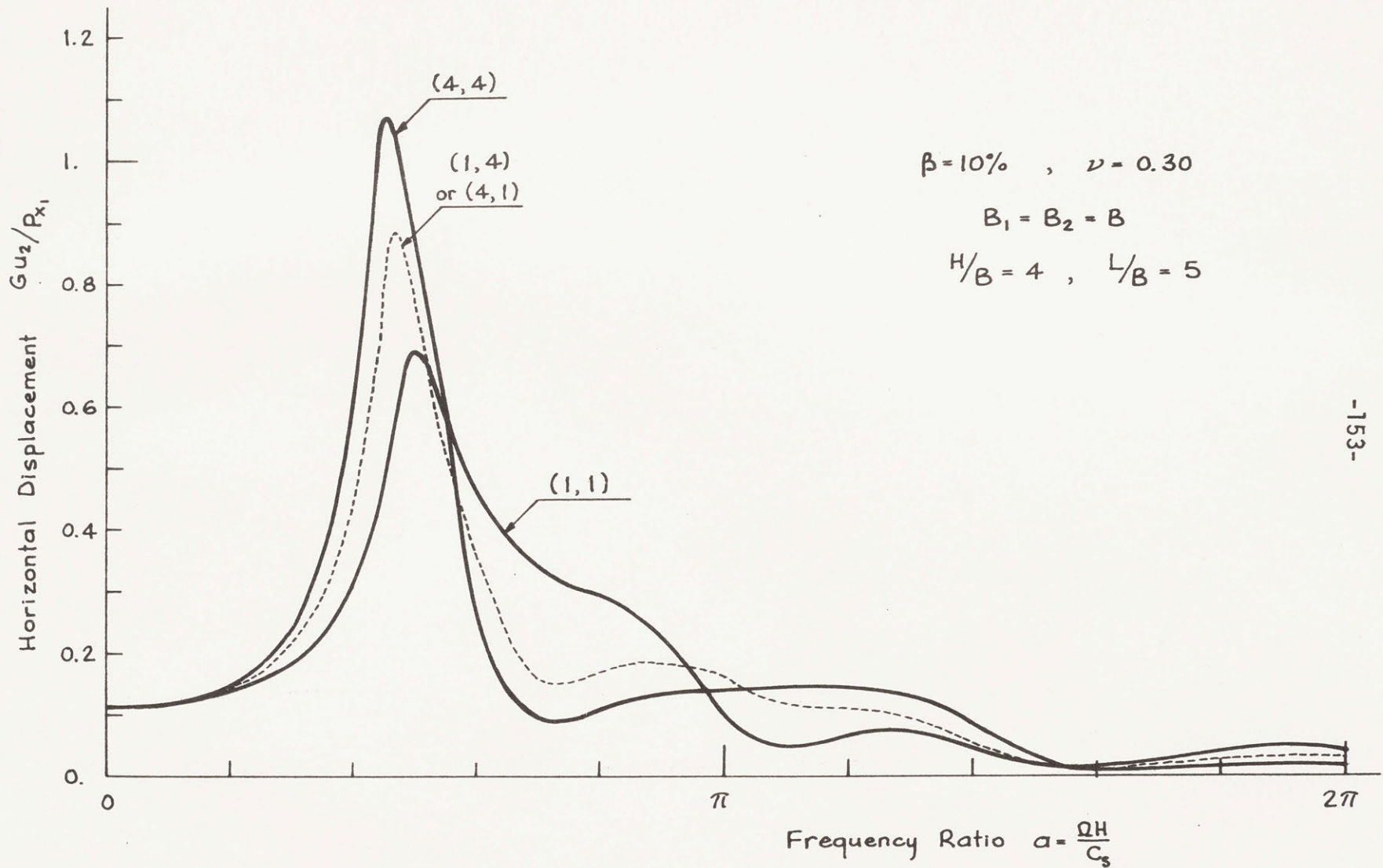


Figure 5-3 Horizontal Displacement in Passive Footing due to Horizontal Force

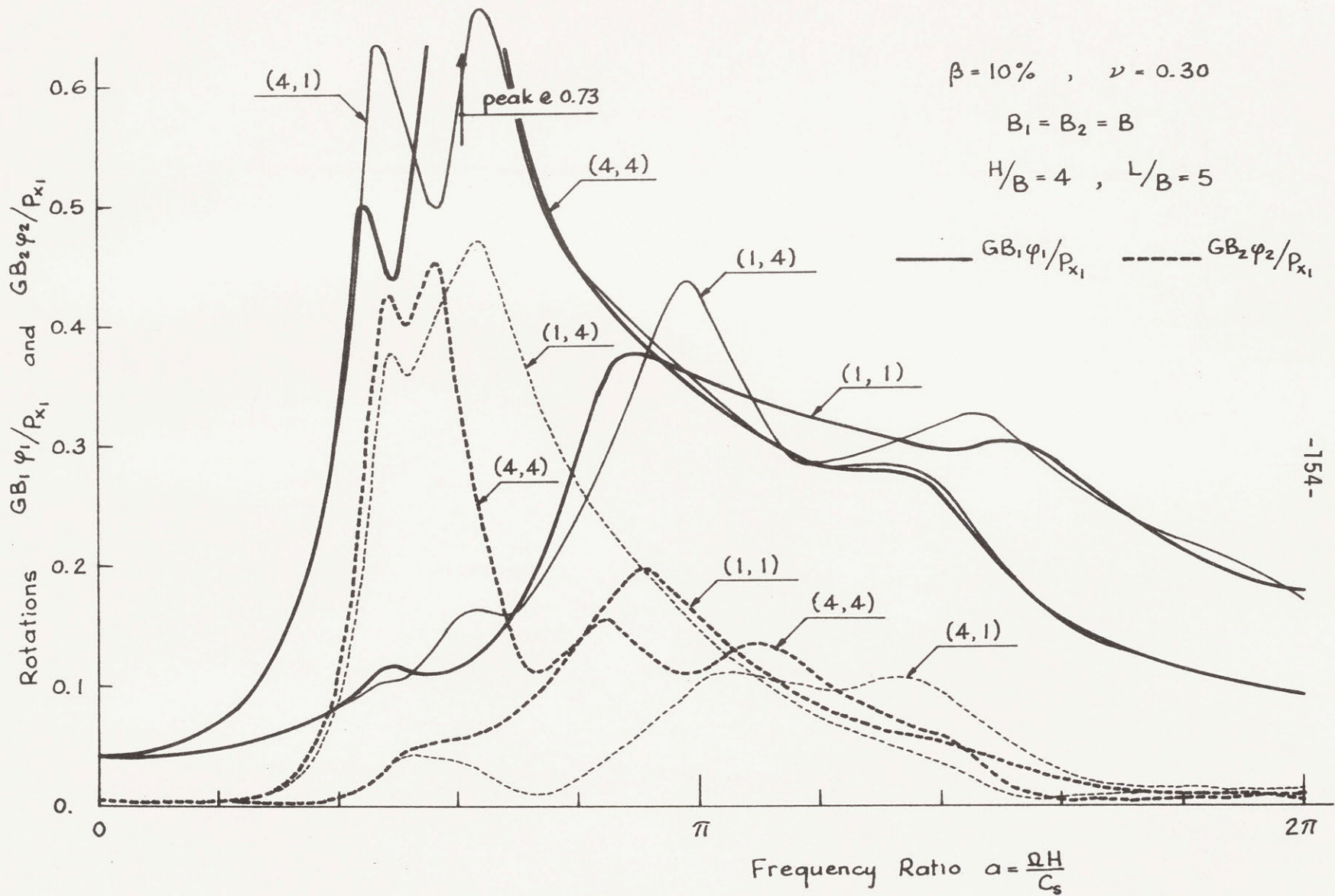


Figure 5-4 Rotations in the Two Footings due to Horizontal Force

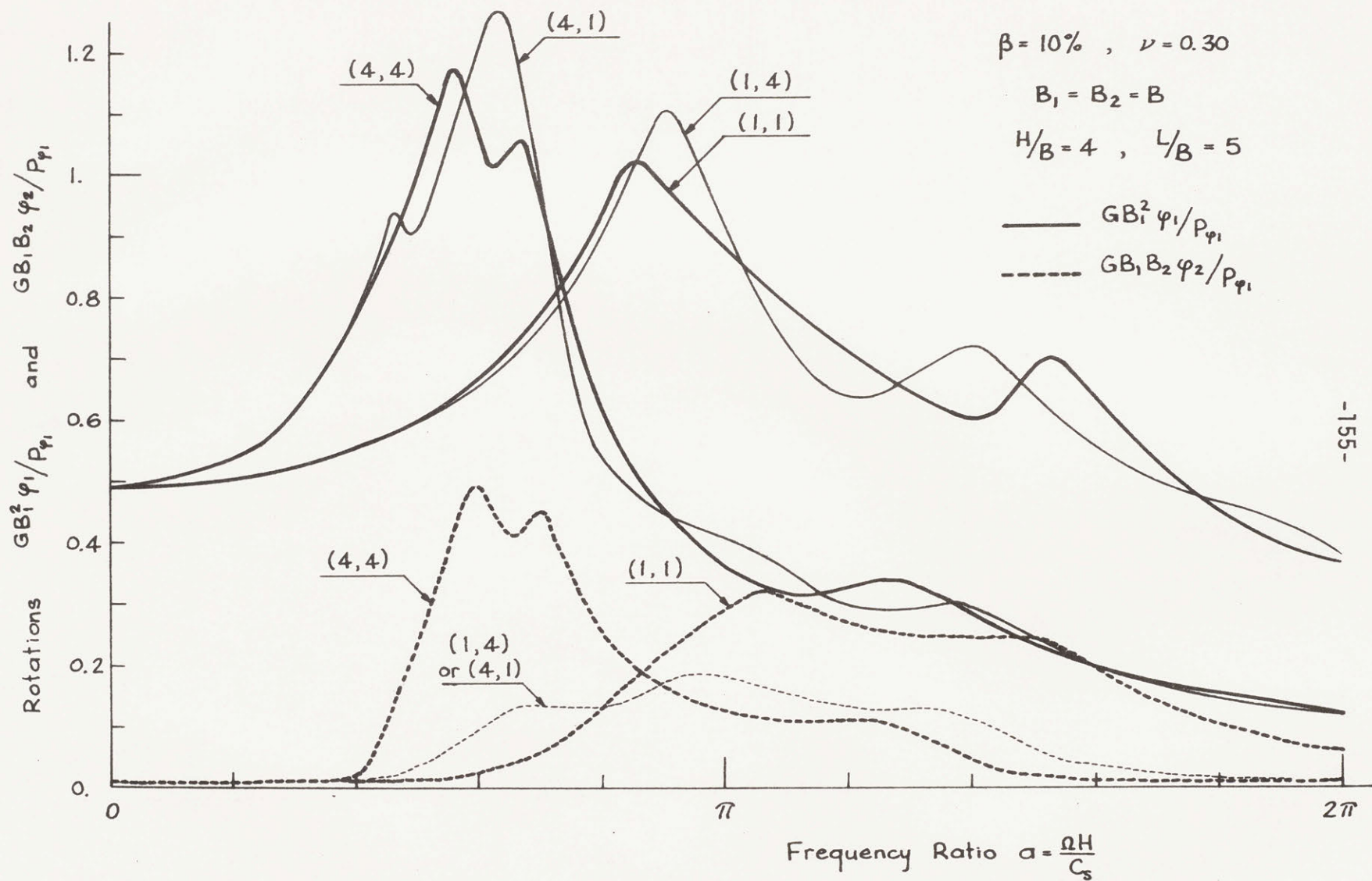


Figure 5-5 Rotations in the Two Footings due to Rocking Moment

Fig. 5-3 shows the horizontal displacement of the unexcited mass. The maximum response of this footing increases when its mass ratio increases and/or when the mass ratio of the excited footing increases. The curves for the two cases (1,4) and (4,1) are exactly equal. The principle of reciprocity extends to the masses, as for the stiffnesses.

The rotations induced by a horizontal force applied on footing 1 are illustrated in Fig. 5-4. The rotation of the excited footing is about twice as large as that of the unexcited footing. For high frequencies, the rotation of footing 2 is very small. In general, the shapes of the response curves for the two masses are similar, for any given pair of mass-ratios. Notice, however, that whereas the response of the excited footing is not affected very much by changing the mass-ratio of the adjacent footing (except at the high peaks), the response of the latter is quite different as any of the two mass ratios changes. The rotation of both footings is in general larger when the mass-ratio increases, at least in the region of the high peaks.

For this relatively deep layer of soil, the dimensionless rotation is of the same order of magnitude as the horizontal translation, and it is this rotation which is responsible in great part for the motion of the unexcited footing (and feedback to the excited footing).

Fig. 5-5 shows the rotations induced in the two footings due to an exciting rocking moment in one of them. The same comments as for Fig. 5-4 apply here. But in this case the important peaks are due

to the vertical resonance of the layer, which is excited by rocking. The rotation of the unexcited mass is negligible until after the first resonance in horizontal translation.

In all these curves, the peaks occur at lower frequencies for larger mass ratios, as is the case for the one-footing problem studied in Chapter 3.

For a very shallow layer, $H/B = 1$, Figs. 5-6 through 5-9 show a few of the response curves.

In Fig. 5-6, the horizontal displacement due to a horizontal exciting force in the same footing is shown. The response is in general smaller than for the relatively deep layer discussed before. It shows two significant peaks at low frequencies, which are due to horizontal and rocking resonances, respectively, and is quite smooth thereafter. For this shallow stratum, the influence of the adjacent mass is imperceptible, at least in the range of mass ratios and for the distance between footings considered here. The first peak decreases as the mass ratio of the excited footing increases, whereas the second peak increases.

Fig. 5-7 shows the rotation in a footing where a rocking moment is applied. Here, as in the previous figure, the frequencies at the peaks shift towards the left as the mass ratio increases. The rotation, as manifested by the vertical displacement of the footing edges, is as large as the horizontal displacement induced by a horizontal force (Fig. 5-6). But the influence on the adjacent footing is very small, one or two orders of magnitude smaller (not shown).

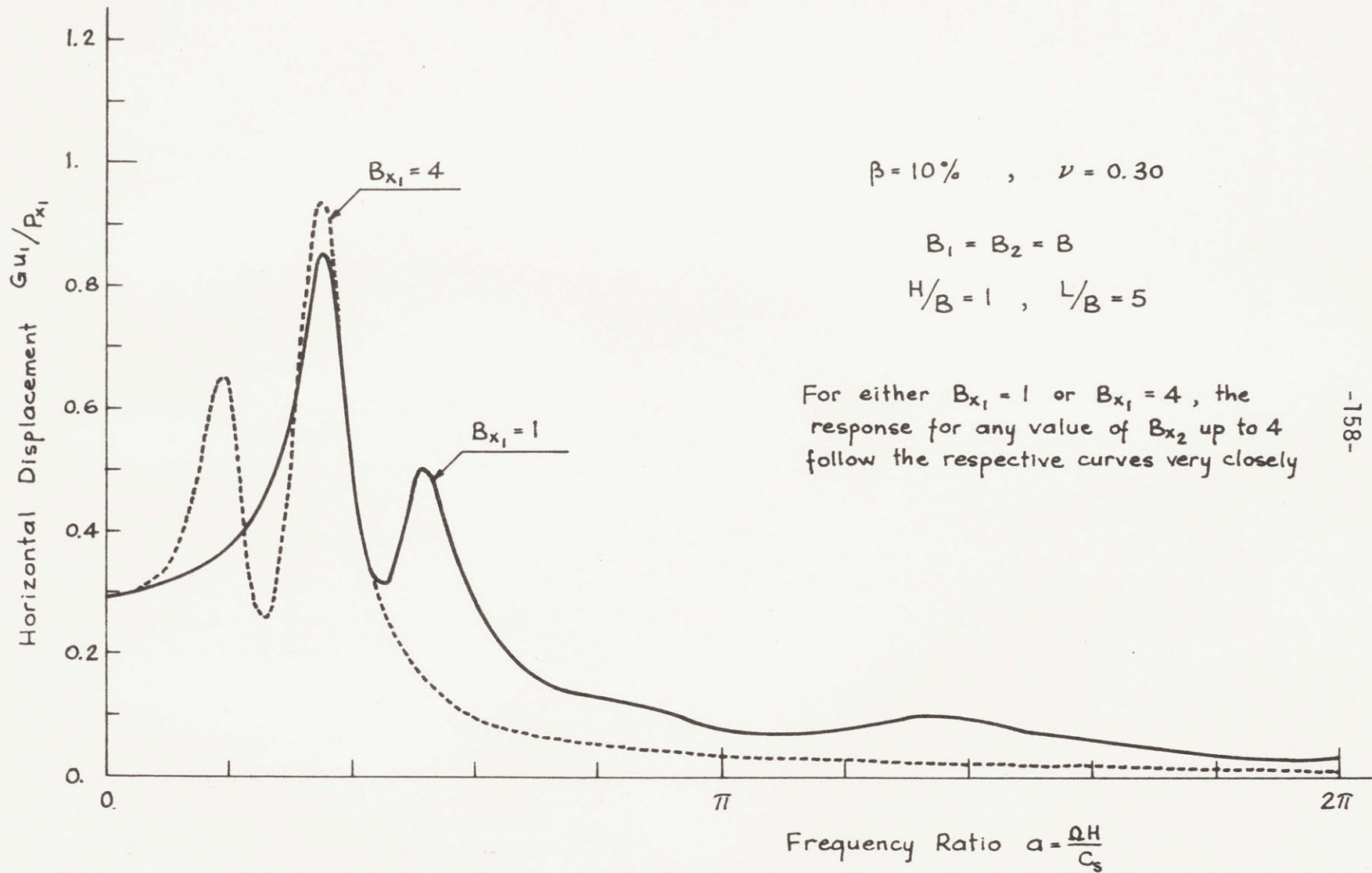


Figure 5-6 Horizontal Displacement in Excited Footing due to Horizontal Force

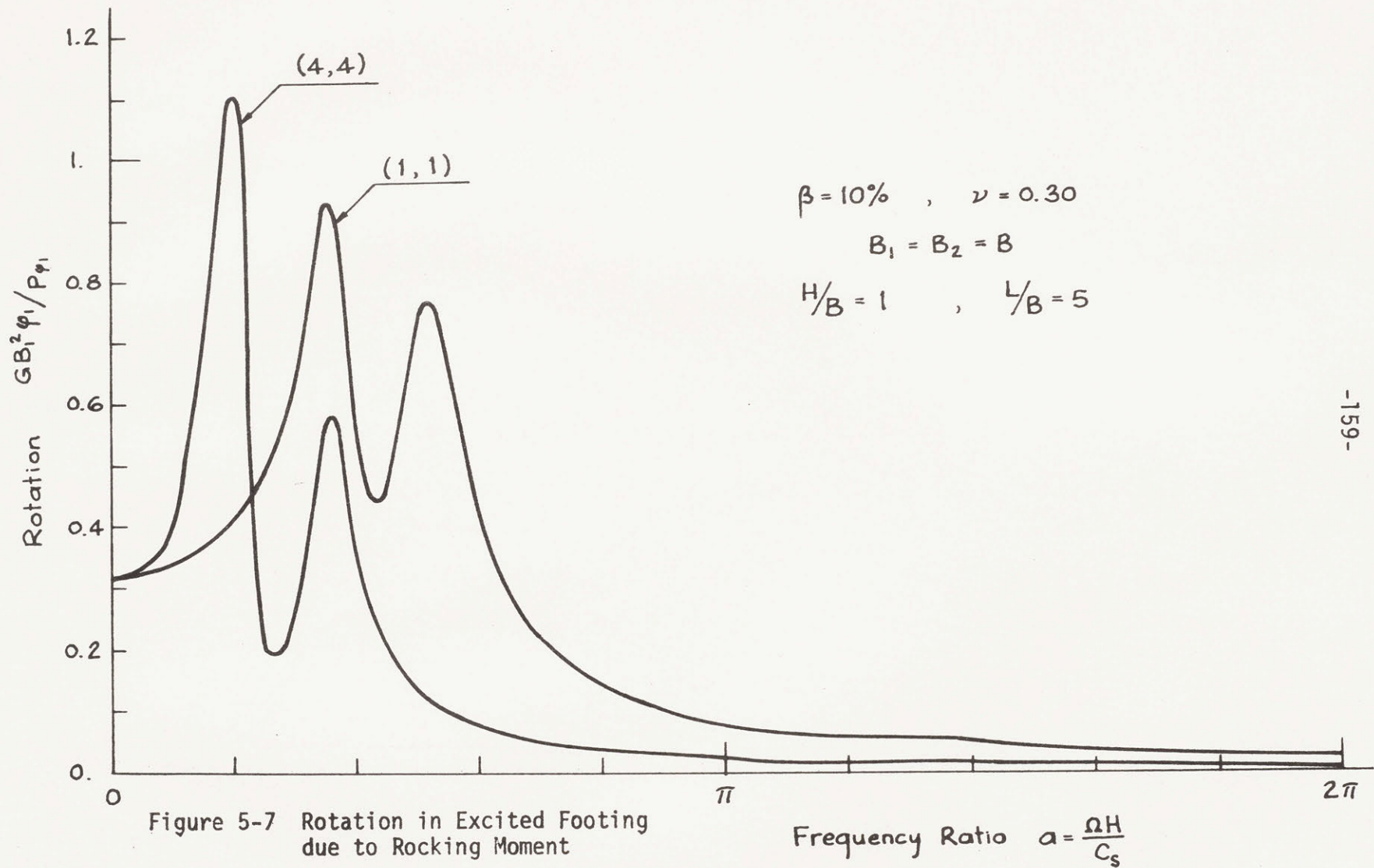
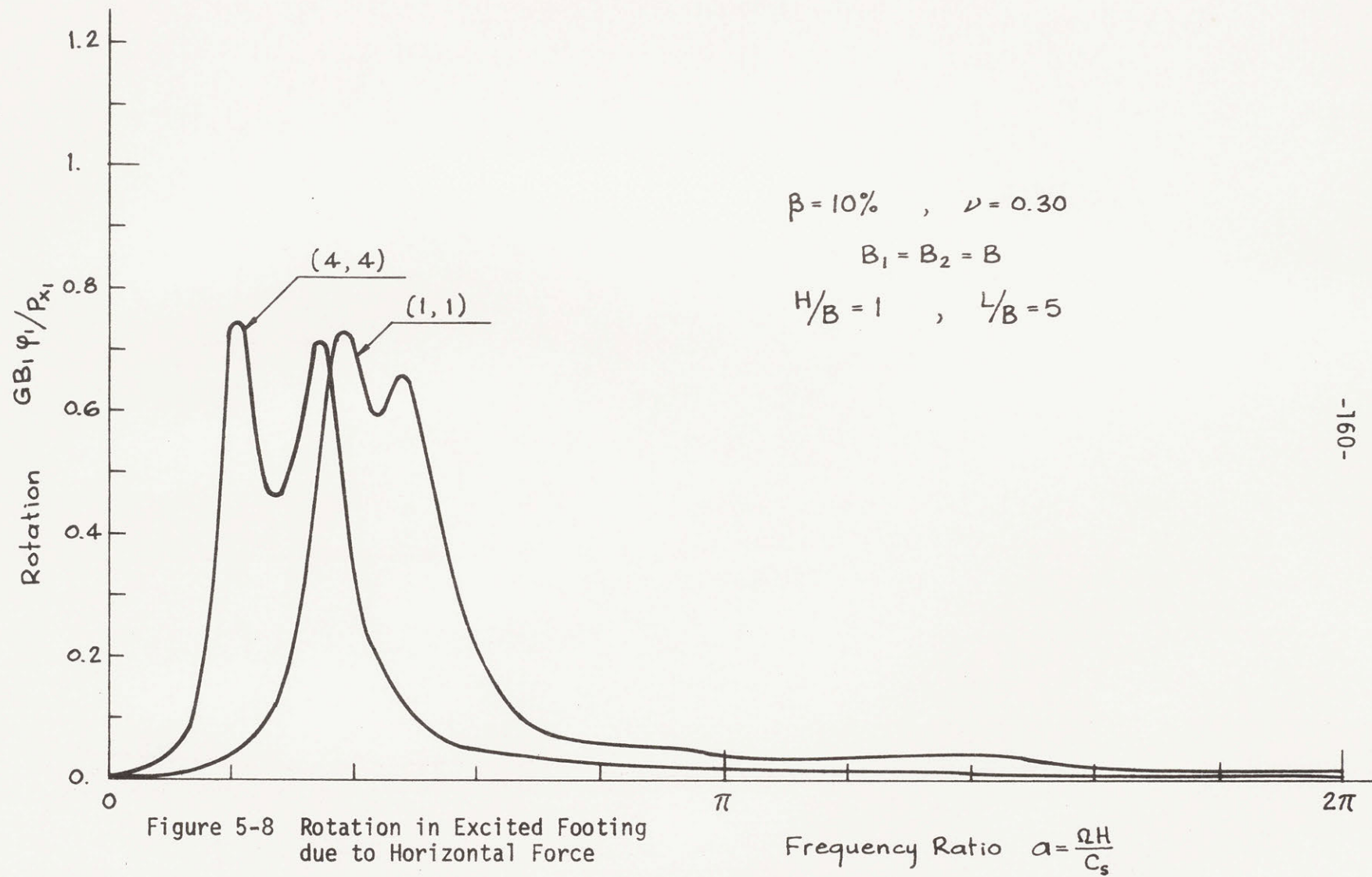


Figure 5-7 Rotation in Excited Footing due to Rocking Moment



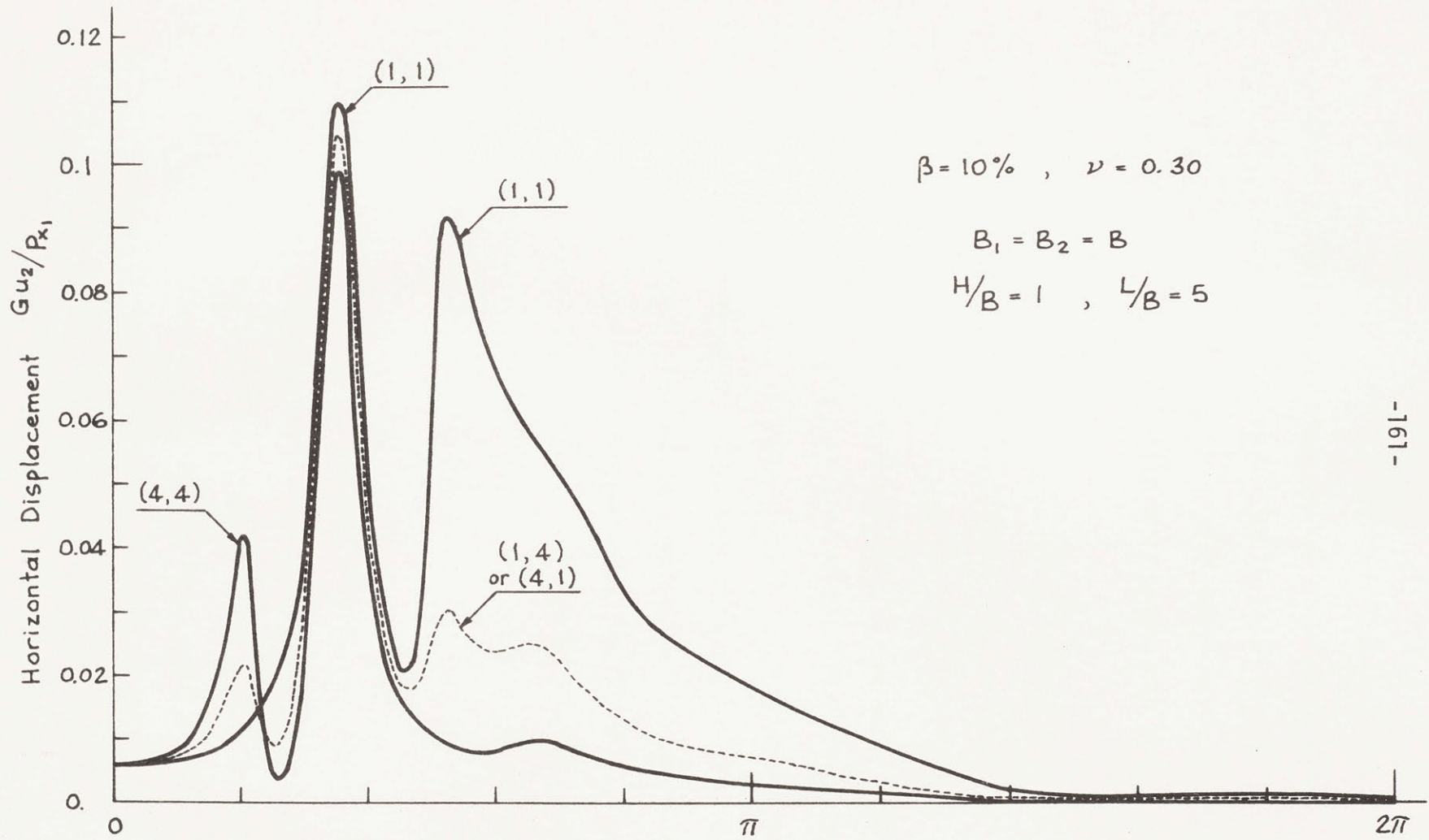


Figure 5-9 Horizontal Displacement in Passive Footing due to Horizontal Force

Frequency Ratio $a = \frac{\Omega H}{C_s}$

In Fig. 5-8, the curves show the horizontal displacement due to a rocking moment or the rotation due to a horizontal force, in the excited footing. These curves have a shape very close to those of Fig. 5-7, and are smaller in magnitude, but still quite appreciable.

The horizontal displacements induced in footing 2 by a horizontal force applied in footing 1 are shown in Fig. 5-9. These displacements are one order of magnitude smaller than those of the excited footing. They show a narrow and high peak, common to all combinations of mass ratios, at a frequency ratio of about 0.36π . When compared with Figs. 5-7 and 5-8, it is seen that all the response curves have a peak around that frequency. Therefore, this peak is caused by the rocking mode primarily. Whereas the combination of light masses (1,1) gives rise to another important peak, the response damps out when one of the two masses is heavy. Again, the case (1,1) is accompanied by considerable rocking; but for the other combinations of masses, the rotation in this footing is small after the high peak at $a = 0.36\pi$.

The effect of the distance between footings is shown in Fig. 5-10 for an excited footing, and in Fig. 5-11 for the adjacent structure. Only the horizontal displacements due to an applied horizontal force in one of them are shown. These curves apply for two equal masses on a layer of four times the half-width of any of them. For the excited mass, the difference in response between having an adjacent structure at a distance of $5B$ or $10B$ is small; but for the

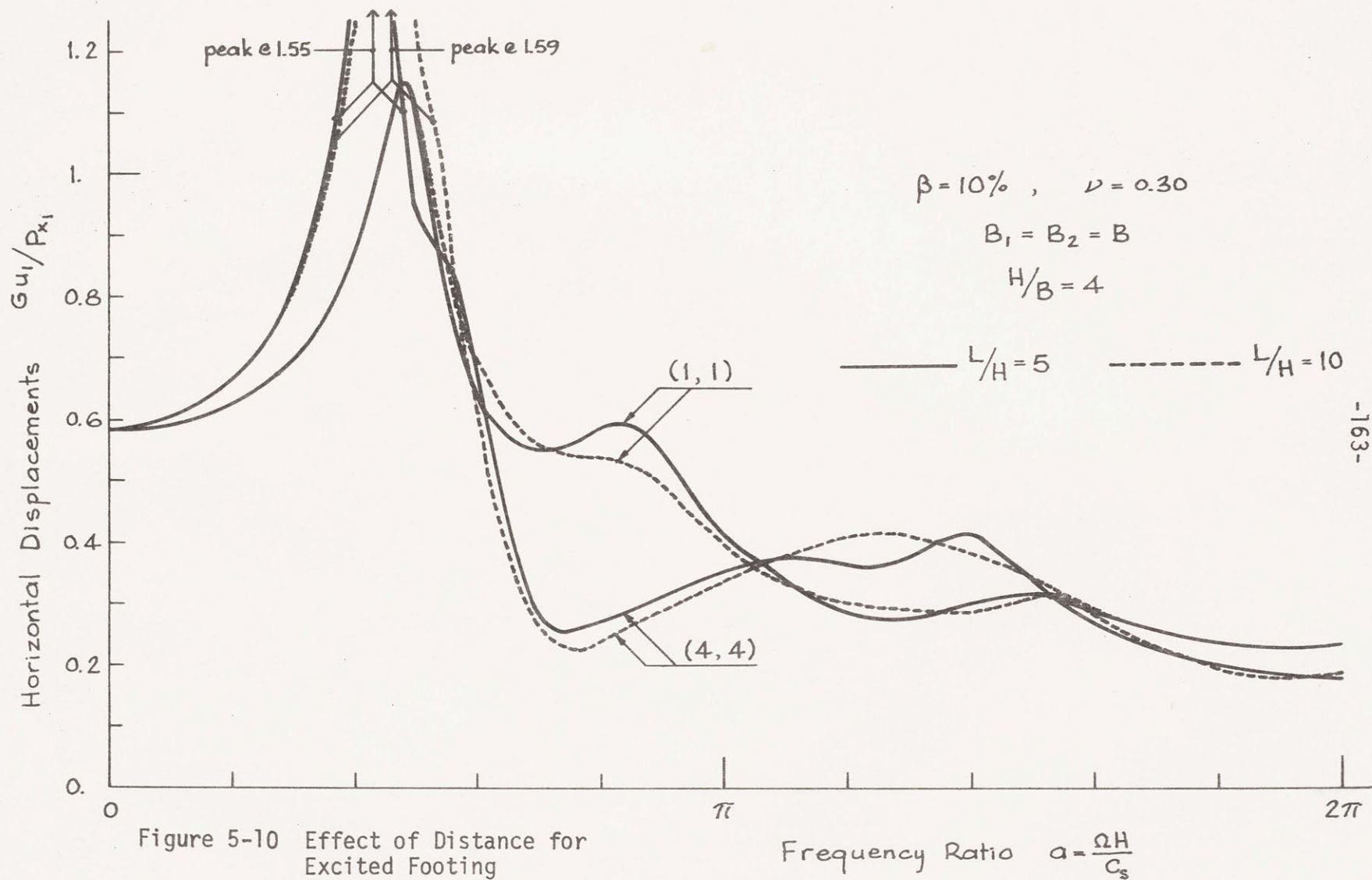


Figure 5-10 Effect of Distance for Excited Footing

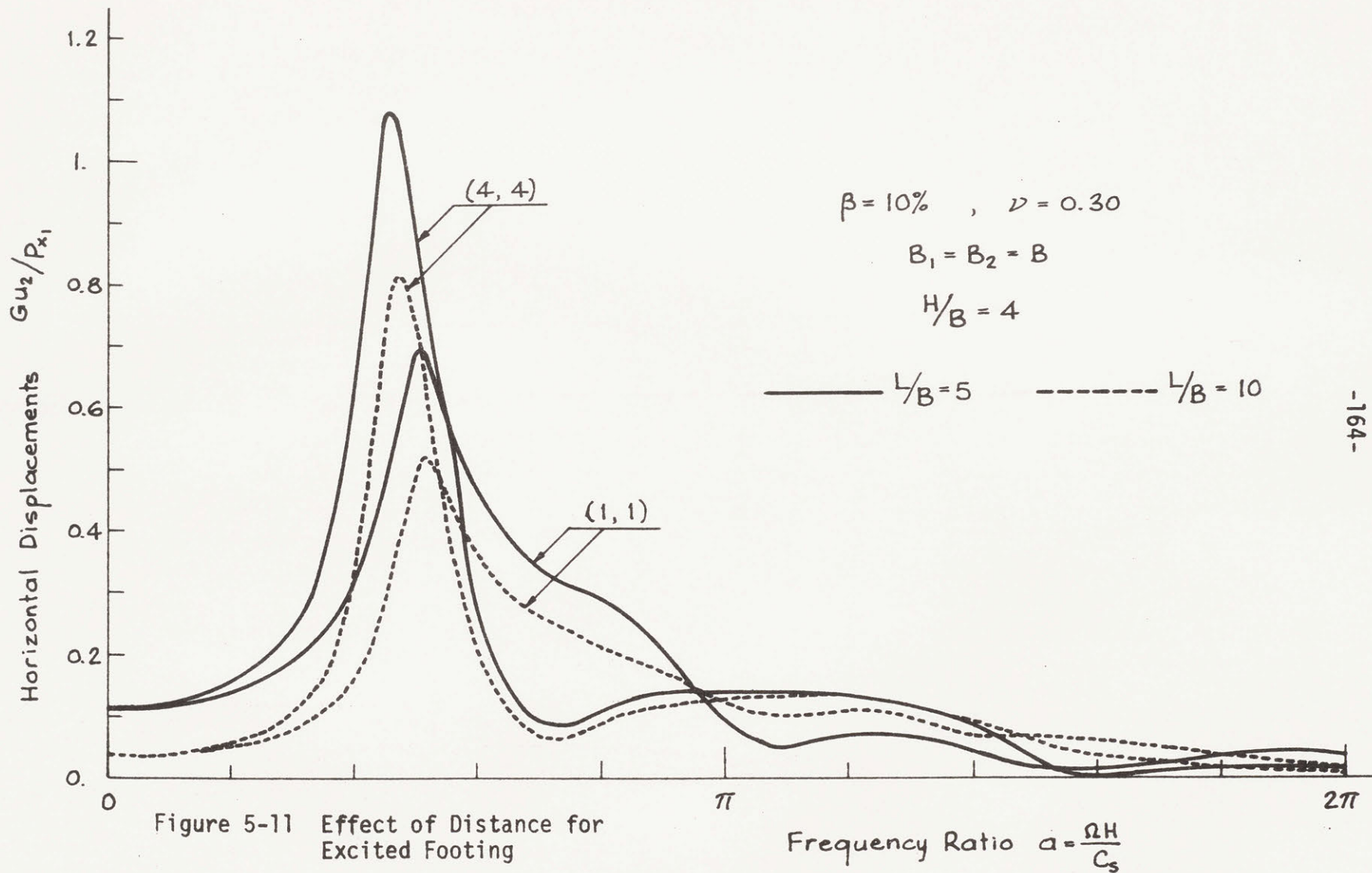


Figure 5-11 Effect of Distance for Excited Footing

unexcited mass, the effect of the distance is important. In the range of frequencies where the induced motion is large, the response is smaller when the excited footing is far, as might be expected. For other (higher) frequencies, the induced motion can be larger when the excited footing is farther; but then, the response is quite small.

5.4 Response to a Prescribed Motion of the Soil

The situation considered in this section is the response of two masses resting on the surface of a soil layer when the free surface moves harmonically in time as $u_0 e^{i\Omega t}$. The response of a mass when there is another body in the neighborhood is shown, as well as the increase or decrease in motion compared to the case of having only one footing.

Two geometrically equal masses are considered first with a ratio $H/B = 2$ and a separation equal to 2.5 times the layer thickness, center-to-center. Figs. 5-12 and 5-13 show the amplification of the free-field displacement as given by u_1/u_0 when the second mass ratio varies from 0 to 4. Fig. 5-12 applies when the footing under investigation is relatively light, $B_{x_1} = 1$, and Fig. 5-13 when it is relatively heavy, $B_{x_1} = 4$.

When the footing is light, the amplification (or deamplification) is not very marked; within 60% to 160% of u_0 . By comparing Figs. 5-12a and 5-12b, it is seen that the peaks in u_1/u_0 follow in general the peaks of u_2/u_0 for any given value of B_{x_2} (in both figures, $B_{x_1} = 1$). At the frequencies of the peaks, both footings tend to reinforce each other.

$$\beta = 10\% \quad , \quad \nu = 0.30$$

$$B_1 = B_2 = B$$

$$H/B = 2 \quad , \quad L/H = 2.5$$

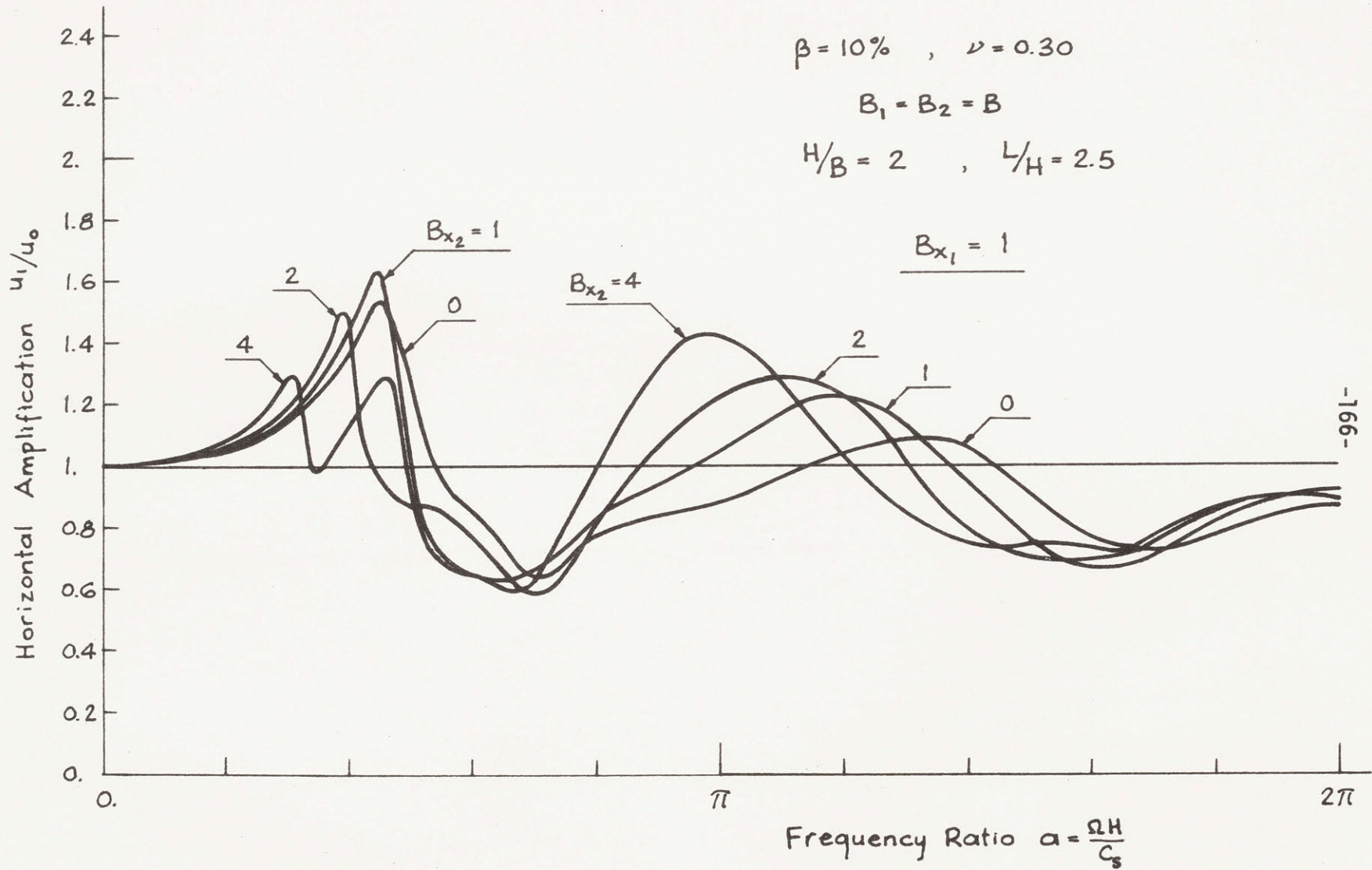


Figure 5-12a Effect of Mass of Adjacent Footing

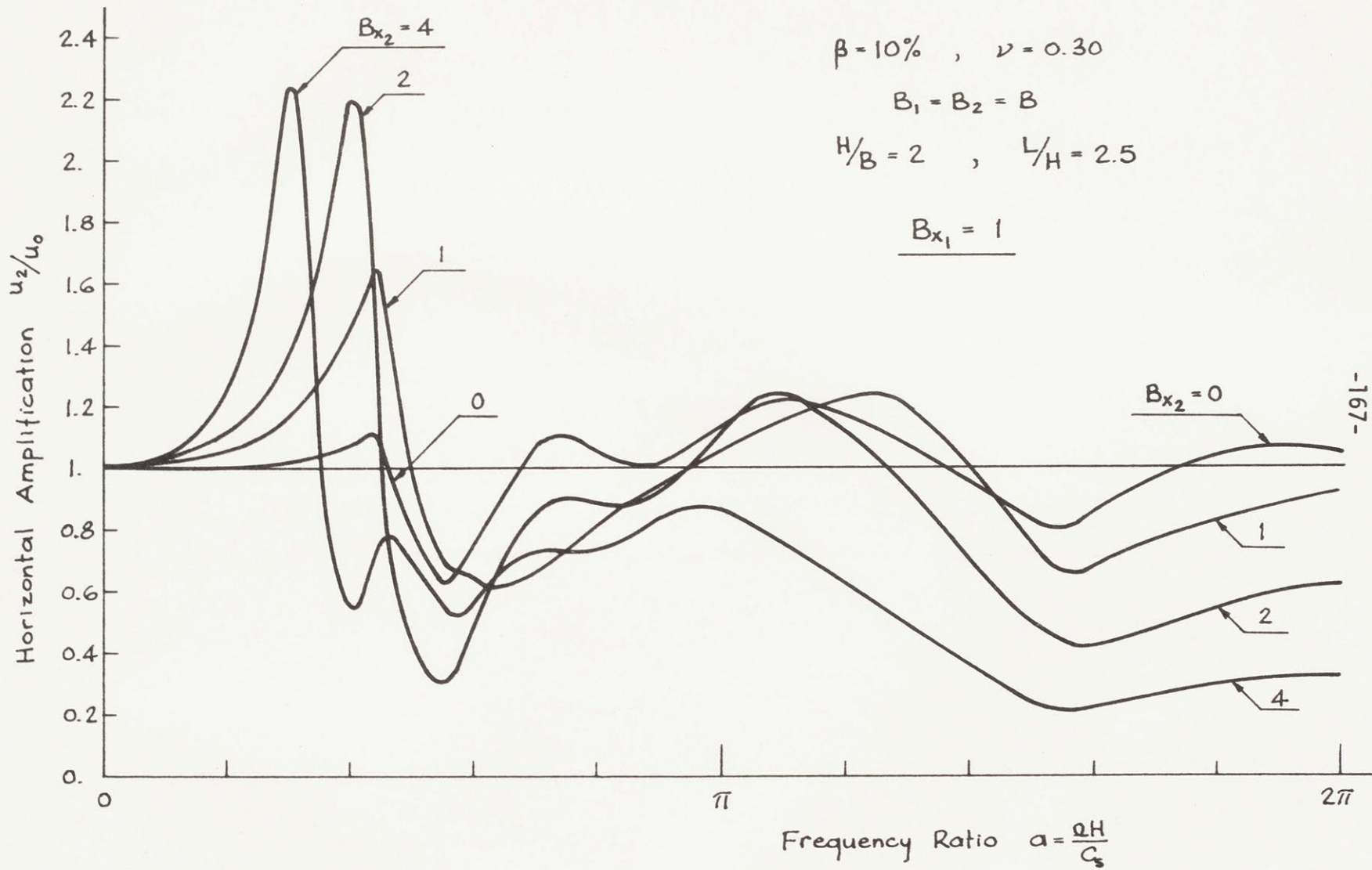


Figure 5-12b Effect of Own Mass

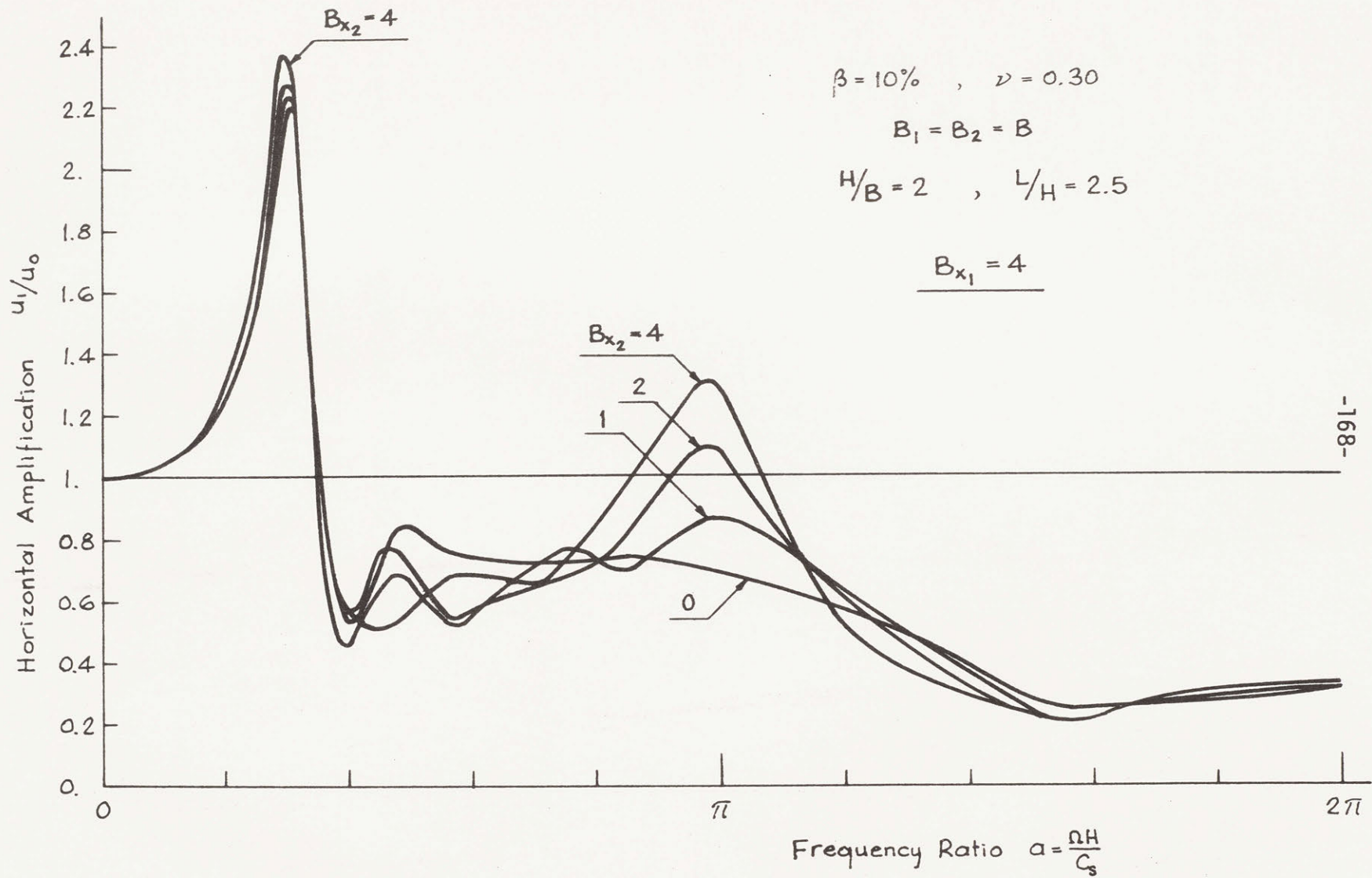


Figure 5-13 Effect of Mass of Adjacent Footing

Observe in Fig. 5-12b that a massless footing, as given by the curve (1,0) also has an amplification of the free-field motion, since the first footing (of $B_{x_1} = 1$) modifies u_0 in its neighborhood, producing horizontal, rocking and vertical displacements in adjacent structures, as well as in itself.

Although not shown here, it is important to point out that the rotation induced on the footings by u_0 can be important at certain frequencies, where $\phi_i B_i / u_0$ may be even larger than u_i / u_0 , $i = 1$ or 2 , and/or greater than 1.

Fig. 5-13 shows u_1 / u_0 when $B_{x_1} = 4$ for different values of B_{x_2} . For this relatively heavy structure, the response is mostly determined by itself. The influence of the second structure is felt almost only around the second important peak near $a = \pi$, which is caused by rocking mainly.

It is of interest to isolate the effect of the second mass on the first. For this purpose, the curves shown in Fig. 5-14 show the ratio of the horizontal displacement u_1 when there is another mass nearby to the displacement produced if the other structure has no mass (but still exists). The only important effect of the second mass occurs when it is relatively heavy, and it is located in the frequency range where rocking is important. The behavior is mostly determined by the second mass, as observed by the closeness of the curves corresponding to (1,1) and (4,1) on one hand, and by (1,4) and (4,4) on the other.

However, in these curves, the second footing's stiffness still

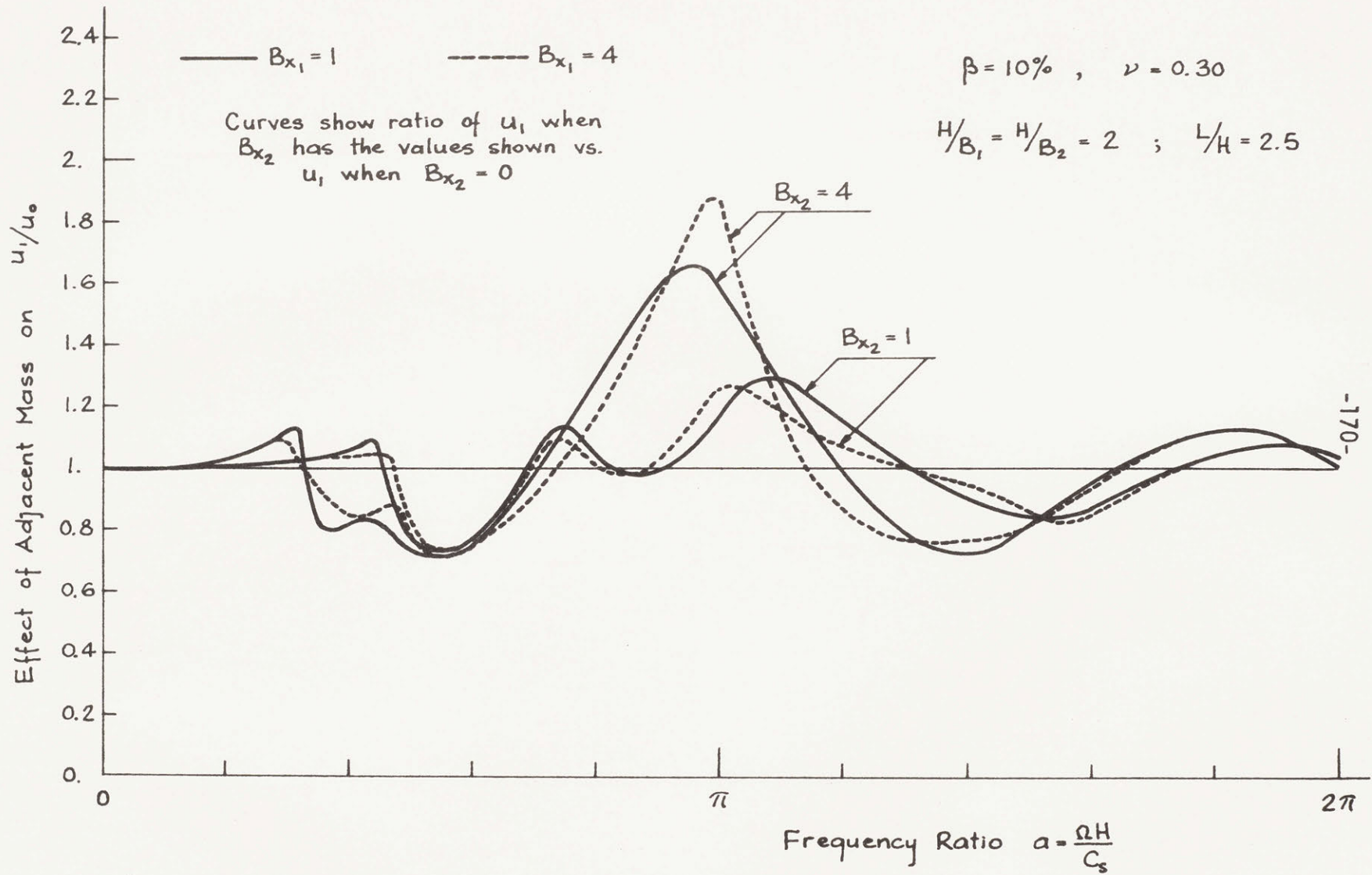


Figure 5-14 Effect of Adjacent Mass

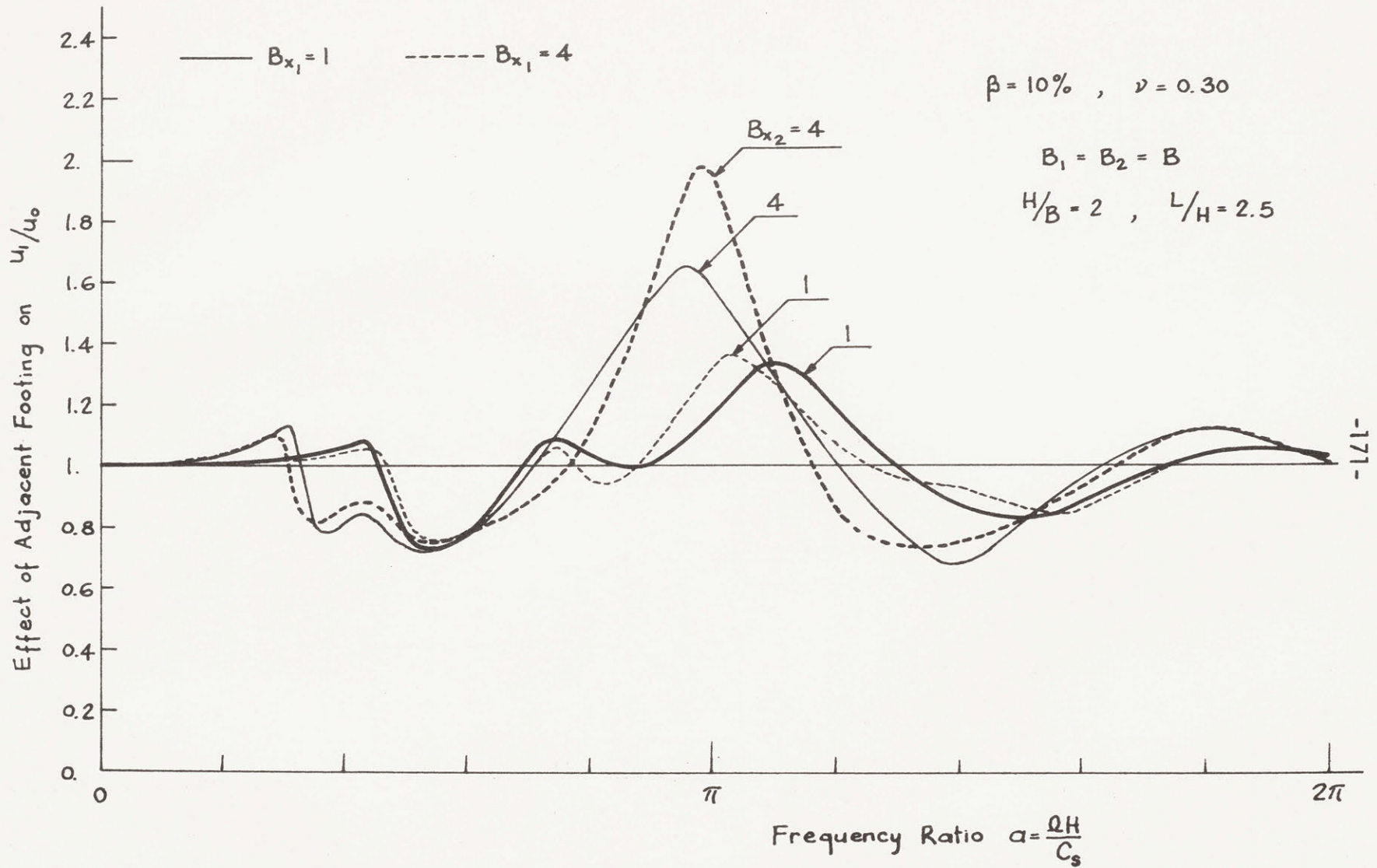


Figure 5-15 Effect of Adjacent Footing

affects the response. In Fig. 5-15, the effect of the second footing is isolated completely, by comparing u_1 when the two footings are present against u_1 when only one exists. Now, other peaks appear at lower frequencies, preceded by a large deamplification. This effect is more noticeable as the mass of the footing increases (cases (4,1) and (4,4)).

Therefore, restraining the surface motion by an adjacent rigid footing produces a feedback, even if it has no mass.

As a last example, the influence of a big structure on a smaller one is presented in Figs. 5-16 through 5-19. The small footing is taken as four times narrower than the large one. They are separated a distance $2.5H$ center to center, as in the preceding example. In terms of dimensionless ratios, $H/B_1 = 4$, $H/B_2 = 1$ and $L/H = 2.5$.

In Fig. 5-16, the small footing is light ($B_{x_1} = 1$). Varying the mass ratio of the second footing changes the response considerably. The peaks move to the left as B_{x_2} increases, and in the region where rocking is important, around $a = \pi$, the magnitude of the peaks is very sensitive to variations in the mass of the large footing. When the first mass is heavy ($B_{x_1} = 4$), as shown in Fig. 5-17, the amplification curves are in general higher than when it is light. The peaks also shift to the left, but varying the second mass from $B_{x_2} = 1$ to 4 does not produce a marked effect on u_1/u_0 in the region around $a = \pi$. The largest variation seems to be from $B_{x_2} = 0$ to 1. It is the inertia forces in the second footing which affect most the response of the first footing.

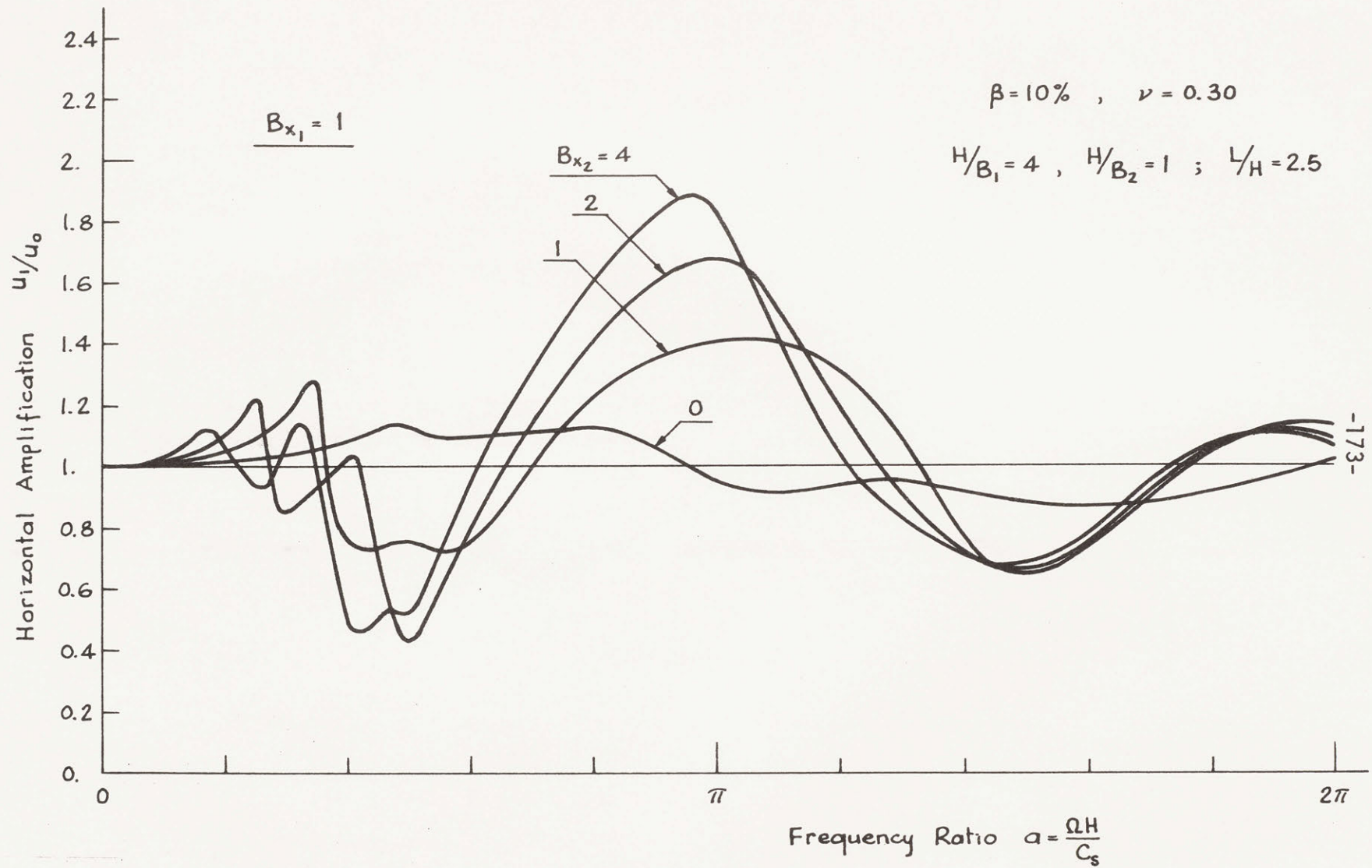


Figure 5-16 Effect of Mass of Adjacent Footing

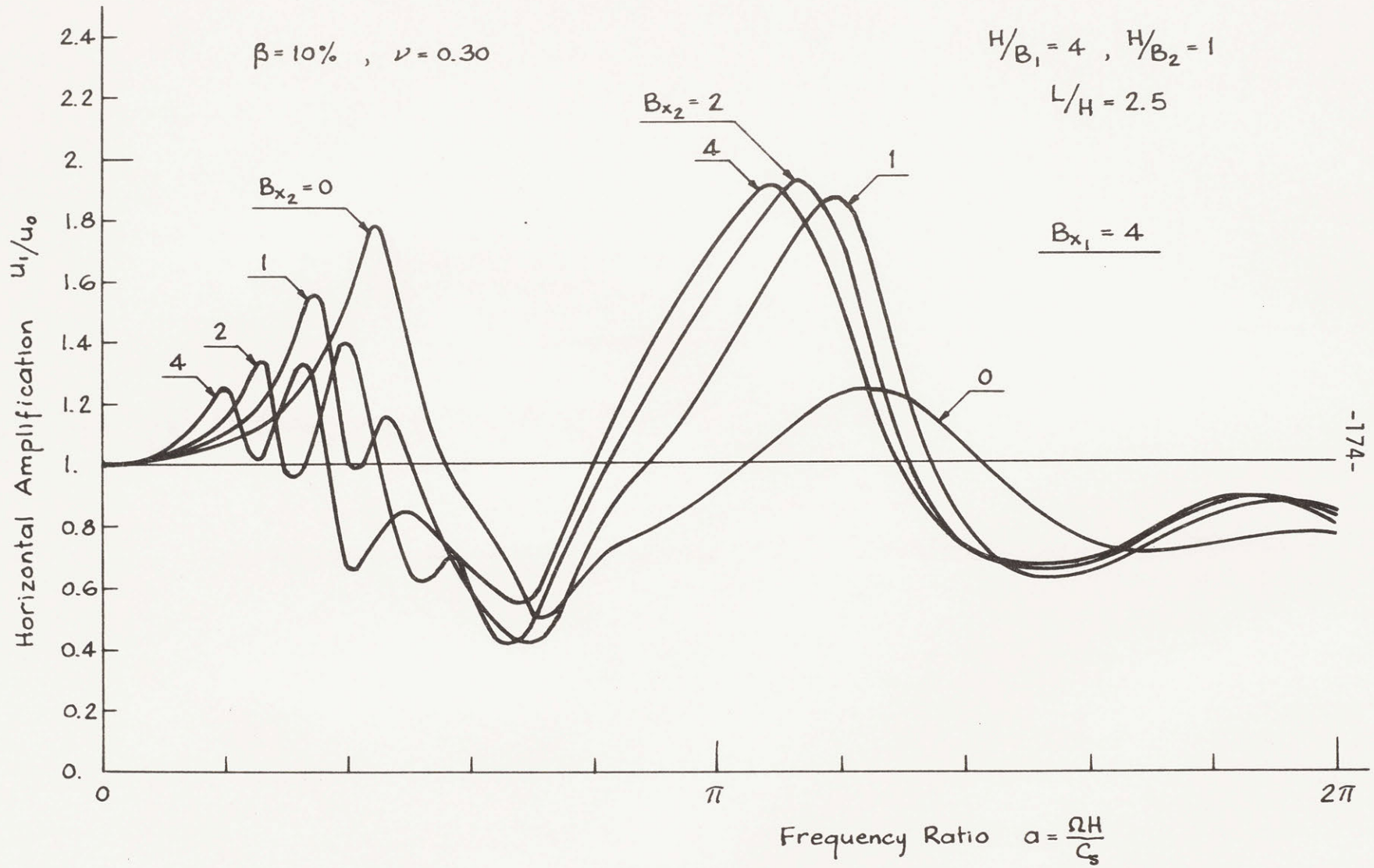


Figure 5-17 Effect of Mass of Adjacent Footing

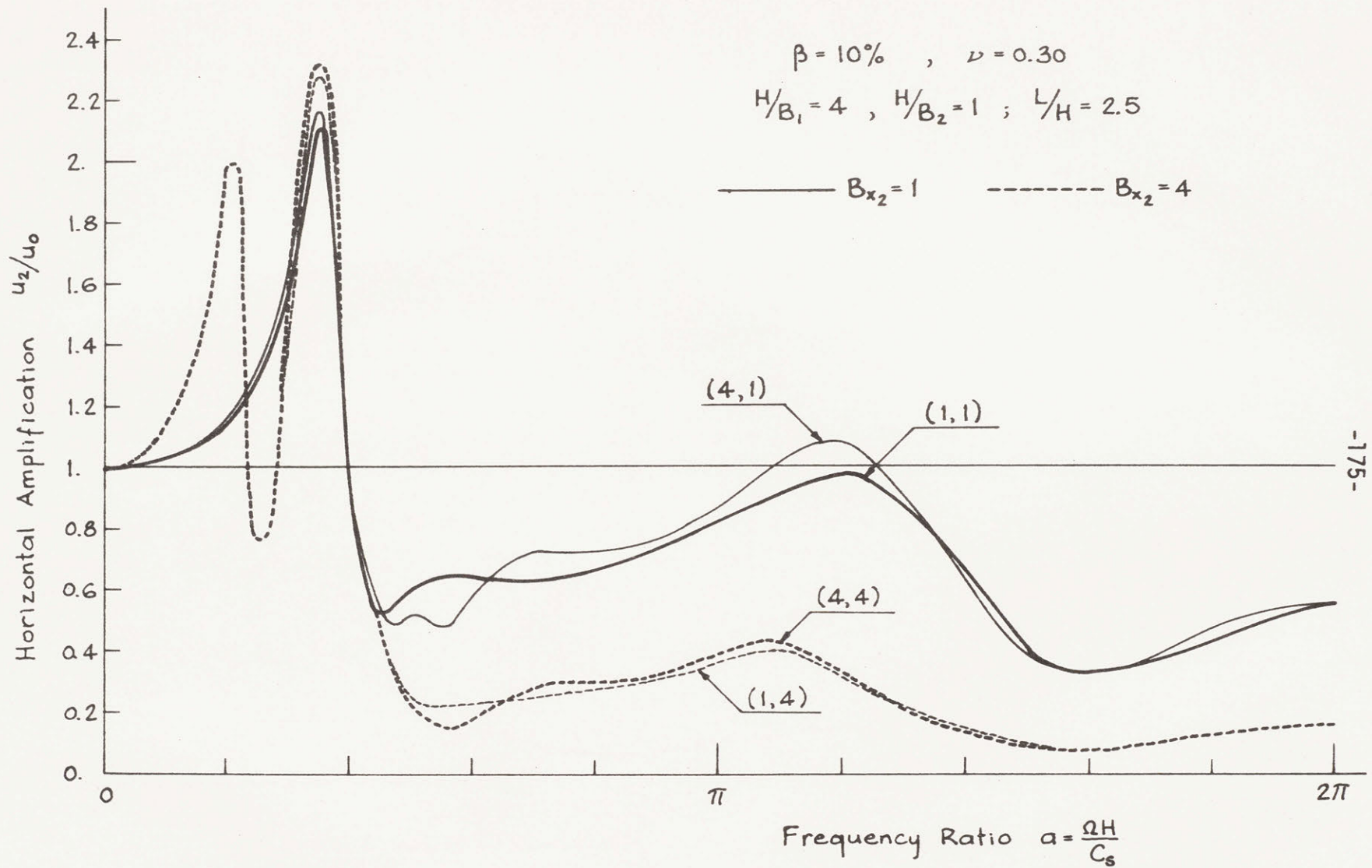


Figure 5-18 Effect of Small Footing on Larger Footing

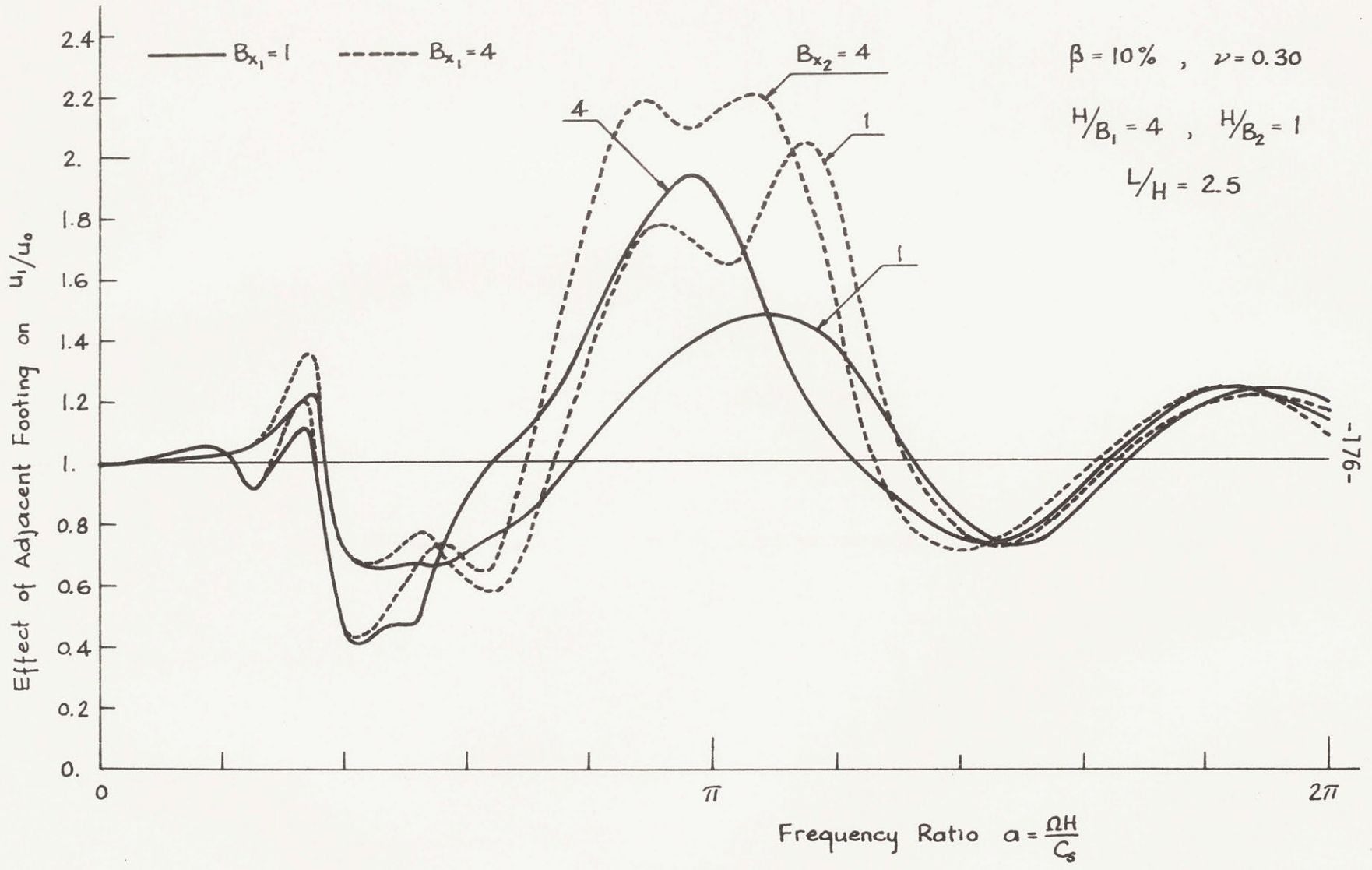


Figure 5-19 Effect of Adjacent Footing

In Fig. 5-18 it is shown how the small footing affects the response of the large one. As expected, the influence is very small. It is felt more when the large footing is light; but for all practical purposes, the large footing can be studied alone as in Chapter 3.

Similarly to Fig. 5-15, Fig. 5-19 shows the ratio of u_1 when the large footing is present against u_1 when only the small footing exists. The amplification due to the large footing is very pronounced. In the average (for a white noise input), the presence of a large footing is detrimental to the small one. Again, rocking is responsible for a large part of this amplification, which increases when either of the mass ratios increases.

CHAPTER 6 - CONCLUSIONS AND RECOMMENDATIONS

6.1 Summary

The response of a rigid strip footing resting on or embedded in a soil stratum was studied. Results were given in terms of dimensionless parameters. For all the examples considered, the soil was taken as homogeneous, isotropic and linearly elastic with hysteretic damping. The cases studied included the excitation of a footing by horizontal forces and rocking moments, and the motion due to a specified displacement at bedrock. The interaction of two footings through the soil was also considered.

Poisson's ratio was kept constant since the rest of the parameters involved in this study was already numerous. For the same reason, almost all results were obtained for only one particular value of damping; but a discussion of the effect of this variable is included.

The model used satisfied equilibrium and compatibility conditions throughout the whole domain. The method was consistent in the sense that it used the same displacement expansions for the derivation of the elastic, damping and inertia forces at any nodal joint. It accounted for the dynamic response of the semi-infinite layered regions, providing displacements continuous in a horizontal direction, and piecewise linearly continuous across the depth of the stratum.

Since there were no available analytical solutions known to the

writer, the results could not be checked rigorously. The solutions presented appear to be reasonable. They follow the trend of other cases studied by several authors in an approximate way for circular or rectangular foundations. As the stratum thickness increased, the solutions found by the present method converged to the known half-space solutions.

Different mesh sizes were used by the originator of the model to determine the accuracy of the method. A few other cases were tested by the writer. No apparent numerical errors arose.

The separation of the amplification effect of the soil from the interaction effect was done using an input motion at the base of the structure consistent with the derived stiffness functions. The adequacy of this procedure was tested by using the program PLAXLY2 to analyze the problem as a whole. The results obtained by both methods gave identical results.

The adequacy of the solutions depends, however, on the validity of an important simplification. It was assumed that the soil could resist tensile stresses and that it would be at all times perfectly welded to the structure.

6.2 Conclusions

Effect of internal damping

The general form of the compliance (or stiffness) functions does not change significantly with the amount of damping, except

for the fact that singularities occur for the undamped case. The use of the correspondence principle to derive solutions for a given percentage of damping starting from the elastic case is, however, inadequate. Only for the half-space, the application of this principle gave results that agreed fairly well with the solution with damping considered implicitly.

Effect of layer thickness

The static horizontal compliance varies more with layer thickness than the rocking compliance, which converges rapidly to the half-space solution as the layer thickness increases. This suggests that the rocking vibration is practically confined within a "bulb of pressure" under the footing.

After the first peak, the compliance functions oscillate around the half-space solution, and tend towards it as the frequency increases, suggesting that the effect of the rigid base under the soil is less important in the high frequency range.

One effect of the mass of the footing is, clearly, to decrease the resonant frequencies. As the mass ratio increases, there is first an increase in the maximum amplification at the first peak, and then a decrease in the value of the amplification as the inertia term predominates over the force due to the stiffness of the soil. A second peak is produced by rocking, and it increases in magnitude as the mass ratio increases. These effects are more pronounced for shallow than for deep layers.

The location of the center of gravity is an important parameter affecting the response. Increasing the height of the center of gravity produces marked changes in the resonant frequency, moving it towards lower values. In the average, the smaller the radius of gyration is, the greater the deamplification of the surface motion.

Effect of embedment

When there is embedment, the theory of one-dimensional amplification will no longer provide the correct input motion at the base of the structure for a separate soil-structure interaction analysis. The motion of the soil is modified in the vicinity of the footing even if it is massless; and the peaks of the amplification curves are reduced as compared to those of the footing on the surface. However, the frequency of these peaks does not change appreciably with embedment, suggesting that it is the total stratum thickness which governs the resonant frequency, rather than the net distance between the bottom of the footing and the rock, as occurs in the case of vertical vibration. In addition to a horizontal motion, there will be now a rotation of the footing. This rocking is small for low frequencies, but can become significant in the high frequency range.

The compliance functions are rather similar for footings with different embedment to layer thickness ratios, when normalized with respect to their static values. Therefore, it would seem that the compliance functions for embedded footings can be found approximately from those corresponding to a footing on the surface by using a scaling factor.

The main effect of embedment is to increase the stiffness of the footing-soil system by the scaling factor mentioned above. As a result, when the footing has mass, the resonant frequencies of the system are higher than if the footing were at the surface. The rocking motion is reduced by embedment if the mass of the structure is higher than the mass of soil lost by the excavation. But the maximum horizontal amplification can be higher for embedded footings than for footings on the surface if the mass ratio is high.

Effect of adjacent structures

From the limited number of cases considered it would appear that the effect of neighboring structures is less important for very shallow layers of soil (on rigid rock) than for layers of moderate thickness. In all cases, the adjoining structure affects only slightly the response of the excited mass, the effect being more noticeable when the latter is small. Results as far as the excited structure is concerned are almost the same for a distance between the two masses of 2.5 or 5 times their base dimension. The significant part of this kind of study would thus be the determination of the vibrations induced in the second structure, rather than the feedback from this one to the excited mass.

For the case of a base motion (simulating an earthquake excitation) the effect of a neighboring structure is particularly significant around the first fundamental frequency of the layer in vertical

motion, indicating that this interaction is primarily due to the rocking effect.

6.3 Recommendations for Further Work

It was the purpose of this work to investigate several factors affecting the soil structure interaction problem: effect of layer thickness (by opposition to an elastic half space), effect of embedment and effect of adjacent structures. Since the number of parameters involved is very large, the cases studied do not cover the complete spectrum of possibilities, and the conclusions presented before have to be interpreted as expressing a trend based on the obtained results, rather than as absolute statements.

Further parametric studies seem warranted in order to validate these conclusions. It would be interesting in particular to consider realistic models of structures rather than rigid masses and to evaluate fully the degree of approximation involved by simplifying assumptions (such as using the compliance functions for the half-space modified by scaling factors to account for layering or embedment). The effect of the rocking motion at the base of the structure in case of embedment should also be investigated in more detail.

While the program used is only applicable in rigor for strip footings, it is used sometimes in practice for the study of rectangular or even circular foundations. A comparison of results obtained with this model and more accurate (but also more expensive) three-

dimensional finite element programs is necessary.

Other improvements can be introduced in the program to study additional factors: among these the possibility of considering non-linear soil properties (by an iterative linear analysis) and the possibility of applying a base motion which is not the same at all points (a travelling disturbance) deserve special consideration. The effect of elastic rock (instead of a rigid base) could also be important in the case of shallow layers.

REFERENCES

1. Agabein, M.E., Parmelee, R.A., and Lee, S.L., "A Model for the Study of Soil-Structure Interaction," Proc. Eighth Congress of the Intl. Assoc. for Bridge and Structural Engng. pp. 1-12, New York, 1968.
2. Ang, A.H.-S., and Harper, G.N., "Analysis of Contained Plastic Flow in Plane Solids," Journ. Engineering Mechanics Div., ASCE, Vol. 90, No. EM5, pp. 397-418, 1964.
3. Arnold, R.N., Bycroft, G.N., and Warburton, G.B., "Forced Vibrations of a Body on an Infinite Elastic Solid," Journ. Applied Mechanics, Trans. ASME, Vol. 22, No. 3, pp. 391-400, 1955.
4. Awojobi, A.O., "Approximate Solution of High-Frequency-Factor Vibrations of Rigid Bodies on Elastic Media," Journ. Applied Mechanics, Trans. ASME, Vol. 38, Ser. E, No. 1, pp. 111-117, 1971.
5. Awojobi, A.O., and Grootenhuis, P., "Vibration of Rigid Bodies on Semi-infinite Elastic Media," Proc. Royal Soc. London, Ser. A, Vol. 287, pp. 27-63, 1965.
6. Baranov, V.A., "On the Calculation of Excited Vibrations of an Embedded Foundation," (in Russian) Voprosy Dynamiki i Prochnosti, No. 14, Polytechnical Inst. of Riga, pp. 195-209, 1967.
7. Beredugo, Y.O., and Novak, M., "Coupled Horizontal and Rocking Vibration of Embedded Footings," Canadian Geotechnical Journal, Vol. 9, No. 4, pp. 477-497, 1972.
8. Bland, D.R., The Theory of Linear Viscoelasticity, Pergamon Press, 1960.
9. Bycroft, G.N., "Forced Vibration of a Rigid Circular Plate on a Semi-infinite Elastic Space and an Elastic Stratum," Phil. Trans. Royal Soc. London, Ser. A., Vol. 248, pp. 327-386, 1956.
10. Chakravorty, M.K., Nelson, M.F., and Whitman, R.V., Approximate Analysis of 3-DOF Model for Soil-Structure Interaction, Research Report 71-11, Dept. of Civil Engrg., MIT, Cambridge, Mass., June 1971.
11. Cooley, J.W., and Tukey, J.W., "An Algorithm for the Machine Calculation of Complex Fourier Series," Mathematical Computation, Vol. 19, pp. 297-301, April 1965.

12. DiMaggio, F.L., and Bleich, H.H., "An Application of a Dynamic Reciprocal Theorem," Journ. Applied Mechanics, Trans. ASME, Vol. 29, pp. 678-679, 1959.
13. Elorduy, J., Nieto, J.A., and Szekely, E.M., "Dynamic Response of Bases of Arbitrary Shape Subjected to Periodical Vertical Loading," Proc. Intl. Symp. on Wave Propagation and Dynamic Properties of Earth Materials, Univ. of New Mexico, Albuquerque, pp. 105-121, 1967.
14. Fleming, J.F., Screwvala, F.N., and Kondner, R.L., "Foundation Superstructure Interaction under Earthquake Motion," Proc. 3rd WCEE, pp. I-22 to I-30, New Zealand, 1965.
15. Fung, Y.C., Foundations of Solid Mechanics, Prentice-Hall, 1965.
16. Gladwell, G.M., "Forced Tangential and Rotatory Vibration of a Rigid Circular Disc on a Semi-infinite Solid," Intl. Journ. Engineering Science, Vol. 6, No. 10, pp. 591-607, 1968.
17. Gupta, D.C., Parmelee, R.A., and Krizek, R.J., "Coupled Sliding and Rocking Vibrations of a Rigid Foundation on an Elastic Medium," Tech. Report, Dept. Civil. Engrg., Northwestern Univ., Evanston, Ill., 1972.
18. Hall, J.R., Jr., "Coupled Rocking and Sliding Oscillations of Rigid Circular Footings," Proc. Intl. Symp. on Wave Propagation and Dynamic Properties of Earth Materials, Univ. of New Mexico, Albuquerque, pp. 139-148, 1967.
19. Hsieh, T.K., "Foundation Vibrations," Proc. Institution of Civil Engineers, Vol. 22, pp. 211-226, 1962.
20. Iljitchov, V.A., "Towards the Soil Transmission of Vibrations from One Foundation to Another," Proc. Intl. Symp. on Wave Propagation and Dynamic Properties of Earth Materials, Univ. of New Mexico, Albuquerque, pp. 641-653, 1967.
21. Jones, T.J., and Roesset, J.M., Soil Amplification of SV and P Waves, Research Report R70-3, Dept. Civil Engrg., MIT, Cambridge, Mass., Jan. 1970.
22. Karasudhi, P., Keer, L.M., and Lee, S.L., "Vibratory Motion of a Body on an Elastic Half Plane," Journ. Applied Mechanics, Trans. ASME, Vol. 35, Ser. E, No. 4, pp. 697-705, 1968.
23. Kobori, T., and Minai, R., "Dynamical Interaction of Multiple Structural Systems on a Soil Medium," Paper 256, Proc. 5th WCEE. Rome, 1973 (in publication).

24. Kobori, T., Minai, R., and Suzuki, T., "The Dynamical Ground Compliance of a Rectangular Foundation on a Viscoelastic Stratum," Bull. of the Disaster Prevention Research Institute, Kyoto Univ., Vol. 20, pp. 289-329, Mar. 1971.
25. Kobori, T., Minai, R., Suzuki, T., and Kusakabe, K., "Dynamical Ground Compliance of Rectangular Foundations," Proc. Sixteenth Natl. Congress for Applied Mechanics, 1966.
26. Kobori, T., Minai, R., Suzuki, T., and Kusakabe, K., "Dynamic Ground Compliance of Rectangular Foundation on a Semi-infinite Viscoelastic Medium," Annual Report, Disaster Prevention Research Institute of Kyoto Univ., No. 11A, pp. 349-367, 1968.
27. Kobori, T., and Suzuki, T., "Foundation Vibrations on a Viscoelastic Multilayered Medium," Proc. Third Japan Earthquake Engrg. Symp., pp. 493-499, Tokyo, 1970.
28. Krizek, R.J., Gupta, D.C., and Parmelee, R.A., "Coupled Sliding and Rocking of Embedded Foundations," Journ. Soil Mech. and Foundations Div., ASCE, Vol. 98, No. SM12, pp. 1347-1358, 1972.
29. Kuhlemeyer, R., Vertical Vibrations of Footings Embedded in Layered Media, Ph. D. thesis, Univ. of California, Berkeley, 1969.
30. Luco, J.E., and Westmann, R.A., "Dynamic Response of Circular Footings," Journ. Engrg. Mechanics Div., ASCE, Vol. 97, No. EM5, pp. 1381-1395, 1971.
31. Luco, J.E., and Westmann, R.A., "Dynamic Response of a Rigid Footing Bonded to an Elastic Half Space," Journ. Applied Mechanics, Trans. ASME, Vol. 39, Ser. E., No. 2, pp. 527-534, 1972.
32. Lycan, D.L., and Newmark, N.M., "Effect of Structure and Foundation Interaction," Journ. Engrg. Mechanics Div., ASCE, Vol. 87, No. EM5, pp. 1-31, 1961.
33. Lysmer, J., Vertical Motion of Rigid Footings, Dept. of Civil Engrg., Univ. of Michigan, Report to WES Contract Report No. 3-115, 1965.
34. Lysmer, J., and Kuhlemeyer, R.L., "Finite Dynamic Model for Infinite Media," Journ. Engineering Mechanics Div., ASCE, Vol. 95, No. EM4, pp. 859-877, 1969.
35. Lysmer, J., and Richart, F.E., Jr., "Dynamic Response of Footings to Vertical Loading," Journ. Soil Mech. and Foundations Div., ASCE, Vol. 92, No. SM1, pp. 65-91, 1966.

36. MacCalden, P.B., and Matthiesen, R.B., "Coupled Response of Two Foundations," Paper 238, Proc. 5th WCEE, Rome, 1973 (in publication).
37. Meek, J.W., and Veletsos, A.S., "Simple Models for Foundations in Lateral and Rocking Motion," Paper 331, Proc. 5th WCEE, Rome, 1973 (in publication).
38. Merritt, R.G., and Housner, G.W., "Effects of Foundation Compliance on Earthquake Stresses in Multi-story Buildings," Bull. Seism. Soc. Am., Vol. 44, No. 4, pp. 551-570, 1954.
39. Novak, M., "The Effect of Embedment on Vibration of Footings and Structures," Paper 337, Proc. 5th WCEE, Rome, 1973 (in publication).
40. Novak, M., and Beredugo, Y.O., "Vertical Vibrations of Embedded Footings," Journ. Soil Mech. and Foundations Div., ASCE, Vol. 98, No. SM12, pp. 1291-1310, 1972.
41. Oien, M.A., "Steady Motion of a Rigid Strip Bonded to an Elastic Half Space," Journ. Applied Mechanics, Trans. ASME, Vol. 38, Ser. E, No. 2, pp. 328-334, 1971.
42. Ratay, R.T., "Sliding-Rocking Vibration of Body on Elastic Medium," Journ. Soil Mech. and Foundations Div., ASCE, Vol. 97, No. SM1, pp. 177-192, 1971.
43. Reissner, E., "Stationäre, axialsymmetrische, durch eine schüttelnde Masse erregte Schwingungen eines homogenen elastischen Halbraumes," Ingenieur-Archiv, Vol. 7, pp. 381-396, 1936.
44. Richardson, J.D., Forced Vibrations of Rigid Bodies on a Semi-infinite Elastic Medium, Ph. D. thesis, Univ. of Nottingham, England, May 1969.
45. Richardson, J.D., Webster, J.J., and Warburton, G.B., "The Response on the Surface of an Elastic Half-Space near to a Harmonically Excited Mass," Journ. Sound and Vibration, 14(3), pp. 307-316, 1971.
46. Robertson, I.A., "Forced Vertical Vibration of a Rigid Circular Disk on a Semi-infinite Solid," Proc. Cambridge Philosophical Soc., Vol. 62A, pp. 547-553, 1966.
47. Roesset, J.M., personal communication of research underway.
48. Roesset, J.M., and Whitman, R.V., Theoretical Background for Amplification Studies, Report No. 5 on "Effect of Local Soil Conditions upon Earthquake Damage," Research Report R69-15, Dept. of Civil Engrg., MIT, Cambridge, Mass., March 1969.

49. Sakurai, J., and Minami, J.K., "Some Effects of Nearby Structures on the Seismic Response of Buildings," Paper 274, Proc. 5th WCEE, Rome, 1973 (in publication).
50. Sarrazin, M.A., Soil-Structure Interaction in Earthquake Resistant Design, Research Report R70-59, Dept. Civil Engrg., MIT, Cambridge, Mass., Sept. 1970.
51. Sinitsyn, A.P., "The Interaction between a Surface Wave and a Structure," Proc. Intl. Symp. on Wave Propagation and Dynamic Properties of Earth Materials, Univ. of New Mexico, Albuquerque, pp. 521-527, 1967.
52. Thomson, W.T., "A Survey of the Coupled Ground-Building Vibration," Proc. 2nd WCEE, Tokyo, 1960.
53. Urlich, C.M., and Kuhlemeyer, R.L., "Coupled Rocking and Lateral Vibrations of Embedded Footings," Canadian Geotechnical Journal, Vol. 10, No. 2, pp. 145-160, 1973.
54. Veletsos, A.S., and Verbic, B., Vibration of Viscoelastic Foundations, Report No. 18, Structural Research at Rice, Dept. of Civil Engrg., Rice Univ., Houston, April 1973.
55. Veletsos, A.S., and Wei, Y.T., Lateral and Rocking Vibration of Footings, Report No. 8, Structural Research at Rice, Dept. of Civil Engrg., Rice Univ., Houston, Jan. 1971.
56. Waas, G., Earth Vibration Effects and Abatement for Military Facilities, Report 3, "Analysis Method for Footing Vibrations through Layered Media," Tech. Report S-71-14, U.S.A.E.W.E.S., Sept. 1972; also Ph. D. thesis, Univ. of California, Berkeley, June 1972.
57. Warburton, G.B., "Forced Vibrations of a Body on an Elastic Stratum," Journ. Applied Mechanics, Trans. ASME, Vol. 24, No. 1, pp. 55-58, 1957.
58. Warburton, G.B., Richardson, J.D., and Webster, J.J., "Forced Vibrations of Two Masses on an Elastic Half Space," Journ. Applied Mechanics, Trans. ASME, Vol. 38, Ser. E., No. 1, 1971.
59. Warburton, G.B., Richardson, J.D., and Webster, J.J., "Harmonic Response of Masses on an Elastic Half Space," Journ. of Engrg. for Industry, Trans. ASME, Paper No. 71-Vibr-59, 1971.
60. Wei, Y.T., "Steady State Response of Certain Foundation Systems," Ph. D. thesis, Rice Univ., Houston, 1971.

61. Whitman, R.V., and Richart, F.E., Jr., "Design Procedures for Dynamically Loaded Foundations," Journ. Soil Mech. and Foundations Div., ASCE, Vol. 93, No. SM6, pp. 169-193, 1967.
62. Zienkiewicz, O.C., The Finite Element Method in Engineering Science, McGraw-Hill, 1971.

BIOGRAPHY

The author was born in Guatemala, Guatemala on June 21, 1945. He married the former Miss France-Anne Pelé on October 24, 1973.

He did his high school studies at the English-American School in Guatemala, and got his diploma of Bachiller en Ciencias y Letras in October, 1962.

Then he attended the School of Civil Engineering at the Universidad de San Carlos de Guatemala, obtaining the degree of Ingeniero Civil in June, 1969 (six-year program plus general exam and thesis).

He was awarded a scholarship by Exploraciones y Explotaciones Mineras de Izabal (EXMIBAL) to pursue graduate studies leading to a Sc. D. degree. During the last term at MIT, he was supported by a research assistantship.

His work experience includes two years as a designer of urban streets and roads for the Municipality of Guatemala City (1965-1967), two years as a structural designer for Ing. J. J. Hermosilla, a private firm (1967-1969); and summer jobs as a construction supervisor for the International Nickel Company at Ontario (1970) and as a structural engineer in Guatemala (1972).

He is a registered Civil Engineer in Guatemala, a member of the Colegio de Ingenieros de Guatemala, a member of the American Concrete Institute, and a student member of the American Society of Civil Engineers.

APPENDIX

PROGRAM PLAXLY2

Identification:

Analysis of plane and axisymmetric layered media of infinite extent subjected to harmonic loads which act within the plane of the cross-section, or to prescribed harmonic motion at the rock-soil interface.

Programmed by Gunter Waas, University of California, Berkeley, June 1972, as PLAXLY. Modified and extended by Víctor Chang Liang and the original author.

Purpose:

Program PLAXLY2 is designed for the analysis of harmonic motion in plane and axisymmetric systems of the type shown in Figs. 2-1a and 2-1b. Materials may be either linearly elastic or viscoelastic. The loads (prescribed nodal forces and nodal displacements) vary harmonically with time. Static loads may be analyzed by setting the frequency zero. The program consists of a main program MAIN and 17 subroutines: INPUTD, ELSTIF, QUAD, BOUMAT, GENEP, SECEVA, BOMAP, INVERT, HANKEL, STIFF, BLOCKS, MODIFY, OUTPUT, RFORCE, OUTDIS, SHAKE and MULT.

Discretization:

The irregular region I (see Figs. 2-1a and 2-1b) is subdivided into finite elements with quadrilateral cross-sections as shown in Fig. 2-3. The layered regions are subdivided into thin sublayers such that the layer interfaces coincide with the finite element nodes at the plane or cylindrical boundaries between the irregular and the layered regions. Any finite element, except those adjacent to the boundaries between the irregular and layered regions, may have zero moduli and zero mass density, while the sublayers of the layered regions must always have non-zero property values.

The numbering of the finite element nodes is arbitrary, with the following restriction. If it exists, the left layered region L (see Fig. 2-3) is connected to the first NUMLL+1 nodes, where NUMLL is the number of sublayers in the left layered regions. The surface layer is connected to nodes 1 and 2, the second layer to nodes 2 and 3, ... , and the bottom layer (numbered NUMLL) to nodes NUMLL and NUMLL+1. The right layered region R, if existing, is connected to the last NUMLR+1 nodes, where NUMLR is the number of sublayers in the right layered region. The surface layer is connected to the nodes NUMNP-NUMLL and NUMNP-NUMLL+1, ... , and the bottom layer to NUMNP-1 and NUMNP, where NUMNP is the total number of nodes. Because the system is supported by a rough rigid base (see Figs. 2-1a and 2-1b) zero displacements must be specified for the nodes at the bottom, or VSR, VSI, VPR and VPI if there is harmonic motion of the rigid base (see input data, item I).

Size Limitations:

The program uses dynamic storage allocation for arrays the lengths of which are problem dependent. The total storage available for these arrays is the length, MTOT, of the array A, which appears in the blank COMMON statement of MAIN. The length requirement is

$$MTOT > MBAND (5MBAND+7) + 3NUMNP + 2NPBB$$

in which

MBAND = maximum half-bandwidth of global stiffness matrix,
i.e. twice the maximum difference between nodal
point numbers of nodes belonging to any element +2

NUMNP = total number of nodal points

NPBB = number of points outside the finite element region
at which motion is to be computed.

If the value of MTOT is reset, then the dimension of the array A in the blank COMMON statement of program PLAXLY must also be adjusted.

This program uses temporary secondary storage with sequential access. The units are referred to by 1, 2, 3, 4 and 8.

Output Information:

The program prints the following output:

- i) Input and generated data.
- ii) Nodal point displacements including amplitudes and phase angles
- iii) Reaction forces for nodes at which non-zero displacements are prescribed, including amplitudes and phase angles.
- iv) Displacement at desired points outside the finite-element region.
- v) One-dimensional amplification when displacements are prescribed at the rock level.

Input Data:

A. START CARD (5H) (Read in MAIN)

The work START must be punched in columns 1 to 5 on a separate card at the beginning of each problem. Several problems can be analyzed in one run.

B. HEADING CARD (12A6) (Read in MAIN)

Columns 1 to 72 contain alphanumerical data to be printed as title on the output.

C. CONTROL CARD (8I5) (Read in MAIN)

Cols.	1-5	No. of nodal points, NUMNP
	6-10	No. of finite elements, NUMEL
	11-15	No. of different materials, NUMMAT
	16-20	No. of sublayers in Region L, NUMLL, less or equal 40
	21-25	No. of sublayers in Region R, NUMLR, less or equal 40
	26-30	No. of points outside of Region I where displacements are to be computed, NPBB
	31-35	No. of frequencies at which the model is to be analyzed, NFRQ
	36-40	If column 40 is left blank, problem is taken to be axisymmetric and NUMLL must be zero. 1 in column 40 indicates a plane problem; 2 indicates plane-strain problem with prescribed horizontal and/or vertical motion at rock level; 3 indicates axisymmetric problem with prescribed vertical motion at rock level (if both VSR and VSI are not equal to 0, an error message will be given, and the particular example will be flushed out).

Note: If NUMLR is input as minus NUMLL, Region R is understood to be a mirror image of Region L, and some computation can be saved.

D. MATERIAL CARDS (2I5, 5F10.0) (Read in INPUTD)

One card for each different material; not more than 40 materials.

Cols. 1-5 Material number, M
6-10 Interpretation parameter, INTPR
 If INTPR=0 Cols. 21-60 contain moduli
 If INTPR=1 Cols. 21-60 contain wave velocities
11-20 Mass density, RHO
21-30 Real component of shear modulus or S-wave velocity, G_1
31-40 Imaginary part of shear modulus or S-wave velocity, G_2
41-50 Real part of Poisson's ratio or P-wave velocity, NU_1
51-60 Imaginary part of Poisson's ratio or P-wave velocity,
 NU_2

E. LAYER CARDS (10I5) (Read in INPUTD)

Cols. 1-5 Material number for sublayer 1
6-10 Material number for sublayer 2
etc.

Note: This data is grouped in sets, one set for each layered region. If there are two layered regions the first set describes Region L and the second set Region R. If NUMLL=0 or NUMLR=0 the respective set is omitted. In the axisymmetric case NUMLL should be zero. Each set consists of as many cards as necessary to contain the material numbers of the layers sequentially, starting with the surface layer and ending with the bottom layer.

F. NODAL POINT CARDS (2I5,4F10.0,I5) (Read in INPUTD)

Cols. 1-5 Nodal point number, NL
6-10 Parameter indicating if displacements or forces are specified, ICODE
11-20 r-ordinate, (x-ordinate in plane case), R(NL)
21-30 z-ordinate, Z(NL)
31-40 U(1,NL) see below (for horiz. rock motion, put a 1.)
41-50 U(2,NL) see below (for vertical rock motion, put a 1.)
51-55 Parameter for nodal point generation, INCL

If ICODE is

- 0 U(1,NL) is specified force in r-direction and U(2,NL) is specified force in z-direction
- 1 U(1,NL) is specified displacement in r-direction and U(2,NL) is specified force in z-direction
- 2 U(1,NL) is specified force in r-direction and U(2,NL) is specified displacement in z-direction
- 3 U(1,NL) is specified displacement in r-direction and U(2,NL) is specified displacement in z-direction

Note: Nodal point cards need not be input in numerical sequence. Suppose cards for nodes NA and NB are input sequentially. If

$(NA-NB) < 1$ then nodal point data will be generated for nodes $NA+INCL, NA+2INCL, \dots, NB-INCL$ where $INCL$ is the integer specified on the card for node NA . The coordinates for these nodal points will be obtained by linear interpolation between nodes NA and NB . The value of $ICODE$ for the generated nodes is 0. If $(NA - NB) > 0$ no data are generated. If left blank $INCL$ is taken as 1.

G. OUTPUT SPECIFICATION CARDS (F5.0, F10.0)(Read in INPUTD)

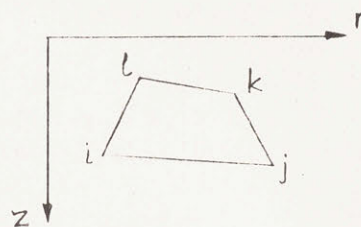
Cols. 1-5 Number of the interface passing through the point at which motion in Region L or Region R is to be computed, RZ . Interfaces are numbered from the surface downward commencing with 1.

6-15 Absolute r -ordinate (horizontal) of point at which motion is to be computed, RZ .

Use one card for each point in Region L and Region R. Cards for points in Region L are placed first. The number of points, $NPBB$, is specified by the Control Card, see C.

H. ELEMENT CARDS (7I5) (Read in ELSTIF)

- Cols. 1-5 Element number, MMM
 6-10 Nodal point i , $IY(1)$
 11-15 Nodal point j , $IY(2)$
 16-20 Nodal point k , $IY(3)$
 21-25 Nodal point l , $IY(4)$
 26-30 Material identification number for element, $IY(5)$.
 If left blank it is taken as 1.
 31-35 Element generation parameter, $INCL$



Note: Order nodal points counter clockwise when the r -axis points horizontally to the right and the z -axis points vertically downwards.

Note: Element data may be generated automatically if the material number is the same for all elements in a series and the nodal point numbers can be obtained as follows:

$$\begin{aligned} IY(1)_i &= IY(1)_j + INCL \\ IY(2)_i &= IY(2)_j + INCL \\ IY(3)_i &= IY(3)_j + INCL \\ IY(4)_i &= IY(4)_j + INCL \end{aligned}$$

where j refers to an element for which the element number MMM_j is one less than the element number MMM_i . In this case only the element card for the first element of the series need be input. However, the last element (highest element number) must always be input. If $INCL$ is left blank then $INCL=1$.

I. FREQUENCY CARDS (F10.0) (Read in MAIN)

- Cols. 1-10 Frequency of the exciting forces and displacements,
CPS
11-20 Real part of specified horizontal rock motion, VSR
21-30 Imaginary part of specified horizontal rock motion,
VSI
31-40 Real part of specified vertical rock motion, VPR
41-50 Imaginary part of specified vertical rock motion,
VPI.

Note: If CPS is positive it is interpreted as the frequency in cycles per second. If CPS is negative it is interpreted as the angular frequency in radians per second. The number of frequency cards is equal to NFRQ specified in the Control Card, see C.

J. STOP CARD (4H) (Read in MAIN)

For normal termination of execution the complete data deck (not each individual problem) finishes with a card with the word STOP punched in columns 1 to 4.